

AD _____

Award Number: DAMD17-99-1-9272

TITLE: Resources for Precision Analysis of Human Breast Cancer

PRINCIPAL INVESTIGATOR: Dr. Peter H. Watson

CONTRACTING ORGANIZATION: University of Manitoba
Winnipeg, Manitoba, R3E 0W3 Canada

REPORT DATE: August 2001

TYPE OF REPORT: Annual

PREPARED FOR: U.S. Army Medical Research and Materiel Command
Fort Detrick, Maryland 21702-5012

DISTRIBUTION STATEMENT: Approved for Public Release;
Distribution Unlimited

The views, opinions and/or findings contained in this report are those of the author(s) and should not be construed as an official Department of the Army position, policy or decision unless so designated by other documentation.

20020401 038

REPORT DOCUMENTATION PAGE

Form Approved
OMB No. 074-0188

Public reporting burden for this collection of information is estimated to average 1 hour per response, including the time for reviewing instructions, searching existing data sources, gathering and maintaining the data needed, and completing and reviewing this collection of information. Send comments regarding this burden estimate or any other aspect of this collection of information, including suggestions for reducing this burden to Washington Headquarters Services, Directorate for Information Operations and Reports, 1215 Jefferson Davis Highway, Suite 1204, Arlington, VA 22202-4302, and to the Office of Management and Budget, Paperwork Reduction Project (0704-0188), Washington, DC 20503

1. AGENCY USE ONLY (Leave blank)		2. REPORT DATE August 2001	3. REPORT TYPE AND DATES COVERED Annual (15 Jul 00 - 15 Jul 01)	
4. TITLE AND SUBTITLE Resources for Precision Analysis of Human Breast Cancer			5. FUNDING NUMBERS DAMD17-99-1-9272	
6. AUTHOR(S) Dr. Peter H. Watson				
7. PERFORMING ORGANIZATION NAME(S) AND ADDRESS(ES) University of Manitoba Winnipeg, Manitoba, R3E 0W3 Canada E-Mail: pwatson@cc.umanitoba.ca			8. PERFORMING ORGANIZATION REPORT NUMBER	
9. SPONSORING / MONITORING AGENCY NAME(S) AND ADDRESS(ES) U.S. Army Medical Research and Materiel Command Fort Detrick, Maryland 21702-5012			10. SPONSORING / MONITORING AGENCY REPORT NUMBER	
11. SUPPLEMENTARY NOTES Report contains color				
12a. DISTRIBUTION / AVAILABILITY STATEMENT Approved for Public Release; Distribution Unlimited				12b. DISTRIBUTION CODE
13. Abstract (Maximum 200 Words) <i>(abstract should contain no proprietary or confidential information)</i> This US Army academic award guarantees ongoing protection and a balance of 75/25% of my time for research/clinical activities. This ensures my continued active contribution to breast cancer research through specific projects underway in my laboratory as well as through efforts to maintain and improve on resources that offer appropriately processed, relevant and pathologically defined tissue samples to other investigators. This award has allowed the PI to 1) continue to advance research projects that are currently ongoing in the laboratory focusing on the role of the psoriasin and lumican genes, the identification and study of additional novel genes associated with progression of pre-invasive DCIS to invasive disease, and 2) continue to direct the NCIC-Manitoba Breast Tumor Bank and offer clinical pathology expertise and advice to many investigators who seek access to appropriate tissues to test their ideas in conjunction with tissues associated with NCIC-clinical trial datasets, and tissues comprising pre-neoplastic and pre-invasive lesions				
14. Subject Terms (keywords previously assigned to proposal abstract or terms which apply to this award) Breast Cancer, Ductal carcinoma in-situ, Tumor Bank				15. NUMBER OF PAGES 104 16. PRICE CODE
17. SECURITY CLASSIFICATION OF REPORT Unclassified	18. SECURITY CLASSIFICATION OF THIS PAGE Unclassified	19. SECURITY CLASSIFICATION OF ABSTRACT Unclassified	20. LIMITATION OF ABSTRACT Unlimited	

NSN 7540-01-280-5500

Standard Form 298 (Rev. 2-89)
Prescribed by ANSI Std. Z39-18
298-102

TABLE OF CONTENTS

Front cover	<i>1</i>
SF298	<i>2</i>
Table of Contents	<i>3</i>
Introduction	<i>4</i>
Body	<i>5-12</i>
Key Research Accomplishments	<i>13</i>
Reportable Outcomes	<i>14-15</i>
Conclusions	<i>16-18</i>
References	<i>19-20</i>
Appendices	<i>21-104</i>

INTRODUCTION.

The past decade has seen dramatic progress in our understanding of the basic cell and molecular biology of breast cancer. However, the translation of this basic science knowledge and ideas has been impeded by the limited numbers of clinician-scientists with skills to effectively collaborate with basic scientists and to accurately interpret tissue pathology, quality and the cellular composition of heterogeneous tissue samples subjected to molecular study. Beyond this there is the problem of access to appropriate human tissue samples. The PI's overall goal is the improvement in our current ability to predict individual risk of development of invasive disease and to predict further progression of invasive disease in terms of resistance to therapies. The specific aims of the PI are 1) continue to advance the two general avenues of research that are currently ongoing in the laboratory and which have direct relevance to important clinical problems in the management of early pre-invasive and the therapy of later advanced disease, 2) continue to direct the NCIC-Manitoba Breast Tumor Bank and offer clinical pathology expertise and advice to many investigators who seek access to appropriate tissues to test their ideas, and 3) to work with others to develop and analyze new tissue resources such as those based on collection of pre-invasive lesions and tissue samples and collection of tumor samples associated with clinical trials.

BODY OF REPORT

The accomplishments over the second year of this award are summarized in four sections with reference to the tasks defined in the original statement of work (entered in *italics* in each section).

Task 1. To develop the National Clinical Trial Tumor Bank Module

- *Complete supervision of collection of material from recently completed NCIC-CTG Trials and conduct histological analysis of all samples (months 0-12)*
- *Continue and refine prospective collection mechanism from collaborating centers (months 0-24)*
- *Travel to new centers in Canada to discuss protocols and enrol in the network (months 0-24)*

The PI has continued to work closely with Dr K. Pritchard (breast site group chair for the NCIC-clinical trials group, NCIC-CTG) and other colleagues across Canada, to develop an NCIC clinical trial breast tumor bank. The PI has participated in 4 conference call meetings and direct discussions concerning this project. The focus this year has been on completion of collection of paraffin tissue blocks associated with the completed MA5 trial and from the outstanding 150 (20%) of cases that we had not previously collected. The project grant from NCIC to Dr K Pritchard was coordinated by the NCIC-CTG central office, and has now ended (July 2001). Given the uncertain future funding of tumor banks in Canada arising from the decision of the NCIC to withdraw from continuing to fund Tumor Banks, no effort to travel has been made to enrol new centers (see conclusions section below).

Task 2. To develop the Pre-neoplastic Tissue Tumor Bank Module

- *Continue supervision of database of Manitoba Breast Surgical Events and collection of representative paraffin blocks from collaborating pathology centers (months 0-36)*
- *Continue to direct accrual of tissue samples and data from collaborating center in Warsaw and conduct histological analysis of all samples (months 0-36)*
- *Travel to Warsaw to discuss protocols and collection system (months 0-12 and 24-36)*

The Manitoba Breast Tumor Bank encompasses 2 major databases, the Manitoba Breast Cancer Database (MBCD, see task 3) and the Manitoba Breast Surgical Events Database (MBED). The first objective in this task was to continue to expand the MBED in order to create a virtual database of patients with breast lesions including preneoplastic and preinvasive lesions within paraffin blocks stored in clinical pathology departments. Initiated in 1996, it now comprises a virtual database linked to specific paraffin blocks in the

archives of 8 pathology departments linked by a common laboratory program. As of July 2001 this database contained 15,154 events on approximately 10,800 patients. This represents a steady rate of case accrual since our last audit in summer 2000 of approximately 2000 patients and 3,073 events. These events include a spectrum of pathological changes limited to only normal tissue, fibrocystic changes, ductal hyperplasia, atypical ductal hyperplasia, in-situ carcinoma, and also cases with invasive carcinoma and combinations of pre-invasive lesions. In time we will create a large dataset of pre-neoplastic lesions in paraffin blocks and a small but invaluable 'longitudinal' dataset comprised of pre-neoplastic/pre-invasive lesions associated with invasive tumors occurring later in the same patients.

A second objective is to further augment the ability of the tumor bank to support research into pre-neoplastic and pre-invasive disease by accruing frozen tissues containing these lesions (in addition to paraffin block tissues encompassed by the MBED). Given the very focal and sporadic nature of such lesions in biopsies, they can only be collected as frozen tissue by systematic accrual and careful analysis of tissues from areas adjacent to breast tumors (where such lesions are most common and can often be identified amongst normal structures). However, this simple strategy, though once feasible, is now very hard to apply in North America where changes in surgical and pathology practice dictate that limited tissue is resected and the peripheral tissue surrounding the tumor is destined for paraffin blocks, required for clinical assessment of margin status. Therefore we have tried to forge collaborations with pathology departments in countries where clinical practice still allows extensive sampling from larger specimens. Although initially successful, our later setbacks in our efforts to achieve this in collaboration with centers in Poland have been detailed previously. We have nevertheless pursued this goal actively, and through close colleagues at the University of Manitoba have now established at least one new potential linkage with a center in Kunming, China. Assurance of ethical review has been obtained from the president of the hospital and a formal letter of invitation to visit and establish a collaboration with the 1st Peoples Hospital of Yunnan Province is in hand. Local ethics review by the Ethics Review Board at the University of Manitoba will now be undertaken prior to proceeding.

Task 3. To direct the NCIC-Manitoba Breast Tumor Bank

- *Continue to direct accrual of primary tumor tissue samples and data and conduct histological analysis of all samples (months 0-36)*
- *Continue to provide advice to external applicants to the Bank (months 0-36)*
- *Continue to supervise the review of applications, and undertake review and selection of appropriate cases for each study (months 0-36)*

The Manitoba Breast Cancer Database (MBCD) section of the Bank contains over 4000 fully processed cases (635 A category cases, 1383 B category cases, 2085 C category cases, 98 D category cases, 60 N category cases) and many further samples collected and partially processed in reserve to maintain the 'stocks'. This represents an increase of 69 (A), 46 (B), 380 (C), 8(D) and 60(N) cases since July 2000. All cases are associated with a database comprising pathological data derived from uniform assessment of the tissue blocks and clinical staging. A subset (all A&B cases) is also associated with complete clinical follow-up.

Overall since the Bank was established in 1993 it has provided support to over 50 projects conducted in research laboratories across North America and Europe. The total aggregate of sections released in support of these projects is 69,747 frozen tumor sections, 12,265 paraffin tumor sections, 10,748 frozen normal tissue sections, 1,227 paraffin normal tissue sections. Over the past year, since July 2000, the Bank has provided material support to 12 investigators including 4 local laboratories, 3 laboratories elsewhere in Canada, and 4 laboratories in the US and 1 laboratory in Europe. This has included 43 batches of cases sent out comprising a total of 7,781 frozen tumor sections, 1,933 paraffin tumor sections, and 96 frozen normal tissue sections and 50 paraffin normal tissue sections.

In addition to continued direction of the NCIC-Manitoba Breast Tumor Bank, the PI has continued to be actively engaged in discussions on the management committee of the Canadian Breast Cancer Research Initiative (CBCRI) concerning breast tumor banking (over 4 meetings this year). The PI has also served as an external consultant and assisted in the development of two proposals, currently under review by the Western Economic Development Agency and the Ontario Cancer Research Network, to establish Tumor Tissue Bank Networks within other Canadian Provinces, Ontario (Coordinating P.I., Mr Pat Lafferty, Price Waterhouse Coopers LLP) and British Columbia (coordinating P.I., Dr Simon Sutcliffe, BCCA).

Task 4. To direct the research program in our laboratory

- *Continue to direct laboratory studies to understand and identify markers of resistance to endocrine therapy and examine the role of estrogen receptor variants and their influence on determination of ER/PR status and response to therapy. (months 0-36)*
- *Continue to direct laboratory studies to understand and identify markers of risk of progression from pre-invasive to invasive disease and examine the role of the psoriasin gene in conferring this risk (months 0-36)*

ER related projects.

Basic research into the mechanisms which underlie the clinical evolution of breast cancer from hormone dependent to hormone independent growth has identified alterations in specific components of the mechanism of estrogen action which may shortcircuit the requirement for estrogen and so contribute to 'hormonal progression'. Over the past year (1999-2000) we have made the following progress, on joint projects and in close collaboration with Dr L C. Murphy's laboratory in our research group;

- The role of active MAP kinase expression was investigated in human breast tumorigenesis and in human breast cancer progression related to hormone independency, using immunohistochemistry and specific antibodies which specifically detect the dually phosphorylated forms of erk 1 and 2. Active MAP kinase expression was detected in approximately 48% of primary human breast tumors, and was found to be significantly increased in the tumors compared to their matched adjacent normal breast tissues (Wilcoxon matched pairs statistical test, $P = 0.027$). No statistically significant correlations were found with grade, cellular composition, ER or PR status. However, a significant positive correlation ($r = 0.38$, $P = 0.0044$, $n = 55$) was obtained between active MAP kinase expression and the presence of lymph node metastases. Moreover, a statistically significant increase in the level of active MAP kinase (Wilcoxon matched pairs test, $P = 0.0098$) was found in concurrent lymph node metastases compared to their matched primary breast tumors. These data support the hypothesis that active MAP kinase may be a marker of breast cancer metastasis and have a functional role in the metastatic process. We also investigated the possibility that active MAP kinase may be a marker of endocrine resistance. However, no statistically significant difference in detection or level of active MAP kinase expression was found in the primary tumors of node negative patients who later were found to respond to tamoxifen treatment (tamoxifen sensitive) or not respond to tamoxifen treatment (tamoxifen resistant). Therefore, active MAP kinase was unlikely to be a marker of endocrine sensitivity, or involved in de novo tamoxifen resistance (1).

Ductal Carcinoma in-situ (DCIS) gene expression projects.

To address the critical issue of the biology of early breast tumor progression and improved determination of risk of progression in pre-invasive lesions, we have applied a novel microdissection approach in combination with our uniquely designed tissue resource and molecular methodologies, in order to directly identify alterations that mark and may contribute to the development pre-invasive lesions and the subsequent development of the invasive phenotype in-vivo. Over the past year;

- We have added two more DCIS cases by microdissection, RNA extraction, hybridization and array analysis (using Research Genetics Array filters to screen for levels of gene expression) and continued our analysis of 8 previously microdissected DCIS tumors.
- To identify molecular alterations underlying the morphological features that separate low from high grade DCIS we have compared gene expression within this total cohort of 10 cases of DCIS (6 high and intermediate-grade DCIS with necrosis and 4 low-grade DCIS without necrosis). A set of 42 cDNAs, from a group of 1,500, has been identified that were consistently differentially expressed and whose expression profile clustered with DCIS grade. Amongst this set, the angio-associated migratory protein (AAMP) was identified as a gene that is consistently higher in high grade DCIS and that is also induced by hypoxia in the T47D breast cancer cell line. Differential expression was confirmed by in situ hybridization and quantitative reverse transcriptase polymerase chain reaction (RT-PCR) analysis of 37 DCIS. AAMP mRNA was associated with high and intermediate-grade DCIS ($p=0.0155$) and DCIS with necrosis ($p=0.023$). However, no relationship was observed between AAMP and angiogenesis, and its functional role in tumorigenesis and breast cancer progression remains to be determined (2).

Specific Progression Gene and related projects.

- In collaboration with Prof Adrian Harris's group, University of Oxford who are leaders in the field of tumor hypoxia and angiogenesis we are also currently examining the role of other hypoxia regulated genes as markers of progression in DCIS and early invasive breast cancer. This is particularly relevant because necrosis, which is thought to be an indicator of severe hypoxia in-vivo is also a marker of high risk of progression of DCIS to recurrence and invasive disease. In this aspect we have recently focused on the carbonic anhydrase genes, CAIX and CAXII that influence intra- and extra- cellular pH and ion transport in varied biological processes, and we have shown are also regulated by hypoxia and are HIF-1 dependent in cell lines including breast cancer cells (3). We then went on to show that expression of CAIX in particular, is associated with necrosis in vivo in both breast and other tumor types (4). Furthermore, in a cohort of 104 invasive breast cancers, CAIX expression was an independent predictor of recurrence free and overall survival (5). By contrast, factors related to differentiation appear to dominate regulation of CAXII in-vivo, and paradoxically high overall expression of CAXII is a good prognostic marker within the same tumor cohort, at least in univariate analysis (6). Next we examined the expression of CAIX and XII in 68 cases of ductal carcinoma in-situ (DCIS; 39 pure DCIS and 29 DCIS associated with invasive carcinoma). As in invasive disease, CA IX was associated with necrosis ($p=0.0053$) and high grade ($p=0.012$). In contrast, CA XII was associated with the

absence of necrosis ($p=0.036$) and low grade ($p=0.012$) but was occasionally observed to be induced adjacent to necrosis within high grade lesions. Assessment of mammographic calcification showed that CA XII expression was also associated with the absence of calcification ($n=43$, $p=0.0083$). Our results demonstrate that induction of CA IX and CA XII occurs in regions adjacent to necrosis in DCIS. Furthermore, these data suggest that hypoxia may be a dominant factor in the regulation of CA IX, and that factors related to differentiation, as determined by tumor grade, dominate the regulation of CA XII. The associations of CAIX with an aggressive phenotype and outcome in invasive tumors suggest that it may be important as a predictor in DCIS and also as a target for therapy through the development of selective inhibitors of carbonic anhydrases, since the latter have recently been shown to prevent tumor invasion (7).

- We have continued to study the psoriasin (S100A7) gene that we have previously identified as differentially expressed between in-situ (DCIS) and invasive carcinoma. We had previously used the yeast 2-hybrid assay to screen a normal breast cell library to identify the centrosome associated protein RanBPM as a possible binding partner. Over this year co-immunoprecipitation of psoriasin and RanBPM- was achieved by cloning by PCR each cDNA into expression vectors downstream of a T7 promoter. Using TNT kits (Promega) ^{35}S -Met labeled proteins were generated and the radiolabelled proteins were added to buffer and immunoprecipitated by addition of anti-HisG antibody. After addition of ProteinG beads and washing steps, the samples were subjected to Tris-Tricine SDS-PAGE and appropriate protein bands were detected by autoradiography to confirm an interaction in-vitro. Co-localization of psoriasin to the centrosome in breast cells in-vivo was done using two different human mammary epithelial cell lines stably transfected with psoriasin (MCF10A and MDA-MB-231). Cells were grown on 4 well slides and psoriasin protein was detected by a specific antibody and visualized by an appropriate FITC labeled secondary antibody. The centrosomal protein pericentrin was also detected by a specific antibody and visualized by an appropriate Cy5 labeled secondary. Using confocal microscopy, psoriasin is observed to co-localize with pericentrin to the region of the centrosome throughout the cell cycle in both cell lines. Psoriasin protein was not observed in non-transfected cells. While preparing this report we have become aware of a second publication concerning RanBPM from the original group that suggests that a) RanBPM is a larger protein than originally described and b) localizes mostly to the nucleus but also to the peri-nuclear and pericentrosomal regions. Nevertheless, the protein-protein interaction observed in yeast between the C-terminal portion of RanBPM and psoriasin is supported by our co-immunoprecipitation and co-localization studies (8).

- Using our microdissection approach we have previously identified lumican and decorin as the most abundant of the small leucine rich proteoglycans (SLRPs) in breast tissue stroma and shown that their expression is altered adjacent to DCIS and in invasive breast tumors, relative to normal breast (9). We are currently examining the prognostic significance of lumican and decorin in a cohort of 140 invasive breast carcinomas by western blot analysis. All cases selected were axillary lymph node negative and treated by adjuvant endocrine therapy, as these represent early stage invasive disease and it is also in this subset of breast cancers that EGFR expression has been shown to be predictive of outcome. The latter criteria is significant as it is believed that decorin is a natural ligand for EGFR and related growth factor receptors. Lumican and decorin expression was highly correlated ($r=0.45$, $p<0.0001$) in these invasive tumors. Low levels of Lumican were associated with higher grade, large size, negative estrogen receptor and progesterone receptor status and increased host inflammatory response (all $p<0.05$) while decorin levels did not show significance with any factor. However, using univariate analysis both were predictive of short recurrence free (lumican $p=0.0013$, decorin $p=0.026$) and poor overall survival (lumican $p=0.001$, decorin $p=0.0076$). Multivariate Cox analysis is currently being performed. These results suggest that higher levels of SLRPs in breast tumors are associated with a worse prognosis in a selected series of invasive breast carcinoma patients (10).

Collaborations

- A. Our work with the SLRPs has interested us in identification of alterations in other intracellular factors. In a collaboration led by Dr Charis Eng, Ohio State Univ., we have begun to examine the existence and role of LOH (loss of heterozygosity) in stroma as opposed to the epithelial elements of breast cancer. By applying laser capture microdissection to 41 cases and tissue samples in both laboratories and analysis of 13 microsatellite markers, we have found frequent LOH in epithelial compartments (25-70%) but also LOH in adjoining stromal compartments (17-61%). This observation has been made previously by others however, we have also shown that stromal LOH at certain loci may be associated with prognostic parameters (eg 6q25.3 associates with low grade). Analysis of larger case sets to determine the significance of stromal LOH is now underway (11,12).
- B. Access to our nationally funded Tumor Bank resource and our tissue expertise is in no way dependent on establishing direct collaborations with the PI. Nevertheless some investigators have sought formal collaborations and assistance in detailed study design and analysis, and the PI also

collaborates with colleagues within the University of Manitoba Breast Cancer Research Group on other projects. In the past year this has resulted in the following additional publications;

- Myal Y, Blanchard A, Watson P, Corrin M, Shiu R, Iwasiou B. Detection of genetic point mutations by PNA-mediated PCR clamping using paraffin embedded specimens. **Anal. Biochem.** 285:169-172, 2000
- Lee J, Weber M, Mejia S, Bone E, Watson P, Orr W. A matrix metalloproteinase inhibitor, batimastat, retards the development of osteolytic bone metastases by MDA-MB-231 human breast cancer cells in Balb C nu/nu mice. **Eur J Cancer.** Jan;37(1):106-113. 2001
- Yu-Hua Tseng, David Vicent, Jianhua Zhu, Yulian Niu, Adewale Adeyinka, Julie S. Moyers, Peter H. Watson and C. Ronald Kahn. Regulation of growth and tumorigenicity of breast cancer cells by the low molecular weight GTPase RAD and NM23. **Cancer Research** 1;61(5):2071-9. 2001

KEY RESEARCH ACCOMPLISHMENTS

In the period July 2000 – July 2001 the PI has contributed through studies in his own laboratory and with others to the following accomplishments;

1. Continued operation and development of the NCIC-Manitoba Breast Tumor Bank and support for new projects
2. Establishing that an interaction occurs in-vitro and in-vivo between Psoriasin and a novel centrosomal protein, RanBPM.
3. Establishing that Lumican and Decorin are the most abundant among the small leucine rich proteoglycan (SLRP) genes in breast tissues, that their expression is altered in breast tumors, and that low levels of these extracellular proteins may be predictive (in univariate analysis) of outcome in node negative invasive breast cancer.
4. Establishing that the carbonic anhydrases genes CAIX and CAXII and hypoxia regulated, that expression of both may be predictive of outcome in invasive breast cancer, and that the altered expression of both occurs between low and high grade DCIS.
5. Establishing that the Angio-Associated Migratory Protein (AAMP) is hypoxia regulated and that the altered expression of AAMP occurs between low and high grade DCIS.
6. Demonstrating that loss of heterozygosity (LOH) can not only occur in stroma adjacent to invasive carcinoma but that this LOH can be associated with clinical-pathological prognostic factors.

REPORTABLE OUTCOMES

PAPERS

1. Myal Y, Blanchard A, Watson P, Corrin M, Shiu R, Iwasiou B. Detection of genetic point mutations by PNA-mediated PCR clamping using paraffin embedded specimens. **Anal. Biochem.** 285:169-172, 2000
2. Leygue E, Snell L, Dotzlaw H, Hole K, Hiller-Hitchcock T, Murphy LC, Roughley PJ, Watson PH. Lumican and decorin are differentially expressed in human breast carcinoma. **J Pathology.** Nov;192(3):313-20. 2000 (listed as in press in previous report)
3. Lee J, Weber M, Mejia S, Bone E, Watson P, Orr W. A matrix metalloproteinase inhibitor, batimastat, retards the development of osteolytic bone metastases by MDA-MB-231 human breast cancer cells in Balb C nu/nu mice. **Eur J Cancer.** Jan;37(1):106-113. 2001
4. C.C. Wykoff, N.J.P. Beasley, P.H. Watson, KJ Turner, J. Pastorek, GD Wilson, H. Turley PH Maxwell, P. Ratcliffe, A.L. Harris. Hypoxia induced regulation of tumor associated carbonic anhydrases. **Cancer Research** Dec 15;60(24):7075-83. 2000
5. Yu-Hua Tseng, David Vicent, Jianhua Zhu, Yulian Niu, Adewale Adeyinka, Julie S. Moyers, Peter H. Watson and C. Ronald Kahn. Regulation of growth and tumorigenicity of breast cancer cells by the low molecular weight GTPase RAD and NM23. **Cancer Research** 1;61(5):2071-9. 2001
6. Charles C. Wykoff, Nigel Beasley, Peter H. Watson, Stephen K. Chia, Ruth English, Jaromir Pastorek, William S. Sly, Peter Ratcliffe, and Adrian L. Harris "Expression of the Tumor Associated Carbonic Anhydrases IX and XII in Ductal Carcinoma In-Situ (DCIS) of the Breast." **Am J Pathology** 158(3):1011-9.2001
7. N.J.P. Beasley, C.C. Wykoff, P.H. Watson, R. Leek, H. Turley, K. Gatter, J. Pastorek, G.J. Cox, P. Ratcliffe, A.L. Harris. Carbonic Anhydrase IX expression in Head and Neck Squamous Cell Carcinoma and its relationship to hypoxia, necrosis and microvessel density. **Cancer Research.** 1;61(13):5262-7. 2001
8. Stephen K. Chia, Charles C. Wykoff, Peter H. Watson, Cheng Han, Russell D. Leek, Jaromir Pastorek, Kevin C. Gatter, Peter Ratcliffe and Adrian L. Harris "Prognostic Significance of a Novel Hypoxia Regulated Marker –Carbonic Anhydrase IX in Invasive Breast Carcinoma." In press **J Clin Oncology**
9. Heidi M. Sowter, Peter J. Ratcliffe, Peter H. Watson, Arnold H. Greenberg and Adrian L. Harris. HIF-1-dependent regulation of hypoxic induction of the cell death factors BNIP3 and NIX in human tumours. In press **Cancer Research.**
10. Keisuke Kurose, Stacy Hoshaw-Woodard, Adewale Adeyinka, Stan Lemeshow, Peter Watson and Charis Eng. Genetic model of multi-step breast carcinogenesis involving the epithelium and stroma: clues to tumour-microenvironment interactions. in press **Hum Mol Genetics**

PAPERS – submitted

- Keisuke Kurose, Stacy Hoshaw-Woodard, Adewale Adeyinka, Stan Lemeshow, Peter Watson and Charis Eng. Differential alterations in the epithelial and stromal compartments of breast cancers correlate with grade and nodal involvement. Submitted to **NEJM**
- “Carbonic Anhydrase XII is a marker of good prognosis in Invasive Breast Carcinoma.” Peter H. Watson, Stephen K. Chia, Charles C. Wykoff, Cheng Han, Russell D. Leek, Sly, Kevin C. Gatter, Peter Ratcliffe, and Adrian L. Harris. Submitted to **British J Cancer**
- “The hypoxia induced genes VEGF and CA IX are differentially regulated in superficial versus invasive bladder cancer”. Kevin J. Turner, Jeremy P. Crew, Charles C. Wykoff, Peter H. Watson, Jaromir Pastorek , David Cranston, Peter J. Ratcliffe, Adrian L. Harris. Submitted to **Cancer Research**
- Activated Mitogen-activated Protein Kinase Expression during Human Breast Tumorigenesis and Breast Cancer Progression. Adewale Adeyinka, Yulian Nui, Tracy Cherlet, Linda Snell, Peter H Watson, Leigh C Murphy. submitted to **British J Cancer**

PRESENTATIONS

- Manitoba Laboratory Congress (MCMLS), “The role of tumor banks in research”, Winnipeg, Oct 2000
- FASEB 2001, “Microdissecting breast cancer tumor banks” Orlando Florida, March 2001
- CBCRI Reasons for Hope conference, “Invasion genes in DCIS, - the real McCoy”, Quebec City, May 2001

DATABASES

- NCIC-Manitoba Breast Tumor Bank – continued operation and development of a unique tissue resource and provision of cases to external investigators across North America

FUNDING

- CIHR grant (PI Dr L.C. Murphy, co-PI Dr Watson) –“mechanisms of estrogen dependence and independence in human breast cancer”, \$117,000, July 2001-2004

CONCLUSIONS

Importance & Implications: It is anticipated that the many studies that will be conducted by the users of the Tumor Bank, will be facilitated and enhanced by access to histologically defined tissues containing invasive and pre-invasive breast lesions. This will lead to the identification of biological markers and cellular alterations that are directly relevant to the prediction of the natural history of onset and the later response to treatment of breast cancer. This knowledge will in turn ultimately contribute to strategies to predict and reduce risk of breast cancer or to circumvent resistance and improve on current treatments for invasive and metastatic disease. Our own research studies described above will hopefully contribute to this knowledge.

Future strategy: In the next year, the PI will continue to pursue the Tasks as outlined in the original Statement of Work.

Task 1 has now been successfully completed.

Tasks 2 and 3 remain dependent on the involvement and motivation of other groups and centers beyond our own. However we will continue to strive to achieve this goal. Task 2 and Task 3 are also undermined by loss of funding and direct involvement from the National Cancer Institute of Canada (NCIC). The NCIC 'tumor bank' program originally funded 4 Banks (Breast, Lung, Brain, Sarcoma) since 1993, all through regular operating grants. However NCIC has become uncomfortable with the funding commitment to Banks, with the view that they are hard to assess in relation to operating grants and should in any case become self-sustaining once launched. As a result, even though some Banks such as the NCIC-Manitoba Breast Tumor Bank has acquired a national and international reputation as a unique resource and for its contribution to cancer research (eg distribution and reputation of users, unsolicited recognition in open forums by CIHR cancer institute director at the "CBCRI Reasons for Hope conference, Quebec City 2001" and the "Future of Health Research and Economic Development in Western Canada", workshop sponsored by Western Economic Development Agency, Chair Dr Henry Friesen, 2001), the NCIC Board decided to cease funding to current Tumor Banks including the Manitoba Breast Tumor Bank, as of June 30, 2001. This followed extensive discussions since spring 1999 to identify a way to reduce NCIC's commitment to these currently established Banks. The PI served as chair of these committee discussions during 1999-2000, which revolved around the premise that NCIC would be willing to support the costs of 'networking' of Banks to create a larger self-sustaining enterprise that

could for example attract outside funding from industry and also develop a user fee schedule. Limited progress was made, reflecting the different interests and resources available to these groups, and also the reluctance of investigators primarily skilled in research, to accept the increased burden of providing these resources and securing income, without core funds and the kind of recognition of value that NCIC bestows. Transformation of a Tumor Bank into a self sustaining enterprise would also occur at the cost of individual research time and priorities.

To continue with Task 2&3 the PI is currently exploring avenues for continued funding and operation of the Tumor Bank as an open resource (by maintaining the integrity of the dataset and the ability of such a Bank to provide a wide selection tissue and data sets in a timely and expert fashion to investigators). This avenues include;

1. Alternative funding agencies:

- NCIC focus has moved away from Tumor Bank resources
- CBCRI (Canadian Breast Cancer Research Initiative) is considering support for breast cancer research infrastructure at the management committee level (on which the PI is a member) but any decision on this is at least a year away
- CIHR (Canadian Institute of Health Research) cancer institute director is considering support for cancer research infrastructure (personal discussion) and has indicated that it is on the Advisory Board agenda but again any decision on this is at least a year away. CIHR offers multiuser equipment grants but a decision on eligibility of a Tumor Bank has as yet to be resolved
- CFI (Canada Foundation for Innovation) will support new resource creation and may offer a mechanism to support CFI created infrastructure, but currently will not support continued operation of an established non-CFI database.
- NCI US has offered several infrastructure type award mechanisms and has included in its NCI 2002 Budget Request a specific objective "To establish and make available tissue resources to researchers to maximize the practical application of molecular signatures to problems in treating cancer. \$17.5M. However recent direct enquiry to NCI has determined that we are not eligible to apply for any of these programs.
- US Army Program has no Tumor Bank infrastructure mechanism

2. User Fees. Feasible on a not-for-profit cost recovery basis to offset costs but requires a parent organisation to oversee financial and ethical responsibility and is not suitable as a core baseline

strategy as funds will be intermittent while maintaining the collection is not. Potential fee schedules and plans have been considered and drafted.

3. Local Institutional Funding

- Cancer Care Manitoba – discussions in progress
- University of Manitoba – discussions in progress

Task 4 revolves around the PI's own research program, and successful renewal of operating grant funding from the CIHR and CBCRI in July 2000 provides the foundation for continued discovery of differentially expressed genes associated with the early stages of breast tumor progression and improved understanding of the biological role and functional importance of novel genes. These studies will include further work on psoriasin & RanBPM (analysis of relationships of expression in breast tumors to centrosomes and the effect of overexpression of both genes on breast cell lines), lumican & decorin (completion of in-vivo expression and outcome study and analysis of effects of overexpression in breast epithelial and fibroblast models), CAIX & CAXII (analysis of roles as predictors of outcome for DCIS), and the AAMP (analysis of expression and protein level and effect on invasiveness in breast cell lines when overexpressed) genes in this process.

REFERENCES

1. Activated Mitogen-activated Protein Kinase Expression during Human Breast Tumorigenesis and Breast Cancer Progression. Adewale Adeyinka, Yulian Nui, Tracy Cherlet, Linda Snell, Peter H Watson, Leigh C Murphy. submitted to **British J Cancer**
2. Angio-Associated Migratory Cell Protein (AAMP) mRNA is associated with necrosis and is differentially expressed between High-grade and Low-grade Ductal Carcinoma In Situ (DCIS) of the Breast. Adewale Aeyinka, Ethan Emberly, Yulian Niu, Linda Snell, Leigh C. Murphy, Hiedi Sowter, Charlie Wykoff, Adrian Harris, and Peter H. Watson. Manuscript in preparation, see data in appendix
3. C.C. Wykoff, N.J.P. Beasley, P.H. Watson, KJ Turner, J. Pastorek, GD Wilson, H. Turley PH Maxwell, P. Ratcliffe, A.L. Harris. Hypoxia induced regulation of tumor associated carbonic anhydrases. **Cancer Research** Dec 15;60(24):7075-83. 2000
4. N.J.P. Beasley, C.C. Wykoff, P.H. Watson, R. Leek, H. Turley, K. Gatter, J. Pastorek, G.J. Cox, P. Ratcliffe, A.L. Harris. Carbonic Anhydrase IX expression in Head and Neck Squamous Cell Carcinoma and its relationship to hypoxia, necrosis and microvessel density. **Cancer Research.** 1;61(13):5262-7. 2001
5. Stephen K. Chia, Charles C. Wykoff, Peter H. Watson, Cheng Han, Russell D. Leek, Jaromir Pastorek, Kevin C. Gatter, Peter Ratcliffe and Adrian L. Harris "Prognostic Significance of a Novel Hypoxia Regulated Marker –Carbonic Anhydrase IX in Invasive Breast Carcinoma." In press **J Clin Oncology**
6. Peter H. Watson, Stephen K. Chia, Charles C. Wykoff, Cheng Han, Russell D. Leek, Sly, Kevin C. Gatter, Peter Ratcliffe, and Adrian L. Harris "Carbonic Anhydrase XII is a marker of good prognosis in Invasive Breast Carcinoma.". Submitted to **British J Cancer**
7. Charles C. Wykoff, Nigel Beasley, Peter H. Watson, Stephen K. Chia, Ruth English, Jaromir Pastorek, William S. Sly, Peter Ratcliffe, and Adrian L. Harris "Expression of the Tumor Associated Carbonic Anhydrases IX and XII in Ductal Carcinoma In-Situ (DCIS) of the Breast." **Am J Pathology** 158(3):1011-9.2001
8. Ethan D. Emberly,, A. Kate Hole, R. Daniel Gietz, Leigh C. Murphy, Peter H. Watson. Psoriasin localizes to the Centrosome and Interacts with Centrosomal Proteins in Human Breast Cancer. Manuscript in perparation, see data in appendix.
9. Leygue E, Snell L, Dotzlaw H, Hole K, Hiller-Hitchcock T, Murphy LC, Roughley PJ, Watson PH. Lumican and decorin are differentially expressed in human breast carcinoma. **J Pathology.** Nov;192(3):313-20. 2000
10. Sandra Troup, Cal Roskelley, Shukti Chakravarti, Peter J. Roughley, Leigh C. Murphy, Peter H. Watson. Reduced expression of the small leucine-rich proteoglycans, Lumican and Decorin, is associated with poor outcome in node negative invasive breast cancer. Manuscript in preparation, see data in appendix.

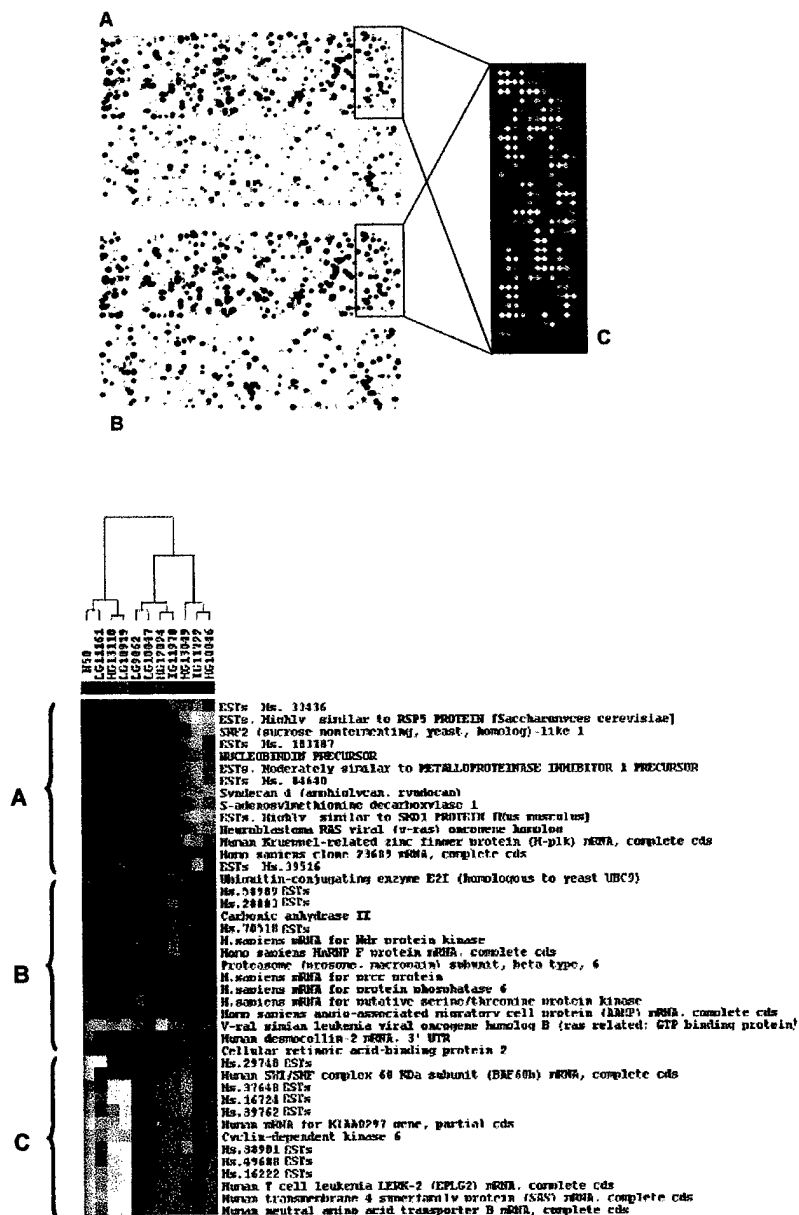
11. Keisuke Kurose, Stacy Hoshaw-Woodard, Adewale Adeyinka, Stan Lemeshow, Peter Watson and Charis Eng. Genetic model of multi-step breast carcinogenesis involving the epithelium and stroma: clues to tumour-microenvironment interactions. in press **Hum Mol Genetics**
12. Keisuke Kurose, Stacy Hoshaw-Woodard, Adewale Adeyinka, Stan Lemeshow, Peter Watson and Charis Eng. Differential alterations in the epithelial and stromal compartments of breast cancers correlate with grade and nodal involvement. Submitted to **NEJM**

APPENDICES A&B

Appendix A. Data and figures associated with references 2,8,10.

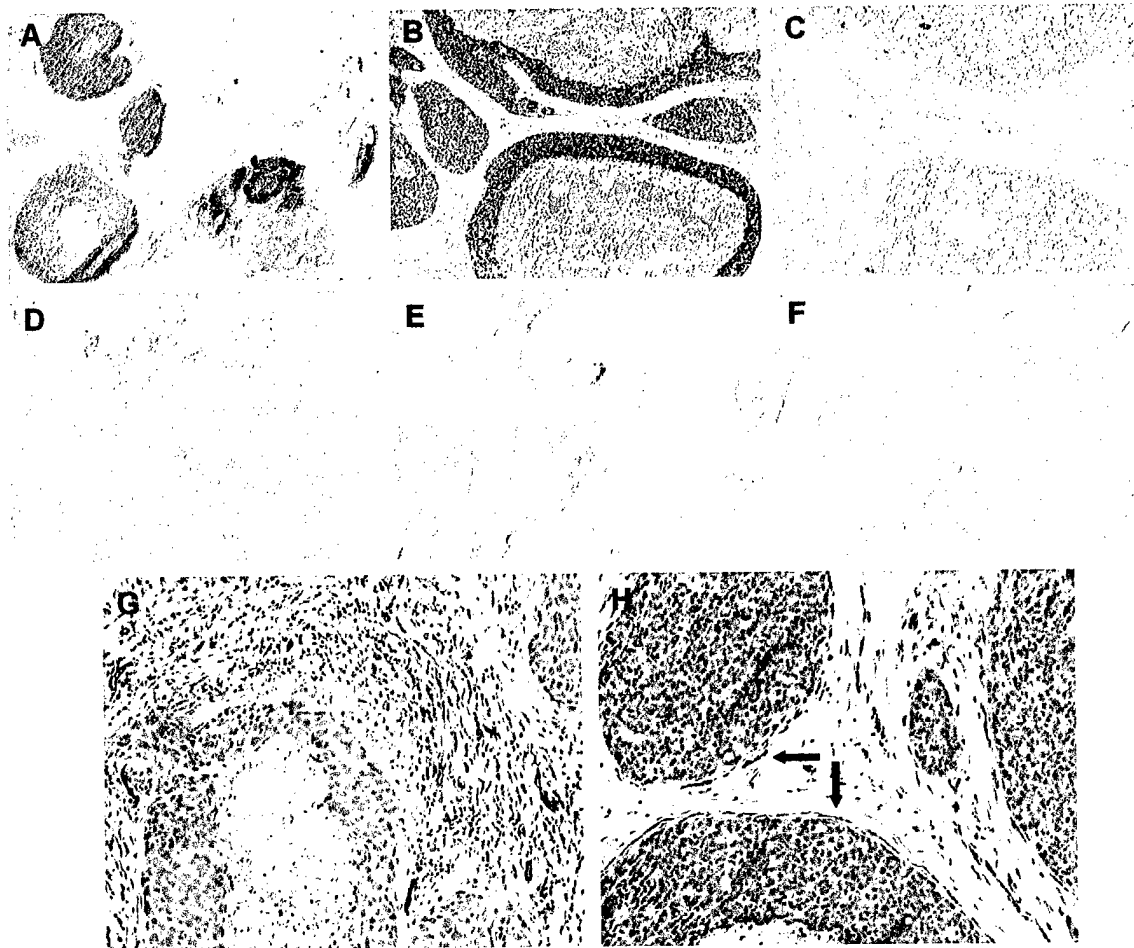
- Angio-Associated Migratory Cell Protein (AAMP) mRNA is associated with necrosis and is differentially expressed between High-grade and Low-grade Ductal Carcinoma In Situ (DCIS) of the Breast. Adewale Aeyinka, Ethan Emberly, Yulian Niu, Linda Snell, Leigh C. Murphy, Hiedi Sowter, Charlie Wykoff, Adrian Harris, and Peter H. Watson. Manuscript in preparation, figure 1 A,B,C and Figure 2
- Ethan D. Emberely,, A. Kate Hole, R. Daniel Gietz, Leigh C. Murphy, Peter H. Watson. Psoriasin localizes to the Centrosome and Interacts with Centrosomal Proteins in Human Breast Cancer. Manuscript in preparation. Figure 1 and figure 2
- Sandra Troup, Cal Roskelley, Shukti Chakravarti, Peter J. Roughley, Leigh C. Murphy, Peter H. Watson. Reduced expression of the small leucine-rich proteoglycans, Lumican and Decorin, is associated with poor outcome in node negative invasive breast cancer. Manuscript in preparation. Figure 1 – survival curves.

Reference #2. Angio-Associated Migratory Cell Protein (AAMP) mRNA is associated with necrosis and is differentially expressed between High-grade and Low-grade Ductal Carcinoma In Situ (DCIS) of the Breast. Adewale Aeyinka, Ethan Emberly, Yulian Niu, Linda Snell, Leigh C. Murphy, Hiedi Sowter, Charlie Wykoff, Adrian Harris, and Peter H. Watson. Data from Manuscript in preparation

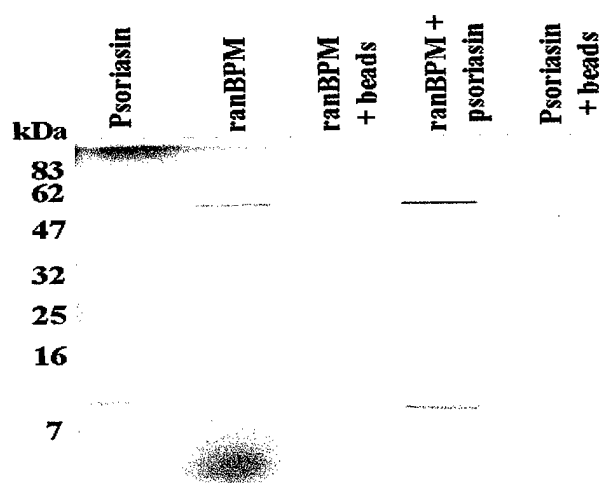


Reference #2, Fig 1. Differential gene expression analysis employing the GF200 cDNA array membrane and the Pathways 2.01 analysis software. Hybridization of 33P-labeled reverse transcribed RNA from a high grade DCIS (A) and a low grade DCIS (B) to Human GF200 cDNA array membranes. (C) Portion of synfilter generated by the Pathways 2.01 analysis software from membranes A and B. Yellow spots show genes expressed equally by both samples, green spots; genes differentially expressed by high grade tumor and red spots; genes differentially expressed by low grade tumor. AAMP is represented by green spot surrounded by blue rectangle. D, Cluster map and phylogenetic tree resulting from an average-linkage cluster analysis of the 42 differentially expressed genes identified in our series of DCIS. Each color patch represents the expression level of the associated gene in that tissue sample with a continuum of expression from bright green (lowest) to bright red (highest). N50 is a normal breast sample, HG, high-grade DCIS; LG, low-grade DCIS; IG, intermediate grade DCIS; 1, cluster of genes and ESTs differentially expressed in low-grade DCIS; 2 and 3, cluster of genes and ESTs differentially expressed in intermediate/high-grade DCIS.

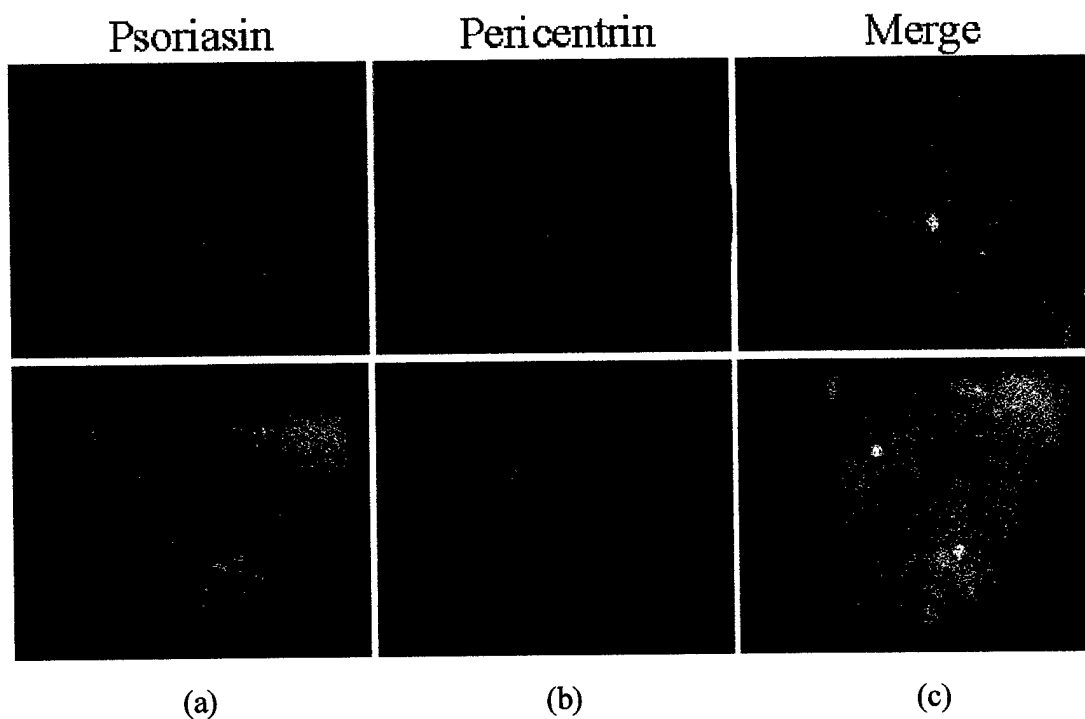
Reference #2, Fig 2. In situ hybridization with ^{33}P -labeled sense probe for AAMP, showing strong signals for AAMP in high-grade ducts with necrosis (A and B) and weaker signals in low-grade DCIS (D). There were no signals with the sense probe (C), x 40. Immunohistochemistry with antibody against the CD34 antigen showing the rim (arrows, E) and stromal (F) patterns of angiogenesis in tumors A and B, respectively, X 100.



Reference:#8: Ethan D. Emberely,, A. Kate Hole, R. Daniel Gietz, Leigh C. Murphy, Peter H. Watson. Psoriasin localizes to the Centrosome and Interacts with Centrosomal Proteins in Human Breast Cancer. Data from Manuscript in perparation



Reference #8, Fig 1. Co-immunoprecipitation of psoriasin and ranBPM to confirm Yeast 2-Hybrid interaction- *in vitro* labeled ^{35}S -Met ranBPM and psoriasin co-immunoprecipitated with annti-HisG antibody, which specifically detects ranBPM. Samples visualized by autoradiography after SDS-PAGE.

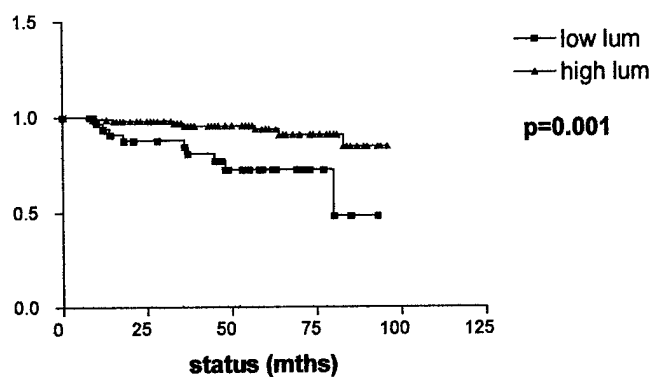


Reference #8, Fig 2. Co-localization of psoriasin to the centrsosome- The human breast cancer cell line MDA-MB-231 was stably transfected to express psoriasin. Upper panels show an interpahse cell, whereas lower panels show a cell in the mitotic stage of the cell cycle. Psoriasin protein (a), is seen throughout the cytoplasm, but is concentrated at a distinct foci in the interpahse cell and multiple locations in the metaphase cell. The centrosomal specific protein pericentrin in (b) is seen to form only one foci in interphase cells, and two foci in mitotic cells. The overlay of images (a) and (b) shows that psoriasin co-localizes to the centrosome (c).

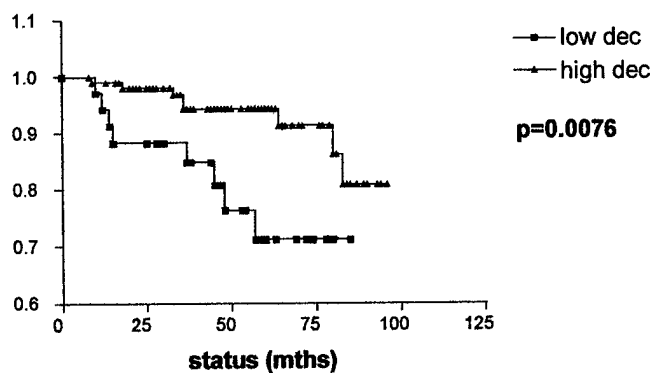
Reference #10. Sandra Troup, Cal Roskelley, Shukti Chakravarti, Peter J. Roughley, Leigh C. Murphy, Peter H. Watson. Reduced expression of the small leucine-rich proteoglycans, Lumican and Decorin, is associated with poor outcome in node negative invasive breast cancer. Data from Manuscript in preparation,

Kaplan Meier plots for association between lumican and decorin expression and survival analysis in a node-negative cohort of invasive breast carcinoma (n=140)

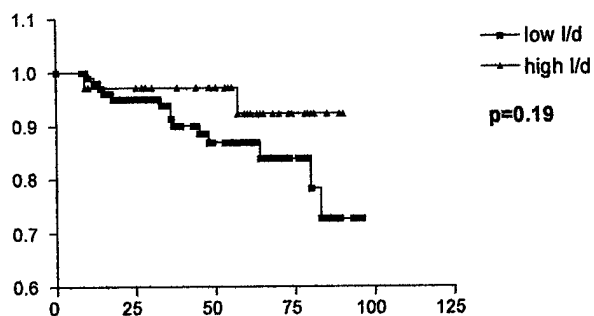
Survival curve: lumican



Survival curve: decorin



**Survival curve:
Lum/dec ratio**



Appendix B. Papers published and in -press.

1. Myal Y, Blanchard A, Watson P, Corrin M, Shiu R, Iwasiou B. Detection of genetic point mutations by PNA-mediated PCR clamping using paraffin embedded specimens. **Anal. Biochem.** 285:169-172, 2000
2. Leygue E, Snell L, Dotzlaw H, Hole K, Hiller-Hitchcock T, Murphy LC, Roughley PJ, Watson PH. Lumican and decorin are differentially expressed in human breast carcinoma. **J Pathology.** Nov;192(3):313-20. 2000 (listed as in press in previous report)
3. Lee J, Weber M, Mejia S, Bone E, Watson P, Orr W. A matrix metalloproteinase inhibitor, batimastat, retards the development of osteolytic bone metastases by MDA-MB-231 human breast cancer cells in Balb C nu/nu mice. **Eur J Cancer.** Jan;37(1):106-113. 2001
4. C.C. Wykoff, N.J.P. Beasley, P.H. Watson, KJ Turner, J. Pastorek, GD Wilson, H. Turley PH Maxwell, P. Ratcliffe, A.L. Harris. Hypoxia induced regulation of tumor associated carbonic anhydrases. **Cancer Research** Dec 15;60(24):7075-83. 2000
5. Yu-Hua Tseng, David Vicent, Jianhua Zhu, Yulian Niu, Adewale Adeyinka, Julie S. Moyers, Peter H. Watson and C. Ronald Kahn. Regulation of growth and tumorigenicity of breast cancer cells by the low molecular weight GTPase RAD and NM23. **Cancer Research** 1;61(5):2071-9. 2001
6. Charles C. Wykoff, Nigel Beasley, Peter H. Watson, Stephen K. Chia, Ruth English, Jaromir Pastorek, William S. Sly, Peter Ratcliffe, and Adrian L. Harris "Expression of the Tumor Associated Carbonic Anhydrases IX and XII in Ductal Carcinoma In-Situ (DCIS) of the Breast." **Am J Pathology** 158(3):1011-9.2001
7. N.J.P. Beasley, C.C. Wykoff, P.H. Watson, R. Leek, H. Turley, K. Gatter, J. Pastorek, G.J. Cox, P. Ratcliffe, A.L. Harris. Carbonic Anhydrase IX expression in Head and Neck Squamous Cell Carcinoma and its relationship to hypoxia, necrosis and microvessel density. **Cancer Research.** 1;61(13):5262-7. 2001
8. Stephen K. Chia, Charles C. Wykoff, Peter H. Watson, Cheng Han, Russell D. Leek, Jaromir Pastorek, Kevin C. Gatter, Peter Ratcliffe and Adrian L. Harris "Prognostic Significance of a Novel Hypoxia Regulated Marker –Carbonic Anhydrase IX in Invasive Breast Carcinoma." In press **J Clin Oncology**
9. Heidi M. Sowter, Peter J. Ratcliffe, Peter H. Watson, Arnold H. Greenberg and Adrian L. Harris. HIF-1-dependent regulation of hypoxic induction of the cell death factors BNIP3 and NIX in human tumours. In press **Cancer Research.**
10. Keisuke Kurose, Stacy Hoshaw-Woodard, Adewale Adeyinka, Stan Lemeshow, Peter Watson and Charis Eng. Genetic model of multi-step breast carcinogenesis involving the epithelium and stroma: clues to tumour-microenvironment interactions. in press **Hum Mol Genetics**

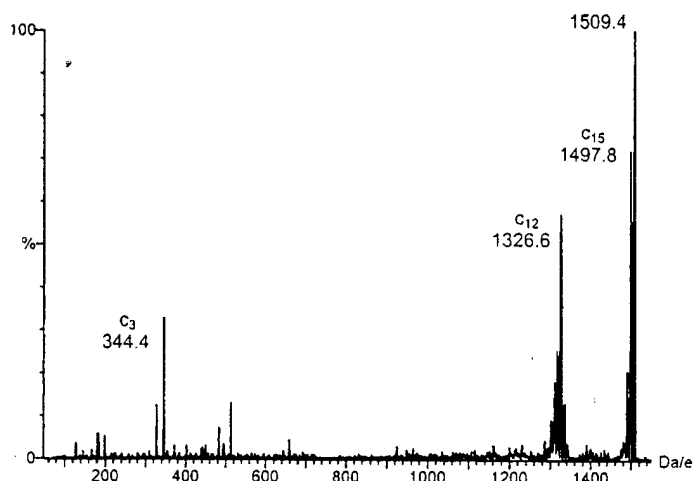


FIG. 2. Collision activated mass spectrum of the doubly charged molecular ion of C-peptide (m/z 1509.4). Collision gas argon at 3×10^{-3} mbar, collision energy 30 V, cone 60 V, capillary 3.5 kV, and source temperature 175°C.

fortified 1 mL of urine with 1% BSA, performed UF with Vivaspins (5000 MW cutoff) for 10 min at 7000g, added 1 mL water to the retentate (25 μ L), mixed, and repeated UF so that a final retentate volume of 200 μ L was reached (concentration factor, 5; purification factor, 8) (see Fig. 1). For the LC/MS analysis, we used the negative electrospray mode and monitored the collision-activated dissociation of the doubly charged molecular ion, m/z 1509.4 to 1326.6 (C_{12} -fragment). Two other important fragments are the C_3 (m/z 344.4) and C_{15} -fragment (m/z 1497.8). As we observed no significant ions with m/z >1510, we only present the spectrum in the range from m/z 50 to 1550 (see Fig. 2).

In conclusion, the adsorption of small proteins to BSA allows the use of UF devices for sample purification and concentration that have considerably higher nominal MW cutoffs than the MW of the analyte of interest. The method has been tested for urinary C-peptide over a concentration range from ~30 to ~170 ng/mL. In future experiments, we also hope to prove the applicability of this method for other peptides and proteins.

Acknowledgments. We acknowledge financial support by the Research Fund of the Ghent University (Grant BOF 01102096) and the National Fund for Scientific Research (Grant 3G0001096).

REFERENCES

1. Vivascience, Ltd. (1999) Vivaspins 500 μ L, 2 mL, and 4 mL; technical data and operating instructions. Lincoln, UK.
2. Filtron Technology Corporation (1999) Microsep Microconcentrators, operating instructions. Northborough, MA.
3. Schleicher & Schuell (1999) Centrex UF Centrifugal Ultrafilters, operating instructions. Keene, NH.

Detection of Genetic Point Mutations by Peptide Nucleic Acid-Mediated Polymerase Chain Reaction Clamping Using Paraffin-Embedded Specimens

Yvonne Myal^{*†}, Anne Blanchard,^{*†}
Peter Watson,^{*†} Michael Corrin,^{*} Robert Shiu,[†]
and Barbara Iwaszow[†]

^{*}Department of Pathology and [†]Department of Physiology,
Faculty of Medicine, University of Manitoba, 770
Bannatyne Avenue, Winnipeg, Manitoba, R3E 0W3 Canada

Received March 20, 2000

Peptide nucleic acid (PNA)²-mediated PCR clamping is a sensitive molecular assay (1) that can detect protooncogene point mutations in patient-derived tissue samples (1, 2). However, to date, PNA-mediated PCR clamping has only been demonstrated on fresh and frozen tissue. In this study, we demonstrate that PNA-mediated PCR clamping can be successfully used to detect point mutations in DNA derived from Formalin-fixed, paraffin-embedded (ffpe) samples, with no loss in sensitivity.

The PNA molecule is a sequence-specific synthetic oligomer that consists of repeating units of (2-aminoethyl)-glycine linked by amide bonds (2). Because of its unique structure, PNA can mimic DNA but cannot serve as a primer molecule during PCR amplification. The PNA molecule binds tightly to the target sequence and blocks amplification only if the two sequences are fully complementary. Thus, because the PNA is made complementary to the wild-type sequence, only the mutant allele is amplified during the PCR reaction.

Because of the frequency of oncogenic point mutations in many human tumors, PNA-mediated PCR clamping is potentially useful to the surgical pathologist as a means of detecting isolated cancer cells amid a population of normal cells (minimal residual disease, MRD). Currently, standard pathologic procedures usually involve the processing of the primary surgical specimen in Formalin followed by embedding in paraffin blocks to allow accurate assessment of tumor and resection margins. Thus, it would be desirable to determine whether PNA-mediated PCR clamping could be applied to ffpe samples. Also, it should be noted that although existing methods such as immunohistochemistry, denaturing gel electrophoresis, or PCR followed by single-stranded conformational polymorphism have

[†] To whom correspondence should be addressed. Fax: (204) 789-3931. E-mail: myal@ms.umanitoba.ca.

² Abbreviations used: PNA, peptide nucleic acid; ffpe, Formalin-fixed, paraffin-embedded; MRD, minimal residual disease.

TABLE 1
Primer Design

Wild type p53 sequence (MCF7)	5' ... CCTCAGCATCTTATCCGAGTGG ... 3'
PNA (15mer)	5' CCTCAGCATCTTATC 3'
Mutant p53 sequence (T47D)	5' ... CCTCAGCATTTTATCCGAGTGG ... 3'
Mutant forward primer (22mer)	5' CCTCAGCATTTTATCCGAGTGG 3'
Reverse primer	5' TTGCAAACCAGACCTCAG 3'

Note. The sequences of the PNA oligomer, the mutant forward primer and the reverse primer are shown. In the T47D human breast cancer cells, the mutant p53 allele contains a T (in bold) instead of a C (also shown in bold) which occurs in the wild-type allele.

been used to detect MRD from ffpe samples, these assays are sometimes unsuccessful either because they are not sensitive enough, resulting in many false negatives or false positives (3–5), or because they require fresh or frozen tissue for efficient PCR. Furthermore, confirmation of the results often requires labor-intensive DNA sequencing protocols. The use of PNA-mediated PCR clamping could address all these limitations.

In testing this application, we developed an *in vitro* assay using serial dilutions of two human breast cancer cell lines, T47D (which carries a p53 gene point mutation at codon 194) and MCF7 (which carries the wild-type gene). The p53 tumor suppressor gene was used as a molecular marker for this study because mutations in this gene constitute the most common genetic change in human cancers. Serial dilutions were generated by mixing the MCF7 cells with increasing numbers of T47D cells. A total of 1×10^7 cells were used for each sample point. Cells were collected in 15-ml tubes and spun at 800 rpm for 5 min. The supernatant was removed and replaced by 1 ml of 4% paraformaldehyde, and the cells quickly dispersed in the fixative. Following a 2-h incubation, the fixed cells were again spun at 800 rpm for 5 min to remove the paraformaldehyde. Two milliliters of molten agar (3%, 43°C) was added to the cell pellets and the mixture was poured into molds (24-well dishes). After 30 min (enough time to allow the agar to set), the molds were placed in embedding cassettes, processed with fixatives [by standard procedures (6)], and followed by infiltration with paraffin. Next, the paraffin blocks were sectioned and used for DNA extraction. For each sample, DNA was extracted from one 5- μ m paraffin section in a final volume of 500 μ l, according to the method of Smith *et al.* (7). For PNA-mediated PCR amplification, 8 μ l of the DNA extract was used per reaction. Although this amount of DNA was too small to measure accurately in all samples, it was the minimum amount of DNA that consistently resulted in a visible PCR product.

The PCR reaction was performed in a total of 50 μ l containing 200 μ M each of deoxynucleoside triphosphates, 50 mM KCl, 1.5 mM MgCl₂, 10 mM Tris-HCl (pH 8.3), 0.2 μ M mutant forward primer and reverse primer (Table 1), 2.5 U *Taq* polymerase (Gibco, BRL),

and 4–5 μ M of PNA primer (Table 1). T_m was an important consideration in primer design. We selected a PNA sequence that had a sufficiently higher T_m than the mutant primer to ensure that the PNA molecule had ample opportunity to anneal to the DNA template. DNA primer PCR amplification consisted of an initial denaturation step of 94°C/5 min, followed by 26 cycles (40 cycles for paraffin-extracted DNA) of 94°C/1 min, 70°C/1 min, 57°C/1 min, and 72°C/1 min, plus an additional final extension cycle at 94°C/1 min and 60°C/10 min. The expected amplified product size was 115 bp.

Figure 1 shows that in the absence of PNA both the mutant and wild-type alleles were amplified. However, in the presence of PNA, only the mutant allele (T47D) was amplified. Amplification of the wild-type p53 allele (in MCF7) was completely inhibited, ruling out the amplification of false positives. Thus, the PNA inhibition of the wild-type p53 gene was indeed allele specific. Higher concentrations of the PNA molecule were no more effective in inhibiting the wild-type allele (data not shown). To rule out nonspecific binding and nonspecific inhibition by the PNA molecule, a 428-bp fragment of the human prolactin-inducible protein (*hPIP*) gene (8) was amplified in the presence and

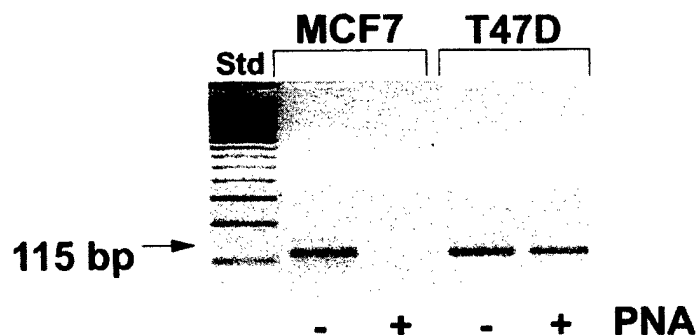


FIG. 1. Inhibition of the wild-type but not the mutant p53 allele by PNA. In the presence of PNA (4 μ M), the amplification of the wild-type p53 allele (MCF7 DNA) is inhibited, but the mutant p53 allele (T47D) is not. Samples were usually carried out in triplicates (not shown here). Experiments were also carried out in triplicates. Thirty microliters of each reaction was electrophoresed on a 3% agarose gel and stained with ethidium bromide. The expected amplified 115-bp product is shown.

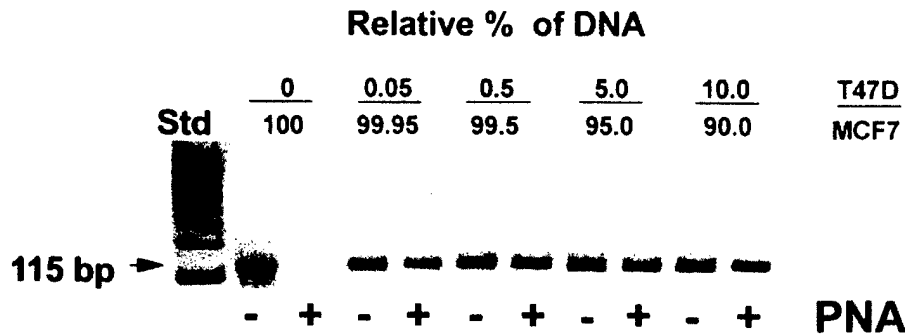


FIG. 2. PNA-mediated PCR clamping of paraffin-embedded cells demonstrates high sensitivity. Cell pellets were fixed (as described in the text) and embedded in paraffin. The percentage of mutant (T47D) alleles to wild type (MCF7) is shown. The total number of cells for each sample was the same but the ratio of T47D to MCF7 cells decreased from right to left. DNA was extracted and PNA-mediated PCR clamping was carried out as described in the text. Thirty microliters of the reaction was electrophoresed on a 3% agarose gel. Suppression of the wild-type alleles by PNA (5 μ M) allowed the detection of 0.05% (the lowest limit tested) or 1 mutant allele in a background of 2000 normal alleles.

absence of the PNA molecule (not shown). The PNA failed to inhibit amplification of the *hPIP* control gene, demonstrating that the PNA molecule was gene specific. When PNA-mediated PCR clamping was carried out on DNA isolated from Formalin-fixed paraffin-embedded cells, suppression of the wild-type p53 allele by the PNA molecule allowed us to detect as little as 0.05% mutant alleles in the sample (Fig. 2). The level of sensitivity for this assay achieved by us (1 mutant allele in 2000-fold excess wild-type alleles) using ffpe samples was higher than that reported earlier (1, 2) using fresh or frozen tissue (1 mutant allele in a 200-fold excess of wild type). The reason for this improved sensitivity is not clear but may reflect the purity of the DNA samples. In addition, the sensitivity of this assay could be further enhanced by Southern blot analysis. However, this strategy was omitted because we wanted to develop a nonradioactive and yet sensitive assay that was rapid, practical, and convenient for a clinical laboratory setting.

In summary, we have shown that PNA-mediated PCR clamping can be performed on DNA from samples that have been embedded in paraffin; and that it is specific and sensitive. We have demonstrated a 10-fold increase in sensitivity over that reported earlier for fresh or frozen tissue (1, 2). Our results and those of others (1, 2) also suggest that this assay could be potentially useful for MRD detection, particularly for the screening of "hot spot" oncogenic lesions in histological samples. Improved methods of detection of MRD are clinically important for accurate disease staging of cancer patients (9) and for appropriate therapeutic management. Since the average length of a PNA molecule is 15 bases, theoretically, one PNA molecule could be used to detect 15 point mutations in a single gene. Used in conjunction with current light microscopy techniques, this assay could enhance our ability to more accurately stage cancer, since oncogenic point

mutations are associated with poor prognosis for some human cancers (10). The main advantage of this approach is that paraffin-derived samples are convenient, require minimal amounts of tissue, and retrospective studies can be carried out on archival material. Finally, ffpe tissues also represent an easily accessible source of specimens, whereas fresh or frozen tissues are sometimes difficult to obtain.

Acknowledgments. This study was supported by a grant from the Health Sciences Centre Research Foundation, Winnipeg, Manitoba (to Y.M.). P.W. is an MRC Clinician Scientist. M.C. is a Government of Canada Summer Placement Career awardee. The authors thank Sandy Troup and Aihua Huang for their assistance in preparing the histological samples. We also thank Dr. Terry Zelinsky and Ms. Molly Pind for reading the manuscript.

REFERENCES

- Thiede, C., Bayerdorffer, E., Blasczyk, R., Wittig, B., and Neubauer A. (1996) Simple and sensitive detection of mutations in the ras proto-oncogenes using PNA-mediated PCR clamping. *Nucleic Acids Res.* **24**, 983-984.
- Behn, M., and Schuermann, M. (1998) Sensitive detection of p53 gene mutations by a 'mutant enriched' PCR-SSCP technique. *Nucleic Acids Res.* **26**, 1356-1358.
- Fisher, C. J., Gillett, C. E., Vojtesek, B., Barnes, D. M., and Millis, R. R. (1994) Problems with p53 immunohistochemical staining: the effect of fixation and variation in the methods of evaluation. *Br. J. Cancer* **69**, 26-31.
- Soong, R., Robbins, P. D., Dix, B. R., Griew, F., Lim, B., Knowles, S., Williams, K. E., Turbett, G. R., House, A. K., and Iacopetta, B. J. (1996) Concordance between p53 protein overexpression and gene mutation in a large series of common human carcinomas. *Hum. Pathol.* **27**, 1050-1055.
- Wynford-Thomas, D. (1992) p53 in tumour pathology: can we trust immunocytochemistry? *Pathology* **166**, 329-330.
- Humanson, G. L. (1967) *Animal Tissue Techniques*, 2nd ed. Freeman, San Francisco.
- Smith, S. A., Easton, D. F., Evans, D. G., and Ponder, B. A. (1992) Allele losses in the region 17q12-21 in familial breast and ovarian cancer involve the wild-type chromosome. *Nat. Genet.* **2**, 128-131.

8. Myal, Y., Robinson, D. B., Iwaszow, B., Tsuyuki, D., Wong, P., and Shiu, R. P. (1991) The prolactin-inducible protein (PIP/GCDFP-15) gene: cloning, structure and regulation. *Mol. Cell Endocrinol.* **80**, 165–175.
9. Sidransky, D., Tokino, T., Helzlsouer, K., Zehnbauser, B., Rausch, G., Shelton, B., Prestigiacomo, L., Vogelstein, B., and Davidson, N. (1992) Inherited p53 gene mutations in breast cancer. *Cancer Res.* **52**, 2984–2986.
10. Brennan, J. A., Mao, L., Hruban, R. H., Boyle, J. O., Eby, Y. J., Koch, W. M., Goodman, S. N., and Sidransky, D. (1995) Molecular assessment of histopathological staging in squamous-cell carcinoma of the head and neck. *N. Engl. J. Med.* **332**, 429–435.

Pharmacokinetic Study and Determination of Imperialine, the Major Bioactive Component in Antitussive *Fritillaria cirrhosa*, in Rat by High-Performance Liquid Chromatography Coupled with Evaporative Light-Scattering Detector

Shun-Wan Chan,* Song-Lin Li,*† Ge Lin,*¹ and Ping Li†

*Department of Pharmacology, Faculty of Medicine, Chinese University of Hong Kong, Shatin, N.T., Hong Kong, SAR, China; and †Department of Pharmacognosy, China Pharmaceutical University, Nanjing, People's Republic of China

Received April 6, 2000

Imperialine (Fig. 1) is the major biologically active isosteroidal alkaloid present in the most commonly used antitussive traditional Chinese medicinal herb, *Bulbus Fritillaria*. It has been identified from several species in genus *Fritillaria*, including *Fritillaria cirrhosa*, the primary plant source for this herbal medicine (1–5). The antitussive effect of imperialine and the crude *fritillaria* alkaloid extracts of various *Fritillaria* spp. has been extensively studied in both *in vitro* and *in vivo* models, and imperialine has been demonstrated to be the most potent *fritillaria* alkaloids (6). However, to date there are no reports on the pharmacokinetic data of imperialine and other *fritillaria* alkaloids. Imposed by the low sensitivity of the chromophore in *fritillaria* alkaloid, a direct HPLC analysis with ultraviolet or fluorescence detection of this type alkaloid is very difficult (7). Consequently, the reported HPLC–UV assay with precolumn derivatization requires extensive sample preparations, and restricted and well-controlled chemical reactions (8). Therefore, the

present study attempts to develop a direct HPLC analytical method for the analysis of imperialine in blood samples by using evaporative light scattering detector (ELSD),² a universal mass detector that responds to all eluates regardless of their structure and/or chromophore (9, 10). Moreover, the pharmacokinetic profiles of imperialine in rats via intravenous and oral administrative routes were investigated by using the developed HPLC–ELSD analytic method.

Materials and methods. Imperialine was isolated from *F. cirrhosa*. The purity and identity were determined by TLC, HPLC, NMR, and MS analyses. Solanidine was purchased from Sigma Chemical Co. (St. Louis, MO). HPLC-grade solvents were obtained from Labscan Asia Co. (Bangkok, Thailand). HPLC analysis was performed on an HP1100 (Hewlett-Packard) system equipped with an Alltech 500 ELSD (Alltech Associates Inc., Deerfield, IL). A Supelco reversed-phase C₈ analytical column (150 × 4.6 mm, i.d., 3 μ) coupled with a C₈ guard column (20 × 4.0 mm, 5 μ) was utilized with a gradient elution at flow rate of 1 ml/min and column temperature of 28°C. The mobile phase consisted of distilled water (A), acetonitrile (B), and methanol containing 0.6% triethylamine (C) was eluted as follows: 0–6 min A:B:C = 7:35:58; 6–7 min linear increase to A:B:C = 0:42:58 and maintained for 25 min, 25–30 min for returning to the initial conditions. The nitrogen gas flow of 2.22 standard liters per minute and drift tube temperature of 72°C were set for ELSD.

Male Sprague–Dawley rats (180–220 g) supplied by the Laboratory Animal Services Centre at the Chinese University of Hong Kong were fed on a standard laboratory diet with free access to water under the controlled temperature at 20–22°C and relative humidity of 50% with 12-h light/dark cycles prior to the study. Rats were surgically cannulated with polyethylene catheters on the right jugular veins under anesthesia with diethyl ether vapor. The animals recovered in individual metabolic cages and fasted but were allowed to have free access to water overnight. Two groups of conscious cannulated rats with at least five in each group were dosed with the HCl salt of imperialine intravenously (20 mg/kg) and orally (100 mg/kg), respectively. Serial venous blood samples (0.25 ml) were collected from the right jugular vein via the cannulated catheter into heparinized tubes at suitable time intervals up to 360 min after dose. At each blood sampling, an equivalent volume of heparinized normal saline (25% v/v, 0.25 ml) was injected into the animals to maintain a constant blood volume.

¹ To whom correspondence should be addressed. Fax: 852-2603-5139. E-mail: linge@cuhk.edu.hk.

² Abbreviation used: ELSD, evaporative light scattering detector.

Original Paper

Lumican and decorin are differentially expressed in human breast carcinoma

Etienne Leygue¹, Linda Snell², Helmut Dotzlaw¹, Sandra Troup², Tamara Hiller-Hitchcock², Leigh C. Murphy¹, Peter J. Roughley³ and Peter H. Watson^{2*}

¹ Department of Biochemistry and Molecular Biology, University of Manitoba, Faculty of Medicine, Winnipeg, Manitoba, Canada, R3E 0W3

² Department of Pathology, University of Manitoba, Faculty of Medicine, Winnipeg, Manitoba, Canada, R3E 0W3

³ Genetics Unit, Shriners Hospital for Children, Montreal, Quebec, Canada, H3G 1A6

*Correspondence to:

Dr P. H. Watson, Department of Pathology, D212-770 Bannatyne Ave, University of Manitoba, Winnipeg, Manitoba R3E 0W3, Canada.

E-mail:

pwatson@cc.umanitoba.ca

Abstract

Previous studies have shown that lumican is expressed and increased in the stroma of breast tumours. Lumican expression has now been examined relative to other members of the small leucine-rich proteoglycan gene family in normal and neoplastic breast tissues, to begin to determine its role in breast tumour progression. Western blot study showed that lumican protein is highly abundant relative to decorin, while biglycan and fibromodulin are only detected occasionally in breast tissues ($n=15$ cases). Further analysis of lumican and decorin expression performed in matched normal and tumour tissues by *in situ* hybridization showed that both mRNAs were expressed by similar fibroblast-like cells adjacent to epithelium. However, lumican mRNA expression was significantly increased in tumours ($n=34$, $p<0.0001$), while decorin mRNA was decreased ($p=0.0002$) in neoplastic relative to adjacent normal stroma. This was accompanied by a significant increase in lumican protein ($n=12$, $p=0.0122$), but not decorin. Further evidence of altered lumican expression in breast cancer was manifested by discordance between lumican mRNA and protein localization in some regions of tumours but not in adjacent morphologically normal tissues. It is concluded that lumican is the most abundant of these proteoglycans in breast tumours and that lumican and decorin are inversely regulated in association with breast tumourigenesis. Copyright © 2000 John Wiley & Sons, Ltd.

Keywords: lumican; decorin; small leucine-rich proteoglycan; breast cancer; tumour progression

Received: 22 June 1999

Revised: 1 February 2000

Accepted: 17 April 2000

Introduction

The development and progression of breast carcinoma are caused by alterations in the expression of multiple genes, most of which are responsible for normal physiological pathways and the necessary cellular interactions to support these functions within the mammary gland. These include alterations in the interactions between the epithelial and stromal cells, which are manifested in tumours by well-recognized morphological changes known as the stromal reaction [1]. Such alterations in stromal-epithelial interactions may influence the risk of transformation of the breast epithelial cell and may contribute to the very early steps in tumourigenesis, as has recently been proposed in other systems [2]. However, the net effect of these alterations in the stroma on the later stages of tumour progression is unresolved [3].

Resolution of this issue is complicated by the recognition that the stroma is a highly complex tissue that includes a variety of different types of fibroblasts [4] and a range of proteins, glycoproteins, and proteoglycans which may play a role in tumour biology. We have recently extended this list by identifying lumican, a member of the small leucine-rich proteoglycans (SLRPs) as an mRNA that is expressed in the stroma of normal breast tissues and

is overexpressed in invasive carcinomas [5]. Members of this family of proteoglycans have been implicated principally in matrix assembly and structure [6], but also more recently in the control of cell growth [7]. While studies of decorin have shown altered expression in neoplastic stroma [3], lumican has previously been studied only in the context of connective tissue and corneal disease [8,9], and the role of SLRPs in human breast cancer is relatively unexplored. To explore further the potential role of lumican and related genes in breast tumour progression, we have now examined the expression of lumican relative to that of other members of the SLRP family, decorin, biglycan and fibromodulin, at both mRNA and protein level, in normal and neoplastic breast tissues.

Materials and methods

Human breast tissues

All breast tumour cases used for this study were selected from the NCIC-Manitoba Breast Tumor Bank (Winnipeg, Manitoba, Canada). As has been previously described [10], tissues are accrued to the bank from cases at multiple centres within Manitoba, rapidly collected, and processed to create matched formalin-fixed, paraffin-embedded, and frozen tissue

blocks with the mirror image surfaces orientated by coloured inks. The histology and cellular composition of every sample in the bank are interpreted in haematoxylin and eosin (H&E)-stained sections from the face of the former tissue block.

For the initial study to compare broadly the expression of different members of the SLRP gene family, a mixed pilot cohort was selected from the Tumor Bank to include nine different invasive carcinomas, three normal tissue samples from patients with cancer, and three normal tissues from normal patients without cancer. The invasive tumours included different tumour types (five ductal, three lobular, and one tubular carcinoma), grades (four high, one moderate, four low Nottingham grades), and oestrogen receptor (ER) levels (three ER < 10 fmol/mg, three ER 10–20, three ER 39–169), and total stromal fractions ranging from 50 to 95% of the cross-sectional area. The mean patient ages were 62, 70, and 28 years for each subgroup, respectively (tumour tissues, normal tissues adjacent to tumours, and normal tissues).

For the subsequent studies to compare lumican and decorin expression, a second more defined and homogeneous cohort of 46 cases was selected to provide matching primary tumour tissues and adjacent normal tissue. This cohort included only invasive ductal carcinomas and was primarily selected to ensure availability of histologically confirmed and distinct regions comprising morphologically normal and tumour tissue elements in different blocks (12 cases, for western blot studies) or the same block (34 cases, for *in situ* hybridization studies). The subset used for western blot studies was also selected to possess equivalent cross-sectional areas [mean section area^(SD) in tumour tissues = $0.86^{(0.44)}$ cm², adjacent normal tissues = $0.85^{(0.35)}$ cm²] and stromal content [mean stromal area^(SD) in tumour tissues = 68⁽¹⁰⁾%, adjacent normal tissues = 89⁽⁶⁾%] between the matching blocks and to incorporate cancer cases from both post-menopausal (six cases mean^(SD) = 76⁽⁷⁾ years) and pre-menopausal patients (six cases mean^(SD) = 44⁽³⁾ years).

Sodium dodecyl sulphate/polyacrylamide gel electrophoresis (SDS/PAGE) and immunoblotting

Total proteins were extracted from frozen tissue sections. These were cut from the face of frozen tissue blocks immediately adjacent to the face of a matching paraffin block [11] from which paraffin sections had been previously cut for pathological assessment and for *in situ* hybridization. For the first cohort of cases, an average of 20 20 µm tissue sections were cut from each typical tissue block (0.5 × 1.0 cm² cross-sectional area) and used for extraction; however, the number of tissue sections was varied for each case according to the measured area of the tissue within individual blocks, to ensure that equivalent volumes of tissue were used for the extraction, which was done as described previously [12]. For the second cohort of matching tissue samples, the same number of frozen sections (20 × 20 µm) was cut from the measured

surface of each tissue block together with a single section from the adjacent paraffin block. This was used as a reference for composition and protein extraction was then performed on the frozen sections with equivalent volumes of extraction buffer. Proteins present in equivalent volumes of extracts were analysed by SDS/PAGE and immunoblotting, using anti-peptide antibodies specific for the carboxyl-terminal regions of the core proteins of lumican, decorin, fibromodulin, and biglycan [12–14]. The specificity of all antibodies was verified by peptide absorption and SLRP cross-reactivity analysis. Protein signals were detected by chemiluminescence and photographed prior to quantitation by video-image analysis and densitometry using an MCID M4 system and software (Imaging Research, St Catherines, Ontario, Canada). All signals were then adjusted with reference to control cartilage samples run with each blot. For the second cohort of matched tissue samples, signals were also adjusted with reference to the measured cross-sectional area and the stromal content of the tissue block to control for equivalent loading. Additional analysis was performed on all signals after further adjustment for relative stromal content of the tissue sections assessed in adjacent H&E sections.

Immunohistochemistry

Immunohistochemistry was performed on paraffin sections using the same antibody to lumican as used for immunoblotting [9,12]. Sections (5 µm thick) were obtained from paraffin-embedded tissue blocks matching the frozen tissue blocks of those cases used for reverse transcription-polymerase chain (RT-PCR) and protein analysis. After deparaffinizing, clearing, and hydrating in TBS buffer (Tris buffered saline, pH 7.6) the sections were pretreated with 3% hydrogen peroxide for 10 min to remove endogenous peroxidases and non-specific binding was blocked with normal swine serum, 1:10 (Vector Laboratories S-4000). TBS was used between steps to rinse and as a diluent. Primary antibody to lumican was applied at a 1:400 dilution overnight at 4°C, followed by biotinylated secondary swine anti-rabbit IgG, 1:200 (DAKO) for 1 h at room temperature. Tissue sections were incubated 45 min at room temperature with an avidin/biotin horseradish peroxidase system (Vectastain ABC Elite, Vector Lab.) followed by detection with DAB (diaminobenzidine), counterstaining with 2% methyl green, and mounting. A positive tissue control (colonic mucosa) and a negative reagent control (no primary antibody) were run in parallel. Immunostaining patterns and intensity were assessed by light microscopic visualization.

In situ hybridization

Paraffin-embedded 5 µm sections of breast tissues were analysed by *in situ* hybridization according to a previously described protocol [5]. For lumican, the plasmid Lumi-398, which consisted of pGEM-T plasmid (Pharmacia Biotech), containing a 398 bp portion of

lumican cDNA between bases 1332 and 1729, was used as a template to generate UTP^{35S} labelled sense and antisense riboprobes using Riboprobe Systems (Promega, Madison, WI, USA) and either the T7 or SP6 promotor at the 5' or 3' end of the lumican sequence according to the manufacturer's instructions. For decorin, the plasmid Dec-322 was used as a template. This consisted of pGEM-T plasmid containing a decorin insert with a comparable length (322 bp) to the lumican probe generated by PCR amplification from the decorin cDNA [12] using primers that corresponded to decorin (sense 5'-AAATGCCCAAACTCTTCAG-3' and antisense 5'-AAACTCAATCCCACTTAGCC-3') [15]. All PCR cDNAs and plasmid inserts were sequenced to confirm their identity. Levels of lumican and decorin expression were assessed in normal and tumour regions by microscopic examination at low magnification and with reference to the negative sense and positive control tumour sections. This was done as previously described [5] by scoring the estimated average signal intensity (on a scale of 0–3) and the proportion of stromal cells showing a positive signal (0, none; 0.1, less than one-tenth; 0.5, less than one-half; 1.0, greater than one-half). The intensity and proportion scores were then multiplied to give an overall score. Regions with a score lower than 1.0 were deemed negative or weakly positive.

Microdissection and protein extraction analysis

To assess protein localization within regions of tumours, two cases were selected that showed marked and well-defined regions within the same tissue section with discrepancies between mRNA and protein expression. This was determined by *in situ* hybridization and immunohistochemistry in adjacent serial sections from paraffin tissue blocks. The mirror image frozen tissue blocks to these paraffin blocks were used for microdissection as previously described [11] and protein was extracted from these histologically defined regions as described above. Briefly, thin 5 µm frozen sections were cut from the faces of the frozen tissue blocks and stained by H&E, and the relevant histological regions of approximately 1–2 mm² distinguished and confirmed by reference to the paraffin sections already studied. Multiple thick frozen sections (20 × 20 µm) were then cut, rapidly stained, and microdissected at room temperature from each section in turn, and the microdissected tissue fragments were frozen again prior to protein extraction.

Results

Identification of lumican as the most abundant SLRP in normal and neoplastic breast tissues

To determine the relative importance of altered lumican expression in breast tumourigenesis, the expression of lumican protein was compared with that of three other members of the SLRP family, decorin, fibromodulin and biglycan, by western blot in a heterogeneous panel of nine breast tumours and six normal tissues.

Lumican was highly abundant in all samples and in both neoplastic and normal tissues (Figure 1). A significant increase was seen in the mean level of lumican protein between normal and tumour [mean^(SD) tissue adjusted optical density units, normal = 0.43^(0.08), tumour = 0.56^(0.15), $p = 0.026$, Mann–Whitney test]. Although an apparent difference in the level of lumican between normal samples from normal patients and normal samples adjacent to tumours was seen, this difference did not persist when the different stromal content of these samples was taken into account. Similarly, there was no difference in the levels in tumour tissues on comparing pre- and post-menopausal patients. Nevertheless, an increase in the overall molecular weight and polydiversity was noted between normal tissues and morphologically normal tissue adjacent to tumours, which might be attributable to either different age or association with tumour in the adjacent breast.

In comparison, decorin, although also present in most samples examined by western blot, was much less abundant relative to the cartilage control (Figure 1). It should be noted that the decorin (in common with biglycan and fibromodulin) signals shown in Figure 1 also required a three-fold longer chemiluminescent exposure time (9 s) than that for lumican (3 s). How-

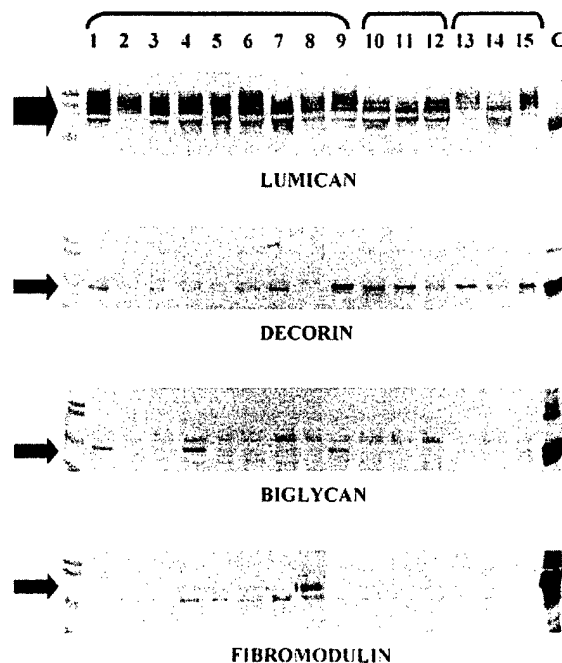


Figure 1. Immunoblotting study of lumican, decorin, biglycan, and fibromodulin protein expression in human breast tumours (lanes 1–9); normal tissues from normal patients (lanes 10–12); and normal tissues adjacent to carcinomas (lanes 13–15). All protein samples were extracted from sets of frozen tissue sections bracketed by sections assessed by H&E stain and light microscopy to confirm content. Chemiluminescent signals for decorin, biglycan, and fibromodulin required three-fold longer exposure times than that for lumican. Molecular markers (left) and cartilage control sample (right) are present in all panels

ever, in contrast to lumican, there was a marked decrease in decorin between normal and tumour samples [mean^(SD) optical density units; normal = 0.21^(0.06), tumour = 0.13^(0.14), $p = 0.066$, Mann-Whitney test]. No difference was seen in the signals between normal samples from normal and cancer patients.

Fibromodulin expression was not detected in normal tissues and at only low levels in 3/9 tumours, where the presence of fibromodulin correlated with those tumours with the highest content of epithelial tumour cells. Biglycan was also only detected at low levels in 2/6 normal tissues and 3/9 tumours, where in contrast to fibromodulin, its presence correlated directly with those tumours with the highest content of collagenous stroma.

Lumican and decorin are differentially expressed between normal and neoplastic tissues

In order to examine further the distinct alterations in the expression of lumican and decorin, the mRNA and protein expression of both genes was examined in 46 cases by *in situ* hybridization (34 cases) and western blot (12 cases) from the second cohort of cases, comprising matched normal and tumour samples.

As previously shown, prominent lumican mRNA expression was detected, using an antisense probe, in stromal fibroblast-like cells within the tumour and immediately adjacent to invasive tumour cells. Assessment of mRNA levels using a semi-quantitative approach, as detailed in the Materials and methods section, also confirmed our previous observations [5] made on a different set of tumours, and lumican mRNA was found to be significantly elevated in the majority of tumours when levels were compared with those present in adjacent normal stroma ($p < 0.0001$, Wilcoxon test, Figures 2 and 3B). Higher levels of lumican (≥ 1) were present in tumour than in normal tissue in 26/34 cases. At the same time, decorin levels also showed a consistent and significant difference, with lower levels seen in stroma associated with tumour, relative to stroma associated with adjacent normal tissue components ($p < 0.0002$, Wilcoxon test,

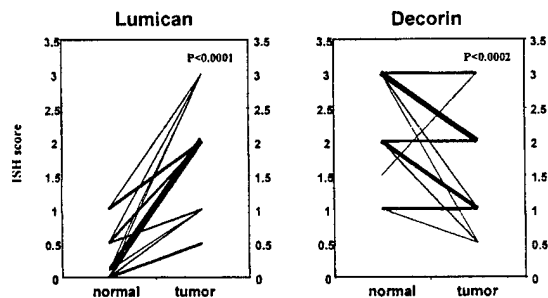


Figure 2. Lumican and decorin mRNA levels in matched normal and tumour tissues, assessed by *in situ* hybridization and semi-quantitative scoring as described in the Materials and methods section. The thickness of each line (on a scale of 1–9) corresponds to the number of cases showing the same differences in scores ($n = 34$ cases)

Figures 2 and 3C), with lower levels of decorin (≥ 1) present in tumour than in normal tissue in 22/34 cases. The pattern of expression of decorin was also identical in sections from the same cases studied with a different *in situ* hybridization riboprobe (data not shown). Although we have previously noted a relationship between lumican and poor prognostic factors, these associations were not found in the present series.

In keeping with the pattern of mRNA expression, the mean lumican protein signal assessed by western blot was also higher in 9/12 tumours relative to normal tissues [mean^(SD) optical density units, normal = 0.22^(0.15), tumour = 0.43^(0.19), $p = 0.0122$ Wilcoxon test]. Once again, in contrast to this, decorin

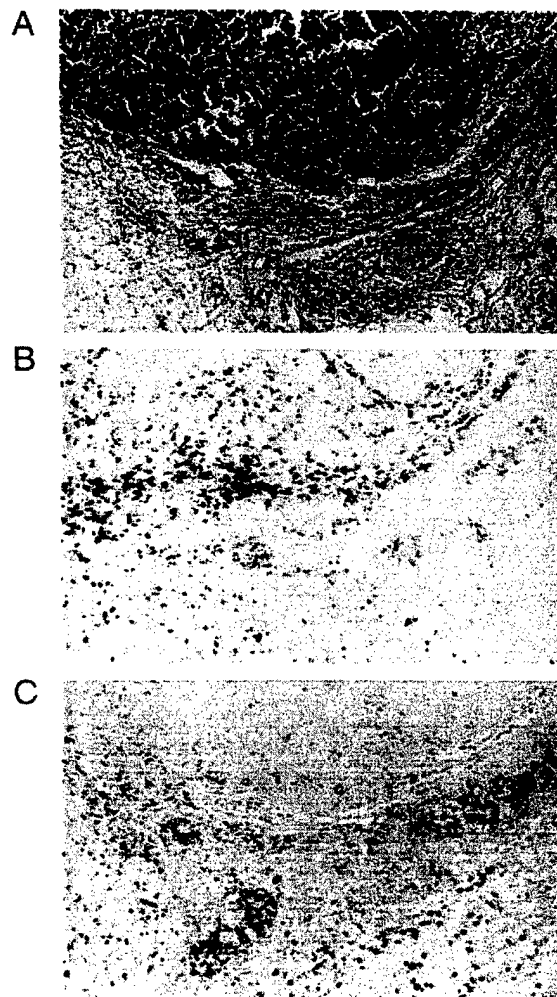


Figure 3. Lumican and decorin mRNA expression detected by *in situ* hybridization within a breast tumour section. Panel A (H&E section) shows the histology including the invasive tumour (upper area), the tumour margin (middle), and adjacent normal tissue including lobular-ductal units (lower area). Lumican expression (B) is high within the tumour and tumour margin and lower in the normal fat and collagenous stroma adjacent to the normal lobules. Decorin (C) shows high expression in the normal stroma adjacent to normal lobules and reduced expression in the tumour. $\times 340$

protein was lower in 7/12 tumours relative to normal tissues, but in this case the differences were not statistically significant [mean^(SD) optical density units, normal = 0.22^(0.19), tumour = 0.17^(0.2), $p = \text{ns}$ (not significant), Wilcoxon test]. These contrasting patterns of lumican and decorin expression also persisted after standardization of western blot signals for relative stromal content (data not shown).

Lumican mRNA and protein expression can occur in different regions within breast tumours

Immunohistochemical study of the lumican distribution within the same tissues that had already been examined by *in situ* hybridization was performed using the same antibody [9,12] that had been employed for western blot analysis (Figure 4). This showed that lumican was abundant throughout the collagenous stroma of both normal and tumour sections, with prominent deposition around small vessels, breast duct, and lobular structures. There was increased deposition within the collagenous stroma of tumours, in particular at the invasive margins and in areas of dense collagen within central regions of some tumours, compared with adjacent normal tissues. However, in some cases there were distinct regions, up to 2 mm in area within the tumour sections, containing loose stroma in which there was a complete absence of lumican detectable by immunohistochemistry (Figures 4C and 4D); but the same regions showed high expression when examined for lumican mRNA by *in situ* hybridization in adjacent sections (Figures 4A and 4B). Similarly, other areas showed strong staining for lumican protein, but low levels of mRNA.

To explore the possibility that the absence of lumican expression detected by immunohistochemistry might be due to the conformation of the native protein or the binding of lumican to other proteins, resulting in the masking of the carboxy-terminal epitope, specific areas measuring approximately 1 mm² each were microdissected from frozen sections of two tumours and lumican protein was assessed under denaturing conditions by SDS/PAGE and western blot. In both cases, those regions with high mRNA expression and negative by immunohistochemistry were also negative by western blot, while areas showing very low mRNA expression but strong staining by immunohistochemistry were positive by western blot (Figure 5).

Discussion

We have shown that lumican is the most abundant proteoglycan in comparison with several other members of the family of small leucine-rich proteoglycans (SLRPs) in breast cancer. We have also extended our previous observations [5], based on the detection of lumican mRNA, in showing that the total lumican protein is also increased in breast tumours relative to adjacent normal tissues. Our results also demonstrate that this pattern of up-regulation of lumican in relation

to breast tumourigenesis is distinct from that of the closely related decorin gene, which is inversely regulated and reduced at mRNA and to a lesser extent at protein levels, in tumour relative to adjacent normal tissue. Finally, we have shown that lumican expression in tumours may also be associated with an abnormal distribution within the stroma, manifested by discordance between mRNA and protein deposition within subregions of breast tumours.

The family of SLRPs share several common features, including a central region of leucine-rich repeats bounded by flanking cysteine residues, and localization in the extracellular matrix. The SLRPs can be separated into three subgroups that include decorin and biglycan, lumican and fibromodulin, and epiphygan and osteoglycin, which are distinguishable by amino acid homologies and also by gene structure [16]. Decorin, probably the best studied of these genes, is known to interact with a variety of extracellular matrix molecules and has been shown to be capable of influencing collagen fibril growth and assembly both *in vitro* and *in vivo* [6,7]. Decorin may also influence tumour cell growth through indirect effects on the availability of growth factors from the extracellular matrix, or directly through activation of the EGF receptor and induction of the p21 cell-cycle inhibitor [18]. In contrast, less is known about lumican and other SLRPs. However, *in vitro* and *in vivo* data indicate that lumican is also important in the regulation of collagen fibril assembly [19]. This view is supported by recent observations based on mice with homozygous deletion of the lumican gene, where loss of corneal transparency and increased skin fragility are associated with disorganized and loosely packed collagen fibres related to increased and irregular fibril size, and interfibrillar spacing, as viewed by light and electron microscopy [8].

The observation that lumican is highly abundant compared with other SLRPs in breast tumours cannot be interpreted to mean that it is necessarily the most important. This is underscored by the recent demonstration that although decorin is apparently more abundant than versican in prostate cancer tissue, only an increase in the larger chondroitin sulphate proteoglycan versican correlates with grade, and inversely with progression-free survival, in prostate cancer [20]. Similarly, the increase in lumican as seen here in association with breast tumourigenesis may be less important than the parallel decrease in decorin. It should also be noted that while the present study was focused primarily on examining the relative expression of SLRPs between matched normal and tumour tissues and was not necessarily designed to compare levels between cases, we did not observe any significant relationship between lumican or decorin and prognostic factors within this tumour cohort, as previously noted [5]. While this leaves open the question of a role for these SLRPs in later tumour progression, the implication of altered expression for the earlier stages of tumourigenesis remains intriguing. It is possible to

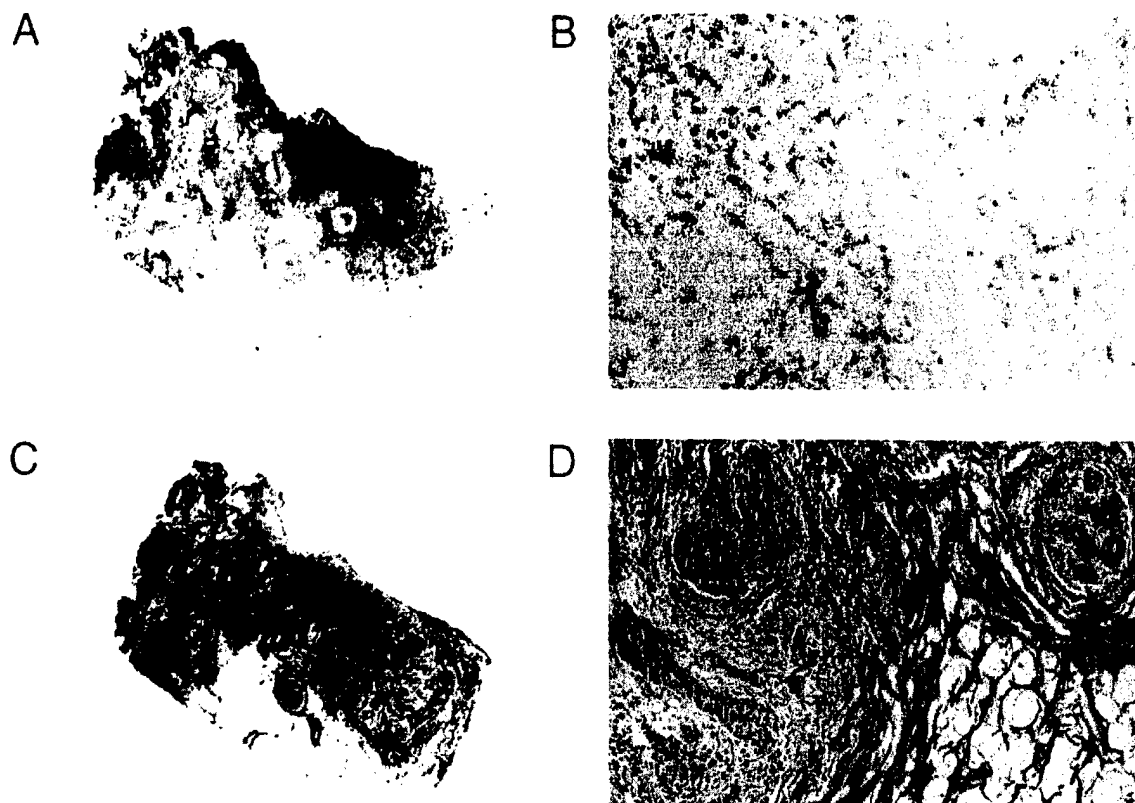


Figure 4. *In situ* hybridization and immunohistochemical study showing regional discordance in lumican mRNA (A, B) and protein expression (C, D) displayed in adjacent sections in breast tumours. Panels A and C show the overall pattern of mRNA (A, black signal) and protein (C, brown staining) within a tissue section (0.4 × 0.8 cm in size) that includes regions of *in situ* and invasive tumour (upper left and upper middle) and adjacent normal tissue (lower left and lower right). Panels B and D show a detailed microscopic view (× 400) of the cellular localization of mRNA and protein within a small region at the invasive edge within the same section (tumour component at left, normal component at right)

speculate that both induction of lumican and decrease in decorin in stromal fibroblasts within the invasive tumour may represent a positive host response, to abrogate the disorganization of collagen within the tumour stroma, encourage macrophage localization [21], and inhibit the growth of epithelial cancer cells, through the increased availability of growth factors inhibitory to breast epithelial cell growth [22]. Alternatively, these alterations may represent a negative host response contributing to early tumour development. Increased lumican mRNA expression may reflect a response to locally increased proteolysis or altered deposition of the lumican protein that is the cause of the disorganization of the collagenous stroma, which in turn facilitates tumour cell invasion. Similarly, a decrease in decorin may remove an inhibitory effect on epithelial tumour cell growth through repression of p21 [7]. A role for and the distinction between these opposing potential effects will clearly require further study.

The differences in lumican levels between normal and tumour tissues observed by both immunohistochemistry and western blot are not as marked as those seen at the level of mRNA expression. While differences in the assays may account for some of this

discrepancy, it is clear that it may also be attributable to the discordance that can exist between lumican mRNA and protein expression detected by *in situ* and immunohistochemical techniques respectively, within the same regions of breast tumour stroma. A similar discordance between mRNA and protein expression has been previously observed in the course of studies on lumican and other large and small proteoglycans in different tissues. For example, in corneal development in the chicken, the mRNA levels for lumican and decorin do not always reflect the rate of synthesis of the corresponding proteins and the efficiency of translation of lumican varies over time [23]. Similar discordance between aggrecan and versican mRNA and protein has been seen in normal tendon [24], between decorin and biglycan mRNA and protein localization in normal and reactive gastric mucosa [25], and in regions of cartilage matrix around vascular channels and the growth plates of long bones in normal cartilage [26]. In this latter instance, the discordance was attributed to a high rate of breakdown and removal at these sites. This conclusion is supported by studies on endothelial cells which show that growth factors such as bFGF can increase not only both biglycan transcription and protein synthesis,

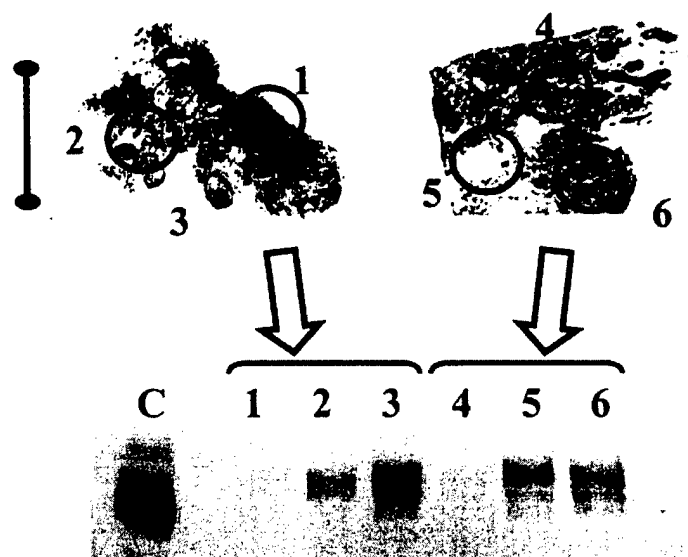


Figure 5. Lumican protein expression detected by immunohistochemistry (upper panel) and western blot (lower panel) demonstrating concordance in the assessment of protein levels in microdissected subregions within two breast tumour sections. The upper panels show IHC sections (tumour A, left; tumour B, right; scale bar = 5 mm). The mRNA and protein signals were detected by *in situ* hybridization (ISH) and immunohistochemistry (IHC) in each region in adjacent sections and ISH/IHC levels were assessed semi-quantitatively (negative, weak +, strong ++) as follows: tumour A: region 1 = ++/+, region 2 = -/+, region 3 (remainder of section) = ++/++; tumour B: region 4 = +/-, region 5 = -/+, region 6 = ++/+. The lower panel shows the western blot (C = cartilage control; lanes 1–6 correspond to regions assessed and microdissected above)

but also the corresponding rate of proteolysis [27]. The absence of protein could also reflect masking of the epitope by conformational changes in the native protein, by changes in post-translational modification, or by binding to another protein. Alternatively, this could reflect reduced translation, increased breakdown, or failure to bind within the immediate stroma and rapid translocation of the protein to adjacent areas of the tissue. Our microdissection experiments, applied to small regions where lumican mRNA is highly expressed, suggest that the corresponding protein is truly absent in these areas and that epitope masking due to conformation or binding proteins is an unlikely explanation for the observation. However, it could also be the case that the necessary binding sites are not available in the immature stroma associated with rapid growth of tumours and that this allows translocation of newly synthesized lumican to binding sites in adjacent tissue.

The reciprocal nature of the changes in the expression of lumican and decorin is intriguing. Although definitive characterization of the stromal cell types awaits primary culture studies, direct comparison of *in situ* hybridization performed on serial sections suggests that expression of both genes apparently occurs in the same fibroblast-like cells in breast tissue stroma. While lumican has not previously been studied in human tumours, the expression of decorin mRNA and proteoglycans incorporating chondroitin sulphate epitopes has been shown to be increased in colon, prostate, and basal cell carcinomas [28–30], but a more recent study of multiple stromal genes in breast

tumours found no difference in the levels of decorin mRNA between tumour and normal tissue, although noting increased expression in the stroma immediately adjacent to *in situ* components [31]. However, the normal tissue examined was selected to be well away from the primary tumour and this, together with differences in the method of quantitation, the definition of tumour regions, and the focus on matched samples, limits a full comparison with our observations. For example, morphologically normal tissue immediately adjacent to carcinomas may be influenced by paracrine growth factors derived from the tumour and may also harbour molecular alterations [32] that might influence local gene expression. However, similar immunohistochemical studies of breast tumours using monoclonal antibodies raised against chondroitin sulphate and dermatan sulphate small proteoglycan have shown reduced decorin expression within invasive as compared with surrounding normal stroma, consistent with our findings [33]. Decorin and other SLRPs are known to be independently regulated and mutually exclusive [26] and compensatory changes in the expression between different SLRPs have been observed [34]. However, this appears to be usually manifested by genes within subgroups of the SLRP family. At the same time, reciprocal changes in the expression between lumican and decorin have not been described in lumican or decorin 'knockout' mice [8,17]. The factors that influence altered expression of these genes in breast tumour stroma remain to be elucidated.

In summary, we have shown that lumican is highly abundant relative to decorin, biglycan, and fibro-

modulin in normal and neoplastic breast tissues. We have also shown that increased lumican protein expression and altered regional localization occur in breast tumours and that different and reciprocal alterations in expression occur between lumican and decorin. The functional significance and the role of alterations in these stromal proteoglycans in breast tumorigenesis and progression remain to be determined.

Acknowledgements

This work was supported by grants from the Medical Research Council of Canada (MRC) and the US Army Medical Research and Materiel Command (USAMRMC). The Manitoba Breast Tumor Bank is supported by funding from the National Cancer Institute of Canada (NCIC). PHW is an MRC Scientist; LCM is an MRC Scientist; and EL is a recipient of a USAMRMC Postdoctoral Fellowship. TH-H is a recipient of an MRC studentship award.

References

1. Peyrol S, Raccourt M, Gerard F, Gleyzal C, Grimaud JA, Sommer P. Lysyl oxidase gene expression in the stromal reaction to *in situ* and invasive ductal breast carcinoma. *Am J Pathol* 1997; **150**: 497–507.
2. Kinzler KW, Vogelstein B. Landscaping the cancer terrain [comment]. *Science* 1998; **280**: 1036–1037.
3. Iozzo RV. Tumor stroma as a regulator of neoplastic behavior. Agonistic and antagonistic elements embedded in the same connective tissue [editorial]. *Lab Invest* 1995; **73**: 157–160.
4. Spanakis E, Brouty-Boye D. Discrimination of fibroblast subtypes by multivariate analysis of gene expression. *Int J Cancer* 1997; **71**: 402–409.
5. Leygue E, Snell L, Dotzlaw H, et al. Expression of lumican in human breast carcinoma. *Cancer Res* 1998; **58**: 1348–1352.
6. Iozzo RV. The family of the small leucine-rich proteoglycans: key regulators of matrix assembly and cellular growth. *Crit Rev Biochem Mol Biol* 1997; **32**: 141–174.
7. Santra M, Mann DM, Mercer EW, Skorski T, Calabretta B, Iozzo RV. Ectopic expression of decorin protein core causes a generalized growth suppression in neoplastic cells of various histogenetic origin and requires endogenous p21, an inhibitor of cyclin-dependent kinases. *J Clin Invest* 1997; **100**: 149–157.
8. Chakravarti S, Magnuson T, Lass JH, Jepsen KJ, LaMantia C, Carroll H. Lumican regulates collagen fibril assembly: skin fragility and corneal opacity in the absence of lumican. *J Cell Biol* 1998; **141**: 1277–1286.
9. Cs-Szabo G, Melching LI, Roughley PJ, Glant TT. Changes in messenger RNA and protein levels of proteoglycans and link protein in human osteoarthritic cartilage samples. *Arthritis Rheum* 1997; **40**: 1037–1045.
10. Watson PH, Snell L, Parisien M. The NCIC-Manitoba Breast Tumor Bank: a resource for applied cancer research. *Cmaj* 1996; **155**: 281–283.
11. Hiller T, Snell L, Watson PH. Microdissection RT-PCR analysis of gene expression in pathologically defined frozen tissue sections. *Biotechniques* 1996; **21**: 38–40.
12. Grover J, Chen XN, Korenberg JR, Roughley PJ. The human lumican gene. Organization, chromosomal location, and expression in articular cartilage. *J Biol Chem* 1995; **270**: 21942–21949.
13. Roughley PJ, White RJ, Cs-Szabo G, Mort JS. Changes with age in the structure of fibromodulin in human articular cartilage. *Osteoarthritis Cart* 1996; **4**: 153–161.
14. Roughley PJ, White RJ, Magny M-C, Liu J, Pearce RH, Mort JS. Non-proteoglycan forms of biglycan increase with age in human articular cartilage. *Biochem J* 1993; **295**: 421–426.
15. Vetter U, Vogel W, Just W, Young MF, Fisher LW. Human decorin gene: intron-exon junctions and chromosomal localization. *Genomics* 1993; **15**: 161–168.
16. Hocking AM, Shinomura T, McQuillan DJ. Leucine-rich repeat glycoproteins of the extracellular matrix. *Matrix Biol* 1998; **17**: 1–19.
17. Danielson KG, Baribault H, Holmes DF, Graham H, Kadler KE, Iozzo RV. Targeted disruption of decorin leads to abnormal collagen fibril morphology and skin fragility. *J Cell Biol* 1997; **136**: 729–743.
18. Moscatello DK, Santra M, Mann DM, McQuillan DJ, Wong AJ, Iozzo RV. Decorin suppresses tumor cell growth by activating the epidermal growth factor receptor. *J Clin Invest* 1998; **101**: 406–412.
19. Ying S, Shiraishi A, Kao CW, et al. Characterization and expression of the mouse lumican gene. *J Biol Chem* 1997; **272**: 30306–30313.
20. Ricciardelli C, Mayne K, Sykes PJ, et al. Elevated levels of versican but not decorin predict disease progression in early-stage prostate cancer. *Clin Cancer Res* 1998; **4**: 963–971.
21. Funderburgh JL, Mitschler RR, Funderburgh ML, Roth MR, Chapes SK, Conrad GW. Macrophage receptors for lumican. A corneal keratan sulfate proteoglycan. *Invest Ophthalmol Vis Sci* 1997; **38**: 1159–1167.
22. Santra M, Skorski T, Calabretta B, Lattime EC, Iozzo RV. *De novo* decorin gene expression suppresses the malignant phenotype in human colon cancer cells. *Proc Natl Acad Sci USA* 1995; **92**: 7016–7020.
23. Cornuet PK, Blochberger TC, Hassell JR. Molecular polymorphism of lumican during corneal development. *Invest Ophthalmol Vis Sci* 1994; **35**: 870–877.
24. Waggett AD, Ralphs JR, Kwan AP, Woodnutt D, Benjamin M. Characterization of collagens and proteoglycans at the insertion of the human Achilles tendon. *Matrix Biol* 1998; **16**: 457–470.
25. Schonherr E, Luger N, Stoll R, Domschke W, Kresse H. Differences in decorin and biglycan expression in patients with gastric ulcer healing. *Scand J Gastroenterol* 1997; **32**: 785–790.
26. Bianco P, Fisher LW, Young MF, Termine JD, Robey PG. Expression and localization of the two small proteoglycans biglycan and decorin in developing human skeletal and non-skeletal tissues. *J Histochem Cytochem* 1990; **38**: 1549–1563.
27. Kinsella MG, Tsoi CK, Jarvelainen HT, Wight TN. Selective expression and processing of biglycan during migration of bovine aortic endothelial cells. The role of endogenous basic fibroblast growth factor. *J Biol Chem* 1997; **272**: 318–325.
28. Adany R, Heimer R, Caterson B, Sorrell JM, Iozzo RV. Altered expression of chondroitin sulfate proteoglycan in the stroma of human colon carcinoma. Hypomethylation of PG-40 gene correlates with increased PG-40 content and mRNA levels. *J Biol Chem* 1990; **265**: 11389–11396.
29. Hunzelmann N, Schonherr E, Bonnekoh B, Hartmann C, Kresse H, Krieg T. Altered immunohistochemical expression of small proteoglycans in the tumor tissue and stroma of basal cell carcinoma. *J Invest Dermatol* 1995; **104**: 509–513.
30. Iozzo RV, Cohen I. Altered proteoglycan gene expression and the tumor stroma. *Experientia* 1993; **49**: 447–455.
31. Brown LF, Guidi AJ, Schnitt SJ, et al. Vascular stroma formation in carcinoma *in situ*, invasive carcinoma, and metastatic carcinoma of the breast. *Clin Cancer Res* 1999; **5**: 1041–1056.
32. Deng G, Lu Y, Zlotnikov G, Thor AD, Smith HS. Loss of heterozygosity in normal tissue adjacent to breast carcinomas. *Science* 1996; **274**: 2057–2059.
33. Nara Y, Kato Y, Torii Y, et al. Immunohistochemical localization of extracellular matrix components in human breast tumours with special reference to PG-M/versican. *Histochem J* 1997; **29**: 21–30.
34. Nelimarkka L, Kainulainen V, Schonherr E, et al. Expression of small extracellular chondroitin/dermatan sulfate proteoglycans is differentially regulated in human endothelial cells. *J Biol Chem* 1997; **272**: 12730–12737.



A matrix metalloproteinase inhibitor, batimastat, retards the development of osteolytic bone metastases by MDA-MB-231 human breast cancer cells in Balb C *nu/nu* mice

J. Lee^a, M. Weber^a, S. Mejia^a, E. Bone^b, P. Watson^a, W. Orr^{a,*}

^aDepartment of Pathology, University of Manitoba, 770 Bannatyne Avenue, Winnipeg, Manitoba, Canada

^bBritish Biotech Pharmaceuticals Limited, Oxford, UK

Received 26 November 1999; received in revised form 17 July 2000; accepted 20 July 2000

Abstract

Bone resorption is a dominant feature of many bone metastases and releases factors from the bone matrix that can promote the expression of the metastatic phenotype in cancer cells. Since proteolytic enzymes, including matrix metalloproteinases (MMPs) contribute to bone destruction by metastatic tumour cells and host cells, we have examined the effect of a MMP inhibitor, batimastat, on the ability of MDA-MB-231 cells to degrade bone *in vitro* and to form bone metastases in BalbC *nu/nu* mice. *In vitro*, the neoplastic cells produced MMP-2 and MMP-9, degraded [³H]-proline-labelled osteoblast matrices, and formed resorption pits in cortical bone. These phenomena were inhibited by ≤ 20 μ M batimastat. To induce vertebral and long bone metastases *in vivo*, 1×10^5 MDA-MB-231 cells were injected into the arterial circulation of BalbC *nu/nu* mice. Test groups were also given 30 mg/kg batimastat intraperitoneally (i.p.). After 21 days, the long bone metastases were characterised by a 67% reduction of metaphyseal medullary bone and complete replacement of marrow by tumour. In tumour-bearing mice that had been treated with 30 mg/kg batimastat i.p., the tumour volume decreased 8-fold, osteolysis was inhibited by 35%, and replacement of the bone marrow by tumour was inhibited by 65%. Similar effects were observed in the vertebral metastases. These data provide evidence that MDA-MB-231 cells can degrade osteoblast matrices and mineralised bone *in vitro* and support the hypothesis that MMPs are involved in the pathogenesis of osteolytic bone metastases *in vivo*. They demonstrate that an agent which inhibits proteolysis can retard the development of osteolytic bone metastases in this model. © 2001 Elsevier Science Ltd. All rights reserved.

Keywords: Neoplasm metastasis; Bone, matrix metalloproteinase; Proteinase inhibitor

1. Introduction

Skeletal metastases are common in patients with advanced cancers of the breast, prostate, lung, thyroid and kidney. Bone resorption is a dominant feature of most bone metastases, mediated by osteoclasts [1], tumour-associated macrophages [2], or metastatic cancer cells [3]. Osteolysis [4] contributes to the pathological progression of bone metastases since the local growth factors that are generated and/or released as part of the bone remodelling process can promote the expression of the metastatic phenotype in osteotropic cancer cells [5]. Moreover, by weakening the structural integrity of bone, osteolysis contributes to the clinical

features of bone metastases which include pain, pathological fractures, spinal cord compression, and hypercalcaemia [6].

The matrix metalloproteinases are mediators of homeostatic bone growth and remodelling [7] and are likely to contribute to the invasion and metastasis of malignant tumours in bone [8,9]. In experimental models of bone metastasis, there is evidence that osteolysis and colonisation of the bone marrow by the tumour can be reduced by strategies that inhibit the release or production of proteases [10,11] or by overexpressing tissue inhibitors of matrix metalloproteinases in metastatic cells [12]. On this basis, we have postulated and show here that a synthetic inhibitor of matrix metalloproteinases, batimastat (BB-94), inhibits the activity of matrix metalloproteinases expressed by MDA-MB-231 human breast carcinoma cells, and blocks the ability of these cells to degrade osteoblast-like matrices or to form

* Corresponding author. Tel.: +1-204-789-3338; fax: +1-204-789-3931.

E-mail address: worr@cc.umanitoba.ca (W. Orr).

resorption pits in cortical bone. *In vivo*, where more than one cell type may be involved in bone destruction, treatment of tumour-bearing animals with batimastat inhibited tumour-associated osteolysis, tumour growth, and the replacement of marrow by tumour.

2. Materials and methods

2.1. Materials

Dulbecco's Minimal Essential Medium (DMEM) was purchased from GibcoBRL (Edmonton, Alberta, Canada). The MDA-MB-231 cells were a generous gift from G.R. Mundy, University of Texas, San Antonio, TX, USA. The SaOS-2 osteosarcoma cells were purchased from the American Type Culture Collection (Rockville, MD, USA). BalbC *nu/nu* mice weighing 18–20 g were purchased from Charles River (Montreal, Quebec, Canada) and housed according to standards established by the University of Manitoba. Batimastat was supplied by British Biotech Pharmaceuticals Ltd, Oxford, UK.

2.2. Tumour cell growth in vitro

4×10^2 MDA-MB-231 human breast cancer cells were seeded into 24 well tissue culture plates and allowed to attach for 2 h. Four replicate wells were then cultured in DMEM with 10% fetal bovine serum, in the presence of batimastat at concentrations ranging from 0 to 50 μ M. Daily counts of viable cells were obtained by a haemocytometer.

2.3. Enzymography

Enzymography was performed as previously described [4]. Briefly, serum-free conditioned medium was collected over 48 h from confluent cultures of MDA-MB-231 cells. Samples of medium were loaded into 10% sodium dodecyl sulphate–polyacrylamide gel electrophoresis (SDS–PAGE) gels containing 0.3% gelatine and resolved by electrophoresis at 4°C at 100 V overnight. The gel was washed in 2.5% Triton X-100 for 2 h at room temperature and incubated for 48 h at 37°C in substrate buffer containing 50 mM Tris–HCl pH 8.9, and 5 mM CaCl_2 with varying concentrations of batimastat. The gel was visualised by staining with Coomassie Blue.

2.4. Degradation of extracellular matrix

SaOS-2 (human osteosarcoma) cells were cultured for 5 days in 96-well plates in the presence of 5 $\mu\text{Ci/ml}$ [^3H]-proline and 25 $\mu\text{g/ml}$ ascorbic acid to form a radiolabelled osteoid-like matrix monolayer on the surface of the tissue culture dish. The osteosarcoma cells were

lysed with 20 mM NH_4OH at 37°C for 20 min. The radiolabelled matrices were washed with serum-free DMEM and incubated for 24 h with 1×10^5 MDA-MB-231 tumour cells in the presence of 0–20 μM batimastat. Replicates of 5–6 wells were included for each condition. 100 μl aliquots of medium were collected, added to 6 ml of Beckman ReadySafeTM scintillation fluid, and counted using a Beckman beta counter [4].

2.5. Resorption of mineralised cortical bone

Fresh bovine long bone was obtained commercially, the marrow removed, and the bones were washed in methanol [4]. The bone was cut into 2-mm slices using an Isomet low-speed diamond-edged saw. The slices were then polished using fine quality sandpaper, 20 μm grit, and then with 10 μm grit accompanied by intermittent washing in water, using an ultrasonicator for 5-min periods. The slices were then dehydrated, and sterilised with ethylene oxide. Before each experiment, the slices were incubated for 24 h in serum-free medium, then incubated with 1×10^5 MDA-MB-231 cells with or without 20 μM batimastat for 60 min. The non-adhering cells were washed off with serum-free medium. The bone slices were then incubated for 30 days at 37°C in the presence or absence of batimastat. The cancer cells were removed by incubating the slices with 0.1% Triton X-100 for 6 h with 5-min washing in the ultrasonicator and the slices fixed in 100% ethanol. The slices were sputter-coated with gold and mounted for examination in a Scanning Electron Microscope. Bones were cultured in quadruplicate for each experimental condition. Between 30 to 50 random fields on the surface of the bone slices were analysed for each condition. Shallow pits with a diameter of 20–30 μm were marked. The mean number of pits per 0.62 mm² field was calculated.

2.6. Experimental bone metastasis

Four groups of 3–4 week old BalbC *nu/nu* mice were established from two sets of littermates, as summarised in Table 1. A normal control group consisted of animals that were neither treated with batimastat nor injected with MDA-MB-231 cells. Two groups of animals were

Table 1
Animal groups used to examine the effects of batimastat on the metastasis of MDA-MB-231 cells to bone

Groups	n	Batimastat	Tumour	Batimastat
(Time line)		2 days		21 days
Normal control	5	–		–
Batimastat control ^a	6	+	–	+
Tumour only ^b	4	–	+	–
Tumour and batimastat ^{a,b}	9	+	+	+

^a 30 mg/kg batimastat injected intraperitoneally (i.p.) daily.

^b 1×10^5 MDA-MB-231 cells injected.

given daily batimastat injections (30 mg/kg intraperitoneally (i.p.)) for a period of 23 days. Two groups of mice were given a single intracardiac left ventricular injection of 1×10^5 MDA-MB-231 cells 21 days before terminating the experiment. One group received both batimastat (beginning 2 days before injection of the tumour cells) and tumour cells. Intracardiac injections of MDA-MB-231 cells were employed to induce the formation of metastatic bone tumours as described by Yoneda and colleagues [12]. Briefly, under anaesthesia, a left parasternal longitudinal incision was made and the second intercostal space located. A needle was inserted until pulsatile blood was observed. 1×10^5 MDA-MB-231 human breast cancer cells in a total volume of 0.1 ml were injected within 20 s. The animals were allowed to recover and housed for 21 days, receiving a daily injection of batimastat or vehicle. The mice were killed by exposure to atmospheric CO_2 . The left femur and the vertebral column were removed and fixed in 10% buffered formalin for 24 h. The vertebrae and femur were decalcified in 10% formic acid for 24 h and then further fixed in formalin for 24 h. The tissues were embedded in paraffin, following standard protocols. A 7- μm thick section of bone was prepared from the centre of the left femur and from the centre of the vertebral column and stained with haematoxylin and eosin. The

metaphyseal medullary bone at the distal end of the left femur and the vertebral bodies were systematically scanned with a $40\times$ objective lens. Five microscopic fields were analysed in each vertebral body with metastases. A Merz graticule was used to perform a morphometric analysis of the percentage area of bone, tumour, and marrow for each section [4,13].

2.7. Batimastat administration

Batimastat stock solution was prepared for use *in vitro* in absolute ethanol at a concentration of 10 mM and diluted in ethanol before each experiment. For experiments *in vivo*, the solution was prepared at a concentration of 3.0 mg/ml in pyrogen-free phosphate buffered saline (GibcoBRL, Edmonton, Alberta, Canada) with 0.01% Tween 80 (Fisher Scientific) and administered by i.p. injection at a daily dose of 30 mg/kg.

3. Results

3.1. Experiments in vitro

Growth curves were obtained to determine if batimastat has an effect on the proliferation of MDA-MB-231

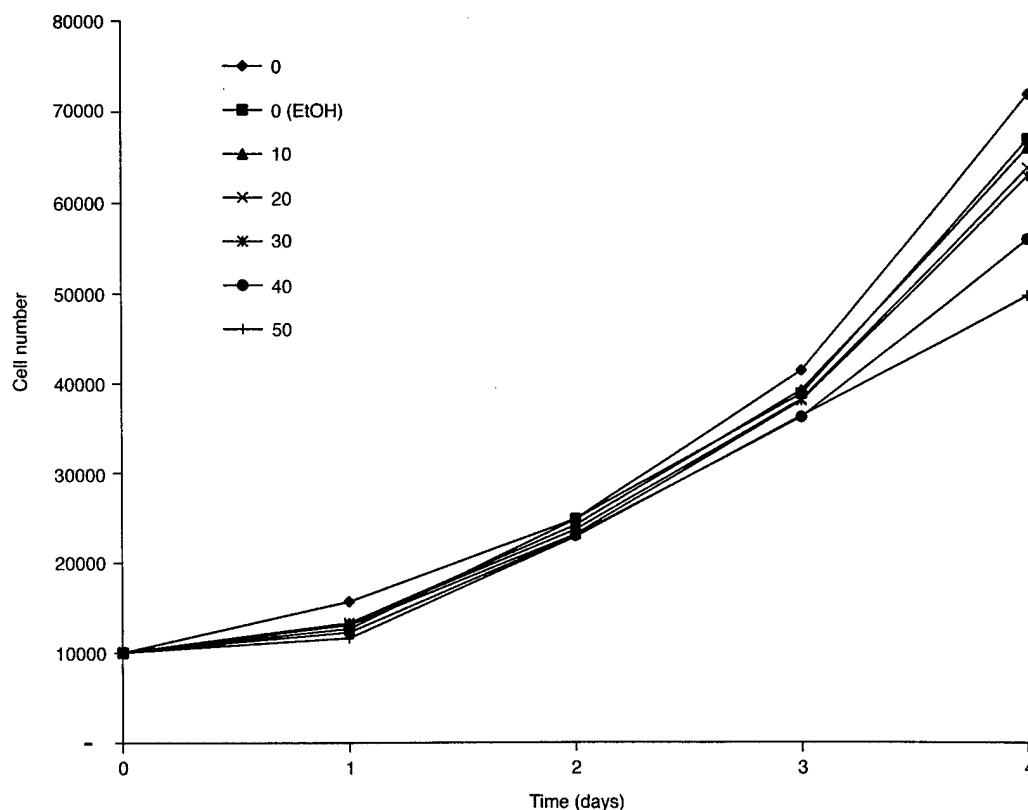


Fig. 1. Effect of batimastat on the growth of MDA-MB-231 human breast cancer cells *in vitro*. 4×10^2 cells were seeded into 24-well tissue culture plates and cultured in the presence of 0–50 μM batimastat. Daily cell counts were obtained by haemocytometer.

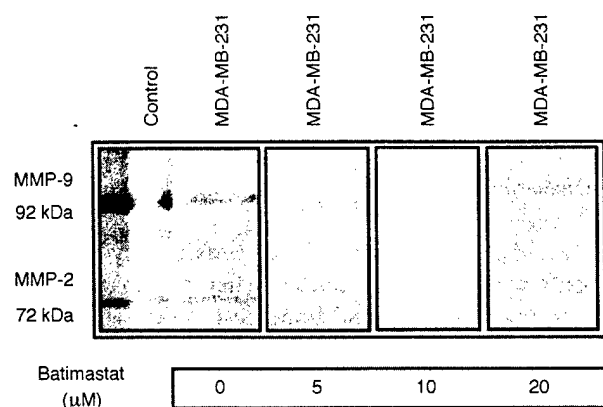


Fig. 2. Effect of batimastat on the expression of MMP-2 and MMP-9 in serum free medium conditioned by MDA-MB-231 cells. Electrophoresis was performed in 10% sodium dodecyl sulphate–polyacrylamide gel electrophoresis (SDS–PAGE) containing 0.3% gelatine. Zymograms were developed over 48 h in substrate buffer containing 0–20 μ M batimastat.

breast cancer cells *in vitro*. After 4 days culture, the proliferation of the MDA-MB-231 cells was inhibited by approximately 4% in the presence of 10 μ M batimastat or the ethanol vehicle and was inhibited up to approximately 30% at concentrations of 50 μ M (Fig. 1).

Using enzymography, the serum-free medium of MDA-MB-231 cells, conditioned for 48 h, exhibited enzymatic activities at molecular weights of 92 kDa and 72 kDa, corresponding to the expression of matrix metalloproteinase (MMP)-9 and MMP-2 respectively. These activities were blocked when batimastat was added to the zymographic substrate buffer at concentrations ≥ 5 μ M (Fig. 2). Metalloproteinase expression was not inhibited in serum-free conditioned medium, collected from cells that had been cultured to confluence in the presence of 5–20 μ M batimastat (data not shown). These results indicated that exposure to batimastat did not alter the expression of MMPs by the neoplastic cells.

Assays to examine the ability of batimastat to inhibit the degradation of non-mineralised bone matrix *in vitro* were performed to model its putative effects on the degradation of non-mineralised osteoid *in vivo*. In three independent experiments, batimastat inhibited the degradation of osteoblast-like matrix by MDA-MB-231 cells in a dose-dependent manner. In all three experiments, matrix degradation was inhibited completely by batimastat at concentrations of 20 μ M with an effective dose (ED)₅₀ \cong 10 μ M (Fig. 3).

Assays to examine the effects of batimastat on the ability of MDA-MB-231 cells to directly degrade mineralised bone were performed as previously described [4,14]. MDA-MB-231 cells cultured on devitalised polished slices of bovine cortical bone generated 1.7 ± 0.2 well-defined surface excavations per 0.62 mm² field after 30 days. In the presence of 20 μ M batimastat,

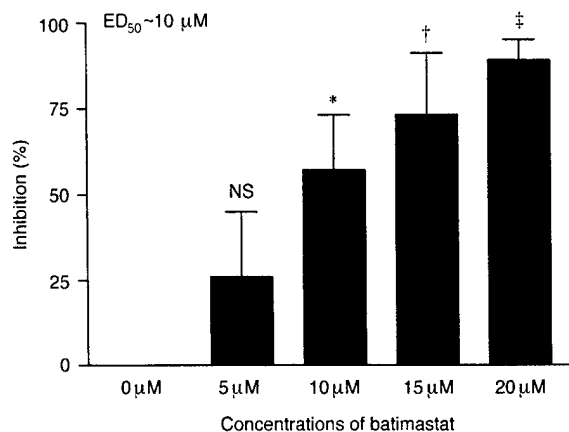


Fig. 3. Effect of batimastat on the degradation of osteoblast-like matrix by MDA-MB-231 cells. MDA-MB-231 cells were cultured on preformed [³H]-proline labelled SaOS-2 osteoblast-like matrix in the presence of 0–20 μ M batimastat. Degradation was determined by counting radioactivity released into the culture medium after 24 h. Not statistically significant by standard Student's *t*-test = NS; Statistically significant = * $P \leq 0.05$; † $P \leq 0.01$; ‡ $P \leq 0.001$. ED, effective dose.

the number of pits decreased by 24% to 1.3 ± 0.2 pits per field ($P \leq 0.076$) (Fig. 4). The areas of these pits were not significantly different ($P \leq 0.32$) between bones cultured in medium (169 ± 15 μ m²) or in the presence of 20 μ M batimastat (148 ± 15 μ m²).

3.2. Experiments *in vivo*

Since metastatic osteolysis can be effected by host-derived osteoclasts and macrophages, as well as by tumour cells, it was important to examine the effects of batimastat *in vivo*. Groups of BalbC *nu/nu* mice were treated according to the protocols described in Table 1. Mice in the tumour-bearing groups were given intracardiac injections of 1×10^5 MDA-MB-231 cells and killed 21 days after tumour cell inoculation. The data obtained by histomorphometric analysis of the distal femoral metaphyses in the two independent experiments are combined in Fig. 5. Compared with non-tumour bearing controls, the non-tumour bearing animals treated with batimastat exhibited a 20% ($P \leq 0.3377$) increase in the area of medullary bone. In the tumour-bearing animals, there was a 67% ($P \leq 0.0001$) reduction of metaphyseal medullary bone at the distal end of the left femur, compared with normal controls. In tumour-bearing mice treated with batimastat, osteolysis was inhibited by 35% ($P \leq 0.02$), compared with untreated tumour-bearing mice. The area of the metaphysis occupied by tumour (tumour burden) was reduced by 68% in tumour-bearing animals treated with batimastat ($P \leq 0.0001$). The distance to which the tumour extended into the metaphysis beyond the epiphyseal growth plate was reduced by 75% ($P \leq 0.0001$). Overall, the total tumour volume decreased from 5.0 ± 0.3 ($\times 10^{-3}$)

mm³ in the untreated tumour-bearing animals to 0.6 ± 0.2 ($\times 10^{-3}$) mm³ in the tumour-bearing batimastat-treated mice ($P \leq 0.0001$). Whereas in normal animals, marrow occupied $85 \pm 2\%$ of the metaphyseal area, this was reduced to 0% ($P \leq 0.0001$) in the tumour-bearing animals. Marrow loss was inhibited by 65% ($P \leq 0.0001$) in tumour-bearing animals treated with batimastat.

In the two experiments, similar results were obtained following analysis of vertebral bone (Table 2). Metastatic tumour was detected in 74% of the vertebral bodies of tumour-bearing animals, but this was reduced to 24% of the vertebral bodies in the tumour-bearing animals treated with batimastat ($P \leq 0.0001$, data not shown). Batimastat treatment was associated with a 96% inhibition of vertebral bone tumour burden

($P \leq 0.0001$), complete inhibition of tumour-associated osteolysis ($P \leq 0.001$), and 53% inhibition of marrow replacement ($P \leq 0.0001$).

4. Discussion

Bone metastases occur in approximately 80% of patients with late stage cancer. They are characterised by cancer cell growth and bone destruction which contribute to their pathophysiological development and clinical presentation. Since bone metastases are not usually detectable until they have become advanced lesions, they are often incurable. The early stages in their formation are asymptomatic and begin as single micrometastatic cells from the bloodstream. As pre-

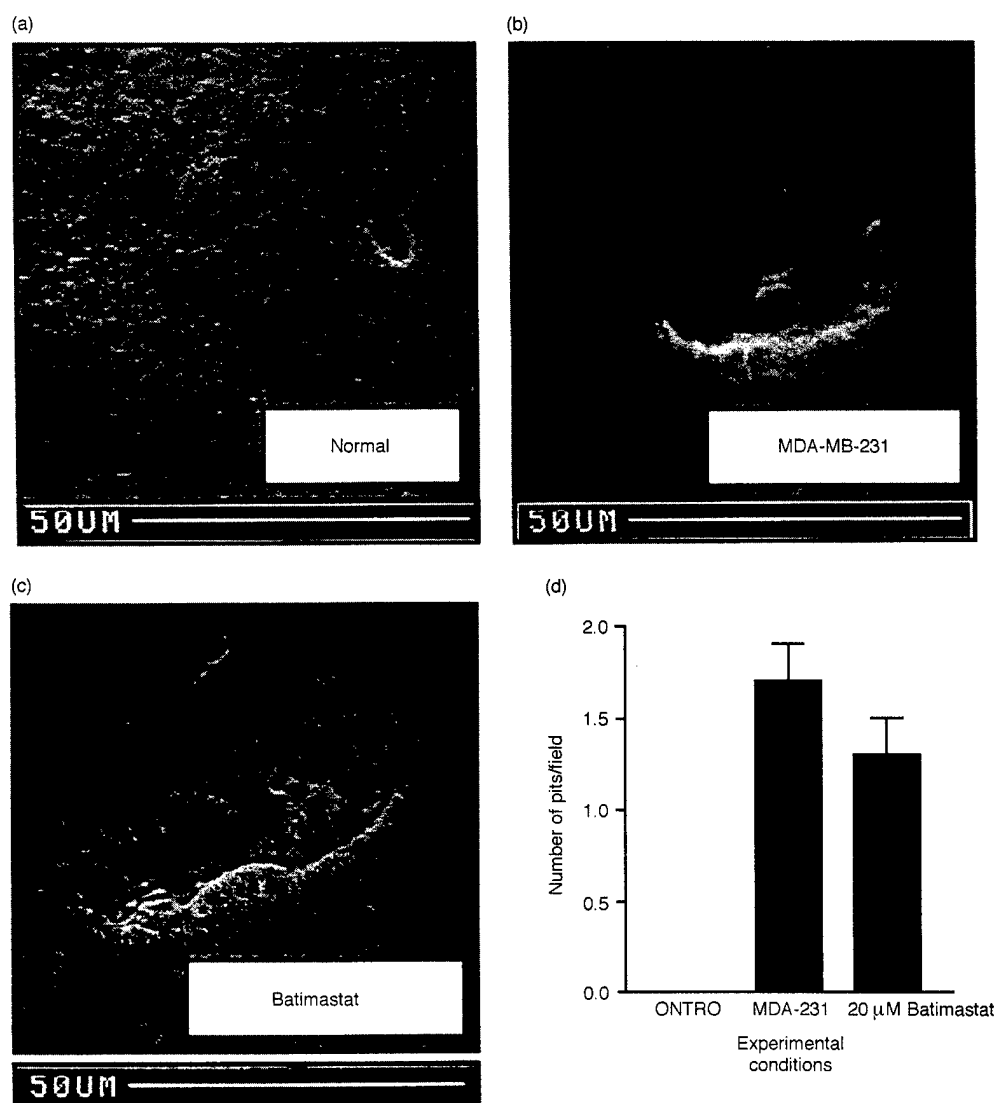


Fig. 4. Effect of batimastat on the formation of cortical bone resorption pits by MDA-MB-231 cells *in vitro*. (a) Appearance of untreated cortical bone after 30 days culture shows an osteocytic lacuna. (b) Resorption pit formed by MDA-MB-231 cells following 30 days coculture with MDA-MB-231 cells. (c) Resorption pit formed by an MDA-MB-231 cell cultured in the presence of batimastat. Scanning electron micrographs $\times 600$. (d) Quantification of pit formation by MDA-MB-231 cells after 30 days incubation in the absence or presence of 20 μ M batimastat. Field = 0.62 mm².

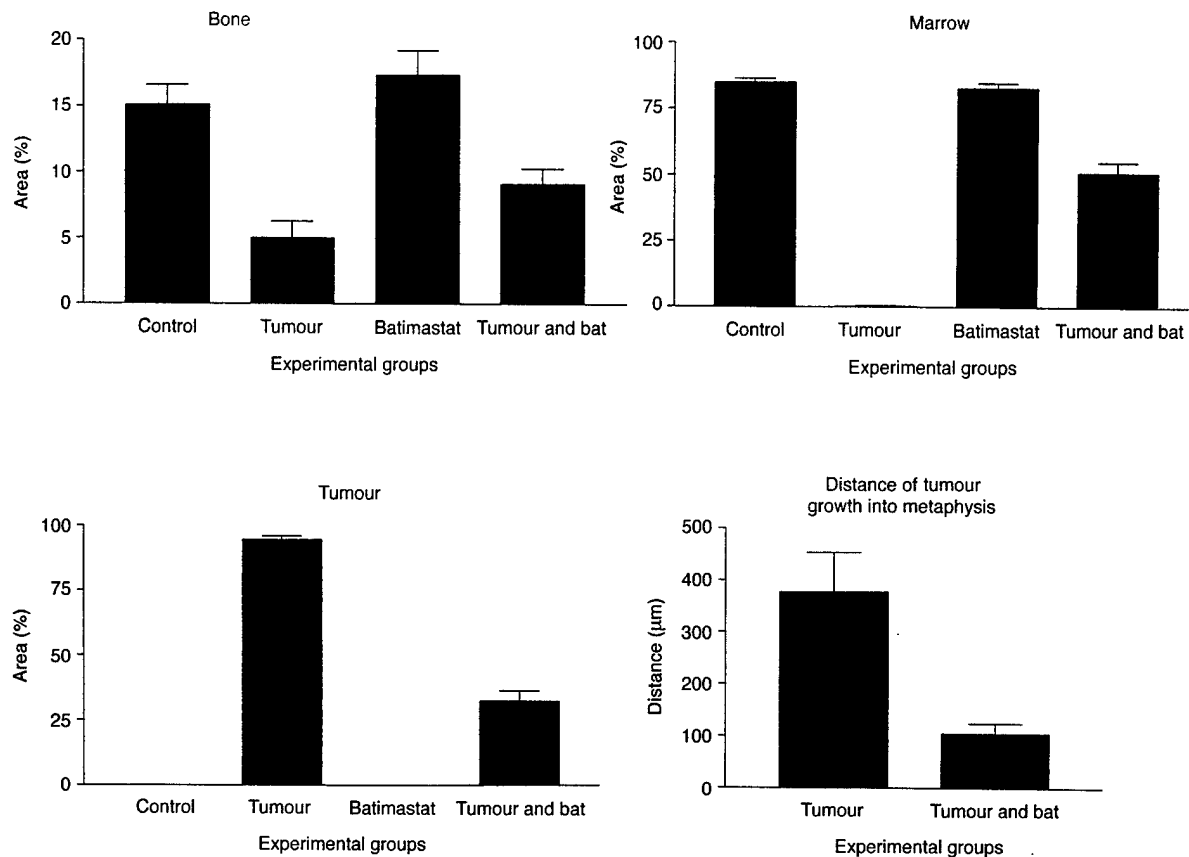


Fig. 5. Effect of batimastat on the development of experimental bone metastases by MDA-MB-231 breast cancer cells in BalbC *nu/nu* mice. Morphometric analysis was performed on histological sections of decalcified left distal femoral metaphysis 21 days after intracardiac injection of tumour cells. The experiment was duplicated to ensure reproducibility. The data presented here are combined from the two independent experiments. Not statistically significant by standard Student's *t*-test = NS; statistically significant by standard Student's *t*-test = * $P \leq 0.05$; † $P \leq 0.01$; ‡ $P \leq 0.001$. BAT, batimastat.

dicted by Paget [15], it has been established that there is a synergistic relationship between the micrometastatic cells and the bone environment, which creates a favourable condition for the development and growth of disseminated tumour cells [5]. Bone resorption mediates the progression of bone metastases by releasing local matrix-derived factors that can promote the expression of metastatic phenotypes in cancer cells including cancer cell chemotaxis [16], tumour growth [17,18], the expression of cell-surface adhesion molecules for bone matrix [19], and expression of MMPs [20,21]. As proteolytic enzymes, including MMPs, contribute to the mechanisms of osteolysis, we postulated that an MMP inhibitor would block osteolysis and interfere with the formation of lesions in established *in vitro* and *in vivo* models of bone metastasis.

Batimastat, an inhibitor of matrix metalloproteinases, acts by binding the zinc ion in the catalytic site, common to all matrix metalloproteinases. In animal models, batimastat has been reported to inhibit the formation of metastases through its inhibitory effects on tumour growth [22,23], tumour cell invasion of extracellular matrix [23–25] or angiogenesis [23,25–27] and by pro-

moting stromal encapsulation [28]. Batimastat has been shown to reduce the activities of the 72-kDa and 92-kDa MMPs expressed by the human breast cancer cell line MDA-MB-435, to inhibit the local regrowth of resected MDA-MB-435 tumours implanted into athymic nude mice, and to inhibit the formation of lung metastases in these animals [29]. The effects of batimastat on bone metastasis do not appear to have been examined previously.

Table 2

Effect of batimastat on the formation of vertebral metastases by MDA-MB-231 breast cancer cells in BalbC *nu/nu* mice^a

Groups	Bone (%)	Marrow (%)	Tumour (%)
Normal control	15±2	85±2	0±0
Tumour only	10±2	34±8	56±6
Batimastat control	16±1	84±1	0±0
Tumour and batimastat	20±2 [†]	78±3*	2±1*

^a Morphometric analysis of decalcified vertebral medullary bone (5 fields/vertebrae, ×200 magnification) was performed 21 days after intracardiac injection of tumour cells. * $P \leq 0.0001$ by Student's *t*-test when compared with the untreated (tumour only) group. †($P \leq 0.0013$).

In our experiments, batimastat did not inhibit the expression of MMP-2 and MMP-9 by the MDA-MB-231 cells but at concentrations $\geq 5 \mu\text{M}$ completely inhibited the gelatinolytic activities of secreted MMPs in serum-free medium and concentrations $\geq 10 \mu\text{M}$ blocked cell-mediated degradation of osteoblast-like matrices. While it is recognised that osteoclastic bone resorption contributes significantly to the osteolytic features of most bone metastases [30], the present experiments confirmed the ability of an osteolytic cancer cell line to induce pit formation in devitalised cortical bone slices in the absence of osteoclasts [4,14]. The ability of a human cancer cell line to cause degradation of mineralised bone was also reconfirmed [14] and was also partially inhibited by batimastat.

The concentrations of batimastat employed in the *in vivo* experiments were based upon precedence from other studies in the literature although they may have exceeded doses required to achieve optimal therapeutic effects. By using histomorphometry to analyse the metastatic lesions, we were able to distinguish between osteolysis, tumour burden, and marrow replacement which can not be accomplished by more conventional radiological measurements. The effects of batimastat treatment on the formation of bone metastases by MDA-MB-231 cells were striking and confirmed in two experiments. The marked osteolytic effects of the tumour were blocked in both femoral and vertebral bone, accompanied by diminished extension of tumour into the medullary long bone, decreased tumour volume, sparing of haematopoietic tissue, and a decrease in the number of metastases found in the vertebral bodies. We were unable to accurately quantify the effects of batimastat on tumour angiogenesis [27,31] as the decalcification procedures we employed appeared to block the ability of established histological markers of angiogenesis to identify blood vessels in our sections. Histomorphometric analysis of the long bones and vertebral bones of non tumour-bearing mice treated with batimastat demonstrated an unexpected increase in the volume of medullary bone, compared with normal untreated controls. An analysis of this phenomenon will be undertaken.

The colonisation of bone marrow by micrometastatic cells is a documented early event in the clinical course of human cancer and is being increasingly regarded as a prognostic factor of clinical significance [32]. Thus, batimastat was administered prior to the injection of tumour cells in order to optimise its potential effects on developing bone metastases rather than to study its actions on established lesions. Given the important contribution of bone resorption to the pathophysiological development of bone metastases, we predict that therapeutic strategies will be most effective if directed at inhibiting the interactions between micrometastatic cells and the bone microcompartment, as opposed to treatment of established lesions.

Acknowledgement

This work was supported by grants to Dr Orr from the Medical Research Council of Canada.

References

1. Mundy GR. Mechanisms of bone metastasis. *Cancer* 1997; **80**, 1546–1556.
2. Quinn JMW, Athanasou NA. Tumour infiltrating macrophages are capable of bone resorption. *J Cell Sci* 1992; **101**, 681–686.
3. Eilon G, Mundy GR. Direct resorption of bone by human breast cancer cells *in vitro*. *Nature* 1978; **276**, 726–728.
4. Sanchez-Sweetman OH, Lee J, Orr FW, Singh G. Direct osteolysis induced by metastatic murine melanoma cells: role of matrix metalloproteinases. *Eur J Cancer* 1997; **33**, 918–925.
5. Orr FW, Lee J, Duivenvoorden WC, Singh G. Pathophysiologic interactions in skeletal metastasis. *Cancer* 2000; **88**, 2912–2918.
6. Rubens RD. Bone metastases — the clinical problem. *Eur J Cancer* 1998; **34**, 210–213.
7. Bord S, Horner A, Hembry RM, Reynolds JJ, Compston JE. Distribution of matrix metalloproteinases and their inhibitor, TIMP-1, in developing human osteophytic bone. *J Anat* 1997; **191**, 39–48.
8. Ueda Y, Imai K, Tsuchiya H, et al. Matrix metalloproteinase 9 (gelatinase B) is expressed in multinucleated giant cells of human giant cell tumor of bone and is associated with vascular invasion. *Am J Pathol* 1996; **148**, 611–622.
9. Barille S, Akhoundi C, Collette M, et al. Metalloproteinases in multiple myeloma: production of matrix metalloproteinase-9 (MMP-9), activation of proMMP-2, and induction of MMP-1 by myeloma cells. *Blood* 1997; **90**, 1649–1655.
10. Stearns ME, Wang M. Effects of alendronate and taxol on pc 3 ml cell bone metastases in scid mice. *Invas Metast* 1996; **16**, 116–131.
11. Kawakami-Kimura N, Narita T, Ohmori K, et al. Involvement of hepatocyte growth factor in increased integrin expression on HepG2 cells triggered by adhesion to endothelial cells. *Br J Cancer* 1997; **75**, 47–53.
12. Yoneda T, Sasaki A, Dunstan C, et al. Inhibition of osteolytic bone metastasis of breast cancer by combined treatment with the bisphosphonate ibandronate and tissue inhibitor of the matrix metalloproteinase 2. *J Clin Invest* 1997; **99**, 2509–2517.
13. Kostenuik PJ, Orr FW, Suyama KL, Singh G. Increased growth rate and tumor burden of spontaneously metastatic Walker 256 cancer cells in the skeleton of bisphosphonate-treated rats. *Cancer Res* 1993; **53**, 5452–5457.
14. Sanchez-Sweetman OH, Orr FW, Singh G. Human metastatic prostate PC3 cell lines degrade bone using matrix metalloproteinases. *Invas Metast* 1999; **18**, 297–305.
15. Paget S. The distribution of secondary growths in cancer of the breast. *Lancet* 1889; **1**, 571–573.
16. Orr FW, Millar-Book W, Singh G. Chemotactic activity of bone and platelet-derived TGF- β for bone-metastasizing rat walker 256 carcinosarcoma cells. *Invas Metast* 1990; **10**, 241–252.
17. Manishen WJ, Sivananthan K, Orr FW. Resorbing bone stimulates tumor cell growth. A role for the host microenvironment in bone metastasis. *Am J Pathol* 1986; **123**, 39–45.
18. Kostenuik PJ, Orr FW, Arsenault L, Millar-Book W, Singh G. Increased expression of c-myc mRNA and protein in walker 256 cancer cells stimulated by bone-derived conditioned media and by transforming factor- β (TGF- β). *Int J Oncol* 1993; **3**, 729–734.
19. Kostenuik PJ, Singh G, Orr FW. Transforming growth factor β upregulates the integrin-mediated adhesion of human prostatic carcinoma cells to type I collagen. *Clin Exp Metast* 1997; **15**, 41–52.

20. Stearns ME. Alendronate blocks TGF-beta1 stimulated collagen I degradation by human prostate PC-3 ML cells. *Clin Exp Metast* 1998, **16**, 332–339.
21. Duivenvoorden WC, Hirte HW, Singh G. Transforming growth factor beta1 acts as an inducer of matrix metalloproteinase expression and activity in human bone-metastasizing cancer cells. *Clin Exp Metast* 1999, **17**, 27–34.
22. Prontera C, Mariani B, Rossi C, Poggi A, Rotilio D. Inhibition of gelatinase A (MMP-2) by batimastat and captopril reduces tumor growth and lung metastases in mice bearing Lewis lung carcinoma. *Int J Cancer* 1999, **81**, 761–766.
23. Tonn JC, Kerkau S, Hanke A, et al. Effect of synthetic matrix-metalloproteinase inhibitors on invasive capacity and proliferation of human malignant gliomas *in vitro*. *Int J Cancer* 1999, **80**, 764–772.
24. Kolkhorst V, Sturzebecher J, Wiederanders B. Inhibition of tumour cell invasion by protease inhibitors: correlation with the protease profile. *J Cancer Res Clin Oncol* 1998, **124**, 598–606.
25. Mira E, Manes S, Lacalle RA, Marquez G, Martinez A. Insulin-like growth factor I-triggered cell migration and invasion are mediated by matrix metalloproteinase-9. *Endocrinology* 1999, **140**, 1657–1664.
26. Bergers G, Javaherian K, Lo KM, Folkman J, Hanahan D. Effects of angiogenesis inhibitors on multistage carcinogenesis in mice. *Science* 1999, **284**, 808–812.
27. Wylie S, MacDonald IC, Varghese HJ, et al. The matrix metalloproteinase inhibitor batimastat inhibits angiogenesis in liver metastases of B16F1 melanoma cells. *Clin Exp Metast* 1999, **17**, 111–117.
28. Brown PD. Matrix metalloproteinase inhibitors: a novel class of anticancer agents. *Adv Enzyme Regul* 1995, **35**, 293–301.
29. Sledge GW Jr, Qulali M, Goulet R, Bone EA, Fife R. Effect of matrix metalloproteinase inhibitor batimastat on breast cancer regrowth and metastasis in athymic mice. *J Natl Cancer Inst* 1995, **87**, 1546–1550.
30. Guise T. Molecular mechanisms of osteolytic bone metastases. *Cancer* 2000, **88**, 2892–2898.
31. Taraboletti G, Garofalo A, Belotti D, et al. Inhibition of angiogenesis and murine hemangioma growth by batimastat, a synthetic inhibitor of matrix metalloproteinases. *J Natl Cancer Inst* 1995, **87**, 293–298.
32. Pantel K, Cote RJ, Fodstad O. Detection and clinical importance of micrometastatic disease. *J Natl Cancer Inst* 1999, **91**, 1113–1124.

Hypoxia-inducible Expression of Tumor-associated Carbonic Anhydrases¹

Charles C. Wykoff, Nigel J. P. Beasley, Peter H. Watson, Kevin J. Turner, Jaromir Pastorek, Amen Sibtain,
George D. Wilson, Helen Turley, Kate L. Talks, Patrick H. Maxwell, Christopher W. Pugh, Peter J. Ratcliffe,²
and Adrian L. Harris

Institute of Molecular Medicine [C. C. W., N. J. P. B., K. J. T., A. L. H.] and the Nuffield Department of Clinical Laboratory Sciences [H. T., K. L. T.], John Radcliffe Hospital, Oxford OX3 9DS, United Kingdom; Department of Pathology, University of Manitoba, Winnipeg, Manitoba, R3E 0W3 Canada [P. H. W.]; Institute of Virology, Slovak Academy of Sciences, 84246 Bratislava, Slovak Republic [J. P.]; Gray Laboratory Cancer Research Trust, Mount Vernon Hospital, Middlesex HA6 2JR, United Kingdom [A. S., G. D. W.]; Wellcome Trust Centre for Human Genetics, Oxford OX3 7BN, United Kingdom [P. H. M., C. W. P., P. J. R.]

ABSTRACT

The transcriptional complex hypoxia-inducible factor-1 (HIF-1) has emerged as an important mediator of gene expression patterns in tumors, although the range of responding genes is still incompletely defined. Here we show that the tumor-associated carbonic anhydrases (CAs) are tightly regulated by this system. Both *CA9* and *CA12* were strongly induced by hypoxia in a range of tumor cell lines. In renal carcinoma cells that are defective for the von Hippel-Lindau (VHL) tumor suppressor, up-regulation of these CAs is associated with loss of regulation by hypoxia, consistent with the critical function of pVHL in the regulation of HIF-1. Further studies of *CA9* defined a HIF-1-dependent hypoxia response element in the minimal promoter and demonstrated that tight regulation by the HIF/pVHL system was reflected in the pattern of CA IX expression within tumors. Generalized up-regulation of CA IX in VHL-associated renal cell carcinoma contrasted with focal perinecrotic expression in a variety of non-VHL-associated tumors. In comparison with vascular endothelial growth factor mRNA, expression of CA IX demonstrated a similar, although more tightly circumscribed, pattern of expression around regions of necrosis and showed substantial although incomplete overlap with activation of the hypoxia marker pimonidazole. These studies define a new class of HIF-1-responsive gene, the activation of which has implications for the understanding of hypoxic tumor metabolism and which may provide endogenous markers for tumor hypoxia.

INTRODUCTION

Tumor hypoxia is an important indicator of cancer prognosis; it is associated with aggressive growth, metastasis, and poor response to treatment (1, 2). Of potential importance for understanding these effects is the role of hypoxia in regulating patterns of gene expression (3–6). Studies of gene expression have defined several classes of hypoxia-inducible genes that are up-regulated in hypoxic regions of tumors and demonstrated that activation of the transcriptional complex HIF-1³ is a key mediator of many of these effects (7–9).

Genes that are up-regulated by microenvironmental hypoxia through activation of HIF include glucose transporters, glycolytic enzymes, and angiogenic growth factors (5, 10, 11). For some HIF targets such as VEGF, a clear function in promoting tumor growth is established (12). However, the full range of HIF target genes has not yet been defined, and identification of additional genes responding to this pathway is likely to provide further insights into the consequences

of tumor hypoxia and HIF activation. Indirect support for the importance of microenvironmental activation of HIF has also been provided by recent demonstrations of constitutive activation of HIF after inactivation of the VHL tumor suppressor gene (13) and amplification of the HIF response by other oncogenic mutations (14–17). Mutations in VHL cause the familial syndrome and are also found in the majority of sporadic RCCs (18). The gene product pVHL forms part of a ubiquitin-ligase complex (19, 20) that targets HIF- α subunits for oxygen-dependent proteolysis (13, 21). In VHL-defective cells, HIF- α is stabilized constitutively, resulting in up-regulation of hypoxia-inducible genes such as VEGF (13). Although the pVHL ubiquitin-ligase complex may have other targets (20) and other functions of pVHL have been proposed that may contribute to tumor suppressor effects (22, 23), these recent findings raise important questions as to the range of genes affected by constitutive HIF activation and the role of these genes in oncogenesis.

In this respect, one interesting group of genes is the tumor-associated transmembrane CAs *CA9* (24–27) and *CA12* (28, 29). CAs catalyze the reversible hydration of carbon dioxide to carbonic acid (30), providing a potential link between metabolism and pH regulation. The membrane-linked isoforms *CA9* and *CA12* were identified by RNA differential display as genes that are down-regulated by pVHL (29), although the effect of hypoxia was not examined and the mechanism of regulation was not defined. Interestingly, *CA9* can confer a variety of features of the transformed phenotype when transfected into NIH 3T3 cells (24).

In this study, we demonstrate that in contrast to constitutive up-regulation in pVHL-defective cell lines, both *CA9* and *CA12* are strongly induced by hypoxia in a broad range of other cell types. The induction of *CA9* by hypoxia was striking and has been studied in detail. We show that the *CA9* promoter is tightly regulated by a HIF-responsive HRE close to its transcriptional start site, and that the gene product is expressed in a perinecrotic manner in many types of human cancer, overlapping with VEGF mRNA and the hypoxia marker pimonidazole. In keeping with constitutive activation of HIF after inactivation of pVHL, the focal pattern of expression observed in most tumors contrasted with that observed in RCCs, where CA IX was globally up-regulated. Our findings define a new biochemical pathway that is regulated by HIF, suggest that CA IX may be a useful marker for HIF activation either by microenvironmental hypoxia or genetic events such as VHL inactivation, and provide additional insights into mechanisms by which the HIF pathway might mediate effects on tumor metabolism.

MATERIALS AND METHODS

Cell Lines. 786-0 cells expressing pVHL or empty vector were a gift from W. G. Kaelin (Dana-Farber Cancer Institute, Boston, MA). RCC4 cells expressing pVHL or empty vector and other RCC lines were as described (13). RT112 human bladder carcinoma cells were a gift from M. Knowles (Imperial Cancer Research Fund, Leeds, United Kingdom). A549, NCI-H460, HeLa, EJ28, MDA-MB-468, MDA-MB-435S, MDA-MB-231, HBL-100, T-47D, and U2 O-S lines were from American Type Culture Collection (ATCC). Cells

Received 6/13/00; accepted 10/18/00.

The costs of publication of this article were defrayed in part by the payment of page charges. This article must therefore be hereby marked *advertisement* in accordance with 18 U.S.C. Section 1734 solely to indicate this fact.

¹ This work was supported by the Wellcome Trust and the Imperial Cancer Research Fund.

² To whom requests for reprints should be addressed, at Wellcome Trust Centre for Human Genetics, Oxford OX3 7BN, United Kingdom. Phone: (44) 1865-287531; Fax: (44) 1865-287533; E-mail: peter.ratcliffe@imm.ox.ac.uk.

³ The abbreviations used are: HIF-1, hypoxia-inducible factor-1; VEGF, vascular endothelial growth factor; VHL, von Hippel-Lindau; RCC, renal cell carcinoma; CA, carbonic anhydrase; *CA9*, carbonic anhydrase 9 gene (including any genomic sequence and mRNA); CA IX, carbonic anhydrase 9 protein; HRE, hypoxia response element; RPA, RNase protection assay; β gal, β -galactosidase; DFO, desferrioxamine; CHO, Chinese hamster ovary.

were grown in DMEM (Sigma) supplemented with 10% FCS (Gibco), L-glutamine (2 mM), penicillin (50 IU/ml), and streptomycin sulfate (50 µg/ml). Studies of inducible gene expression were performed on cells approaching confluence. Parallel incubations were performed on aliquots of cells in normoxia (humidified air with 5% CO₂) and either hypoxia or DFO mesylate (100 µM; Sigma). Hypoxic conditions were generated in a Napco 7001 incubator (Precision Scientific) with 0.1% O₂, 5% CO₂, and balance N₂, unless otherwise specified. Experimental exposures were performed in normal growth medium for 16 h.

RNA Analysis. Total RNA was extracted by a modified acid/guanidinium thiocyanate/phenol/chloroform method (RNAzol B; Cinna/Biotec Laboratories), dissolved in hybridization buffer (80% formamide, 40 mM PIPES, 400 mM sodium chloride, and 1 mM EDTA, pH 8) and analyzed by RPA. To generate appropriate riboprobe templates, cDNA fragments of human *CA9* (nucleotides 3632–3771, accession number Z54349) and *CA12* (nucleotides 301–450, accession number AF037335) were amplified by PCR and ligated into pSP72 (Promega). DNA templates for generating ³²P-labeled RNA probes were linearized for 16 h with *Bgl*II and transcribed with SP6 RNA polymerase. For *CA9* and *CA12*, RPAs were performed on 30 µg of total RNA, using an internal control assay for U6 small nuclear RNA as described (13).

Construction of Reporter Plasmids. To generate plasmids p-506 and p-173, sequences of the *CA9* gene between –506 and +43 relative to the transcriptional start site were amplified by PCR from genomic DNA. PCR products were ligated into pGL3-basic, a promoterless and enhancerless luciferase expression vector (Promega). To generate plasmids p-36, MUT1, and MUT2, complementary oligonucleotides with ends corresponding to the 5' restriction cleavage overhangs of *Bgl*II and *Mlu*I were annealed and ligated into *Bgl*II/*Mlu*I-digested pGL3-basic. Oligonucleotides (sense strand) were: p-36 (forward), 5'-cgcgCTCCCCACCCAGCTCTCGTTTCCAATGCA-CGTACAGCCCGTACACACCG-3'; MUT1 (forward), 5'-cgcgCTCCCCACCCAGCTCTCGTTTCCAATGCTTTTACAGCCCGTACACACCG-3'; MUT2 (forward), 5'-cgcgCTCCCCACCCAGCTCTCGTTTCCAATGCAAGTACAGCCCGTACACACCG-3'. Nucleotides introduced for cloning are lowercased; mutations are underlined. All *CA9* promoter sequences were confirmed by dideoxy sequence analysis.

Transient Expression Assays. Cells at ~70% confluence in 60-mm dishes were transfected with 1 µg of a luciferase reporter construct and 0.4 µg of control plasmid, pCMV-βgal (Promega), using FuGENE 6 (Roche Diagnostic) according to the manufacturer's instructions. Cells were then incubated at 20% O₂ for 8 h, followed by 20% or 0.1% O₂ for 16 h.

Luciferase activity was determined in cell lysates using a commercial assay system (Promega) and a TD-20e luminometer (Turner Designs). βgal activity in cell lysates was measured using o-nitrophenyl-β-D-galactopyranoside as substrate in a 0.1 M phosphate buffer (pH 7.0) containing 10 mM KCl, 1 mM MgSO₄, and 30 mM β-mercaptoethanol. To correct for variable transfection efficiencies between experimental conditions, the luciferase:βgal ratio was determined for each sample. For cotransfection assays, cells also received 0.1–1 µg each of pCDNA3/HIF-1α or pCDNA3/HIF-2α containing the entire human HIF-1α or HIF-2α open reading frame, respectively. Transfections were balanced with various amounts of pCDNA3 (Invitrogen) and pCDNA3/HIF-α such that all cells received the same total quantity of DNA.

Cell Lysis and Immunoblotting. Whole-cell protein extracts were prepared from tissue culture cells by 10-s homogenization in denaturing conditions as described (31). Whole-cell protein extracts were prepared from tumors by fine section of frozen tissue and 30-s homogenization in denaturing conditions identical to tissue culture extracts. For Western analysis, aliquots were separated by SDS-PAGE and transferred to Immobilon-P membranes. CA IX was detected using the mouse monoclonal antihuman CA IX antibody M75 (1:50) as described (32). Horseradish peroxidase-conjugated goat-antimouse immunoglobulin (DAKO; 1:2000) was applied for 1 h at room temperature. ECL Plus (Amersham Pharmacia) was used for visualization.

Immunohistochemistry. Formalin-fixed, paraffin-embedded tissue specimens collected by standard surgical oncology procedures were obtained from the Pathology Department, John Radcliffe Hospital (Oxford, United Kingdom). Immunostaining of paraffin sections was performed after dewaxing and rehydrating 4-µm sections. For CA IX detection, endogenous peroxidase was blocked with 0.5% hydrogen peroxide in water for 30 min. To block, 10% normal human serum in TBS was applied for 15 min. M75 (see "Immunoblotting"; 1:50) was applied for 30 min at room temperature. Secondary

polymer from Envision kit (DAKO) was applied for 30 min at room temperature. For pimonidazole detection, sections were digested with 0.01% Pronase (Sigma) in PBS for 30 min at 37°C. Endogenous peroxidase was blocked with 0.1% hydrogen peroxide in water for 30 min. To block, Protein Block (DAKO) was applied for 5 min. Anti-pimonidazole IgG1 antibody (Natural Pharmacia; 1:100) was applied for 1 h at room temperature. Biotinylated rabbit antimouse secondary (DAKO; 1:200) was applied for 1 h at room temperature. ABC complex horseradish peroxidase conjugate (DAKO) was applied for 1 h at room temperature. Visualization of CA IX and pimonidazole staining was by diaminobenzidine substrate. Slides were counterstained with hematoxylin before mounting in Aquamount (BDH). Substitution of primary antibody with PBS was used as a negative control for both antibodies.

CA IX and pimonidazole were studied in semiserial tissue sections. The percentage of tumor cells showing positive staining for CA IX or pimonidazole and the extent of overlap between these regions within each tissue section was assessed by light microscopy at low magnification by three observers (C. C. W., P. H. W., and H. T.) and a consensus was determined.

In Situ mRNA Hybridization. Specific localization of VEGF mRNA was accomplished by *in situ* hybridization using an antisense riboprobe. Briefly, pBluescript (Stratagene) containing 517 consecutive complementary nucleotides of the VEGF₁₂₁ transcript (439 consecutive nucleotides of which are complementary to VEGF₁₆₅, VEGF₁₈₉, and VEGF₂₀₆) was linearized with *Eco*RV for 16 h at 37°C. Labeled transcripts were synthesized using T7 (antisense) and SP6 (sense) polymerase in the presence of [³⁵S]UTP (>800 Ci/mmol; Amersham Pharmacia). The methods for pretreatment, hybridization, washing, and dipping of slides in Ilford K5 for autoradiography were as described for formalin-fixed, paraffin-embedded tissue (33). The presence of hybridizable mRNA in tissue sections was established in semiserial sections using an antisense β-actin probe. Hybridizations using a sense probe were used to control for nonspecific signal. Autoradiography was at 4°C (two exposures per section for VEGF visualization at 10 and 18 days), before developing in Kodak D19 and counterstaining by Giemsa's method. Sections were examined under conventional and reflected light/dark-field conditions.

Pimonidazole Administration. Patients with squamous or basal cell carcinomas of the skin and patients with newly diagnosed transitional cell bladder carcinoma were studied. Signed informed consent was obtained in all cases. Pimonidazole hydrochloride was selected as the hypoxia marker because of its high water solubility, chemical stability, efficient tumor uptake, and low toxicity. Patients received 500 mg/m² of pimonidazole hydrochloride, 1-[(2-hydroxy-3-piperidinyl)propyl]-2-nitroimidazole hydrochloride (Hypoxprobe) in 100 ml of normal saline i.v. over 20 min. This dose is 25% of the maximum tolerated dose (34). Patients with tumors in skin underwent incisional or Trucut biopsy under local anesthetic 2–24 h after pimonidazole infusion. Patients with bladder carcinoma underwent transurethral resection of the tumor under general anesthetic 2–24 h after pimonidazole infusion. Tissue samples were immediately placed in 10% neutral buffered formalin, protected from light, and then processed into formalin blocks.

RESULTS

VHL-dependent Regulation of *CA9* and *CA12* mRNAs by Hypoxia. Expression of mRNAs encoding *CA9* and *CA12* was analyzed by RPA. To confirm the previous report of down-regulation by pVHL (29), we first examined expression in the VHL-defective RCC line RCC4 and a stable transfectant expressing a human VHL cDNA (RCC4/VHL). In normoxic cells, both mRNAs were down-regulated by pVHL. However, when cells were exposed in parallel to normoxia or hypoxia (0.1% oxygen), induction by hypoxia was observed in RCC4/VHL cells, whereas in RCC4 cells the high level of expression in normoxia was unchanged by hypoxia (Fig. 1A). We also examined expression in other RCC lines that are either defective (KRL140, SKRC28, UMRC2, and 786-0) or wild type (Caki-1) for VHL, and in a stable transfectant of 786-0 re-expressing wild-type pVHL (WT 8). Representative results from three cell lines are illustrated in Fig. 1A. In the VHL-defective cells, both *CA9* and *CA12* were constitutively expressed and unresponsive to changes in oxygen tension. In the

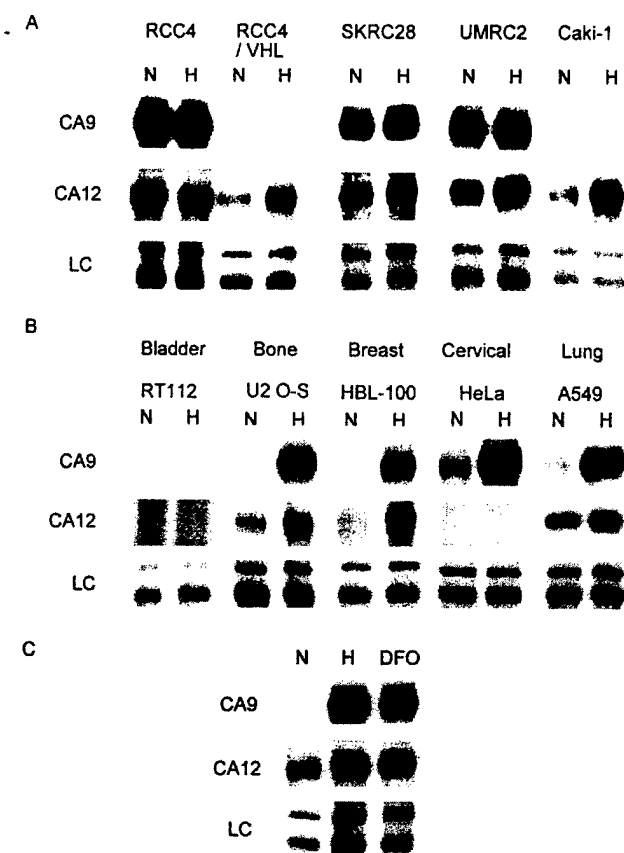


Fig. 1. Induction of *CA9* and *CA12* mRNA by hypoxia. Cells were exposed to either normoxia (N; 20% O₂) or hypoxia (H; 0.1% O₂) for 16 h. *CA9* and *CA12* mRNA was examined by RPA. A, induction by hypoxia in renal carcinoma-derived cell lines is VHL dependent. RCC4, SKRC28, and UMRC2 are VHL defective. RCC4/VHL is a pVHL stable transfectant of RCC4. Caki-1 is VHL competent. B, induction by hypoxia in nonrenal-derived cell lines from indicated tissue type. C, comparison of induction by hypoxia and DFO (each applied for 16 h) in A549 cells. LC, signal from internal control assay for the constitutively expressed U6 small nuclear RNA.

wild-type VHL cell lines, both genes, when expressed, were induced by hypoxia.

To examine regulation by hypoxia across a range of cell types, we performed RPAs for *CA9* and *CA12* on mRNA samples from normoxic and hypoxic cultures of 11 additional cell lines derived from five different tissue types: bladder (RT112 and EJ-28), bone (U2 O-S), breast (HBL-100, MDA-MB-435S, MDA-MB-468, MDA-MB-231, and T-47D), cervical (HeLa), and lung (A549 and NCI-H460). With the exception of bladder cell lines RT112 and EJ-28, every cell type expressed one or both CA isoforms, and in each case where expression was observed, it was induced by hypoxia. The amplitude of induction by hypoxia was particularly high for *CA9*; mRNA levels were at or below the limit of detection in normoxia, yet strikingly induced by hypoxia. Representative illustrations of one cell line from each tissue type are depicted in Fig. 1B. Because many hypoxia-inducible genes are up-regulated by treatment of cells with the iron chelator DFO (35), we also tested the effect of DFO and found a similar induction of both *CA9* and *CA12* mRNA (Fig. 1C).

CA9 Promoter Analysis. To investigate the unusually tight regulation of *CA9* mRNA by hypoxia, we tested for oxygen-dependent function of the *CA9* promoter. In the first set of experiments, we tested luciferase reporter genes containing ~0.5 kb of *CA9* 5' flanking sequences (–506 to +43) and a deletion to nucleotide –173 (–173 to +43) in transiently transfected HeLa cells. Both constructs showed very low levels of activity in normoxic cells but were induced strongly

by hypoxia (Fig. 2A). By contrast, a similar reporter linked to a minimal SV40 promoter showed no induction by hypoxia.

To test whether these responses were dependent on HIF-1, we performed further transfections using a CHO mutant cell (Ka13) that is functionally defective for the HIF-1 α subunit and cannot form the HIF-1 transcriptional complex (36). In the CHO wild-type parental subline C4.5, the –173 nucleotide promoter conferred 17-fold transcriptional induction by hypoxia. In contrast, in the HIF-1 α -deficient Ka13 subline, this hypoxic induction was absent (Fig. 2B). Cotransfection of human HIF-1 α restored hypoxia-inducible activity to the *CA9* promoter in the Ka13 cells and increased normoxic activity in both C4.5 and Ka13 (Fig. 2B). In C4.5 and Ka13 cells at 0.1% O₂, luciferase expression was increased 1.6- and 17-fold, respectively, by cotransfection of human HIF-1 α . Thus, hypoxia-inducible activity of the *CA9* promoter is completely dependent on HIF-1 and strongly influenced by the level of HIF-1 α . Activity of the *CA9* promoter in Ka13 cells could also be restored by cotransfection of HIF-2 α , although normoxic activity was higher and fold induction by hypoxic stimulation was reduced (data not shown).

Inspection of the *CA9* 5' flanking sequences revealed a consensus HRE beginning 3 bp 5' to the transcriptional start site, orientated on the antisense strand, reading 5'-TACGTGCA-3' (Fig. 2, left). To test the importance of this site, we constructed a *CA9* minimal promoter containing this sequence (–36 to +14). This minimal promoter retained hypoxia-inducible activity in C4.5 cells but had no inducible activity in Ka13 cells (Fig. 2C). Absolute levels of activity were lower in comparison to the –173 nucleotide promoter construct, being reduced ~8 fold, indicating that although sequences –173 to –36 amplified promoter activity, responsiveness to hypoxia was conveyed by the minimal sequence containing the HRE. To confirm the importance of this HRE, two mutations were made within its core (antisense strand): a 3-bp substitution from CGT → AAA (MUT1), and a single substitution of G → T (MUT2; Fig. 2, left). Both mutations completely ablated hypoxia-inducible activity, although basal activity was preserved or slightly increased for MUT1 (Fig. 2C).

Regulation of CA IX Protein by Oxygen. As a first step toward understanding the significance of hypoxia-inducible expression of *CA9* mRNA, the effect of hypoxia was examined on CA IX protein levels in whole-cell extracts. Immunoblots of representative cells using anti-CA IX monoclonal antibody M75 are illustrated in Fig. 3A. Striking induction of CA IX protein by hypoxia was observed in multiple cell lines, whereas the VHL-defective RCC4 cells showed constitutive up-regulation of CA IX protein. Thus, hypoxic up-regulation of *CA9* mRNA is clearly reflected at the protein level. We next examined the response of CA IX to increasing degrees of hypoxia (Fig. 3B). The level of CA IX hypoxic induction after 16 h of exposure increased with decreasing oxygen tensions from 5 to 0.1%. Because the original description of CA IX was as an antigen induced by culture of cells at high density (37), we also compared the effects of culture at high density with those of hypoxia. In normoxic cultures of A549 cells, high density clearly induced CA IX, although the effect was considerably smaller than that of hypoxia (Fig. 3C).

CA IX Expression in Human Tumors. We next sought to determine whether regulation of *CA9* by hypoxia in tissue culture cells was reflected in patterns of expression within naturally occurring human tumors. To confirm the specificity of M75 immunostaining in our laboratory, we first compared immunohistochemical staining with CA IX immunoblot signals in pellets of cultured cells. Pellets were prepared from normoxic cultures of RCC4 and RCC4/VHL cells and processed in parallel for whole-cell protein extraction and immunohistochemistry. In keeping with the immunoblotting results, immunostaining of these sections with M75 revealed strong membrane expression of CA IX in RCC4 cells (Fig. 4A) and no staining in

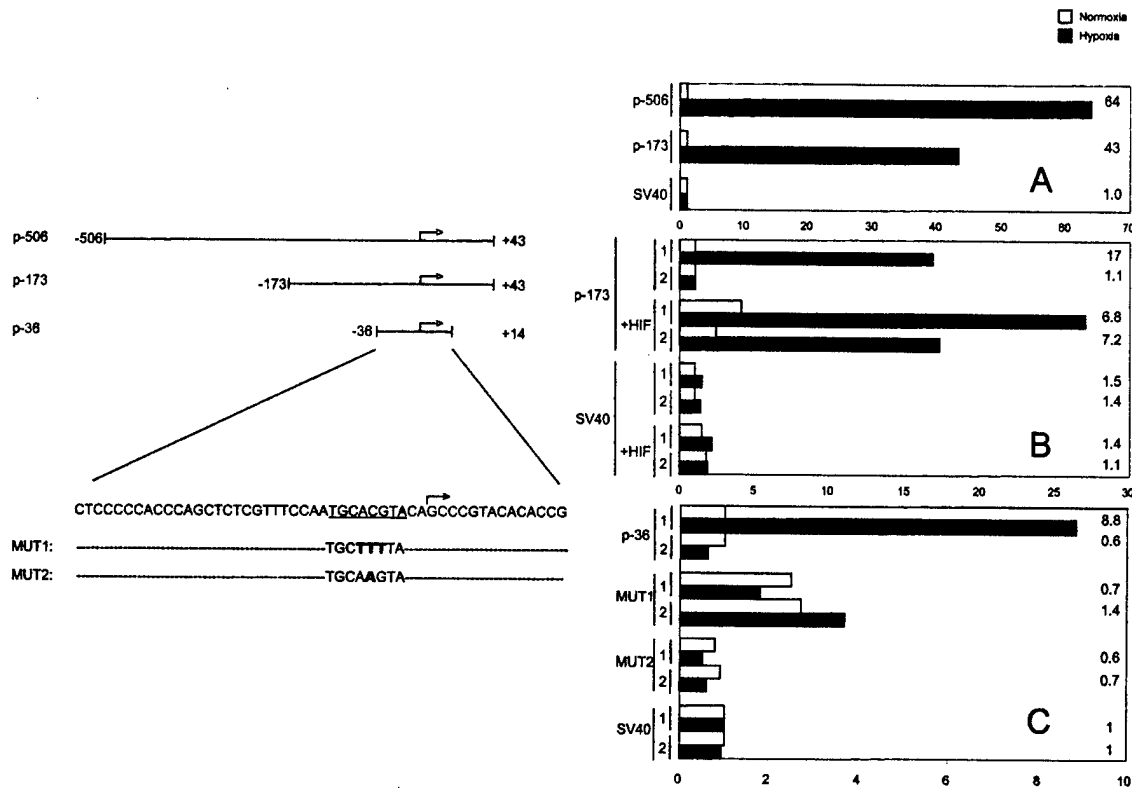


Fig. 2. Functional analysis of human *CA9* 5'-flanking sequences in transient expression assays. *Left panel*, schematic diagram of reporter genes; the indicated *CA9* wild-type and mutant sequences were inserted 5' to a promoterless luciferase reporter gene. *Arrow*, 5' transcriptional initiation site. *Underlined sequence*, *CA9* putative HRE. *Right panels*, reporter gene activities in transiently transfected cells. *CA9* promoter sequences are indicated to the left of each column. *SV40*, control minimal SV40 promoter. *A*, activities in normoxic and hypoxic HeLa cells. *B* and *C*, activities in wild-type CHO (C4.5) cells (columns 1) and HIF-1 α -deficient CHO (Ka13) cells (columns 2). *A*, hypoxia-inducible activity of the *CA9* promoter. *B*, hypoxia-inducible activity of the *CA9* promoter is ablated in Ka13 cells. Cotransfection of HIF-1 α restores induction by hypoxia in Ka13 cells and augments *CA9* promoter activity in both wild-type and Ka13 cells. In comparison, minimal effects are seen on the SV40 promoter. *C*, a minimal *CA9* promoter retains HIF-1 α -dependent, hypoxia-inducible activity. Two mutations within the putative HRE, MUT1 and MUT2, completely ablate hypoxia-inducible activity, whereas basal transcription is preserved. Columns, mean luciferase activities corrected for transfection efficiency from a typical experiment performed in duplicate. Each duplicate experiment was repeated two to six times. Numbers to the right are the ratios of hypoxic to normoxic expression of the indicated reporter construct. Transfected cells were incubated at 20% O₂ for 8 h and then incubated at 20% O₂ (normoxia) or 0.1% O₂ (hypoxia) for 16 h.

normoxic RCC4/VHL cells (Fig. 4B). Then, we compared immunostaining and immunoblots of tissue extracts from similar regions of tumor and normal tissue in four sets of paired samples from surgical excisions of head and neck tumors. By immunostaining, CA IX

expression was low or absent in normal tissue surrounding the tumors but was expressed at significant levels in each tumor specimen. Results of immunoblot analysis correlated closely with immunostaining, signals being very low or undetectable in each normal tissue sample, and correlated with the extent of CA IX immunostaining in tumor samples (data not shown).

Of particular interest to regulation by hypoxia is the relationship of CA IX expression to zones of tumor necrosis. This was first examined in a series of nine tumors of head and neck, breast, and ovary, each of which showed well-defined zones of necrosis. Three tumors of each type were analyzed. In each specimen, a predominantly or even exclusively perinecrotic expression pattern was observed for CA IX. Representative sections from each tumor type are illustrated in Fig. 4. Expression was localized to the cellular membrane. Tracing a line from the necrotic center to adjacent viable cells revealed a gradient of CA IX expression, with the highest levels observed in cells closest to or within necrotic regions (Fig. 4, C-F).

Because pVHL inactivation leads to loss of *CA9* regulation by oxygen in cultured cells and is common in clear cell renal carcinoma but not other renal tumors, we next compared expression patterns in a second series of 35 clear cell renal tumors and eight papillary renal tumors. Representative sections from a clear cell and a papillary tumor are illustrated in Fig. 4, G and H. Expression patterns were markedly different. In 33 of 35 clear cell tumors, (both sporadic and derived from VHL syndrome patients), CA IX was expressed throughout

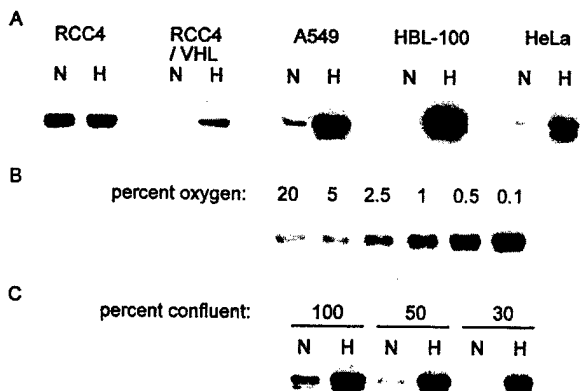


Fig. 3. Regulation of CA IX protein by hypoxia and cell density. Western blots of whole-cell extracts using anti-CA IX monoclonal antibody M75 are shown. *A*, cells exposed to either normoxia (N; 20% O₂) or hypoxia (H; 0.1% O₂) for 16 h. Expression is constitutive in the VHL-defective cell line, RCC4, but inducible by hypoxia in RCC4/VHL transfectants and a range of nonrenal cell lines. *B*, effects of graded hypoxia; A549 cells, 16 h exposure to the indicated oxygen concentration. *C*, comparison of induction by increasing cell density and hypoxia; A549 cells, 16 h exposure to hypoxia.

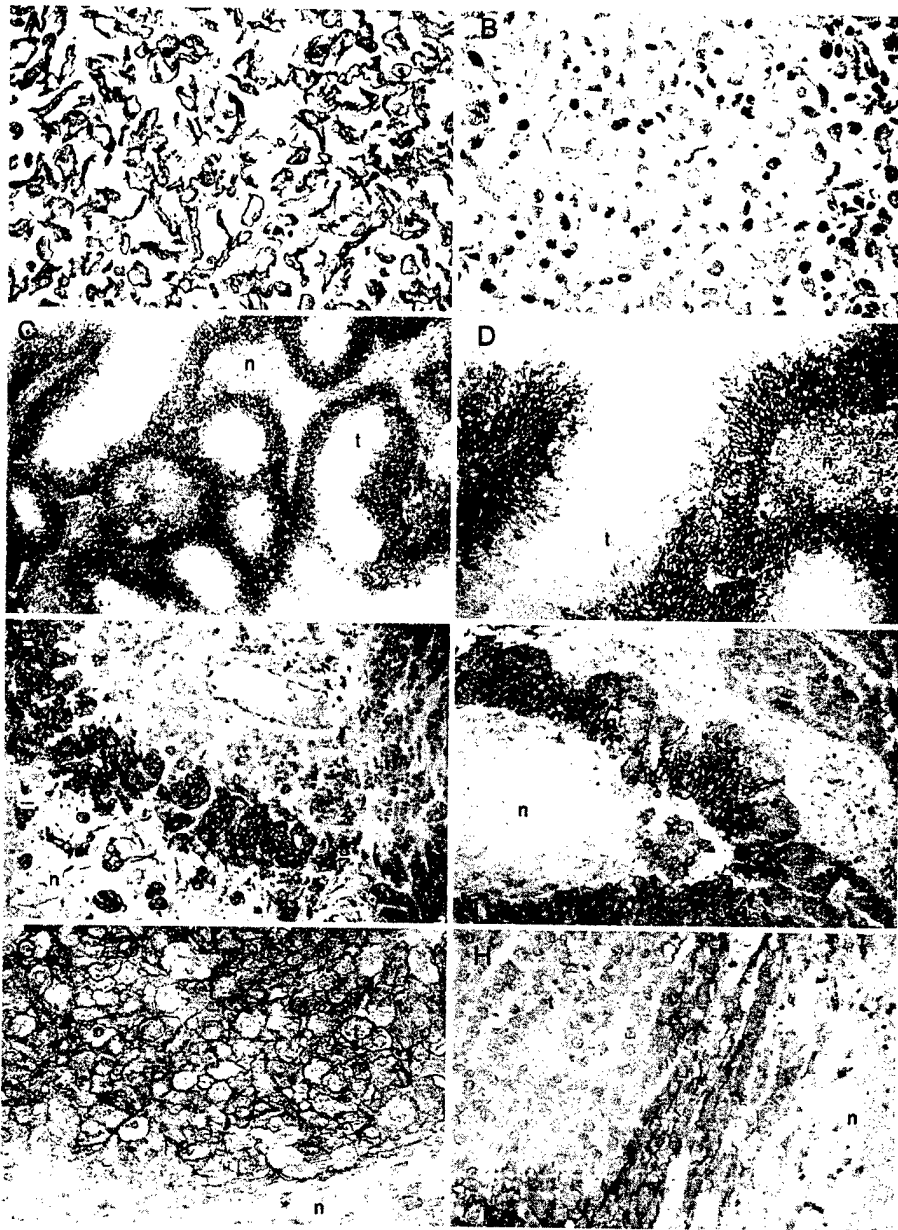


Fig. 4. Immunohistochemical analysis of CA IX expression in cell pellets and tumor biopsies. Sections were stained with anti-CA IX monoclonal antibody M75. *A* and *B*, paraffin-embedded cell pellets of normoxic RCC4 and RCC4/VHL respectively. Tumor sections showing the relationship of CA IX expression to regions of necrosis: *C* and *D*, head and neck carcinoma; *E*, breast adenocarcinoma; *F*, ovarian adenocarcinoma; *G*, clear cell renal carcinoma from a VHL syndrome patient; *H*, papillary renal carcinoma. Staining is predominantly membranous. A focal perinecrotic pattern is observed in all tumors except clear cell renal carcinomas. *n*, regions of necrosis; *t*, regions of viable tumor cells. *A*, *B*, and *D-H*, $\times 200$; *C*, $\times 100$.

tumor tissue; strong membrane staining was observed in tumor cells, regardless of proximity to necrosis or vessels (*G*). In contrast, in papillary renal tumors CA IX immunostaining was much less evident but was observed in tumors containing areas of necrosis, where, as with the nonrenal tumors, staining was strikingly focal and perinecrotic (four of eight papillary tumors contained necrosis, and all four showed focal CA IX positivity; Fig. 4*H*). Thus, the tight regulation of CA9 expression by oxygen observed in cell culture appeared to be reflected in strikingly focal patterns of expression around areas of necrosis.

Relationship of CA IX Expression with an Endogenous and an Administered Hypoxia Marker in Human Tumors. To compare CA IX expression with potential markers of tumor hypoxia, we examined expression of VEGF mRNA and activation of the bioreductive hypoxia marker pimonidazole in relationship to CA IX staining. Serial sections of a subset of our first series of tumors were analyzed for VEGF mRNA expression by *in situ* hybridization, and

CA IX expression was analyzed by immunostaining. Representative views from an ovarian and head and neck tumor sample are illustrated in Fig. 5. VEGF mRNA was expressed at varying levels throughout tumor tissue but was increased greatly in regions adjacent to necrosis. CA IX immunostaining showed strong overlap but was more tightly limited to perinecrotic regions.

For comparison of pimonidazole staining with CA IX expression, a series of 14 transitional cell bladder carcinomas and 6 squamous or basal cell skin carcinomas derived from patients who had received pimonidazole prior to surgical excision of tumor tissue was analyzed. Representative views of pimonidazole- and CA IX-stained sections are illustrated in Fig. 6, and assessment of pimonidazole and CA IX staining with corresponding overlap for each tumor biopsy are indicated in Table 1. In most tumors (16 of 20), pimonidazole staining was more extensive across tumor sections than CA IX staining, being primarily banded around necrotic areas (Fig. 6, *C* and *E*) and the periphery of papillary structures in bladder carcinomas (Fig. 6*A*).

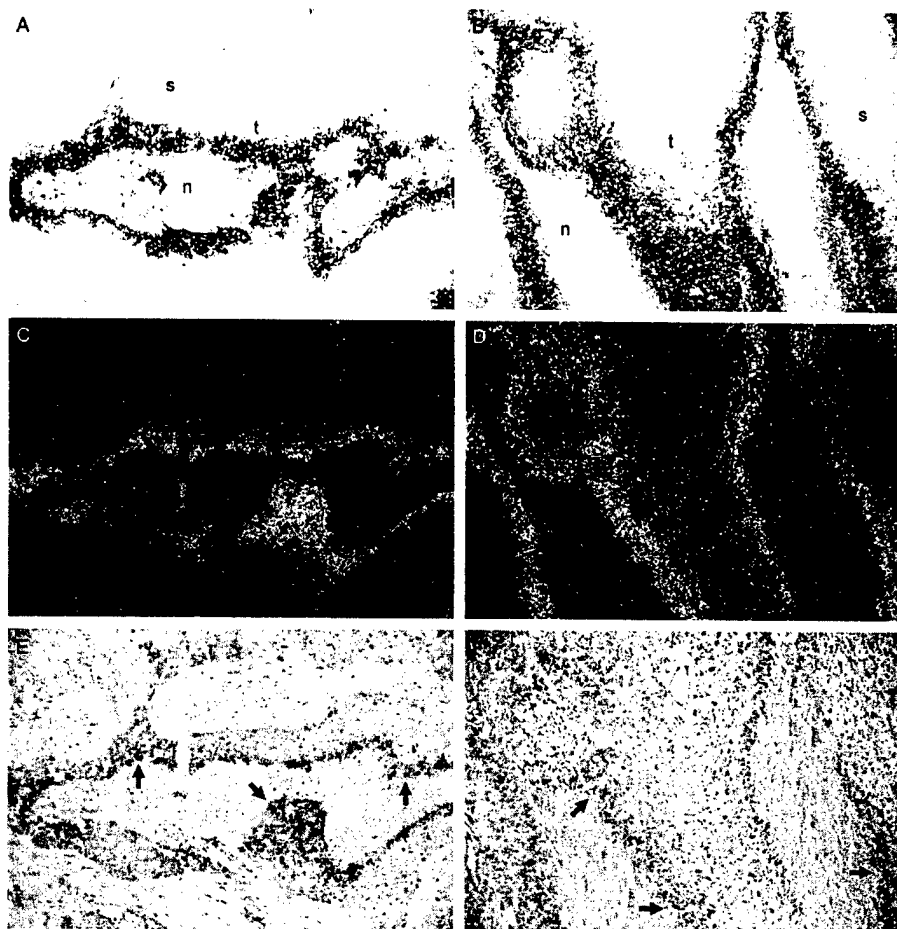


Fig. 5. Comparison of expression patterns for CA IX and VEGF in tumor biopsies. Immunohistochemical detection of CA IX using anti-CA IX monoclonal antibody M75 and *in situ* mRNA analysis of VEGF is shown. A, C, and E, ovarian adenocarcinoma. B, D, and F, head and neck carcinoma. A and B, CA IX immunostaining. C and D, dark-field views of *in situ* hybridization for VEGF mRNA on sections serial to the CA IX-immunostained sections. E and F, bright-field views of VEGF *in situ*. Arrows within necrotic areas (n) in bright-field views point toward the boundary with viable tumor cells. s, stroma; t, regions of viable tumor cells. All panels, $\times 100$.

Although less extensive, the large majority of CA IX immunostaining localized within regions of pimonidazole adduct formation and was also associated with necrosis (Fig. 6, D and F) or the periphery of papillary structures in bladder carcinomas (Fig. 6B). Some regions containing CA IX were observed that were slightly farther removed from necrosis than regions staining positive for pimonidazole (Fig. 6, C and D). In 4 of 20 cases, CA IX staining was more extensive than pimonidazole staining. In these cases, in addition to the characteristic perinecrotic and peripheral papillary expression, a proportion of CA IX expression was not obviously associated with such regions in the plane of the section. Nevertheless, within these four tumors the pimonidazole-positive regions were consistently localized within regions of CA IX positivity, again demonstrating the overlap between these markers. Despite the relationship between pimonidazole and CA IX at the microscopic level in all tumors, we did not observe an overall correlation between the percentage of tumor stained for pimonidazole and CA IX (Table 1).

DISCUSSION

In this work, we have demonstrated that the tumor-associated CAs CA9 and CA12 are strongly inducible by hypoxia in a broad range of tumor cells. Our findings also explain up-regulation of these CA isoforms in VHL-defective renal tumors, indicating that they are expressed constitutively at a high level in VHL-defective cells as a consequence of constitutive activation of HIF. The work therefore extends the range of HIF target genes to a new class of molecule that may have important implications for understanding the consequences

of microenvironmental tumor hypoxia, as well as the tumor-promoting effects of VHL inactivation. The regulation of CA9 was particularly tightly controlled by oxygen, and we analyzed the hypoxia-inducible response of this gene in detail.

Studies of the CA9 promoter demonstrated that sequences close to the transcriptional initiation site were sufficient to convey a hypoxia-inducible response, that this activity was mediated by HIF, and that it was dependent on a consensus HRE lying adjacent to the initiation site. The CA9 promoter contains neither a TATA box nor a consensus initiator sequence at the cap site (38). The association of this unusual anatomy with tight regulation by hypoxia is therefore of interest and suggests that it may be informative to pursue the mechanism by which HIF interacts with the basal transcriptional machinery operating on this gene. Furthermore, irrespective of the mechanism, the strong inducibility conveyed by the minimal CA9 promoter is unusual and may itself be of utility, for instance in the refinement of gene therapy vectors seeking to target therapeutic gene expression to hypoxic regions of tumors (39, 40).

Our findings also raise a number of issues relevant to recently published analyses of the CA9 promoter that did not examine the effect of hypoxia: (a) they provide an explanation for the remarkably low levels of CA9 promoter activity recently reported under standard culture conditions (41), because promoter activity is so strongly dependent on hypoxia; (b) they are consistent with the positive activity demonstrated for sequences -173 to $+31$ (41) and show that the transcriptional effects mediated by these sequences interact with the HRE in the minimal promoter to amplify the response to hypoxia; (c)

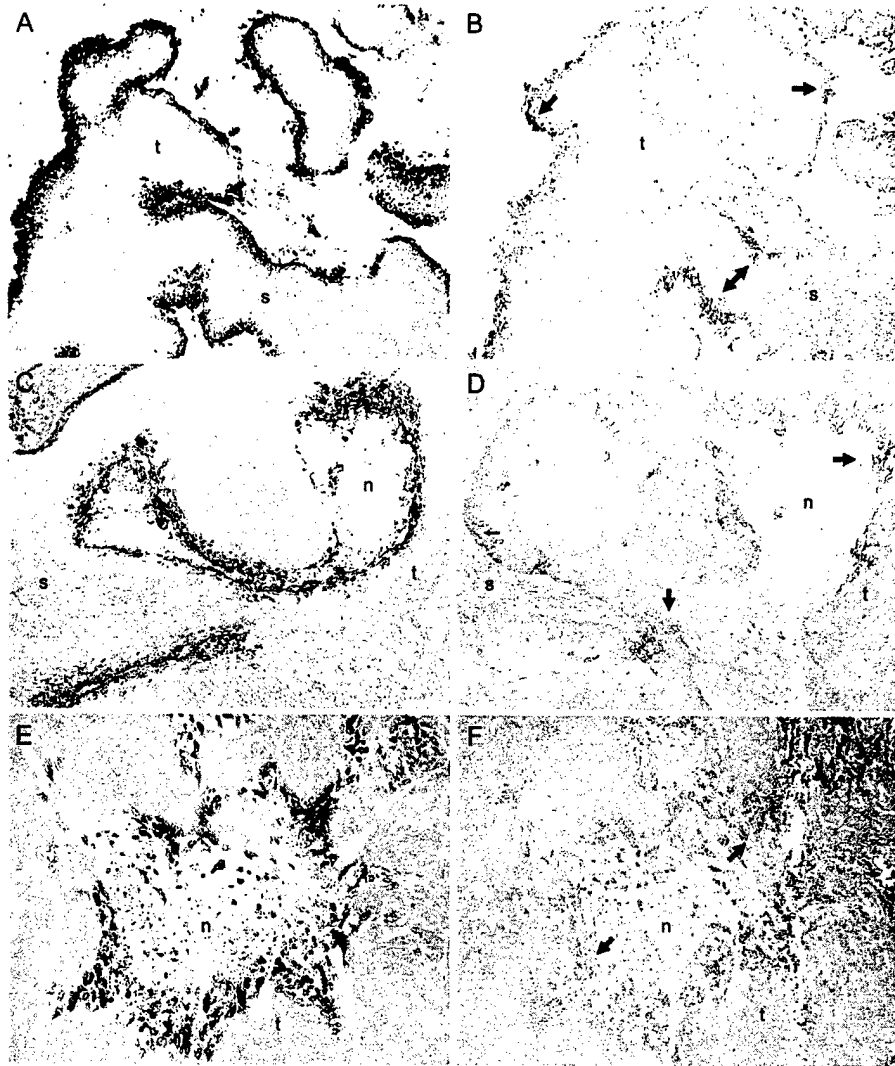


Fig. 6. Comparison of patterns of CA IX expression and pimonidazole adduct formation. A–D, bladder carcinomas; E and F, skin carcinoma. Left-hand panels, pimonidazole immunostaining. Right-hand panels, CA IX immunostaining on semiserial sections. Large arrows within CA IX-stained sections point toward regions of CA IX positivity that overlap with pimonidazole staining. Small arrow (D) highlights region of CA IX positivity farther removed from necrosis than pimonidazole-stained region. n, regions of necrosis; s, stroma; t, regions of viable tumor cells. All panels, $\times 50$.

they are consistent with the absence of a DNase I footprint in the region of the HRE (41), because even in hypoxia it has been shown that HIF-1 binding characteristics are such that an *in vitro* footprint is not demonstrated (42); (d) they provide a potential explanation for the repressive effects of p53 expression on the activity of the *CA9* promoter in some cells (43), because it has been suggested that p53 can interact with the regulation of HIF-1 α stability so as to reduce activity of the HIF/HRE complex (15, 16).

In tissue culture, *CA9* demonstrated a very marked difference between constitutive expression in VHL-defective RCC cells and strong induction by hypoxia in cells known or presumed to be VHL competent. This provided an opportunity to determine the extent to which these contrasting patterns of regulation in culture were reflected in patterns of expression within native tumors. In our series of renal tumors, we found a striking contrast between generalized expression in clear cell carcinomas, which are usually defective in VHL, and focal perinecrotic expression in papillary renal tumors, which are usually wild type for VHL. Notwithstanding the absence of direct ascertainment of VHL genotype in all of the tumors analyzed, this strongly suggests that effects of VHL status on HIF-dependent, hypoxia-inducible gene expression are reflected in patterns of expression within native tumors. Up-regulation by constitutively active HIF therefore provides an explanation for the utility of *CA9* as a marker for

clear cell carcinoma. The pattern of diffuse expression in clear cell carcinoma is in agreement with findings of a previous analysis of CA IX expression in which the authors focused on high levels of expression in clear cell carcinoma *versus* absent expression in a variety of benign lesions and postulated that CA IX expression might be useful as a marker of malignant change (25). That study also noted focal expression in papillary renal carcinoma, although the authors did not comment on the relation to necrosis. In our studies, we found that the striking localization of focal CA IX expression to zones of necrosis is not just observed in papillary renal carcinoma but also in several series of nonrenal tumors. The pattern is similar to that first described for VEGF mRNA (5), and we compared directly the pattern of CA IX immunostaining with that of *in situ* mRNA hybridization for VEGF in several types of tumors. In this work, we used *in situ* mRNA hybridization for VEGF to localize the site of production, because, in contrast with CA IX, some isoforms of VEGF are secreted. Patterns of expression for CA IX and VEGF mRNA were clearly concordant. However, CA IX expression was more strikingly delimited, being essentially limited to regions surrounding zones of necrosis.

The concordance of hypoxia-inducible *versus* constitutive patterns of expression in tissue culture with focal perinecrotic *versus* diffuse patterns of expression in tumors strongly supports the view that the focal perinecrotic pattern of expression is driven by microenviron-

Table 1 CA IX expression and pimonidazole activation in bladder and skin carcinomas

Tumor type	CA IX ^a	pim ^a	Overlap ^b
Bladder	25	25	+
Bladder	25	25	+
Bladder	50	30	++ (+ +)
Bladder	5	50	++
Bladder	5	25	++
Bladder	5	25	++
Bladder	5	25	++
Bladder	5	25	++
Bladder	5	20	++
Bladder	10	15	++
Bladder	0	25	NA
Bladder	0	5	NA
Bladder	10	0	NA
Skin	10	2	– (+ +)
Skin	50	15	– (+ +)
Skin	50	25	++ (+ +)
Skin	20	50	++
Skin	0	5	NA
Skin	0	0	NA

^a Semiquantitative estimate of the percentage of tumor cells within the entire tumor section staining positive for either CA IX or pim (pimonidazole).

^b Semiquantitative estimate of the percentage of tumor staining positive for CA IX that also stained positive for pimonidazole. Numbers in parentheses, semiquantitative estimate of the percentage of tumor staining positive for pimonidazole that also stained positive for CA IX in the four tumors in which CA IX staining was more extensive than pimonidazole staining. ++, 90–100%; +, 50–90%; –, <50%; NA, not applicable (no staining for one or both antigens).

mental hypoxia. Furthermore, the particularly tight regulation of CA9 by hypoxia suggested that it might be useful as a hypoxia marker. It was, therefore, of interest to compare the pattern of CA IX immunostaining with staining for the hypoxia marker pimonidazole (44–46). Our analysis demonstrated clear overlap of the staining patterns, supporting expression of CA IX in hypoxic regions. Previous studies have compared the distribution of immunodetectable pimonidazole adducts with VEGF immunostaining. One study concluded that pimonidazole and VEGF displayed the same pattern of staining on adjacent sections during the angiogenesis associated with a model of liver fibrogenesis (47), whereas an earlier study emphasized the discrepancies between pimonidazole and VEGF staining, although regions of overlap were demonstrated (48). Among the explanations considered for the differences between the distribution of VEGF staining and pimonidazole adducts were regulation of VEGF by nonhypoxic stimuli and diffusion of VEGF from hypoxic sites of production. For CA9, basal expression in normoxic cells was lower than we have observed for VEGF, induction by hypoxia was more striking, and the protein was not secreted. Despite this, we also observed differences in pimonidazole and CA IX staining. The substantial regions of overlap presumably reflect regions where tumor hypoxia was of sufficient duration and severity to activate both markers. Regions of nonoverlap could reflect the operation of additional positive or negative influences on expression or activation or different time frames of induction or activation. For instance, pimonidazole adducts are formed over a relatively short period of time and are then long-lived (45, 46), whereas we have found that CA IX is a stable protein that, in tissue culture, accumulated over a long period of hypoxia (data not shown). Thus, CA IX induction might only be expected in regions of relatively chronic tumor hypoxia and would reflect a different hypoxic time frame from pimonidazole activation. Correlation of focal CA IX expression with direct measurements of tumor oxygenation and with clinical parameters of outcome will be of interest.

The demonstration that an extracellular CA is up-regulated by microenvironmental tumor hypoxia has potentially important implications for understanding the regulation of tumor pH and the response to hypoxia. It has been widely held that lactate production by glyco-

lysis is a major cause of the acidic extracellular pH of tumors (49), and indeed glycolytic enzymes are induced by hypoxia (11), as is lactate production (50). However, tumors grown from mutant cells with glycolytic defects show a similar extracellular acidosis in the absence of lactate accumulation (51, 52), indicating that other mechanisms must be involved. Recently, it has been proposed that extracellular CAs could convert CO₂ diffusing from oxygenated areas to carbonic acid and promote the generation of bicarbonate and hydrogen ions (29, 52). Bicarbonate might then be exchanged for intracellular chloride, providing a mechanism for maintaining the characteristic extracellular acidosis and intracellular alkalosis that is postulated to promote tumor growth (53). Thus, it is likely that the hypoxia-inducible behavior of tumor-associated CAs could exert important biological effects through an influence on microenvironmental pH. This could have therapeutic implications because CA inhibitors have been shown to inhibit the invasion of renal cell carcinoma lines in model culture systems (54) and have synergistic effects with other chemotherapeutic agents in animal models (55). The potential for strong induction by hypoxia will now need to be considered in assessing the diagnostic and therapeutic implications of tumor-associated extracellular CAs.

ACKNOWLEDGMENTS

We thank Richard Poulsom, Rosemary Jeffery, and Jan Longcroft (Imperial Cancer Research Fund, Lincoln's Inn Fields, London, United Kingdom) for assistance with the *in situ* hybridization studies.

REFERENCES

- Höckel, M., Schlenger, K., Aral, B., Mitze, M., Schaffer, U., and Vaupel, P. Association between tumor hypoxia and malignant progression in advanced cancer of the uterine cervix. *Cancer Res.*, 56: 4509–4515, 1996.
- Brizel, D. M., Scully, S. P., Harrelson, J. M., Layfield, L. J., Bean, J. M., Prosnitz, L. R., and Dewhirst, M. W. Tumor oxygenation predicts for the likelihood of distant metastases in human soft tissue sarcoma. *Cancer Res.*, 56: 941–943, 1996.
- Heacock, C. S., and Sutherland, R. M. Induction characteristics of oxygen regulated proteins. *Int. J. Radiat. Oncol. Biol. Phys.*, 12: 1287–1290, 1986.
- Price, B. D., and Calderwood, S. K. Gadd45 and Gadd153 messenger RNA levels are increased during hypoxia and after exposure of cells to agents which elevate the levels of the glucose-regulated proteins. *Cancer Res.*, 52: 3814–3817, 1992.
- Shweiki, D., Itin, A., Soffer, D., and Keshet, E. Vascular endothelial growth factor induced by hypoxia may mediate hypoxia-initiated angiogenesis. *Nature (Lond.)*, 359: 843–845, 1992.
- Koong, A. C., Denko, N. C., Hudson, K. M., Schindler, C., Swiersz, L., Koch, C., Evans, S., Ibrahim, H., Le, Q. T., Terris, D. J., and Giaccia, A. J. Candidate genes for the hypoxic tumor phenotype. *Cancer Res.*, 60: 883–887, 2000.
- Maxwell, P. H., Dachs, G. U., Gleadle, J. M., Nicholls, L. G., Harris, A. L., Stratford, I. J., Hankinson, O., Pugh, C. W., and Ratcliffe, P. J. Hypoxia inducible factor-1 modulates gene expression in solid tumors and influences both angiogenesis and tumor growth. *Proc. Natl. Acad. Sci. USA*, 94: 8104–8109, 1997.
- Carmeliet, P., Dor, Y., Herbert, J. M., Fukumura, D., Brusselmans, K., Dewerchin, M., Neeman, M., Bono, F., Abramovitch, R., Maxwell, P., Koch, C. J., Ratcliffe, P., Moons, L., Jain, R. K., Collen, D., and Keshet, E. Role of HIF-1 α in hypoxia-mediated apoptosis, cell proliferation and tumour angiogenesis. *Nature (Lond.)*, 394: 485–490, 1998.
- Ryan, H. E., Lo, J., and Johnson, R. S. HIF-1 α is required for solid tumor formation and embryonic vascularization. *EMBO J.*, 17: 3005–3015, 1998.
- Ebert, B. L., Firth, J. D., and Ratcliffe, P. J. Hypoxia and mitochondrial inhibitors regulate expression of glucose transporter-1 via distinct *cis*-acting sequences. *J. Biol. Chem.*, 270: 29083–29089, 1995.
- Semenza, G. L., Roth, P. H., Fang, H.-M., and Wang, G. L. Transcriptional regulation of genes encoding glycolytic enzymes by hypoxia-inducible factor 1. *J. Biol. Chem.*, 269: 23757–23763, 1994.
- Kim, K. J., Li, B., Winer, J., Armanini, M., Gillett, N., Phillips, H. S., and Ferrara, N. Inhibition of vascular endothelial growth factor-induced angiogenesis suppresses tumour growth *in vivo*. *Nature (Lond.)*, 362: 841–844, 1993.
- Maxwell, P., Wiesener, M., Chang, G.-W., Clifford, S., Vaux, E., Cockman, M., Wykoff, C., Pugh, C., Maher, E., and Ratcliffe, P. The tumour suppressor protein VHL targets hypoxia-inducible factors for oxygen-dependent proteolysis. *Nature (Lond.)*, 399: 271–275, 1999.
- Jiang, B. H., Agani, F., Passaniti, A., and Semenza, G. L. V-SRC induces expression of hypoxia-inducible factor 1 (HIF-1) and transcription of genes encoding vascular endothelial growth factor and enolase 1: involvement of HIF-1 in tumor progression. *Cancer Res.*, 57: 5328–5335, 1997.
- Blagosklonny, M. V., An, W. G., Romanova, L. Y., Trepel, J., Fojo, T., and Neckers, L. p53 inhibits hypoxia-inducible factor-stimulated transcription. *J. Biol. Chem.*, 273: 11995–11998, 1998.

16. Ravi, R., Mookerjee, B., Bhujwalla, Z. M., Sutter, C. H., Artemov, D., Zeng, Q., Dillehay, L. E., Madan, A., Semenza, G. L., and Bedi, A. Regulation of tumor angiogenesis by p53-induced degradation of hypoxia-inducible factor 1 α . *Genes Dev.*, 14: 34–44, 2000.
17. Zundel, W., Schindler, C., Haas-Kogan, D., Koong, A., Kaper, F., Chen, E., Gottschalk, A., Ryan, H., Johnson, R., Jefferson, A., Stokoe, D., and Giaccia, A. Loss of *PTEN* facilitates HIF-1-mediated gene expression. *Genes Dev.*, 14: 391–396, 2000.
18. Gnarr, J. R., Tory, K., Weng, Y., Schmidt, L., Wei, M. H., Li, H., Latif, F., Liu, S., Chen, F., Duh, F.-M., Lubensky, I., Duan, D. R., Florence, C., Pozzatti, R., Walther, M. M., Bander, N. H., Grossman, H. B., Brauch, H., Pomer, S., Brooks, J. D., Isaacs, W. B., Lerman, M. I., Zbar, B., and Linehan, W. M. Mutations of the *VHL* tumour suppressor gene in renal carcinoma. *Nat. Genet.*, 7: 85–90, 1994.
19. Lisztwan, J., Imbert, G., Wirbelauer, C., Gstaiger, M., and Krek, W. The von Hippel-Lindau tumor suppressor protein is a component of an E3 ubiquitin-protein ligase activity. *Genes Dev.*, 13: 1822–1833, 1999.
20. Iwai, K., Yamanaka, K., Kamura, T., Minato, N., Conaway, R. C., Conaway, J. W., Klausner, R. D., and Pause, A. Identification of the von Hippel-Lindau tumor-suppressor protein as part of an active E3 ubiquitin ligase complex. *Proc. Natl. Acad. Sci. USA*, 96: 12436–12441, 1999.
21. Cockman, M. E., Masson, N., Mole, D. R., Jaakkola, P., Chang, G. W., Clifford, S. C., Maher, E. R., Pugh, C. W., Ratcliffe, P. J., and Maxwell, P. H. Hypoxia inducible factor- α binding and ubiquitination by the von Hippel-Lindau tumor suppressor protein. *J. Biol. Chem.*, 275: 25733–25741, 2000.
22. Pause, A., Lee, S., Loneragan, K. M., and Klausner, R. D. The von Hippel-Lindau tumor suppressor gene is required for cell cycle exit on serum withdrawal. *Proc. Natl. Acad. Sci. USA*, 95: 993–998, 1998.
23. Ohh, M., Yauch, R. L., Loneragan, K. M., Whaley, J. M., Stemmer-Rachamimov, A. O., Louis, D. N., Gavin, B. J., Kley, N., Kaelin, W. G., Jr., and Iliopoulos, O. The von Hippel-Lindau tumor suppressor protein is required for proper assembly of an extracellular fibronectin matrix. *Mol. Cell*, 1: 959–968, 1998.
24. Pastorek, J., Pastorekova, S., Callebaut, I., Mornon, J., Zelnik, V., Opavsky, R., Zatovicova, M., Liao, S., Portetele, D., Stanbridge, E., Zavada, J., Burny, A., and Kettmann, R. Cloning and characterization of MN, a human tumor-associated protein with a domain homologous to carbonic anhydrase and a putative helix-loop-helix DNA binding segment. *Oncogene*, 9: 2877–2888, 1994.
25. Liao, S.-Y., Aurelio, O., Jan, K., Zavada, J., and Stanbridge, E. Identification of the MN/CA9 protein as a reliable diagnostic biomarker of clear cell carcinoma of the kidney. *Cancer Res.*, 57: 2827–2831, 1997.
26. Saarnio, J., S. P., Parkkila, A.-K., Haukipuro, K., Pastorekova, S., Pastorek, J., Kairaluoma, M., and Karttunen, T. Immunohistochemical study of colorectal tumors for expression of a novel transmembrane carbonic anhydrase, MN/CA IX, with potential value as a marker of cell proliferation. *Am. J. Pathol.*, 153: 279–285, 1998.
27. Vermeylen, P., Roufosse, C., Burny, A., Verhest, A., Bosschaerts, T., Pastorekova, S., Ninane, V., and Sculier, J. P. Carbonic anhydrase IX antigen differentiates between preneoplastic malignant lesions in non-small cell lung carcinoma. *Eur. Respir. J.*, 14: 806–811, 1999.
28. Tureci, O., Sahin, U., Vollmar, E., Siemer, S., Gottert, E., Seitz, G., Parkkila, A. K., Shah, G. N., Grubb, J. H., Pfeundscher, M., and Sly, W. S. Human carbonic anhydrase XII: cDNA cloning, expression, and chromosomal localization of a carbonic anhydrase gene that is overexpressed in some renal cell cancers. *Proc. Natl. Acad. Sci. USA*, 95: 7608–7613, 1998.
29. Ivanov, S. V., Kuzmin, I., Wei, M.-H., Pack, S., Geil, L., Johnson, B. E., Stanbridge, E. J., and Lerman, M. I. Down-regulation of transmembrane carbonic anhydrases in renal cell carcinoma cell lines by wild-type von Hippel-Lindau transgenes. *Proc. Natl. Acad. Sci. USA*, 95: 12596–12601, 1998.
30. Sly, W. S., and Hu, P. Y. Human carbonic anhydrases and carbonic anhydrase deficiencies. *Annu. Rev. Biochem.*, 64: 375–401, 1995.
31. Wiesener, M. S., Turley, H., Allen, W. E., William, C., Eckardt, K.-U., Talks, K. L., Wood, S. M., Gatter, K. C., Harris, A. L., Pugh, C. W., Ratcliffe, P. J., and Maxwell, P. H. Induction of endothelial PAS domain protein-1 by hypoxia: characterization and comparison with hypoxia-inducible factor-1 α . *Blood*, 92: 2260–2268, 1998.
32. Pastorekova, S., Zavados, Z., Kostal, M., Babusikova, O., and Zavada, J. A novel quasi-viral agent, Ma Tu, is a two-component system. *Virology*, 187: 620–626, 1992.
33. Senior, P. V., Critchley, D. R., Beck, F., Walker, R. A., and Varley, J. M. The localization of laminin mRNA and protein in the postimplantation embryo and placenta of the mouse: an *in situ* hybridization and immunocytochemical study. *Development (Camb.)*, 104: 431–446, 1988.
34. Kennedy, A. S., Raleigh, J. A., Perez, G. M., Calkins, D. P., Thrall, D. E., Novotny, D. B., and Varia, M. A. Proliferation and hypoxia in human squamous cell carcinoma of the cervix: first report of combined immunohistochemical assays. *Int. J. Radiat. Oncol. Biol. Phys.*, 37: 897–905, 1997.
35. Wang, G. L., and Semenza, G. L. Desferrioxamine induces erythropoietin gene expression and hypoxia-inducible factor 1 DNA-binding activity: implications for models of hypoxia signal transduction. *Blood*, 82: 3610–3615, 1993.
36. Wood, S. M., Wiesener, M. S., Yeates, K. M., Okada, N., Pugh, C. W., Maxwell, P. H., and Ratcliffe, P. J. Selection and analysis of a mutant cell line defective in the hypoxia-inducible factor-1 α subunit (HIF-1 α). *J. Biol. Chem.*, 273: 8360–8368, 1998.
37. Zavada, J., Zavados, Z., Pastorekova, S., Ciampor, F., Pastorek, J., and Zelnik, V. Expression of MaTu-MN protein in human tumor cultures and in clinical specimens. *Int. J. Cancer*, 54: 268–274, 1993.
38. Opavsky, R., Pastorekova, S., Zelnik, V., Gibadulinova, A., Stanbridge, E. J., Zavada, J., Kettmann, R., and Pastorek, J. Human MN/CA9 gene, a novel member of the carbonic anhydrase family: structure and exon to protein domain relationships. *Genomics*, 33: 480–487, 1996.
39. Dachs, G. U., Patterson, A. V., Firth, J. D., Ratcliffe, P. J., Townsend, K. M. S., Stratford, I. J., and Harris, A. L. Targeting gene expression to hypoxic tumour cells. *Nat. Med.*, 3: 515–520, 1997.
40. Griffiths, L., Binley, K., Iqbal, S., Kan, O., Maxwell, P., Ratcliffe, P., Lewis, C., Harris, A., Kingsman, S., and Naylor, S. The macrophage—a novel system to deliver gene therapy to pathological hypoxia. *Gene Ther.*, 7: 255–262, 2000.
41. Kaluz, S., Kaluzova, M., Opavsky, R., Pastorekova, S., Gibadulinova, A., Dequiedt, F., Kettmann, R., and Pastorek, J. Transcriptional regulation of the MN/CA 9 gene coding for the tumor-associated carbonic anhydrase IX. Identification and characterization of a proximal silencer element. *J. Biol. Chem.*, 274: 32588–32595, 1999.
42. Semenza, G. L., and Wang, G. L. A nuclear factor induced by hypoxia via *de novo* protein synthesis binds to the human erythropoietin gene enhancer at a site required for transcriptional activation. *Mol. Cell. Biol.*, 12: 5447–5454, 1992.
43. Kaluzova, M., Pastorekova, S., Pastorek, J., and Kaluz, S. p53 tumour suppressor modulates transcription of the TATA-less gene coding for the tumour-associated carbonic anhydrase MN/CA IX in MaTu cells. *Biochim. Biophys. Acta*, 1491: 20–26, 2000.
44. Arteel, G. E., Thurman, R. G., Yates, J. M., and Raleigh, J. A. Evidence that hypoxia markers detect oxygen gradients in liver: pimonidazole and retrograde perfusion of rat liver. *Br. J. Cancer*, 72: 889–895, 1995.
45. Azuma, C., Raleigh, J. A., and Thrall, D. E. Longevity of pimonidazole adducts in spontaneous canine tumors as an estimate of hypoxic cell lifetime. *Radiat. Res.*, 148: 35–42, 1997.
46. Arteel, G. E., Thurman, R. G., and Raleigh, J. A. Reductive metabolism of the hypoxia marker pimonidazole is regulated by oxygen tension independent of the pyridine nucleotide redox state. *Eur. J. Biochem.*, 253: 743–750, 1998.
47. Rosmorduc, O., Wendum, D., Corpechot, C., Galy, B., Sebbagh, N., Raleigh, J., Housset, C., and Poupon, R. Hepatocellular hypoxia-induced vascular endothelial growth factor expression and angiogenesis in experimental biliary cirrhosis. *Am. J. Pathol.*, 155: 1065–1073, 1999.
48. Raleigh, J. A., Calkins-Adams, D. P., Rinker, L. H., Ballenger, C. A., Weissler, M. C., Fowler, W. C., Jr., Novotny, D. B., and Varia, M. A. Hypoxia and vascular endothelial growth factor expression in human squamous cell carcinomas using pimonidazole as a hypoxia marker. *Cancer Res.*, 58: 3765–3768, 1998.
49. Griffiths, J. R. Are cancer cells acidic? *Br. J. Cancer*, 64: 425–427, 1991.
50. Heacock, C. S., and Sutherland, R. M. Enhanced synthesis of stress proteins caused by hypoxia and relation to altered cell growth and metabolism. *Br. J. Cancer*, 62: 217–225, 1990.
51. Newell, K., Franchi, A., Pouyssegur, J., and Tannock, I. Studies with glycolysis-deficient cells suggest that production of lactic acid is not the only cause of tumor acidity. *Proc. Natl. Acad. Sci. USA*, 90: 1127–1131, 1993.
52. Yamagata, M., Hasuda, K., Stamato, T., and Tannock, I. F. The contribution of lactic acid to acidification of tumours: studies of variant cells lacking lactate dehydrogenase. *Br. J. Cancer*, 77: 1726–1731, 1998.
53. Martinez-Zaguilan, R., Seftor, E. A., Seftor, R. E., Chu, Y. W., Gillies, R. J., and Hendrix, M. J. Acidic pH enhances the invasive behavior of human melanoma cells. *Clin. Exp. Metastasis*, 14: 176–186, 1996.
54. Parkkila, S., Rajaniemi, H., Parkkila, A.-K., Kivela, J., Waheed, A., Pastorekova, S., Pastorek, J., and Sly, W. Carbonic anhydrase inhibitor suppresses invasion of renal cancer cells *in vitro*. *Proc. Natl. Acad. Sci. USA*, 97: 2220–2224, 2000.
55. Teicher, B. A., Liu, S. D., Liu, J. T., Holden, S. A., and Herman, T. S. A carbonic anhydrase inhibitor as a potential modulator of cancer therapies. *Anticancer Res.*, 13: 1549–1556, 1993.

Regulation of Growth and Tumorigenicity of Breast Cancer Cells by the Low Molecular Weight GTPase Rad and Nm23¹

Yu-Hua Tseng, David Vicent, Jianhua Zhu, Yulian Niu, Adewale Adeyinka, Julie S. Moyers, Peter H. Watson, and C. Ronald Kahn²

Research Division, Joslin Diabetes Center, Department of Medicine, Harvard Medical School, Boston, Massachusetts 02215 [Y.-H. T., D. V., J. Z., J. S. M., C. R. K.]; and Department of Pathology, University of Manitoba, Winnipeg, Manitoba R3E 0W3, Canada [Y. N., A. A., P. H. W.]

ABSTRACT

Rad is the prototypic member of a family of novel Ras-related GTPases that is normally expressed in heart, skeletal muscle, and lung and that has been shown to exhibit a novel form of bi-directional interaction with the nm23 metastasis suppressor. In the present study, we have investigated the expression of Rad in normal and neoplastic breast tissues by Western blot and immunohistochemistry and the functional effect of altered Rad expression in breast cancer cell lines. We found that, although Rad is frequently expressed in normal breast tissue (23/30 Rad+ve), expression is usually lost in adjacent invasive carcinoma (8/30 Rad+ve; $P < 0.0001$). However, where Rad expression persists in a small proportion of tumors, it is associated with higher grade, larger size, and extensive axillary nodal involvement ($n = 48$; $P = 0.035$, $P = 0.016$, $P = 0.022$, respectively). Furthermore, Rad is also highly expressed in a breast cancer cell line with high tumorigenic and metastatic potential (MDA-MB231). To further examine the role of Rad in breast cancer, we stably transfected a Rad-ve breast cancer cell line (MDA-MB435). We observed an increase in growth and marked increased colony formation in soft agar *in vitro* ($P < 0.05$) and an increase in tumor growth rate in nude mice ($P < 0.05$). Moreover, coexpression of nm23 with wild-type Rad inhibited the effect of Rad on growth of these cells in culture and markedly inhibited tumor growth *in vivo*. Additional transfection studies with mutated Rad cDNAs revealed that the growth-promoting effects of Rad appeared to be mediated through its NH₂- and COOH-terminal regions, rather than its GTPase domain, and might involve acceleration of cell cycle transition. These findings suggest that Rad may act as an oncogenic protein in breast tissues and demonstrate a potential mechanism by which interaction between Rad and nm23 may regulate growth and tumorigenicity of breast cancer.

INTRODUCTION

Development and progression of breast cancer is a complex process involving both hormonal and genetic factors. Among the several hormones known to stimulate both normal and malignant mammary cell proliferation are steroids, such as estrogen (1) and progesterone (2), and peptide growth factors, such as prolactin (3), insulin (4), and insulin-like growth factor-1 (5). Alterations of a number of genes in breast cancer have also been identified, some of which have been proposed as molecular markers to help predict the prognosis. These include breast cancer susceptibility genes *BRCA-1* and -2, p53, Her-2/neu (c-erbB-2), and some regulatory proteins of cell cycle such as cyclin D1 and p27Kip1. Still further altered genes may emerge from investigations centered on chromosomal regions showing loss of heterozygosity (for review, see Ref. 6). Despite the recognition of these factors, the molecular mechanisms of formation of breast cancer still remain unclear, and identification of regulatory genes in the

process of tumorigenesis and metastasis is one of the major goals of cancer research.

Rad is a M_r 35,000 small GTPase that was initially cloned by subtractive cloning as a mRNA overexpressed in skeletal muscle of some type-2 diabetic humans and is normally highly expressed in heart and lung (7). It is the prototypic member of a newly emerged Ras-related GTPase family with several unique characteristics, including Gem/Kir, Rem, Rem2 and Ges. Gem/Kir was found by its overexpression in activated T lymphocytes (8) and in v-abl-transformed pre-B cells (9). Rem was cloned as a product of PCR amplification using oligonucleotide primers derived from conserved regions of Rad and Gem/Kir as a mRNA that was repressed by lipopolysaccharide in mice (10). Rem2 mRNA is expressed in rat brain and kidney and possesses a novel cellular localization signal that is different from most Ras-related proteins (11). Ges is expressed in the endothelium and functions as a promoter of cytoskeleton reorganization (12). All of these G proteins possess several structural features that are distinct from other Ras-related GTPases, including major NH₂- and COOH-terminal extensions, a lack of typical prenylation motifs, and several nonconservative changes in the sequence of the GTP-binding domain. The NH₂ terminus of Rad is extended by 88 amino acids, and the COOH-terminus is extended by 31 amino acids as compared with Ras. As a result of the lack of a prenylation motif, Rad is primarily a cytosolic protein that associates with the cytoskeleton in a nonlipid-dependent manner (13). Rad, Gem, and Rem differ from each other and from other Ras-like molecules in the pupative effector (G2) domain. They also contain residues in the G3 consensus sequence for guanine nucleotide binding that are divergent from Ras (7). By expression cloning and coimmunoprecipitation, Rad can be shown to interact with CaM,³ CaMKII (14), and β -tropomyosin (15). These interactions are enhanced by an increase in calcium influx and favor the GDP-bound form of Rad. Overexpression of Rad in 3T3-L1 adipocytes and C2C12 myocytes causes a marked reduction in insulin-stimulated glucose uptake (16). However, the exact function of Rad is still unknown.

Our laboratory has recently identified a novel form of bi-directional interaction between Rad and nm23 (17). In this complex, nm23 acts as both a GTPase-activating protein and a guanine nucleotide exchange factor for Rad, determining the balance between GTP-Rad and GDP-Rad. The first nm23 gene (*nm23-M1*) was originally identified by subtractive cloning in murine melanoma cell lines as a putative tumor metastasis suppressor (18). Since then, an additional murine nm23 gene, *nm23-M2* (19), and five human nm23 genes, namely *nm23-H1* (20), *nm23-H2* (21), *DR-nm23* (22), *nm23-H4* (23), and *nm23-H5* (24), have been identified. The metastasis suppressor function of nm23 has been demonstrated by both *in vivo* and *in vitro* experiments that show reduced incidence of primary tumor formation and a significant reduction in metastatic potential on transfection of nm23-M1 and nm23-H1 cDNA into highly metastatic murine melanoma cells (25) and human breast cancer cells (26), respectively. In addition,

Received 5/22/00; accepted 1/10/01.

The costs of publication of this article were defrayed in part by the payment of page charges. This article must therefore be hereby marked advertisement in accordance with 18 U.S.C. Section 1734 solely to indicate this fact.

¹Supported by the NIH Grant DK-45935 (to C. R. K.). P. H. W. is supported by a Scientist Award from the Medical Research Council of Canada. The National Cancer Institute of Canada-Manitoba Breast Tumor Bank is funded by the National Cancer Institute of Canada.

²To whom requests for reprints should be addressed, at Joslin Diabetes Center, One Joslin Place, Boston, MA 02215. Phone: (617) 732-2635; Fax: (617) 732-2593; E-mail: c.ronald.kahn@joslin.harvard.edu.

³The abbreviations used are: CaM, calmodulin, CaMKII, calmodulin-dependent protein kinase II; Wt, wild-type.

nm23 transfection inhibits motility of human and murine tumor cells in response to different factors (27). Nm23 possesses several enzymatic activities, including a nucleoside diphosphate kinase activity (28), a histidine kinase activity (29), and a serine protein kinase activity (30). Rad has been shown to enhance the nucleoside diphosphate kinase activity of nm23 and decrease its autophosphorylation (17).

In addition to its potential function on suppression of tumor metastasis, several reports have suggested that nm23 has a role in cell differentiation and proliferation (for review, see Ref. 31). Nm23 H2 has been found to be identical to the c-myc transcription factor, PuF (32). The homologue of nm23 in *Drosophila* is the Awd (abnormal wing discs) protein (33). Mutation in *awd* causes abnormal structures of imaginal disc during wing development (34). A correlation between increased nm23 expression and cell proliferation has also been suggested by other investigations. The levels of nm23 expression strictly correlate with cell growth rate and DNA synthesis in the human breast epithelial cell line, MCF-10A (35, 36). Overexpression of nm23 in rat pheochromocytoma PC12 cells enhances nerve growth factor-induced sympathetic neuronal cell differentiation by delaying cell cycle transition and increasing neurite outgrowth (37). Nevertheless, the biochemical mechanism of nm23 action is unknown to date.

In this report, we show that Rad is expressed in some human breast cancer and breast cancer cell lines and that expression is related to features of poor prognosis *in vivo*. In cultured cells, overexpression of Rad causes a marked increase in growth and increased colony formation in soft agar, and these effects are inhibited by nm23. Moreover, similar effects are seen when these cells are injected into nude mice. These findings suggest that the Rad-nm23 interaction may regulate growth and tumorigenicity of human breast cancer cells.

MATERIALS AND METHODS

Human Breast Cancer Specimens. All of the breast tumor cases used for this study were selected from the National Cancer Institute of Canada-Manitoba Breast Tumor Bank (Winnipeg, Manitoba, Canada). As described previously (38), tissues are rapidly collected and processed to create matched formalin-fixed-embedded and frozen tissue blocks for each case. The histology of every sample in the bank is uniformly interpreted by a pathologist in H&E-stained sections from the face of the paraffin tissue block. For each case, interpretation data include an estimate of the cellular composition of the section used for study, tumor type, and tumor grade (Nottingham score; Ref. 39). Steroid receptor status was determined for all of the cases by ligand binding assay performed on an adjacent portion of tumor tissue. Tumors with estrogen and progesterone receptor levels above 3 fmol/mg and 15 fmol/mg of total protein, respectively, were considered estrogen-receptor or progesterone-receptor positive.

Two cohorts of tumors were selected. The first cohort comprised a series of 24 invasive ductal tumors selected only to ensure >25% tumor cells/section. Frozen sections from these cases were cut and used for protein extraction and Western blot analysis in our preliminary survey of Rad expression. The second cohort of 48 invasive ductal carcinomas was selected to comprise tumors with approximately equivalent numbers of each tumor grade [low, intermediate, and high (15, 16, and 17 cases, respectively)] and a range of estrogen receptor, progesterone receptor, nodal status, and tumor sizes (Table 1). Additional selection criteria also included high tissue quality, presence of invasive tumor within >25% of the cross-section of the paraffin block, and, where possible, normal ducts or lobules adjacent to the tumor to allow comparison between tumor and normal tissue.

Immunohistochemistry. Immunohistochemistry was performed using polyclonal anti-Rad antibody (1:200 dilution) and the AEC Kit (DAKO Envision System, Toronto, Ontario, Canada) following the manufacturer's instructions. Slides were counterstained with H&E. Rad expression was assessed by brightfield microscopic examination at low (10× objective) magnification with reference to negative control tumor sections run with each batch. Levels of expression were scored semiquantitatively by assessing the average signal

Table 1 Rad expression status relative to the clinical-pathological features of the cohort of invasive breast tumors studied

		Total No.	Rad -ve	Rad +ve	P ^a
ER ^b	+ve	37 (77) ^c	26 (54)	11 (23)	ns ^b
	-ve	11 (23)	8 (17)	3 (6)	
PR ^b	+ve	30 (62.5)	20 (42)	10 (21)	ns
	-ve	18 (37.5)	14 (29)	4 (8)	
Grade	I	15 (31)	15 (31)	0 (0)	0.035
	II	16 (33.5)	8 (17)	8 (17)	
	III	17 (35.5)	11 (23)	6 (12)	
Size ^d	0-2	12 (25)	11 (23)	1 (2)	0.022
	2-5	22 (46)	17 (35.5)	5 (10.5)	
	>5	7 (14.5)	3 (6)	4 (8.5)	
	Unknown	7 (14.5)	4 (8.5)	3 (6)	
NS ^b	0	18 (37.5)	15 (31)	3 (6)	0.016
	+ve (1-2)	9 (19)	8 (17)	1 (2)	
	+ve ≥3	14 (29)	6 (12)	8 (17)	
	Unknown	7 (14.5)	5 (11)	2 (4)	

^a P, χ^2 test for trend.

^b ER, estrogen receptor status; PR, progesterone receptor status; NS, nodal status; ns, not significant.

^c Numbers in parentheses represent approximate percentage values.

^d Tumor size in cm².

intensity (on a scale of 0 to 3) and the proportion of tumor cells showing a positive signal (0, none; 0.1, less than one tenth; 0.5, less than one half; 1.0, greater than one half). The intensity and proportion scores were then multiplied to give an overall score. Tumors with a score equal to or higher than 1.0 were deemed positive.

Cell Culture and Transfection of Cell Lines. Human breast carcinoma cell lines MDA-MB435 expressing pCMV vector or pCMVnm23-H1 construct (cell lines C-100 and H1-177, respectively; Ref. 26) were generous gifts from Dr. Patricia S. Steeg (National Cancer Institute, Bethesda, Maryland). These cells were transfected with pBabe puromycin resistance vector only (Puro) or expressing full-length human Wt Rad cDNA, the Rad S105N mutant, the Rad N88 mutant, the Rad C249 mutant, or the full-length cDNA of Gem by calcium phosphate method (14, 15). Stable cell lines were established by selection in puromycin-containing media (2 μ g/ml). Cells were maintained in DMEM containing 10% fetal bovine serum in a 5% CO₂ environment.

Immunoblotting. Cells grown on a 100-mm dish were washed twice with ice-cold PBS and scraped into 1 ml of lysis buffer as described previously (14). For the preparation of tissue extracts, about 2 mg of normal or tumor human breast tissues from frozen samples were homogenized in 400 μ l of lysis buffer. Protein concentrations were determined using the Bradford protein assay (Bio-Rad). Lysates (50 μ g) were subjected to SDS-PAGE followed by Western immunoblotting using specific antisera and detection with chemiluminescence (Amersham Pharmacia Biotech, Piscataway, NJ). Rad polyclonal antiserum was used at 1:1000 dilution as described (15). Monoclonal antibody against human nm23 H1 was purchased from Santa Cruz (Catalogue #SC-465; Santa Cruz, CA) and used at 1:500 dilution.

Growth Assays. For anchorage-dependent growth assay, 1×10^4 cells were plated/well in multiple 24-well plates and incubated at 37°C for varying times, and the numbers of cells were determined by trypsinization and counting in a hemocytometer or Coulter particle counter. Soft-agar colonization assay was performed using 3×10^3 cells in 0.5 ml of medium containing 0.3% (w/v) agar over a 0.5 ml plug of medium containing 0.5% (w/v) agar. Colonies were counted after 14 days of incubation. All of the data were obtained from three independent experiments with each group represented by triplicate wells.

Cell Cycle Analysis by Flow Cytometry. Cells (1.5×10^6) were plated in a 60-mm dish and grown for overnight. The cells were washed twice with PBS, kept in serum-deprived medium for 84 h, and then reexposed to 10% fetal bovine serum for 12 or 24 h. Cells were collected by trypsinization followed by centrifugation, washed once with PBS, and resuspended in 0.2 ml of ice-cold PBS. The cells were fixed in 70% ethanol [in 50 mM glycine buffer (pH 2.0)]. After at least 24 h of fixation, DNA was stained with 2.5 μ g/ml propidium iodide, and the content was analyzed in a FACScan at the Dana-Farber Cancer Institute flow cytometry facility (Boston, MA).

Tumor Growth Assay. A suspension of 5×10^5 (in 0.2 ml of PBS) MDA-MB435 cells expressing vector alone (Puro), Wt Rad, or Rad S105N in the absence or presence of coexpression of nm23 was injected s.c. into the left hind flank of 5-week-old female NIH Swiss Nude mice (Taconic, German-

town, New York). There were five mice in each treatment group, and the experiments were repeated twice. Tumors were measured with calipers in three dimensions twice weekly. All of the animals were treated in accordance with animal welfare guidelines. The entire experiment was halted after any animal had a visible tumor more than 25 mm in one dimension. At autopsy, all of the organs were examined for gross metastases. Primary tumors, lymph nodes, lungs, spleens, and livers were collected and fixed in 10% formalin. H&E-stained sections were prepared from these formalin-fixed and paraffin-embedded tissues. Slides were reviewed using a light microscope (4× and 20× objectives) and certified by other pathologists.

RESULTS

Rad Was Highly Expressed in a Tumorigenic Breast Cancer Cell Line and a Number of Breast Cancer Tissues. Many small G proteins may act as positive or negative effectors of cell growth; however, the exact function of the small GTPase Rad remains unknown. To explore a possible role for Rad in breast cancer, Western blot analysis was performed on protein extracts of breast tissue samples from a number of patients with breast cancer. This demonstrated a variable level of Rad expression, from very low or undetectable in most cases to very high in a few (Fig. 1*B*). To examine Rad expression further, immunohistochemical analysis was conducted in a second cohort of 48 human breast cancer specimens, selected to allow exploration of the relative cellular expression of Rad in breast. These included normal and neoplastic components in the majority of cases. This revealed that Rad was expressed within both normal breast epithelium and tumor cells. Rad expression was often present and at high levels in normal ductal and lobular epithelium (23/30 cases). By contrast, expression was commonly lost in adjacent invasive carcinoma in the same patient (8/30 Rad+ve; $P < 0.0001$; Wilcoxon matched pairs test). Nevertheless, where persistence of high levels of Rad expression was present in breast tumors, this was associated with higher grade, larger size, and extensive axillary nodal involvement

($n = 48$; $P = 0.035$, $P = 0.016$, $P = 0.022$, respectively; χ^2 test for trend; Fig. 1*C*; Table 1).

In an attempt to find cell models to study Rad action further, several cultured cell lines were screened for Rad expression. Whereas the levels of Rad expression were low in the C2C12 myocytes and in the breast cancer cell line MDA-MB435, Rad was highly expressed in MDA-MB231 breast cancer cells (Fig. 1*A*).

Rad Induces Both Anchorage-dependent and Anchorage-independent Growth in Breast Cancer Cells, and Nm23 Blunts These Effects. Our laboratory has recently demonstrated a novel form of bi-directional interaction between Rad and nm23 (17). To determine whether the Rad-nm23 interaction may have a role in growth of breast cancer cells, we established cell lines overexpressing Wt Rad in the presence or absence of coexpression of nm23 in the MDA-MB435 breast cancer cells, which have a low level of endogenous Rad. Drug-resistant clones were pooled together, and both anchorage-dependent and anchorage-independent growth were monitored in these cells. Rad expression resulted in accelerated cell growth on tissue culture plastics by almost 3-fold, and an increased number of colonies formed in soft agar by almost 2.5-fold (Fig. 2, *A* and *B*). Coexpression of nm23 slightly increased the basal levels of growth in both of these *in vitro* assays, although these increases were not statistically significant. More strikingly, however, nm23 almost completely blocked the growth-promoting effects of Rad. Similar results were obtained from isolated individual clones (data not shown). These data suggested that Rad was able to accelerate both anchorage-dependent and anchorage-independent growth in the breast cancer cells and that this effect may be modified by its interaction with nm23.

The Growth-promoting Effects of Rad Required Its NH₂- and COOH-terminal Regions. To further study the structure-function relationship of Rad on cell growth, we generated several cell lines with either Wt Rad or a series of mutants of Rad in the MDA-MB435

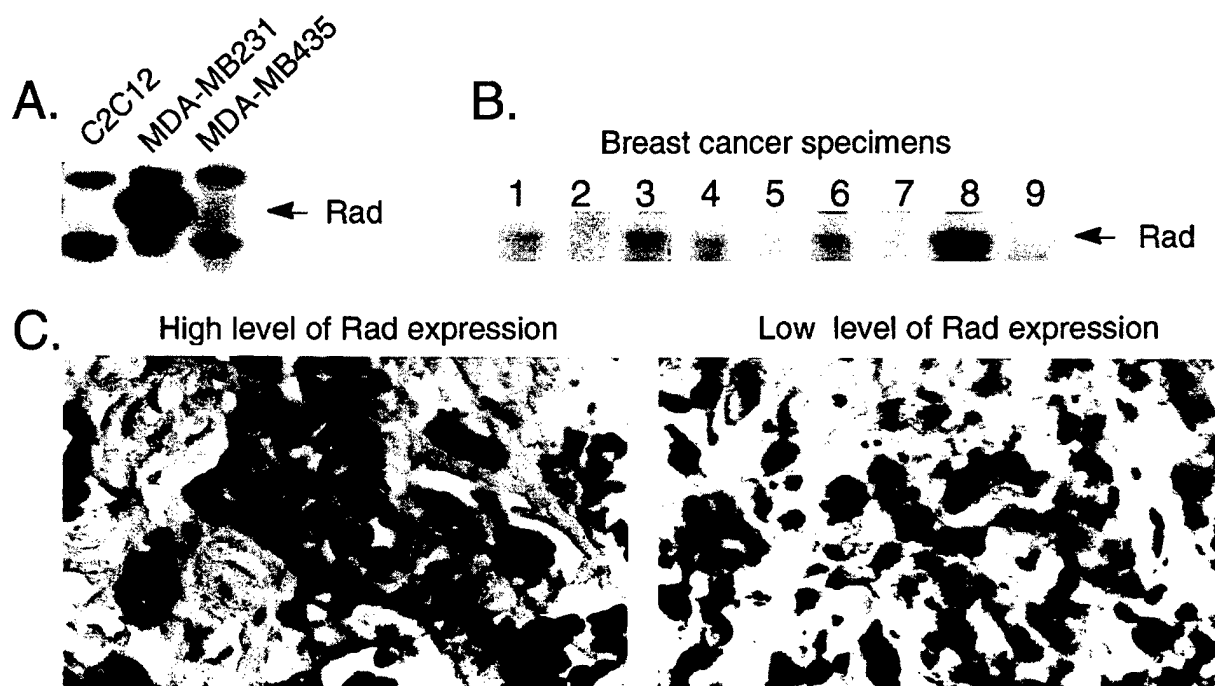


Fig. 1. Rad expression in cell lines and human breast cancer tissues. *A*, Western blot analysis of Rad expression in different cell lines. C2C12 is a murine myocyte line; MDA-MB231 and MDA-MB435 are human breast cancer cell lines. *B*, Western blot analysis of Rad expression in human breast cancer specimens. Protein extracts (50 μ g) from randomly selected human breast cancer specimens were analyzed using a polyclonal antibody against human Rad (15). *C*, representative immunohistochemical staining of high (left panel) and low (right panel) levels of Rad expression in human breast cancer tissues. Cells with red-brown staining in the cytoplasm are considered as positive. Original magnification, $\times 400$.

cells. These mutants included the Rad S105N mutant, the Rad N88 mutant, and the Rad C249 mutant (Fig. 3A). The Rad S105N mutant contained a Ser to Asn mutation at position 105, which is analogous to the S17N mutation in Ras and results in a loss of GTP-binding activity favoring GDP binding (15). The other two mutants, Rad N88 and Rad C249, have deletions in the NH₂-terminal 88 amino acids or the COOH-terminal 59 amino acids (residues 249–308), respectively. Both regions have been shown to be important for CaM binding (14). These constructs were transfected into the MDA-MB435 cell with or without coexpression of nm23. Western blotting revealed an over 100-fold overexpression for both Wt Rad and Rad S105N, about a 40-fold increase for Rad C249, and about a 30-fold increase for Rad N88. The extra bands comigrating with Rad C249 and Rad N88 were nonspecific and were not shown when ¹²⁵I-labeled protein A detection system was used (14). The relatively lower levels of expression of the latter two were consistent with our previous studies demonstrating that the NH₂ terminus and possibly the COOH terminus of Rad may be critical for antibody recognition, protein expression, and/or stability (Ref. 14; Fig. 3B).

Analysis in tissue culture revealed that Wt Rad, as well as the Rad S105N mutant, were able to accelerate cell growth (Fig. 3C, *Left Panel*). This occurred primarily by shortening the lag time required for entering exponential growth, rather than altering the doubling time (Fig. 3, D and E). Interestingly, the GDP-bound form of Rad (S105N) had an effect equal to or greater than that of the Wt protein. This is similar to our previous observation that Rad S105N is more potent in interacting with CaM, CaMKII (14), and tropomyosin (15), all of which favor the GDP form of Rad. Cells overexpressing either the NH₂- or COOH-terminal truncation mutant of Rad, in which their interactions with CaM were affected, did not show any change in lag time as compared with the control cells. Similar structure-function relationships were observed in the soft agar colonization assay (Fig. 3F). Overall, coexpression of nm23 increased slightly, but not significantly, both anchorage-dependent and anchorage-independent growth as shown in both Fig. 2 and Fig. 3. These data agreed with other investigations on a positive correlation of levels of nm23 expression and cell growth rates (35). Taken together, our data suggested that the growth-promoting effects of Rad might be mediated through its NH₂- and COOH-terminal regions and CaM binding, rather than being dependent on the GTPase activity of Rad. Gem, another member of the Rad family of GTPases that binds CaM (40), was also able to shorten the lag time when transfected into the MDA-MB-435 cells (Fig. 3D). However, it was unable to promote colony formation in soft agar (Fig. 3F). No significant difference was observed in growth rates of all cell lines during exponential growth (Fig. 3E). Again, coexpression of nm23 blunted the growth-accelerating effects of Rad in these cells (Fig. 3, D–F).

Rad Promoted Cell Growth by Accelerating Cell Cycle Transitions. Potential mechanisms by which Rad might regulate cell growth *in vitro* include induction of the expression of autocrine factors, increasing plating efficiency, and/or acceleration of cell cycle. To see if Rad induced the expression of autocrine factors, we collected conditioned media from the Puro, Rad Wt, or Rad S105N cultures, added them to control Puro cells, and measured growth. No significant difference was found among these culture media (data not shown). In addition, we treated the cells with mitomycin-C to prevent DNA replication and then replated these cells into tissue culture plates to look for the possibility of changing the plating efficiency of cells by Rad. Again, no difference in plating efficiency was observed among the Puro, Rad Wt, and Rad S105N cells (data not shown). Finally, we determined if Rad had any effect on cell cycle transition. The cells were synchronized by 84 h of serum-starvation (Fig. 4, A–C) and then treated with serum for

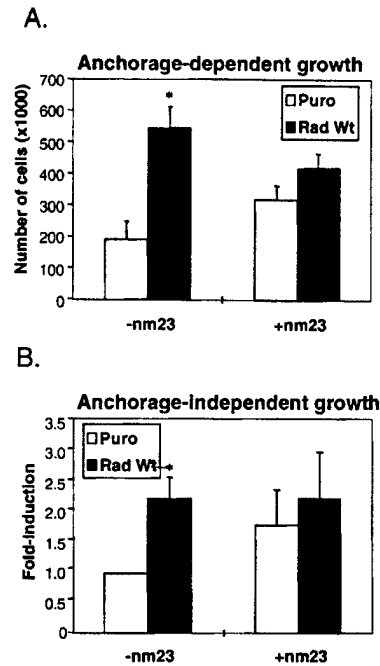


Fig. 2. Effects of Rad and nm23 on anchorage-dependent and anchorage-independent growth. *A*, anchorage-dependent growth of MDA-MB435 cells overexpressing Rad and/or nm23. Cells (1×10^4) were plated/well in multiple 24-well plates and incubated for 6 days, and numbers of cells were determined by trypsinization and counting in a hemocytometer or Coulter particle counter. *B*, soft-agar colonization of MDA-MB435 cells overexpressing Rad and/or nm23. Cells (3×10^3) were plated in 0.5 ml of medium containing 0.3% agar over a 0.5 ml plug of medium containing 0.5% agar. Colonies were counted after 14 days of incubation. In this panel, data are presented as fold-induction by expression of Rad and/or nm23 relative to the Puro control in the absence of nm23 coexpression. All of the data were obtained from three independent experiments with each group represented by triplicate wells. Significance was determined relative to corresponding control by Student's *t* test; * = $P < 0.05$.

12 or 24 h, and cell cycle distributions were determined by flow cytometry of propidium iodide-stained cells. Overexpression of Wt Rad or the S105N mutant caused a large portion of cells to shift into S/G₂M phases after 24 h of serum treatment (Fig. 4, H and I). This suggests that the mechanism by which Rad promotes cell growth involves, at least in part, induction of cell cycle transitions rather than secretion of some autocrine growth factors or change in plating efficiency.

The Rad-Nm23 Interaction Regulated Tumor Formation in Nude Mice. The above experiments indicate that Rad is able to increase numbers of colonies formed in soft agar, and this effect is blunted in the presence of nm23 (Fig. 2B and Fig. 3F). To determine whether Rad and/or nm23 could affect the growth of tumors derived from human breast cancer cells *in vivo*, a suspension of 5×10^5 MDA-MB435 cells expressing either Wt Rad or Rad S105N in the absence or presence of coexpression of nm23 was injected s.c. into the left hind flank of 5-week-old, female NIH Swiss Nude mice, and tumor growth was monitored. Mice that received cells overexpressing either Rad Wt or Rad S105N in the absence of nm23 developed larger tumors than mice receiving the control cells (Fig. 5, A and B). A significant increase was observed in the percentage of Rad Wt or Rad S105N mice that developed detectable tumors at early times after injection (day 33 and day 27; Fig. 5C). Furthermore, by day 33 there was a significant increase in the size of tumors in the Rad Wt positive/nm23 negative group relative to the corresponding Puro control (Fig. 5D). This is in agreement with the *in vitro* data that also showed Rad affecting the early time points of cell growth (Fig. 3D). Interestingly, as in the *in vitro* experiments, the growth-promoting

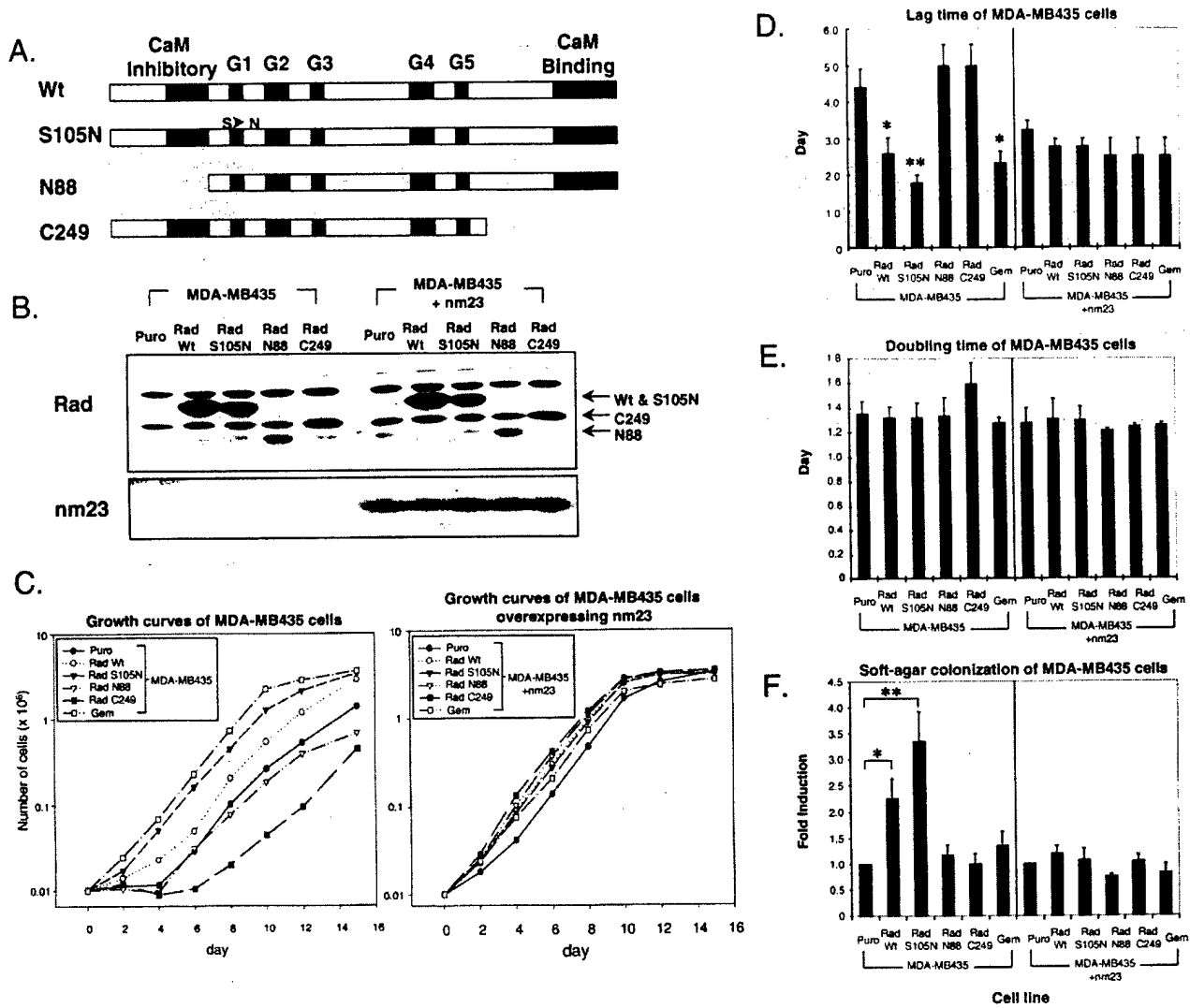


Fig. 3. Structure-function relationship of Rad on growth. *A*, schematic diagram shows the structures of Wt and mutants of Rad. G1-G5 refer to the conserved domains found similar in members of the Ras family of GTPases. Regions that bind or interfere CaM binding were indicated. *B*, Western blot analysis of cells expressing Wt or mutant forms of Rad in the absence or presence of coexpression of nm23. *C*, growth curves of Rad/nm23 overexpressors. *D* and *E*, lag time and doubling time of Rad/nm23-overexpressing cell lines. Lag times were determined by the period of adaptation after subculture before entering exponential growth. Doubling times were determined by calculating growth rates during exponential growth. *F*, soft-agar colonization of Rad/nm23 overexpressors. Data are presented as fold-induction by expression of either Wt Rad or different mutants of Rad or Gem relative to the Puro controls for each nm23 \pm group. Cells were grown and assayed as described in Fig. 2. Data were obtained from three or four independent experiments. Significance was determined relative to corresponding Puro control using Student's *t* test; * = $P < 0.05$; ** = $P < 0.01$.

effect of Rad was blocked in the cells coexpressing nm23, suggesting that nm23 may play a role as a dominantly negative regulator for Rad in tumor growth (Fig. 5, *A*, *B*, and *D*). Moreover, nm23 caused significant decreases in the probabilities of tumor formation at days 27 and 33, and this effect appeared to be independent of the presence of Rad Wt or Rad S105N (Fig. 5*C*). With only one exception, spontaneous metastases were not evident at 67 days after injection, at which time the mice were sacrificed under animal welfare guidelines, because of the primary tumor sizes of mice.

The histological appearance of tumor resembled typical medullary carcinoma, consistent with the origin of the cells (41). Histological analysis of cross-sections of tumors also revealed that Rad Wt tumors showed a relatively larger area (approximately 30–40% of the cross-section area) with degenerative changes (picnotic nuclei, necrosis, and hemorrhage) as compared with the Puro controls that contain only about 10% of the area involved with degenerative changes (Fig. 6).

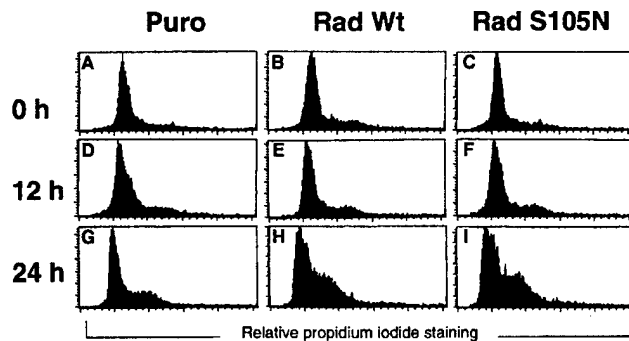


Fig. 4. Effects of Rad on cell cycle distribution. MDA-MB435 cells overexpressing Wt Rad, S105N mutant, or empty vector control (Puro) were serum-starved for 84 h and then treated with 10% serum for 12 and 24 h. DNA content was determined by propidium iodide staining and flow cytometry analysis. The experiments were repeated twice. A representative experiment is shown.

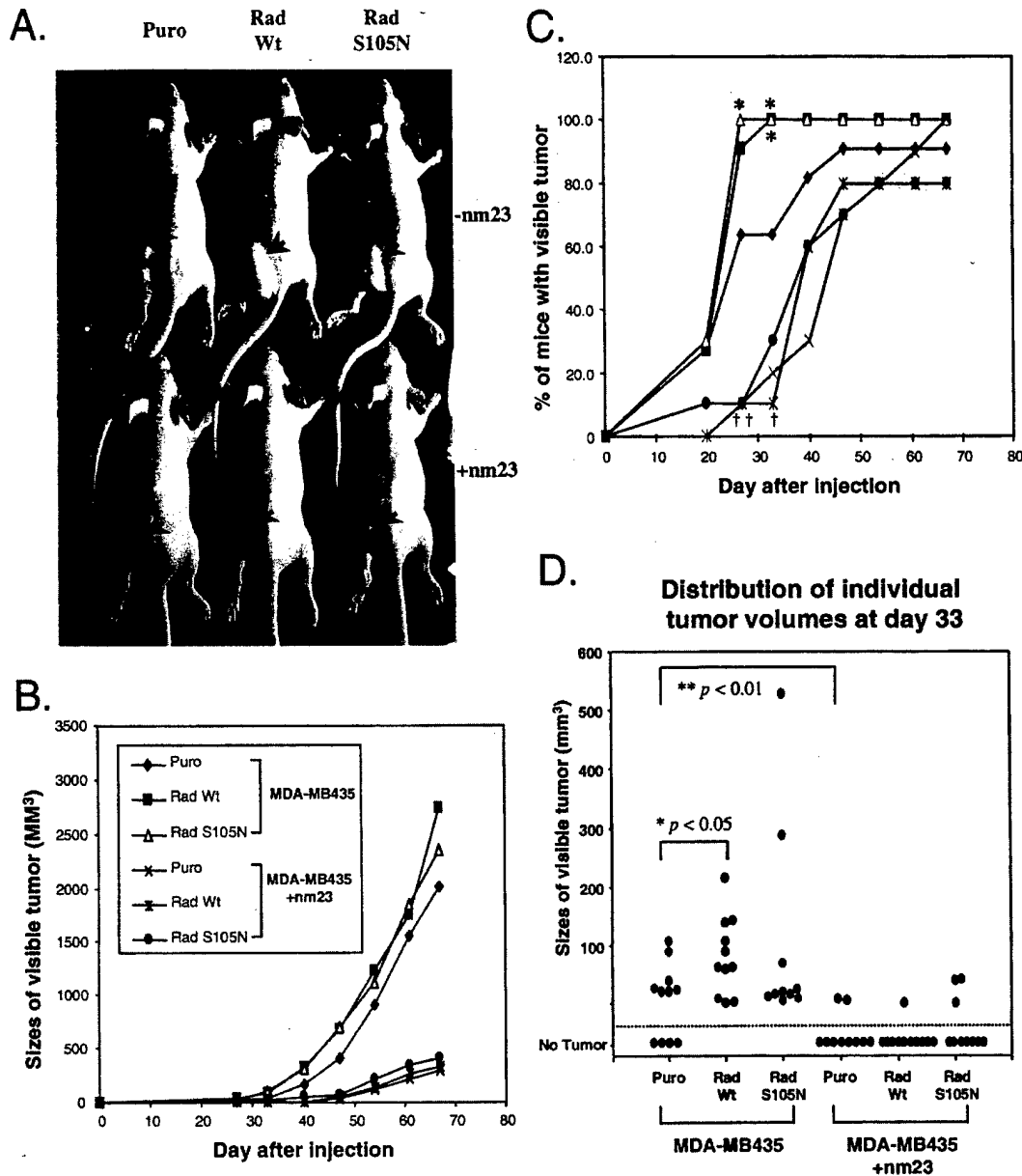


Fig. 5. Effects of Rad and nm23 on tumor growth in nude mice. Five-week old NIH Swiss Nude mice received injections in the left hind flank with 5×10^5 cells expressing either Wt or mutant Rad with or without coexpression of nm23. *A*, shows representative mice from each treatment group at day 67 after injection. Arrows indicate tumors. *B*, growth curves of tumors in nude mice. Data are presented as average volume of tumors from mice receiving either control or Rad overexpressors in the presence or absence of coexpression of nm23 ($n = 10$ or 11). *C*, percentage of mice with visible tumors; * = $P < 0.05$ as determined relative to corresponding Puro control, statistical significance was determined using the Fisher's exact test; † = $P < 0.05$; †† = $P < 0.001$ as determined relative to corresponding nm23 negative. *D*, distribution of individual tumor volumes at day 33. Significance was determined relative to the control using a nonparametric Mann-Whitney test; * = $P < 0.05$; ** = $P < 0.01$.

DISCUSSION

Ras-related GTP-binding proteins comprise a superfamily of molecules that play important roles in a wide variety of cellular processes including cell proliferation and differentiation (42), apoptosis (43), intracellular vesicular trafficking (44), cytoskeletal rearrangement (45), cell cycle regulation (46), and glucose transportation in cells (16, 47). Activating mutations of Ras occur in about 30% of all of human tumors, including breast cancer (48, 49). Rad itself has not been implicated in tumor development, although another member of the Rad family, Gem, was originally identified by its overexpression in mitogen-stimulated T lymphocytes and v-abl-transformed pre-B cells (8, 9). In the present study, we have demonstrated not only that Rad

is present in some human breast cancers, but also that it is able to accelerate growth of breast cancer cells *in vitro* and increase the tumorigenicity of these cells when injected into nude mice.

Rad was originally identified to be highly expressed in the skeletal muscle of some type-2 diabetic humans and is normally also highly expressed in heart and lung (7). When overexpressed in skeletal muscle, Rad alters contractility and potentiates high fat diet-induced insulin resistance.⁴ In transgenic mice with overexpression of Rad in the heart, there is cardiac hypertrophy and an increase in metabolic

⁴ J. Ilany, P. J. Bilan, S. Kapur, J. S. Caldwell, M-E. Patti, A. Marette, and C. R. Kahn. Overexpression of Rad in muscle of mice worsens high-fat-diet-induced insulin resistance and glucose intolerance and lowers plasma triglyceride level, manuscript in preparation.

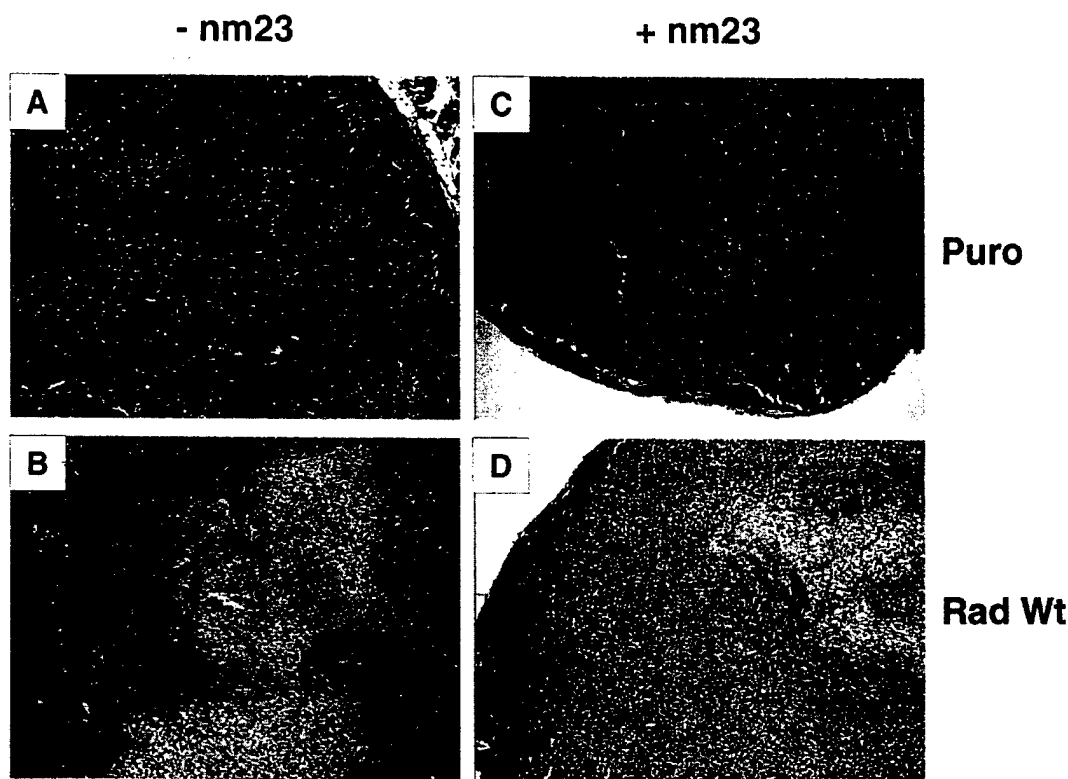


Fig. 6. Histological analysis of tumors from mice that received injections with MDA-MB435 cells. Tumors removed from mice were fixed in 10% formalin and stained with H&E. All of the tumors show typical morphology of medullary breast carcinoma. Lighter staining areas in *B* and *D* show degeneration. Original magnification, $\times 40$.

activity.⁵ Moreover, epidemiological evidence has suggested hyperinsulinemia and insulin resistance found in type-2 diabetes mellitus are risk factors for the development of breast cancer (50, 51). *In vivo* experiments using euglycemic, hyperinsulinemic clamps have shown that insulin is able to stimulate Rad expression (52). This raises the possibility that Rad overexpression found in some patients with type-2 diabetes mellitus may be the results of hyperinsulinemia rather than the cause of insulin resistance. Taken together with the data presented in this study, which indicate a growth-accelerating role of Rad in human breast cancer, these data suggest that in type-2 diabetes, Rad may be more closely related to changes in cell growth than changes in cell metabolism.

Studies on the structure-function relationship reveal that the growth-promoting effects of Rad *in vitro* may be mediated through its NH₂- and COOH-terminal regions. Previously (14), we have identified a CaM-binding region in residues 278–297 at the COOH terminus of Rad and a potential negatively regulatory region of Rad-CaM interaction in the NH₂ terminus of Rad which, when removed, increases the binding of Rad to CaM. In the current study, we found that deletions of either the CaM-binding domain (C249) or the CaM-inhibitory domain (N88) of Rad results in losing its growth-promoting effect. Gem, which can also bind CaM (40), also accelerated breast cancer cell growth *in vitro* but differed from Rad in its inability to promote colony formation in soft agar. These data suggest that interaction of these GTPases with CaM through their COOH-terminal extensions may be important for their ability to accelerate anchorage-dependent cell growth, although additional sequences in the NH₂ terminus may also be critical. It has been shown that CaM regulates the G₁-S transition of the cell cycle by increasing the activities of cyclin-dependent kinase 4, cyclin-dependent kinase 2, and retinoblas-

toma protein phosphorylation (53). In this study, we also found that overexpression of Rad in the MDA-MB435 cells results in acceleration of cell cycle transitions in response to serum stimulation. Taken together, these data suggest that Rad may regulate the growth of breast cancer cells through its interaction with CaM and an acceleration of cell cycle transition.

Another potential mechanism by which Rad may regulate cell growth is related to changes in cytoskeletal adhesion and cell motility. This is suggested by its ability to interact with CaM, CaMKII (14), and β -tropomyosin (15). Tropomyosin clearly plays a role in contraction and cytoskeletal organization, both of which contribute to cell motility (54). CaM and CaMKII have also been shown to be involved in calcium-mediated cell movement (55). Interestingly, there are several lines of well-documented evidence concerning the involvement of small G proteins in cell adhesion and migration (for review, see Ref. 56). Aberrations in these events lead to cell transformation, tumor invasion, and metastasis; *e.g.*, the Rho family proteins, including cdc42, Rac1, and RhoA, have been suggested by multiple studies (57, 58) to play an important role in cytoskeletal rearrangements, cell adhesion, tumor invasion, and metastasis. It seems likely that Rad may regulate growth of tumor cells via similar mechanisms used by the Rho family small G proteins. This is an interesting topic for future studies.

Data from our *in vitro* and *in vivo* studies suggest that nm23 may act as a dominant negative regulator of Rad and that coexpression of nm23 with Rad abolishes its growth-promoting effects. Nm23 possesses several enzymatic activities and mediates a number of biological functions, including proliferation, differentiation, cell motility, and suppression of metastasis (31). We have demonstrated previously (59) a coordinate, bi-directional, and bimolecular interaction between Rad and nm23. In the present study, we find that this interaction appears to play a significant role in control of tumor cell growth. This

⁵ L. Field, P. J. Bilan, and C. R. Kahn, manuscript in preparation.

is particularly interesting because the expression of *nm23* gene has been shown to inversely correlate with metastatic potential in several tumor types (60, 61). To date, the exact mechanism of these effects has been unclear. It has been shown that *nm23* may mediate part of its effects by altering cell motility (27). Taken together with the fact that Rad may also affect motility via interactions with CaM, CaMKII (14), and β -tropomyosin (15), it is possible that the Rad-*nm23* complex acts in a coordinated manner to regulate growth of tumor cells via pathways involved in cytoskeletal organization and cell motility. Furthermore, in this complex, *nm23* functions as a GTPase-activating protein and a guanine nucleotide exchange factor for Rad, determining the balance between GTP- and GDP-Rad (17). However, the GTPase activity of Rad does not appear to be critical to its effects on *in vitro* growth of breast cancer cells because this effect appears to favor the GDP-bound form of Rad (the S105N mutant) more than the Wt protein. This is similar to the ability of Rad to interact with CaM, CaMKII, and tropomyosin, all of which favor the GDP form of Rad (14, 15). However, both the Wt Rad and the S105N mutant have similar effects on promoting tumor growth *in vivo*. These phenomena may be explained by having distinct cellular environments between *in vitro* and *in vivo*, which may differentially regulate the activities of Rad and *nm23*.

In the present study, we have also shown that Rad expression in cell lines significantly increases the tumor growth and the percentage of mice that develop tumors *in vivo* at early times after injection of breast cancer cells. This agrees with the *in vivo* studies where we have observed that high levels of Rad expression are significantly associated with several features indicative of more aggressive tumors, including larger size, higher grade, and more extensive nodal metastasis. Interestingly, the latter features are also those with which loss of *nm23* was initially associated (62). However, whereas subsequent investigation has not always confirmed these associations (63), in some of the larger studies, a relationship between persistence of *nm23* and longer disease-free and metastasis-free survival has emerged (60, 61). Our current findings, that the positive effects of Rad on tumor growth can be abrogated by interaction with *nm23* and the implication that the interaction between these proteins may be significant in prognosis, may be important in resolving the discrepancies between such studies to determine the role of *nm23*. However, a more extensive study on a much larger cohort of cases than the cohort used in this study will be required to determine the *in vivo* significance in human tumors of an interaction with *nm23* and the prognostic significance of Rad expression.

In summary, we have shown that some human breast cancers express the small G protein, Rad, and that Rad is able to regulate growth of breast cancer cells both *in vitro* and *in vivo*. Furthermore, we have shown that this effect of Rad is blocked by coexpression of *nm23*. These results suggest a novel mechanism by which interaction between Rad and *nm23* may play an important role in the regulation of growth and tumorigenicity of breast cancer. Rad may also provide both a new diagnostic test for staging of breast cancer and a new therapeutic target for its treatment.

ACKNOWLEDGMENTS

We thank S. E. Curtis for assistance in injection of cells into nude mice. We are also grateful to T-L. Azar and J. Konigsberg for excellent secretarial assistance.

REFERENCES

- McManus, M. J., and Welsch, C. W. The effect of estrogen, progesterone, thyroxine, and human placental lactogen on DNA synthesis of human breast ductal epithelium maintained in athymic nude mice. *Cancer (Phila.)*, 54: 1920-1927, 1984.
- Papa, V., Hartmann, K. K., Rosenthal, S. M., Maddux, B. A., Siiteri, P. K., and Goldfine, I. D. Progestins induce down-regulation of insulin-like growth factor-I (IGF-I) receptors in human breast cancer cells: potential autocrine role of IGF-II. *Mol. Endocrinol.*, 5: 709-717, 1991.
- Clevenger, C. V., Chang, W. P., Ngo, W., Pasha, T. L., Montone, K. T., and Tomaszewski, J. E. Expression of prolactin and prolactin receptor in human breast carcinoma. Evidence for an autocrine/paracrine loop. *Am. J. Pathol.*, 146: 695-705, 1995.
- Osborne, C. K., Bolan, G., Monaco, M. E., and Lippman, M. E. Hormone responsive human breast cancer in long-term tissue culture: effect on insulin. *Proc. Natl. Acad. Sci. USA*, 73: 4536-4540, 1976.
- Rasmussen, A. A., and Cullen, K. J. Paracrine/autocrine regulation of breast cancer by the insulin-like growth factors. *Breast Cancer Res. Treat.*, 47: 219-233, 1998.
- Dahiya, R., and Deng, G. Molecular prognostic markers in breast cancer. *Breast Cancer Res. Treat.*, 52: 185-200, 1998.
- Reynet, C., and Kahn, C. R. Rad, a member of the ras family overexpressed in muscle of type II diabetic humans. *Science (Washington DC)*, 262: 1441-1444, 1993.
- Maguire, J., Santoro, T., Jensen, P., Siebenlist, U., Yewdell, J., and Kelly, K. Gem. An induced, immediate early protein belonging to the Ras family. *Science (Washington DC)*, 265: 241-244, 1994.
- Cohen, L., Mohr, R., Chen, Y. Y., Huang, M., Kato, R., Dorin, D., Tamanoi, F., Goga, A., Afar, D., Rosenberg, N., and Witte, O. Transcriptional activation of a *ras*-like gene (*kir*) by oncogenic tyrosine kinases. *Proc. Natl. Acad. Sci. USA*, 91: 12448-12452, 1994.
- Finlin, B. S., and Andres, D. A. Rem is a new member of the Rad- and Gem/Kir Ras-related GTP-binding protein family repressed by lipopolysaccharide stimulation. *J. Biol. Chem.*, 272: 21982-21988, 1997.
- Finlin, B. S., Shao, H., Kadono-Okuda, K., Guo, N., and Andres, D. A. Rem2, a new member of the Rem/Rad/Gem/Kir family of Ras-related GTPases. *Biochem. J.*, 347: 223-231, 2000.
- Pan, J. Y., Fieles, W. E., White, A. M., Egerton, M. M., and Silberstein, D. S. Ges, a human GTPase of the Rad/Gem/Kir family, promotes endothelial cell sprouting and cytoskeleton reorganization. *J. Cell Biol.*, 149: 1107-1116, 2000.
- Bilan, P. J., Moyers, J. S., and Kahn, C. R. The Ras-related protein Rad associates with the cytoskeleton in a non lipid-dependent manner. *Exp. Cell Res.*, 242: 391-400, 1998.
- Moyers, J. S., Bilan, P. J., Zhu, J., and Kahn, C. R. Rad, and Rad-related GTPases interact with calmodulin and calmodulin-dependent protein kinase II. *J. Biol. Chem.*, 272: 11832-11839, 1997.
- Zhu, J., Bilan, P. J., Moyers, J. S., Antonetti, D. A., and Kahn, C. R. Rad, a novel ras-related GTPase, interacts with skeletal muscle β -tropomyosin. *J. Biol. Chem.*, 271: 768-773, 1996.
- Moyers, J. S., Bilan, P. J., Reynet, C., and Kahn, C. R. Overexpression of Rad inhibits glucose uptake in cultured muscle and fat cells. *J. Biol. Chem.*, 271: 23111-23116, 1996.
- Zhu, J., Tseng, Y. H., Kantor, J. D., Rhodes, C. J., Zetter, B. R., Moyers, J. S., and Kahn, C. R. Interaction of the Ras-related protein associated with diabetes Rad and the putative tumor metastasis suppressor Nm23 provides a novel mechanism of GTPase regulation. *Proc. Natl. Acad. Sci. USA*, 96: 14911-14918, 1999.
- Steeg, P. S., Bevilacqua, G., Kopper, L., Thorgerisson, U. P., Talmadge, J. E., Liotta, L. A., and Sobel, M. E. Evidence for a novel gene associated with low tumor metastatic potential. *J. Natl. Cancer Inst. (Bethesda)*, 80: 200-204, 1988.
- Urano, T., Takamiya, K., Furukawa, K., and Shiku, H. Molecular cloning and functional expression of the second mouse *nm23/NDP* kinase gene, *nm23-M2*. *FEBS Lett.*, 309: 358-362, 1992.
- Rosengard, A. M., Kruttsch, H. C., Shearn, A., Biggs, J. R., Barker, E., Margulies, I. M. K., King, C. R., Liotta, L. A., and Steeg, P. S. Reduced Nm23/Awd protein in tumour metastasis and aberrant *Drosophila* development. *Nature (Lond.)*, 342: 177-170, 1989.
- Stahl, J. A., Leone, A., Rosengard, A. M., Porter, L., King, C. R., and Steeg, P. S. Identification of a second human *nm23* gene, *nm23-H2*. *Cancer Res.*, 51: 445-449, 1991.
- Venturelli, D., Martinez, R., Melotti, P., Casella, I., Peschle, C., Cucco, C., Spampinato, G., Darzynkiewicz, Z., and Calabretta, B. Overexpression of DR-nm23, a protein encoded by a member of the *nm23* gene family, inhibits granulocyte differentiation and induces apoptosis in 32Dcl3 myeloid cells. *Proc. Natl. Acad. Sci. USA*, 92: 7435-7439, 1995.
- Milon, L., Rousseau-Merck, M., Munier, A., Erent, M., Lascu, I., Capeau, J., and Lacombe, M. *nm23-H4*, a new member of the family of human *nm23/nucleoside diphosphate kinase* genes localized on chromosome 16p13. *Hum. Genet.*, 99: 550-557, 1997.
- Munier, A., Feral, C., Milon, L., Phung-Ba Pinon, V., Gyapay, G., Capeau, J., Guellaen, G., and Lacombe, M-L. A new human *nm23* homologue (*nm23-H5*) specifically expressed in testis germinal cells. *FEBS Lett.*, 434: 289-294, 1998.
- Leone, A., Flatow, U., King, C. R., Sandeen, M. A., Margulies, I. M. K., Liotta, L. A., and Steeg, P. S. Reduced tumor incidence, metastatic potential, and cytokine responsiveness of *nm23*-transfected melanoma cells. *Cell*, 65: 25-35, 1991.
- Leone, A., Flatow, U., VanHoutte, K., and Steeg, P. S. Transfection of human *nm23-H1* into the human MDA-MB-435 breast carcinoma cell line: effects on tumor metastatic potential, colonization and enzymatic activity. *Oncogene*, 8: 2325-2333, 1993.
- Kantor, J. D., McCormick, B., Steeg, P. S., and Zetter, B. R. Inhibition of cell motility after *nm23* transfection of human and murine tumor cells. *Cancer Res.*, 53: 1971-1973, 1993.
- Wagner, P. D., and Vu, N. D. Phosphorylation of ATP-citrate lyase by nucleoside diphosphate kinase. *J. Biol. Chem.*, 270: 21758-21764, 1995.

29. Freije, J. M., Blay, P., MacDonald, N. J., Manrow, R. E., and Steeg, P. S. Site-directed mutation of Nm23-H1. Mutations lacking motility suppressive capacity upon transfection are deficient in histidine-dependent protein phosphotransferase pathways *in vitro*. *J. Biol. Chem.*, 272: 5525-5532, 1997.
30. MacDonald, N. J., De La Rosa, A., Benedict, M. A., Freije, J. M. P., Kruttsch, H., and Steeg, P. S. A serine phosphorylation of nm23, and not its nucleoside diphosphate kinase activity, correlates with suppression of tumor metastatic potential. *J. Biol. Chem.*, 268: 25780-25789, 1993.
31. Lombardi, D., Lacombe, M. L., and Paggi, M. G. nm23. Unraveling its biological function in cell differentiation. *J. Cell. Physiol.*, 182: 144-149, 2000.
32. Postel, E. H. NM23/Nucleoside diphosphate kinase as a transcriptional activator of c-myc. *Curr. Top. Microbiol. Immunol.*, 213: 233-252, 1996.
33. Biggs, J., Hersperger, E., Steeg, P. S., Liotta, L. A., and Shearn, A. A *Drosophila* gene that is homologous to a mammalian gene associated with tumor metastasis codes for a nucleoside diphosphate kinase. *Cell*, 63: 933-940, 1990.
34. Rosengard, A. M., Kruttsch, H. C., Shearn, A., Biggs, J. R., Barker, E., Margulies, I. M. K., King, C. R., Liotta, L. A., and Steeg, P. S. Reduced Nm23/Awd protein in tumour metastasis and aberrant *Drosophila* development. *Nature (Lond.)*, 342: 177-180, 1989.
35. Caligo, M. A., Cipollini, G., Fiore, L., Calvo, S., Basolo, F., Collecchi, P., Ciardiello, F., Pepe, S., Petrin, M., and Bevilacqua, G. NM23 gene expression correlates with cell growth rate and S-phase. *Int. J. Cancer*, 60: 837-842, 1995.
36. Cipollini, G., Berti, A., Fiore, L., Rainaldi, G., Basolo, F., Merlo, G., Bevilacqua, G., and Caligo, M. A. Down-regulation of the nm23.h1 gene inhibits cell proliferation. *Int. J. Cancer*, 73: 297-302, 1997.
37. Gervasi, F., D'Agnano, I., Vossio, S., Zupi, G., Sacchi, A., and Lombardi, D. nm23 influences proliferation and differentiation of PC12 cells in response to nerve growth factor. *Cell Growth Differ.*, 7: 1689-1695, 1996.
38. Hiller, T., Snell, L., and Watson, P. H. Microdissection RT-PCR analysis of gene expression in pathologically defined frozen tissue sections. *Biotechniques*, 21: 38-40, 1996.
39. Elston, C. W., and Ellis, I. O. Pathological prognostic factors in breast cancer. I. The value of histological grade in breast cancer: experience from a large study with long-term follow-up. *Histopathology (Oxf.)*, 19: 403-410, 1991.
40. Fischer, R., Wei, Y., Anagli, J., and Berchtold, M. W. Calmodulin binds to and inhibits GTP binding of the Ras-like GTPase Klr/Gem. *J. Biol. Chem.*, 271: 25067-25070, 1996.
41. Brinkley, B. R., Beall, P. T., Wible, L. J., Mace, M. L., Turner, D. S., and Cailleau, R. M. Variations in cell form and cytoskeleton in human breast carcinoma cells *in vitro*. *Cancer Res.*, 40: 3118-3129, 1980.
42. Lange-Carter, C. A., and Johnson, G. L. Ras-dependent growth factor regulation of MEK kinase in PC12 cells. *Science (Washington DC)*, 265: 1458-1461, 1994.
43. Evan, G., and Littlewood, T. A matter of life and cell death. *Science (Washington DC)*, 281: 1317-1322, 1998.
44. Zerial, M., and Stenmark, H. Rab GTPases in vesicular transport. *Curr. Opin. Cell Biol.*, 5: 613-620, 1993.
45. Hall, A. Small GTP-binding proteins and the regulation of the actin cytoskeleton. *Annu. Rev. Cell Biol.*, 10: 31-54, 1994.
46. Yang, J. J., Kang, J. S., and Krauss, R. S. Ras signals to the cell cycle machinery via multiple pathways to induce anchorage-independent growth. *Mol. Cell. Biol.*, 18: 2586-2595, 1998.
47. Cormont, M., Bortoluzzi, M. N., Gautier, N., Mari, M., Van Obberghen, E., and Le Marchand-Brustel, Y. Potential role of Rab4 in the regulation of subcellular localization of Glut4 in adipocytes. *Mol. Cell. Biol.*, 16: 6879-6886, 1996.
48. Bos, J. L. *ras* oncogenes in human cancer: a review. *Cancer Res.*, 49: 4682-4689, 1989.
49. Clark, G. J., and Der, C. J. Aberrant function of the Ras signal transduction pathway in human breast cancer. *Breast Cancer Res. Treat.*, 35: 133-144, 1995.
50. DeMali, K. A., and Kazlauskas, A. Activation of Src family members is not required for the platelet-derived growth factor β receptor to initiate mitogenesis. *Mol. Cell. Biol.*, 18: 2014-2022, 1998.
51. Volkert, N. Diabetes and cancer: scientists search for a possible link. *J. Natl. Cancer Inst. (Bethesda)*, 92: 192-194, 2000.
52. Laville, M., Auboeuf, D., Khalfallah, Y., Vega, N., Riou, J. P., and Vidal, H. Acute regulation by insulin of phosphatidylinositol-3-kinase, Rad, Glut4, and lipoprotein lipase mRNA levels in human muscle. *J. Clin. Investig.*, 98: 43-49, 1996.
53. Taulés, M., Ruis, E., Talaya, D., López-Girona, A., Bachs, O., and Agell, N. Calmodulin is essential for cyclin-dependent kinase 4 (Cdk4) activity and nuclear accumulation of cyclin D1-Cdk4 during G₁. *J. Biol. Chem.*, 273: 33279-33286, 1998.
54. Babcock, G. G., and Fowler, V. M. Isoform-specific interaction of tropomodulin with skeletal muscle and erythrocyte tropomyosins. *J. Biol. Chem.*, 269: 27510-27518, 1994.
55. Pauly, R. R., Bilato, C., Sollott, S. J., Monticone, R., Kelly, P. T., Lakatta, E. G., and Crowe, M. T. Role of calcium/calmodulin-dependent protein kinase II in the regulation of vascular smooth muscle cell migration. *Circulation*, 91: 1107-1115, 1995.
56. Blanchard, J. M. Small GTPases, adhesion, cell cycle control and proliferation. *Pathol. Biol.*, 48: 318-327, 2000.
57. Mohri, T., Adachi, Y., Ikehara, S., Hioki, K., Tokunaga, R., and Taketani, S. Activated Rac1 selectively up-regulates the expression of integrin $\alpha 6 \beta 4$ and induces cell adhesion and membrane ruffles of nonadherent colon cancer Colo201 cells. *Exp. Cell Res.*, 253: 533-540, 1999.
58. Evers, E. E., Zondag, G. C., Malliri, A., Price, L. S., ten Klooster, J. P., van der Kammen, R. A., and Collard, J. G. Rho family proteins in cell adhesion and cell migration. *Eur. J. Cancer*, 36: 1269-1274, 2000.
59. Aprile, J. A., Russo, M., Pepe, M. S., and Loughran, T. P., Jr. Activation signals leading to proliferation of normal and leukemic CD3+ large granular lymphocytes. *Blood*, 78: 1282-1285, 1991.
60. Heimann, R., Ferguson, D. J., and Hellman, S. The relationship between nm23, angiogenesis, and the metastatic proclivity of node-negative breast cancer. *Cancer Res.*, 58: 2766-2771, 1998.
61. Charpin, C., Garcia, S., Bonnier, P., Martini, F., Andrarc, L., Horschowski, N., Lavaut, M. N., and Allasia, C. Prognostic significance of Nm23/NDPK expression in breast carcinoma, assessed on 10-year follow-up by automated and quantitative immunocytochemical assays. *J. Pathol.*, 184: 401-407, 1998.
62. Bevilacqua, G., Sobel, M. E., Liotta, L. A., and Steeg, P. S. Association of low nm23 RNA levels in human primary infiltrating ductal breast carcinomas with lymph node involvement and other histopathological indicators of high metastatic potential. *Cancer Res.*, 49: 5185-5190, 1989.
63. Sawa, A., Lascu, I., Veron, M., Anderson, J. J., Wright, C., Horne, C. H., and Angus, B. NDP-K/nm23 expression in human breast cancer in relation to relapse, survival, and other prognostic factors: an immunohistochemical study. *J. Pathol.*, 172: 27-34, 1994.

Expression of the Hypoxia-Inducible and Tumor-Associated Carbonic Anhydrases in Ductal Carcinoma *in Situ* of the Breast

Charles C. Wykoff,* Nigel Beasley,*
Peter H. Watson,[†] Leticia Campo,*
Stephen K. Chia,[‡] Ruth English,[§]
Jaromir Pastorek,[¶] William S. Sly,^{||}
Peter Ratcliffe,** and Adrian L. Harris*

From the Institute of Molecular Medicine* and the Breast Screening Program,[‡] John Radcliffe Hospital, Oxford, United Kingdom; the Wellcome Trust Centre for Human Genetics,** Oxford, United Kingdom; the Department of Pathology,[†] University of Manitoba, Winnipeg, Manitoba, Canada; the Division of Medical Oncology,[‡] British Columbia Cancer Agency, Vancouver, British Columbia, Canada; the Institute of Virology,[¶] Slovak Academy of Sciences, Bratislava, Slovak Republic; and the Edward A. Doisy Department of Biochemistry,^{||} St. Louis University School of Medicine, St. Louis, Missouri

Carbonic anhydrases (CA) influence intra- and extracellular pH and ion transport in varied biological processes. We recently identified CA9 and CA12 as hypoxia-inducible genes. In this study we examined the expression of these tumor-associated CAs by immunohistochemistry in relation to necrosis and early breast tumor progression in 68 cases of ductal carcinoma *in situ* (DCIS) (39 pure DCIS and 29 DCIS associated with invasive carcinoma). CA IX expression was rare in normal epithelium and benign lesions, but was present focally in DCIS (50% of cases) and in associated invasive carcinomas (29%). In comparison, CA XII was frequently expressed in normal breast tissues (89%), in DCIS (84%), and in invasive breast lesions (71%). In DCIS, CA IX was associated with necrosis ($P = 0.0053$) and high grade ($P = 0.012$). In contrast, CA XII was associated with the absence of necrosis ($P = 0.036$) and low grade ($P = 0.012$). Despite this, augmented CA XII expression was occasionally observed adjacent to necrosis within high-grade lesions. Neither CA IX nor CA XII expression was associated with regional or overall proliferation as determined by MIB1 staining. Assessment of mammographic calcification showed that CA XII expression was associated with the absence of calcification ($n = 43$, $P = 0.0083$). Our results demonstrate that induction of CA IX and CA XII occurs in regions adjacent to necrosis in DCIS. Furthermore, these data suggest that proliferation status does not influence expression of either CA in breast tissues, that hypoxia

may be a dominant factor in the regulation of CA IX, and that factors related to differentiation, as determined by tumor grade, dominate the regulation of CA XII. The existence of differential regulation and associations with an aggressive phenotype may be important in the development of selective inhibitors of CAs, because the latter have recently been shown to prevent tumor invasion. (*Am J Pathol* 2001, 158:1011–1019)

The management of pre-invasive ductal carcinoma *in situ* (DCIS) of the breast has become an increasingly significant problem. This is due in part to both the increasing number of these lesions detected by mammography,^{1,2} and the impetus provided by the demonstration that invasive breast cancer may be delayed or inhibited by tamoxifen therapy in women at high risk.^{3,4} Assessment of DCIS and the risk of progression to invasive disease is complicated by the small size and focal nature of most breast lesions, and has traditionally been based primarily on morphological classification and grading of pre-invasive disease by the pattern of growth into comedo and noncomedo subtypes. Recently, radiological studies have suggested that abnormal patterns of calcification may be associated with high-grade DCIS,^{5,6} whereas pathological studies have developed more reproducible and discriminating schema for classification of DCIS lesions.⁷ Consequently, the presence of necrosis and nuclear grade^{8,9} have emerged as important aspects to consider when assessing breast lesions, although consistent recognition and quantification of both parameters remains problematic.¹⁰

Necrosis is believed to represent the extreme manifestation of hypoxia within tissues.¹¹ Interestingly, tumor hypoxia has been shown to be a prognostic indicator for many tumor types, being associated with aggressive growth, metastasis, and poor response to treatment not

Supported by the Imperial Cancer Research Fund and the Wellcome Trust. P. H. W. is supported by a Scientist Award from the Medical Research Council of Canada, an Academic Award from the U. S. Army Medical Research and Materiel Command, and a Research Travel Fellowship from Burroughs Wellcome. S. K. C. is supported by the Shane Fellowship and the Canadian Breast Cancer Foundation.

Accepted for publication December 4, 2000.

Address reprint requests to Dr. Peter Watson, Dept. of Pathology, University of Manitoba, D212-770 Bannatyne Ave., Winnipeg, Manitoba, R3E 0W3, Canada. E-mail: pwatson@cc.umanitoba.ca.

only in patients treated with radiotherapy, but also in those treated with surgery alone.¹²⁻¹⁶ Of potential importance for understanding these effects is the role of hypoxia in regulating patterns of gene expression. Studies of gene expression have defined several classes of genes that are up-regulated by hypoxia and demonstrated that activation of the transcriptional complex hypoxia-inducible factor-1 is a key mediator of many of these effects.^{17,18} Genes that are up-regulated by microenvironmental hypoxia through hypoxia-inducible factor-1 activation include glucose transporters, glycolytic enzymes, and angiogenic growth factors.

We recently identified the two tumor-associated transmembrane carbonic anhydrases (CA) CA9¹⁹⁻²¹ and CA12^{20,22} as being up-regulated by hypoxia in epithelial tumor cell lines.²³ Furthermore, we demonstrated focal perinecrotic expression of CA IX in invasive human tumors, co-localizing with vascular endothelial growth factor mRNA expression and pimonidazole activation.²³

CA9 and CA12 are members of a family of catalytically active CAs that share the capacity to catalyze the reversible hydration of carbon dioxide to carbonic acid.²⁴ CA IX^{19,21,25} has been studied extensively in several tumor types including lung, kidney, colon, and cervix, where its expression has been established as a marker of cellular proliferation and early dysplasia.²⁶⁻³⁰ CA XII was initially identified in renal carcinoma,²² and subsequently shown to be associated with colon carcinoma where altered expression occurs in early stages of tumorigenesis.³¹ However, the expression of these CAs in breast cancer has not been examined.

We investigated CA IX and CA XII expression in breast cancer in anticipation that their expression might serve as indicators of tissue hypoxia, altered pH, and tumor progression. Specifically we wished to assess the pattern of expression of these genes in DCIS, where the appearance of necrosis and abnormal calcification is associated with a high risk of progression to invasive disease.

Materials and Methods

Tissue Specimens

Sixty-eight pathological specimens containing DCIS of the breast were selected from review of surgical resections collected from 1997 to 1999 at the John Radcliffe Hospital and the Churchill Hospital, Oxford, UK. The cohort comprised 39 cases of pure DCIS (DCIS-) and 29 cases of DCIS associated with invasive carcinoma in the same biopsy (DCIS+), either independent from or directly associated with adjoining invasive carcinoma.

All DCIS lesions were classified into histological grades on the basis of the predominant grade present in the tissue section studied for gene expression according to the Van Nuys grading system.^{9,32} The presence of intraductal necrosis within any component of DCIS within the tissue section was evaluated in hematoxylin and eosin-stained sections by light microscopy. The radiological appearance was classified according to the presence and pattern of calcification^{5,6} in preoperative mammo-

grams for a subset of cases in which films were available ($n = 43$). These classifications were performed by a single pathologist (PHW) and radiologist (RE), respectively, without reference to the cohort's immunohistochemical data and outcome. Among the series of cases, the histological grades were as follows: 18 low grade (8 DCIS-, 10 DCIS+), 24 intermediate grade (15 DCIS-, 9 DCIS+), and 26 high grade (16 DCIS-, 10 DCIS+). Intraductal necrosis was present in 51 cases (75%), among which 29 were DCIS- and 22 DCIS+. Mammographic calcifications were present in 35 of 43 cases, among which 27 of 35 were DCIS- and eight of 35 DCIS+. The pattern of calcification was classified as linear type (14 cases) if the presence of any linear calcification was seen, nonlinear type (21 cases), or absent (eight cases).

Cell Lines and Immunoblotting

MDA-MB-231 and ZR-75.1 cell lines were from ATCC (Rockville, MD). Hypoxic conditions were generated in a Napco 7001 incubator (Precision Scientific, Winchester, VA) with 0.1% O₂, 5% CO₂, and balance N₂ for 16 hours. Whole-cell protein extracts were prepared from tissue culture cells by 10 seconds of homogenization in denaturing conditions as described.³³ Whole-cell protein extracts were prepared from tumors by fine section of frozen tissue and 30 seconds of homogenization in denaturing conditions identical to tissue-culture extracts. For Western analysis, aliquots were separated under reducing conditions by sodium dodecyl sulfate-polyacrylamide gel electrophoresis and transferred to Immobilon-P membranes (Millipore, Hertfordshire, UK). CA IX was detected using the mouse monoclonal anti-human CA IX antibody M75 (1:50) as described.³⁴ CA XII was detected using a rabbit polyclonal anti-human CA XII antibody (1:2000) as described.²² horseradish peroxidase-conjugated goat-anti-mouse and swine anti-rabbit immunoglobulins (DAKO, Cambridgeshire, UK) (1:2000), respectively, were applied for 1 hour at room temperature. ECL Plus (Amersham Pharmacia, Buckinghamshire, UK) was used for visualization.

Immunohistochemistry (IHC)

Formalin-fixed, paraffin-embedded tissue specimens collected by standard surgical oncology procedures were obtained from the Pathology Department, John Radcliffe Hospital, Oxford, UK. Immunostaining of paraffin sections was performed after dewaxing and rehydrating 5- μ m sections. Staining for CA IX, CA XII, and MIB1 was performed on serial sections. Endogenous peroxidase was blocked with 0.5% hydrogen peroxide in water for 30 minutes. Ten percent normal human serum in Tris-buffered saline was applied for 15 minutes at room temperature to block nonspecific protein binding. Primary antibodies: anti-human CA IX murine monoclonal antibody M75 (1:50);³⁵ anti-human CA XII rabbit polyclonal antibody (1:2000); anti-human Ki67 murine monoclonal antibody MIB1 (1:50) (Immunotech). Primary antibodies were

incubated for 30 minutes at room temperature in Tris-buffered saline with 5% normal human serum, followed by a 30-minute incubation with a peroxidase-conjugated secondary antibody. After each incubation, slides were washed twice with Tris-buffered saline for 5 minutes. Visualization of staining was by diaminobenzidine substrate for 8 minutes. Slides were counterstained with hematoxylin before mounting in Aquamount (BDH). Substitution of primary antibody with PBS was used as a negative control for each antibody. All staining was performed on an automated IHC stainer (MiniPrep 75; Tecan) at room temperature.

Assessment of CA IX, CA XII, and MIB1 Staining

Immunostaining for CA IX and CA XII was assessed by light microscopy and semiquantitative scoring was performed by a single pathologist (PHW), independently of the pathological assessment. Expression and intensity was scored (0, no staining; 1, weak staining; 2, moderate staining; and 3, strong staining), together with the percentage of normal or neoplastic epithelial cells showing expression within the tissue section (0 to 100%). The product of the intensity and the percentage gave a final immunostaining score (0 to 300; IHC score). MIB1 expression was assessed using a Chalkley point array method adapted from methods used to assess vascular density in breast sections.¹¹ Briefly, MIB1-immunostained section was reviewed at low magnification and five areas showing the highest density of MIB1-positive tumor cells were selected. These hot spots were then assessed at higher magnification ($\times 25$ objective) and the number of grid points that coincided with positive and negative tumor cell nuclei was counted. The mean ratio of MIB1-positive/MIB1-negative cells was then calculated. Each hot spot contained between 200 and 1000 tumor cells depending on DCIS histology.

Results

CA IX and CA XII Antibody Specificity

The anti-CA IX and anti-CA XII antibodies used in this study have been previously characterized for immunostaining in many human tissues.^{22,31,34,36} However, neither antibody has been applied extensively to breast specimens. Therefore, initial experiments were performed to compare IHC profiles with immunoblotting signals from a set of six invasive breast ductal carcinomas. By IHC, two cases exhibited strong membranous staining for CA IX that was restricted to the invasive ductal carcinoma cells, one was weakly positive, and three were negative (data not shown). Two of the tumors that were either negative or weakly positive for CA IX by IHC exhibited strong membranous staining for CA XII, whereas four cases were negative (data not shown). Immunoblotting for CA IX and CA XII was performed in parallel on protein lysates obtained from the same tumor specimens. As shown in Figure 1A, immunoblotting for CA IX revealed a 54- to 58-kd doublet restricted to the two cases

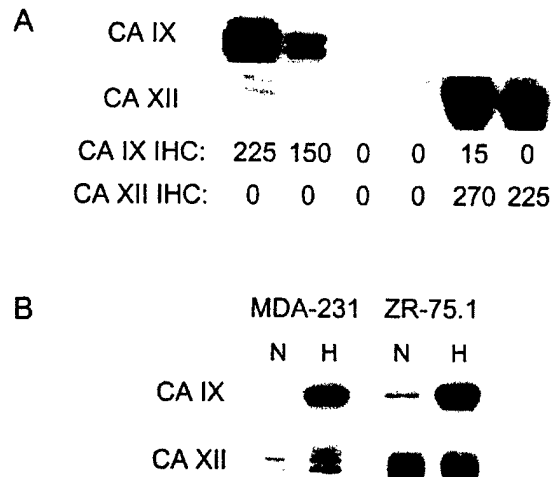


Figure 1. Immunoblotting for CA IX and CA XII. **A:** CA IX and CA XII expression detected by Western blot correlates with the respective immunostaining (IHC) score in invasive breast carcinomas. CA IX and CA XII are detected in tumor extracts that are strongly positive for CA IX or CA XII by IHC in adjacent paraffin sections (IHC score for each CA is indicated). **B:** CA IX and CA XII expression and response to hypoxia in two breast tumor cell lines exposed to either normoxia (N; 20% O₂) or hypoxia (H; 0.1% O₂) for 16 hours.

that were strongly positive by IHC. Similarly, immunoblotting for CA XII revealed a 46- to 48-kd doublet restricted to the two cases that were positive by IHC.

CA IX and CA XII Expression in Breast Cell Lines

We have previously demonstrated wide-spread hypoxic induction of CA9 and CA12 mRNA in various tumor cell lines.²³ Here we compared hypoxic induction of CA IX and CA XII in two breast cell lines selected as representative of estrogen receptor (ER)-negative and poorly differentiated (MDA-MB-231), and ER-positive and well-differentiated (ZR-75.1) breast cancer (Figure 1B). CA IX had an undetectable or low basal level of expression and was markedly induced by hypoxia. In comparison, CA XII had a higher level of normoxic expression and was further induced by hypoxia in one of the two cell lines.

CA IX Expression in Breast Tissues

A series of 68 DCIS breast cases were studied for CA IX expression by IHC. Subsets of these cases also contained normal lobular and ductal components ($n = 47$), and invasive ductal carcinoma components ($n = 29$). CA IX expression was present in normal epithelium in one of 47 cases (2%), and in this case was limited to focal expression adjacent to the site of a recent biopsy. In many cases, benign breast lesions were present within the tissue section, including cystic changes, apocrine metaplasia, blunt duct, and sclerosis adenosis. No expression was observed in any benign breast lesion. In DCIS lesions, focal membranous CA IX staining, typically adjacent to areas of necrosis, was present in 34 of 68 (50%) cases, including 23 of 39 (59%) pure DCIS and 11 of 29 (38%) DCIS associated with invasive disease. In those cases in which invasive disease was present on the

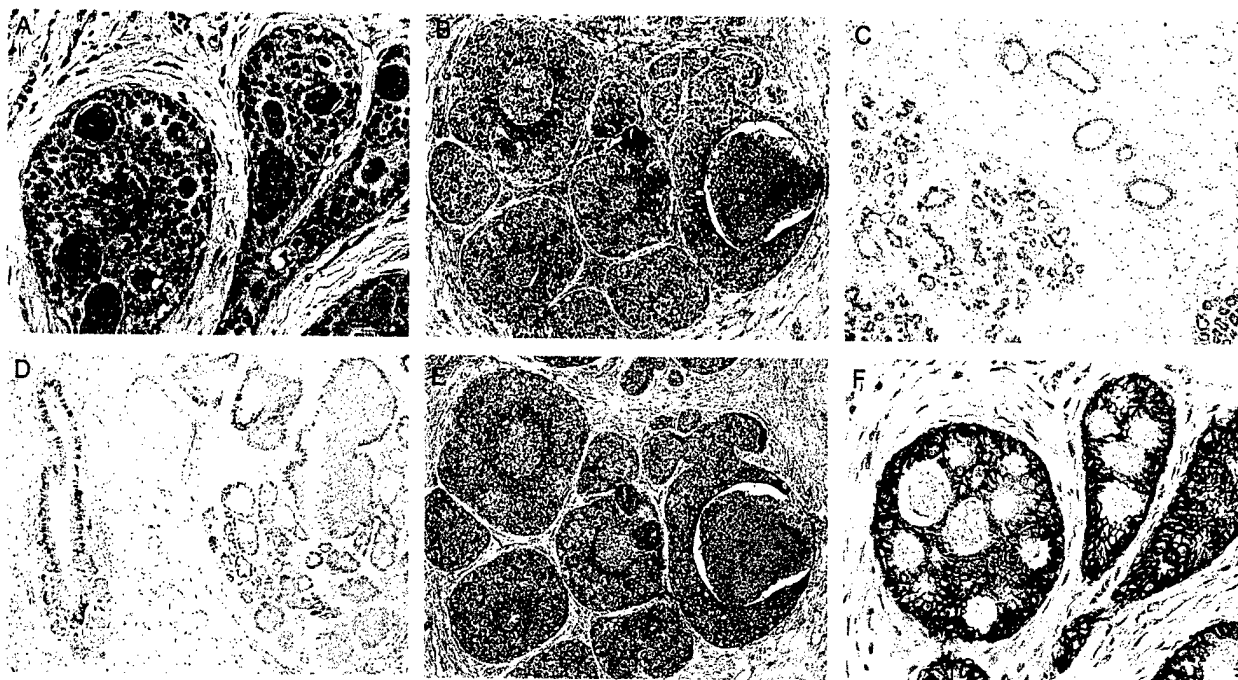


Figure 2. CA IX and CA XII have different expression profiles in non-neoplastic and neoplastic breast tissues. Low levels of CA IX expression are detected in low-grade DCIS (A) and more prominently in high-grade DCIS associated with central necrosis (B). CA XII expression in normal breast lobules and ducts (C), in ductal hyperplasia (D), in high-grade DCIS with accentuation adjacent to central luminal necrosis (E), and at higher levels in low-grade DCIS (F). Original magnifications, $\times 10$ (B-E) and $\times 20$ (A and F).

same tumor section, CA IX was expressed adjacent to regions of necrosis where this was present within the invasive component in four of 14 cases (29%). The presence of CA IX staining in both DCIS and invasive components was correlated ($r = 0.55$, $P = 0.04$). The focal perinecrotic nature of expression was reflected in the distribution of IHC scores with only 13 (19%) tumors scoring >10 (potential range of IHC score was 0 to 300, as described in Materials and Methods). The range of IHC scores was from 0 to 100 (median, 1; mean, 9; and SD, 17). Representative examples of low and high CA IX expression are illustrated in Figure 2, A and B. CA IX was significantly associated with high grade (grade low versus intermediate versus high; mean (SD), 2 (5), 11 (16), 13 (22), $P = 0.012$ analysis of variance) and the presence of necrosis (necrosis negative versus positive; mean (SD), 2 (5), 12 (19), $P = 0.0053$, Mann Whitney; Figure 3 and Table 1).

CA XII Expression in Breast Tissues

The expression of CA XII was assessed by IHC in sections adjacent to CA IX-stained sections for all 68 DCIS cases. Membranous staining of the basal-lateral aspects of breast epithelial cells was present in normal lobular and normal ductal epithelium in 42 of 47 (89%) cases and in every benign breast lesion observed (Figure 2, C and D). In ductal hyperplasia, CA XII expression was predominantly limited to basal epithelial cells. In DCIS lesions, widespread membranous CA XII staining was present in 57 of 68 (84%) cases, including 31 of 39 (79%) pure DCIS and 26 of 29 (90%) DCIS associated with invasive dis-

ease. In those cases in which invasive disease was present on the same tumor section, CA XII was expressed in 10 of 14 cases (71%). The presence of CA XII staining in both DCIS and invasive components was highly correlated ($r = 0.91$, $P < 0.0001$). Although expression in DCIS was typically homogeneous throughout the tumor section, in intermediate- and high-grade DCIS where CA XII expression tended to be lower, expression was increased adjacent to areas of necrosis (Figure 2E).

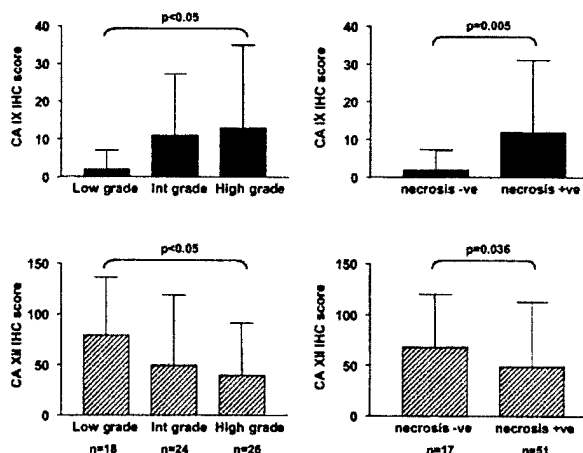


Figure 3. CA IX and CA XII expression are inversely related to grade and the presence of necrosis in DCIS. CA IX expression shown relative to grade (upper left) and necrosis (upper right) and CA XII expression shown relative to grade (lower left) and necrosis (lower right). Columns (CA IX, black; CA XII, hatched) represent the mean IHC score with bars showing SD relative to DCIS grade (low, intermediate, high) and necrosis (absent, present).

Table 1. Relationship between CA IX or CA XII Expression and Grade, Necrosis, and MIB1 Staining

DCIS parameter	No.	CA IX			CA XII		
		Negative	Positive		Negative	Positive	
Grade							
Low	18	14	4	$P = 0.0091$ $P = 0.0023$ (t)	7	11	ns ($P = 0.072$) $P = 0.025$ (t)
Intermediate	24	12	12		15	9	
High	26	8	18		19	7	
Necrosis							
Negative	17	14	3	$P = 0.002$	7	10	ns ($P = 0.55$)
Positive	51	20	31		17	34	
MIB1							
Low	13	6	7	ns ($P = 0.42$)	6	7	ns ($P = 0.69$)
High	13	4	9		5	8	

Statistical significance estimated by χ^2 test and χ^2 test for trend (t).

The distribution of IHC scores was wider than for CA IX, with 17 (25%) tumors scoring 60 or more (potential range, 0 to 300). The range of IHC scores was from 0 to 270 (median, 40; mean, 54; and SD, 61). Representative examples of low and high CA XII expression are illustrated in Figure 2, E and F. CA XII was significantly associated with low grade (grade low *versus* intermediate *versus* high; mean (SD), 79(57), 50(69), 40(52), $P = 0.012$ analysis of variance) and the absence of necrosis (necrosis negative *versus* positive; mean (SD), 68(52), 49(64), $P = 0.036$, Mann Whitney; Figure 3 and Table 1).

CA IX and CA XII Expression Relative to the Proliferation Marker MIB1

A correlation between CA IX and proliferation has been suggested previously.²⁶ We therefore examined the relationship between proliferation and CA IX and CA XII in our breast tissue specimens (Figure 4). Comparison of mitotic rates within positively stained ducts for CA IX and CA XII and within different zones in these ducts (adjacent to the stroma or the lumen), indicated that neither CA IX nor CA XII expression correlated regionally with mitosis. Whereas CA IX expression was typically localized to areas adjacent to necrosis, mitotic figures did not show a similar distribution, being most numerous in the cells adjacent to stroma and farthest removed from necrosis. Similarly, CA XII expression was not restricted to the areas of highest mitotic activity and was typically uniform throughout the intraductal epithelium, with occasional accentuation in luminal cells adjacent to necrosis. To confirm these morphological observations, a random subset of cases ($n = 26$) were immunostained for the proliferation marker MIB1 and the MIB1 score was determined by Chalkley counting. In agreement with previous observations,³⁷ we found MIB1 to be associated with both grade (low *versus* intermediate *versus* high; mean (SD), 0.16(0.07), 0.4(0.18), 0.56(0.33), $P = 0.0026$ analysis of variance) and the presence of necrosis (necrosis negative *versus* positive; mean (SD), 0.19(0.09), 0.51(0.28), $P = 0.001$ Mann Whitney; Figure 5). However, MIB1 was not significantly related to the expression of either CA IX or CA XII (CA IX negative *versus* positive; MIB1 mean (SD), 0.44(0.37), 0.37(0.21); CA XII negative *versus* positive; MIB1 mean (SD), 0.43(0.31), 0.38(0.26); Table 1).

Similarly, when CA IX and CA XII expression were divided into low and high expression using the median IHC score of the series for each (CA IX positive, >1 and CA XII negative, >40), no association was detected between the expression of either CA and MIB1 staining.

CA IX and CA XII Expression Relative to Mammographic Calcification

CA IX and CA XII expression were assessed in relation to the presence and pattern of calcification detected in preoperative mammograms in a subset of cases in which films were available for review ($n = 43$). The presence of calcification was associated with the presence of necrosis ($P = 0.0036$, chi-square) and higher grade ($P = 0.0057$, chi-square) (Table 2). When CA gene expression was classified as low or high on the basis of the median IHC score of the series (CA IX positive, >1 and CA XII positive, >40) a significant relationship was observed between lower CA XII expression and the presence of calcification ($P = 0.0083$, chi-square), as shown in Table 2. The level of CA XII expression was also inversely associated with calcification (calcification absent *versus* present, mean (SD), 94(60), 42(60), $P = 0.03$, Mann Whitney). The pattern of calcification was not significantly different with respect to either CA gene expression. Despite this, comparison of cases with nonlinear *versus* cases with some component of linear calcification revealed a trend toward an increased proportion of CA IX positive cases (8 of 21 vs. 9 of 14 or 38% vs. 64%), whereas the proportion of CA XII positive cases was no different (6 of 21 vs. 3 of 14 or 29% vs. 21%). Additionally, cases with linear calcification tended to be associated with higher levels of CA IX expression than cases with nonlinear calcification (CA IX IHC score mean (SD), 9 (12) vs. 5 (10), $P = \text{n.s.}$) whereas there was no such trend for CA XII (CA XII IHC score, 41 (69) vs. 43 (55), $P = \text{n.s.}$).

Discussion

We have shown that the tumor-associated CAs CA IX and CA XII are both expressed by malignant breast epithelium. CA IX expression was rare in normal ductal and lobular epithelium, and in benign breast lesions, occur-

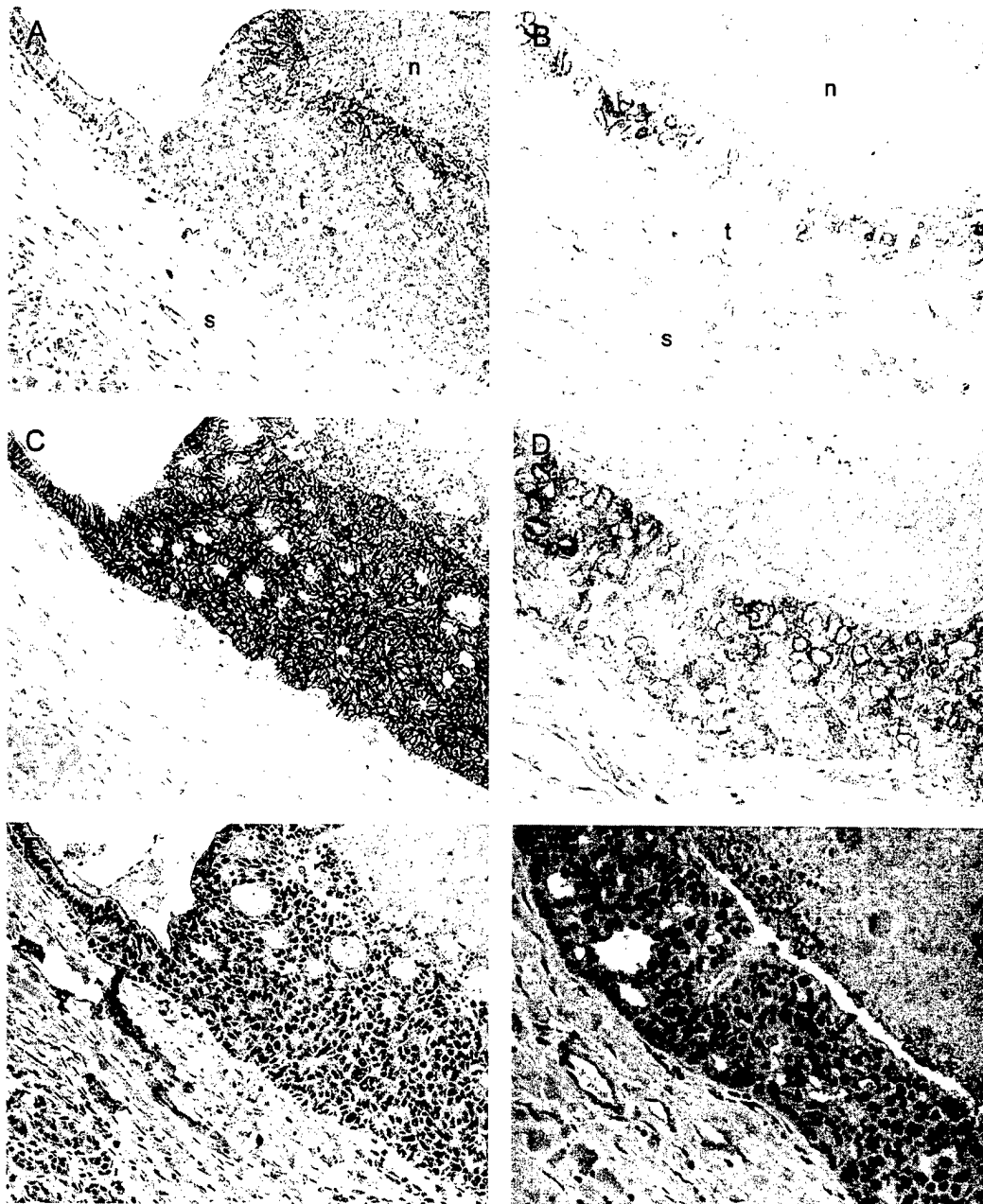


Figure 4. CA IX and CA XII expression is unrelated to MIB1 expression. The pattern of expression of CA IX (A and B), CA XII (C and D), and MIB1 (E and F), was assessed in serial sections from intermediate-grade DCIS (left column) and high-grade DCIS (right column). CA IX expression is restricted to the inner zone of luminal epithelium adjacent to central necrosis. CA XII expression is present throughout the duct wall, but accentuated adjacent to necrosis in high-grade DCIS, and also in the adjacent portion of non-neoplastic ductal epithelium (C, upper left). In contrast, MIB1-positive nuclei are distributed throughout the duct in both intermediate- and high-grade DCIS, and are absent from normal epithelium (E, upper left). Arrows within F indicate MIB1-positive nuclei. Original magnifications, $\times 20$.

ring primarily in pre-invasive DCIS and invasive breast carcinomas. In DCIS, expression was focal and specifically associated with regions of necrosis and high-grade lesions. In contrast, CA XII was frequently expressed in normal breast tissue as well as in benign, pre-invasive, and invasive breast lesions. In DCIS, expression was typically homogeneous and associated with the absence of necrosis and low-grade lesions. However, focal induction of CA XII was observed in high-grade DCIS adjacent to necrosis. The finding that both CA IX and CA XII are

induced *in vivo* in breast tumor cells adjacent to regions of necrosis suggests that these CAs may be important components of the breast epithelial cellular response to hypoxia. This observation is compatible with our recent findings in a variety of tissue-culture cell lines,²³ where both CA9 and CA12 are induced by hypoxia, and that at least for CA9 this induction is hypoxia-inducible factor-1-dependent. However, future studies to establish co-localization of CA expression with hypoxia-inducible factor-1 in tissue sections will be important to confirm *in vivo*.

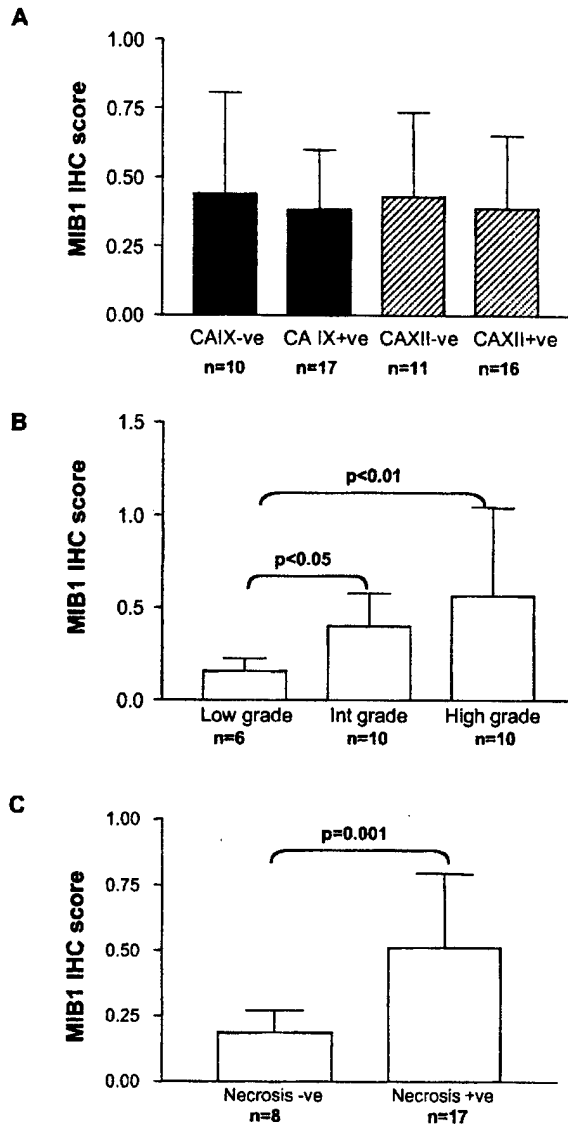


Figure 5. MIB1 expression relative to CA IX or CA XII expression, DCIS grade, and the presence of necrosis. Columns (CA IX, black; CA XII, hatched; MIB1, clear) represent the mean MIB1 IHC score with bars showing SD relative to CA IX or CA XII expression (negative, positive), DCIS grade (low, intermediate, high), and necrosis (absent, present).

CAs have been studied in a spectrum of tumor types in relation to their potential role as diagnostic and prognostic markers. Earlier studies focusing on CAs I, II, and IV revealed no clear relationships with tumorigenesis.²⁶ More recently, CA9 has been identified as overexpressed in multiple tumor cell lines and in several human tumor types. In various studies, CA9 has been found to be associated with aspects of early tumorigenesis,^{20,26,30,35,38} and it has therefore been proposed to serve as a biomarker for dysplasia. In accordance with these findings, we have shown that whereas CA IX expression is rare in normal or benign breast lesions, CA IX expression occurs in pre-invasive DCIS of the breast where it is limited to malignant epithelium. In the breast specimens examined, CA IX expression was not related to proliferation and was strongly associated with necrosis, indicating that hypoxia may be an important pathway for induction of CA IX in breast tumors *in vivo*.

CA12 was initially identified as a renal carcinoma-associated gene^{20,22} and has subsequently been found to be expressed in a range of normal tissues including endometrium, pancreas, and colon.^{31,39,40} Interestingly, in the normal colon CA XII is expressed highly by the differentiated surface epithelium relative to the cells of the crypt base, and whereas no change in the surface expression occurs with tumorigenesis, increased basal/deep mucosal expression is associated with increasing dysplasia and invasive tumor stage.³¹ Similarly, and in striking contrast to CA IX expression, we have observed constitutive expression of CA XII in normal breast epithelium and benign ductal hyperplasia. This suggests that CA XII may play a role in the control of pH in normal breast tissue. The function of this membrane-associated extracellular CA may be coupled to that of an intracellular CA such as CA II, as has been hypothesized for other secretory/excretory organs such as the salivary glands, pancreas, and kidney.⁴⁰ Clearly, a detailed examination of the interplay between the many CAs is warranted. We have also shown that CA XII expression persists in malignant pre-invasive DCIS. Although focal induction of CA XII was observed in areas adjacent to necrosis, the differentiation status of the DCIS lesion (as indicated by grade) had a more dominant role in determining CA XII

Table 2. Relationship in DCIS between the Presence of Calcification and CA IX or CA XII Expression, Necrosis, and Grade

DCIS parameter	No.	Mammogram calcification		
		Negative	Positive	
CA IX				
Negative	21	3	18	ns ($P = 0.477$)
Positive	22	5	17	
CA XII				
Negative	28	2	26	$P = 0.0083$
Positive	15	6	9	
Necrosis				
Negative	10	5	5	$P = 0.0036$
Positive	33	3	30	
Grade				
Low	9	5	4	$P = 0.0057$, $P = 0.0137$ (t)
Intermediate	15	1	14	
High	19	2	17	

Statistical significance estimated by χ^2 test and χ^2 test for trend (t).

expression, which was reflected in the pattern of expression observed in the ER-negative and ER-positive cell lines examined. Of note, differentiation has been proposed to play a role in the expression of other CAs, including CA I whose induction is associated with differentiation in the colon,⁴¹ and CA II whose expression is associated with differentiation in pancreatic cell lines under the influence of tumor necrosis factor- α .⁴²

An abnormal pattern of calcification in a breast mammogram is an important indicator of DCIS.⁵ In particular, the presence of linear type calcification is associated with high-grade DCIS and may predict outcome of associated small invasive tumors.^{5,6,43,44} Calcification is believed to reflect a disruption of the normal vascular architecture caused by abnormal proliferation within the intraductal epithelium.⁴⁵ This leads to a reduction in luminal pH, changes in the equilibria of many ions, and resulting calcification.⁴⁶ Inherited alteration and deficiency of CA II activity causes metabolic acidosis and ectopic tissue calcification.⁴⁷ Similarly, changes in extracellular pH influenced by CA IX and CA XII expression may affect the extent and pattern of calcification in DCIS of the breast. In the current series, increased mammographically detectable calcification was associated with reduced CA XII expression, as well as the presence of high-grade DCIS and necrosis, as previously reported.⁴⁸ Our inability to demonstrate a relationship between calcification and CA IX staining could relate to the fact that CA IX staining was only present very focally. Therefore, the tissue block assessed for CA IX expression may not correspond to the status of the area of the mammogram assessed for calcification, which encompassed the entire biopsy. Furthermore, our results suggest that whereas overall loss of CA XII expression is important in the development of calcification, local gain of CA IX expression adjacent to the ductal lumen may influence the pattern of calcification. However the significance of these observations awaits confirmation by larger studies as this subset of cases is small and includes a disproportionate number of cases with calcification present, reflecting the fact that calcification is a key factor in detection of tumors by mammography.⁵

The effect on local pH and the significance for breast tumor progression of reciprocal changes in the expression of these CAs remains to be determined. However, there is additional evidence to suggest that a switch in pH regulatory pathways may occur in breast tumor progression. Although a decrease in the activity of the Na⁺/H⁺ exchanger was noted in response to serum deprivation in nontumor breast cells, stimulation of this exchanger and an increased capacity for extracellular acidification was observed in tumor cells.⁴⁹ In terms of tumor progression, maintenance of high levels of CA XII may be important for both the function and survival of the ductal epithelium in normal tissue. Loss of CA XII expression with progression to higher grade DCIS may reflect the acquisition of alternative cellular responses to ameliorate the effects of disruption of tissue architecture, altered pH, and hypoxia.^{18,50} One facet of this adaptation may be provided by the induction of other CAs such as CA IX to modulate the effects of local hypoxia. This view predicts that overall

loss of CA XII and/or gain of CA IX expression may be associated with a high risk of progression to invasive disease and therefore be of prognostic significance. Interestingly, inhibition of CA activity has recently been demonstrated to suppress invasion of some tumor cell lines.⁵¹

In conclusion, we have shown that CA IX and CA XII are expressed in breast tissues, and that the profile of expression of these CAs in DCIS suggests that whereas hypoxia may be a dominant factor in the regulation of CA IX, the regulation of CA XII is dominated by other factors related to cellular differentiation.

References

1. Ernster VL, Barclay J, Kerlikowske K, Grady D, Henderson C: Incidence of and treatment for ductal carcinoma in situ of the breast. *JAMA* 1996, 275:913-918
2. Ernster VL, Barclay J: Increases in ductal carcinoma in situ (DCIS) of the breast in relation to mammography: a dilemma. *J Natl Cancer Inst Monogr* 1997, 22:151-156
3. Fentiman IS: Trials of treatment for non-invasive breast cancer. *Recent Results Cancer Res* 1998, 152:135-142
4. Fisher B: Highlights from recent National Surgical Adjuvant Breast and Bowel Project studies in the treatment and prevention of breast cancer. *CA Cancer J Clin* 1999, 49:159-177
5. Holland R, Hendriks JH: Microcalcifications associated with ductal carcinoma in situ: mammographic-pathologic correlation. *Semin Diagn Pathol* 1994, 11:181-192
6. Tabar L, Chen HH, Duffy SW, Yen MF, Chiang CF, Dean PB, Smith RA: A novel method for prediction of long-term outcome of women with T1a, T1b, and 10-14 mm invasive breast cancers: a prospective study. *Lancet* 2000, 355:429-433
7. Shoker BS, Sloane JP: DCIS grading schemes and clinical implications. *Histopathology* 1999, 35:393-400
8. Fisher ER, Costantino J, Fisher B, Palekar AS, Redmond C, Mamounas E: Pathologic findings from the National Surgical Adjuvant Breast Project (NSABP) Protocol B-17. Intraductal carcinoma (ductal carcinoma in situ). The National Surgical Adjuvant Breast and Bowel Project Collaborating Investigators. *Cancer* 1995, 75:1310-1319
9. Silverstein MJ, Lagios MD, Craig PH, Waisman JR, Lewinsky BS, Colburn WJ, Poller DN: A prognostic index for ductal carcinoma in situ of the breast. *Cancer* 1996, 77:2267-2274
10. Schnitt SJ, Harris JR, Smith BL: Developing a prognostic index for ductal carcinoma in situ of the breast. Are we there yet? *Cancer* 1996, 77:2189-2192
11. Leek RD, Landers RJ, Harris AL, Lewis CE: Necrosis correlates with high vascular density and focal macrophage infiltration in invasive carcinoma of the breast. *Br J Cancer* 1999, 79:991-995
12. Wetzels RH, Kuijpers HJ, Lane EB, Leigh IM, Troyanovsky SM, Holland R, van Haelst UJ, Ramaekers FC: Basal cell-specific and hyperproliferation-related keratins in human breast cancer. *Am J Pathol* 1991, 138:751-763
13. Vaupel P, Hoeckel M: Predictive power of the tumor oxygenation status. *Adv Exp Med Biol* 1999, 471:533-539
14. Dachs GU, Chaplin DJ: Microenvironmental control of gene expression: implications for tumor angiogenesis, progression, and metastasis. *Semin Radiat Oncol* 1998, 8:208-216
15. Brizel DM, Sibley GS, Prosnitz LR, Scher RL, Dewhirst MW: Tumor hypoxia adversely affects the prognosis of carcinoma of the head and neck. *Int J Radiat Oncol Biol Phys* 1997, 38:285-289
16. Valenta S, Wetterling M, Lehrke M, Schwickert G, Sundfor K, Rofstad EK, Mueller-Klieser W: High lactate levels predict likelihood of metastases, tumor recurrence, and restricted patient survival in human cervical cancers. *Cancer Res* 2000, 60:916-921
17. Maxwell PH, Dachs GU, Gleadle JM, Nicholls LG, Harris AL, Stratford IJ, Hankinson O, Pugh CW, Ratcliffe PJ: Hypoxia-inducible factor-1 modulates gene expression in solid tumors and influences both angiogenesis and tumor growth. *Proc Natl Acad Sci USA* 1997, 94:8104-8109

18. Zhong H, De Marzo AM, Laughner E, Lim M, Hilton DA, Zagzag D, Buechler P, Isaacs WB, Semenza GL, Simons JW: Overexpression of hypoxia-inducible factor 1 α in common human cancers and their metastases. *Cancer Res* 1999, 59:5830-5835
19. Grabmaier K, Vissers JL, De Weijert MC, Oosterwijk-Wakka JC, Van Bokhoven A, Brakenhoff RH, Noessner E, Mulders PA, Merks G, Figdor CG, Adema GJ, Oosterwijk E: Molecular cloning and immunogenicity of renal cell carcinoma-associated antigen G250. *Int J Cancer* 2000, 85:865-870
20. Ivanov SV, Kuzmin I, Wei MH, Pack S, Geil L, Johnson BE, Stanbridge EJ, Lerman MI: Down-regulation of transmembrane carbonic anhydrases in renal cell carcinoma cell lines by wild-type von Hippel-Lindau transgenes. *Proc Natl Acad Sci USA* 1998, 95:12596-12601
21. Opavsky R, Pastorekova S, Zelnik V, Gibadulinova A, Stanbridge EJ, Zavada J, Kettmann R, Pastorek J: Human MN/CA9 gene, a novel member of the carbonic anhydrase family: structure and exon to protein domain relationships. *Genomics* 1996, 33:480-487
22. Tureci O, Sahin U, Vollmar E, Siemer S, Gottert E, Seitz G, Parkkila AK, Shah GN, Grubb JH, Pfreundschuh M, Sly WS: Human carbonic anhydrase XII: cDNA cloning, expression, and chromosomal localization of a carbonic anhydrase gene that is overexpressed in some renal cell cancers. *Proc Natl Acad Sci USA* 1998, 95:7608-7613
23. Wykoff C, Beasley NJP, Watson PH, Turner KJ, Pastorek J, Sibbain A, Wilson GD, Turley H, Talks K, Maxwell PH, Pugh CW, Ratcliffe PJ, Harris AL: Hypoxia inducible expression of tumor associated carbonic anhydrases. *Cancer Res* 2000, 60:7075-7083
24. Jiang W, Gupta D: Structure of the carbonic anhydrase VI (CA6) gene: evidence for two distinct groups within the alpha-CA gene family. *Biochem J* 1999, 344:385-390
25. Pastorek J, Pastorekova S, Callebaut I, Morion JP, Zelnik V, Opavsky R, Zlatovicova M, Liao S, Portetelle D, Stanbridge EJ: Cloning and characterization of MN, a human tumor-associated protein with a domain homologous to carbonic anhydrase and a putative helix-loop-helix DNA binding segment. *Oncogene* 1994, 9:2877-2888
26. Nogradi A: The role of carbonic anhydrases in tumors. *Am J Pathol* 1998, 153:1-4
27. Liao SY, Stanbridge EJ: Expression of the MN antigen in cervical Papanicolaou smears is an early diagnostic biomarker of cervical dysplasia. *Cancer Epidemiol Biomarkers Prev* 1996, 5:549-557
28. Liao SY, Aurelio ON, Jan K, Zavada J, Stanbridge EJ: Identification of the MN/CA9 protein as a reliable diagnostic biomarker of clear cell carcinoma of the kidney. *Cancer Res* 1997, 57:2827-2831
29. Liao SY, Stanbridge EJ: Expression of MN/CA9 protein in Papanicolaou smears containing atypical glandular cells of undetermined significance is a diagnostic biomarker of cervical dysplasia and neoplasia. *Cancer* 2000, 88:1108-1121
30. Vermylen P, Roufosse C, Burny A, Verhest A, Bosschaerts T, Pastorekova S, Ninane V, Sculier JP: Carbonic anhydrase IX antigen differentiates between preneoplastic malignant lesions in non-small cell lung carcinoma. *Eur Respir J* 1999, 14:806-811
31. Kivela A, Parkkila S, Saarnio J, Karttunen TJ, Kivela J, Parkkila AK, Waheed A, Sly WS, Grubb JH, Shah G, Tureci O, Rajaniemi H: Expression of a novel transmembrane carbonic anhydrase isozyme XII in normal human gut and colorectal tumors. *Am J Pathol* 2000, 156:577-584
32. Silverstein MJ, Poller DN, Waisman JR, Colburn WJ, Barth A, Gierson ED, Lewinsky B, Gamagami P, Slamon DJ: Prognostic classification of breast ductal carcinoma-in-situ. *Lancet* 1995, 345:1154-1157
33. Wiesener MS, Turley H, Allen WE, Willam C, Eckardt KU, Talks KL, Wood SM, Gatter KC, Harris AL, Pugh CW, Ratcliffe PJ, Maxwell PH: Induction of endothelial PAS domain protein-1 by hypoxia: characterization and comparison with hypoxia-inducible factor-1 α . *Blood* 1998, 92:2260-2268
34. Pastorekova S, Zavadova Z, Kostal M, Babusikova O, Zavada J: A novel quasi-viral agent, MaTu, is a two-component system. *Virology* 1992, 187:620-626
35. Saarnio J, Parkkila S, Parkkila AK, Haukipuro K, Pastorekova S, Pastorek J, Kairaluoma MI, Karttunen TJ: Immunohistochemical study of colorectal tumors for expression of a novel transmembrane carbonic anhydrase, MN/CA IX, with potential value as a marker of cell proliferation. *Am J Pathol* 1998, 153:279-285
36. Saarnio J, Parkkila S, Parkkila AK, Waheed A, Casey MC, Zhou XY, Pastorekova S, Pastorek J, Karttunen T, Haukipuro K, Kairaluoma MI, Sly WS: Immunohistochemistry of carbonic anhydrase isozyme IX (MN/CA IX) in human gut reveals polarized expression in the epithelial cells with the highest proliferative capacity. *J Histochem Cytochem* 1998, 46:497-504
37. Zafrani B, Leroy A, Fourquet A, Laurent M, Trophime D, Validire P, Sastre-Garau X: Mammographically-detected ductal in situ carcinoma of the breast analyzed with a new classification. A study of 127 cases: correlation with estrogen and progesterone receptors, p53 and c-erbB-2 proteins, and proliferative activity. *Semin Diagn Pathol* 1994, 11:208-214
38. Turner JR, Odze RD, Crum CP, Resnick MB: MN antigen expression in normal, preneoplastic, and neoplastic esophagus: a clinicopathological study of a new cancer-associated biomarker. *Hum Pathol* 1997, 28:740-744
39. Karhamaa P, Parkkila S, Tureci O, Waheed A, Grubb JH, Shah G, Parkkila A, Kaunisto K, Tapanainen J, Sly WS, Rajaniemi H: Identification of carbonic anhydrase XII as the membrane isozyme expressed in the normal human endometrial epithelium. *Mol Hum Reprod* 2000, 6:68-74
40. Nishimori I, Fujikawa Adachi K, Onishi S, Hollingsworth MA: Carbonic anhydrase in human pancreas: hypotheses for the pathophysiological roles of CA isozymes. *Ann NY Acad Sci* 1999, 880:5-16
41. Sowden J, Leigh S, Talbot I, Delhanty J, Edwards Y: Expression from the proximal promoter of the carbonic anhydrase 1 gene as a marker for differentiation in colon epithelia. *Differentiation* 1993, 53:67-74
42. Franz MG, Winkler BC, Norman JG, Fabri PJ, Gower Jr WR: Tumor necrosis factor- α induces the expression of carbonic anhydrase II in pancreatic adenocarcinoma cells. *Biochem Biophys Res Commun* 1994, 205:1815-1821
43. Evans AJ, Pinder SE, Snead DR, Wilson AR, Ellis IO, Elston CW: The detection of ductal carcinoma in situ at mammographic screening enables the diagnosis of small, grade 3 invasive tumours. *Br J Cancer* 1997, 75:542-544
44. Holland R, Hendriks JH, Vebeek AL, Mravunac M, Schuurmans Stekhoven JH: Extent, distribution, and mammographic/histological correlations of breast ductal carcinoma in situ. *Lancet* 1990, 335:519-522
45. Engels K, Fox SB, Whitehouse RM, Gatter KC, Harris AL: Distinct angiogenic patterns are associated with high-grade in situ ductal carcinomas of the breast. *J Pathol* 1997, 181:207-212
46. Stubbs M, Rodrigues L, Howe FA, Wang J, Jeong KS, Veech RL, Griffiths JR: Metabolic consequences of a reversed pH gradient in rat tumors. *Cancer Res* 1994, 54:4011-4016
47. Sly WS, Sato S, Zhu XL: Evaluation of carbonic anhydrase isozymes in disorders involving osteopetrosis and/or renal tubular acidosis. *Clin Biochem* 1991, 24:311-318
48. Evans AJ, Pinder S, Ellis IO, Sibbering M, Elston CW, Poller DN, Wilson R: Screening-detected and symptomatic ductal carcinoma in situ: mammographic features with pathologic correlation. *Radiology* 1994, 191:237-240
49. Reshkin SJ, Bellizzi A, Albarani V, Guerra L, Tommasino M, Paradiso A, Casavola V: Phosphoinositide 3-kinase is involved in the tumor-specific activation of human breast cancer cell Na(+)/H(+) exchange, motility, and invasion induced by serum deprivation. *J Biol Chem* 2000, 275:5361-5369
50. Tannock IF, Rotin D: Acid pH in tumors and its potential for therapeutic exploitation. *Cancer Res* 1989, 49:4373-4384
51. Parkkila S, Rajaniemi H, Parkkila AK, Kivela J, Waheed A, Pastorekova S, Pastorek J, Sly WS: Carbonic anhydrase inhibitor suppresses invasion of renal cancer cells in vitro. *Proc Natl Acad Sci USA* 2000, 97:2220-2224

Carbonic Anhydrase IX, an Endogenous Hypoxia Marker, Expression in Head and Neck Squamous Cell Carcinoma and its Relationship to Hypoxia, Necrosis, and Microvessel Density

Nigel J. P. Beasley, Charles C. Wykoff, Peter H. Watson, Russell Leek, Helen Turley, Kevin Gatter, Jaromir Pastorek, Graham J. Cox, Peter Ratcliffe, and Adrian L. Harris¹

Oxford Centre for Head and Neck Oncology, Radcliffe Infirmary, Oxford OX2 6HE, United Kingdom [N. J. P. B., G. J. C.]; ICRF Molecular Oncology Group, Institute of Molecular Medicine [C. C. W., P. H. W., R. L., H. T., A. L. H.] and Nuffield Department of Clinical Laboratory Sciences [K. G.], John Radcliffe Hospital, Oxford OX3 9DU, United Kingdom; Institute of Virology, Slovak Academy of Sciences, Bratislava, Slovak Republic [J. P.]; and Wellcome Trust Centre for Human Genetics, Oxford OX3 7BN, United Kingdom [P. R.]

ABSTRACT

Carbonic anhydrase IX (CA IX) is a transmembrane glycoprotein with an active extracellular enzyme site. We have shown previously that it was hypoxia inducible and may therefore be an endogenous marker of hypoxia. It is overexpressed in some tumors, particularly renal cell carcinoma. The aim of this study was to examine the expression and localization of CA IX in head and neck squamous cell carcinoma (HNSCC) and relate this to the location of tumor microvessels, angiogenesis, necrosis, and stage. Expression of CA IX was determined by immunoblotting in three HNSCC cell lines grown in normoxia and hypoxia (pO₂ 0.1%) and three paired tumor and normal tissue samples of HNSCC. Archived paraffin sections (79) of HNSCC were immunostained with antibodies to CA IX and CD34 to determine microvessel density (MVD). By double staining sections with CA IX and CD34, the distance between blood vessels and the start of CA IX expression and necrosis was calculated. CA IX was induced by hypoxia in all three HNSCC cell lines and overexpressed in HNSCC tumor tissue. Overexpression was localized to the perinecrotic area of the tumor on immunostaining, and the percentage area of the tumor expressing CA IX was significantly higher with more tumor necrosis ($P = 0.001$), a high MVD ($P = 0.02$), and advanced stage ($P = 0.033$) on univariate analysis and necrosis ($P = 0.0003$) and MVD ($P = 0.0019$) on multivariate analysis. The median distance between a blood vessel and the start of CA IX expression was 80 μ m (range, 40–140 μ m). CA IX is overexpressed in HNSCC because of hypoxia and is a potential biomarker for hypoxia in this tumor. Overexpression may help to maintain the intracellular pH, giving tumor cells a survival advantage and enhancing resistance to radiotherapy and chemotherapy. CA IX is a potential target for future therapy in HNSCC.

INTRODUCTION

Carbonic anhydrases are encoded by three independent gene families: α -CA, β -CA, and γ -CA. CA9² is one of the α -CA isoenzymes. Carbonic anhydrases catalyze the reversible conversion of carbon dioxide to carbonic acid and are involved in respiration, calcification, acid-base balance, and the formation of aqueous humor, cerebrospinal fluid, saliva, and gastric acid. The different carbonic anhydrases have different tissue distribution, subcellular localization, biological function, kinetic properties, and susceptibility to inhibitors (1).

CA9 is a novel member of the carbonic anhydrase family which codes for a transmembrane glycoprotein that possesses an extracellu-

lar catalytic domain with weak enzymatic activity. It has homology also to basic helix-loop-helix domain proteins. Transfection into murine fibroblast NIH mouse fibroblast cells promotes proliferation, and it may be involved in control of cell proliferation and oncogenesis (1, 2).

There is abundant expression of CA IX protein in normal human upper GI mucosa and GI-associated structures, such as pancreas, gallbladder, and liver (3–5). Expression is most prominent on the basolateral surfaces of the crypt enterocytes in the duodenum and jejunum. This suggests that it might serve as a ligand or a receptor for another protein that regulates intercellular communication or cell proliferation (6). Interestingly, expression is lost in gastric adenocarcinoma (5). Normal human heart, lung, kidney, prostate, peripheral blood, brain, placenta, and muscle do not express CA IX (3).

CA IX overexpression has been identified in a number of solid tumors, including renal carcinoma and particularly clear cell adenocarcinoma (7–10), cervical squamous carcinoma (11, 12), ovarian carcinoma (13), colorectal carcinoma (14), esophageal carcinoma (15), bladder carcinoma (16), and non-small cell lung carcinoma (17). In some epithelial tissues, expression has been observed in areas of severe dysplasia, e.g., cervix (12), but in most, no expression is present until malignant invasion occurs, where it is often an early indicator of malignancy, e.g., lung carcinoma (17). There appears to be an inverse correlation between CA IX expression and stage and grade in some tumors (7, 11, 14, 15), and low expression of CA IX has been correlated with poor prognostic factors, such as lymph node metastases and depth of invasion (11, 14, 15).

Clear cell renal carcinoma where CA IX expression is particularly high is almost always associated with mutation of the VHL tumor suppressor gene and loss of function of pVHL (18). CA IX is also overexpressed in mutant VHL renal cell carcinoma cell lines. This overexpression is reversed by transfection of the wt VHL gene back into the cell (19).

After the recent description of VHL regulation of HIF-1 α (20), we investigated the hypoxic regulation of CA IX and have shown it is inducible by hypoxia. A HIF binding site in the 5' promoter region of CA9 was found, and we showed that a hypoxia response element and HIF-1 α were essential for CA9 transcription under hypoxia.

HNSCC is known to be a particularly hypoxic tumor with the degree of hypoxia having a significant impact on its response to radiotherapy chemotherapy and prognosis (22–25). The aim of this study was to examine the induction of CA IX by hypoxia in HNSCC cells lines and to analyze its expression and localization in HNSCC. Expression has been examined in relation to MVD as a measure of angiogenesis and necrosis as an indicator of the effects of hypoxia. Additionally, the distance of CA IX expression from blood vessels was analyzed as a surrogate assessment of the relation to hypoxia.

Received 1/16/01; accepted 4/24/01.

The costs of publication of this article were defrayed in part by the payment of page charges. This article must therefore be hereby marked *advertisement* in accordance with 18 U.S.C. Section 1734 solely to indicate this fact.

¹ To whom requests for reprints should be addressed, at ICRF Molecular Oncology Group, Institute of Molecular Medicine, John Radcliffe Hospital, Oxford OX3 9DU, United Kingdom. E-mail: aharris.lab@icrf.icnet.uk.

² The abbreviations used are: CA9, carbonic anhydrase 9 (gene); CA IX, carbonic anhydrase IX (protein); HIF-1 α , hypoxia inducible factor 1 α ; HNSCC, head and neck squamous cell carcinoma; MVD, microvessel density; TBS, Tris-buffered saline; VHL, von Hippel Lindau; MoAb, monoclonal antibody; wt, wild type; pH_i, intracellular pH; pH_e, extracellular pH; GI, gastrointestinal.

MATERIALS AND METHODS

Cell Lines. Human HNSCC lines UM-SCC22A, UM-SCC22B (courtesy of Dr. T. Carey, University of Michigan; Ref. 26), and SCC-25 (American Type Culture Collection) were maintained in DMEM with 10% heat-inactivated FCS and 2 mM fresh glutamine. Cells were exposed to normoxia or hypoxia (94.9% N₂, 5% CO₂, and 0.1% O₂) for 16 h. Cells were harvested on ice and homogenized in lysis buffer [8 M urea, 10% glycerol, 10 mM Tris-HCl (pH 6.8), 1% SDS, 5 mM phenylmethylsulfonyl, 1 µg/ml aprotinin, 10 µg/ml pepstatin, and 10 µg/ml leupeptin] using an IKA Ultra-Turrax T8 homogenizer (Janke & Kinkel, Staufen, Germany) for 30 s at full speed.

Primary renal adenocarcinoma cell lines expressing pVHL (RCC4/VHL) or empty vector (RCC4) were a gift from C. H. C. M. Buys (University of Groningen) and used as positive and negative controls as described (20). Cells were maintained in DMEM, 10% heat-inactivated FCS, 2 mM fresh glutamine, and 1 mg/ml G418 (G418 was removed from the medium 24 h before collection of samples). Cells were harvested on ice and prepared in 8 M urea lysis buffer as above. Whole cell preparations for immunostaining were harvested and fixed in 10% neutral buffered formalin overnight. Cell pellets were embedded in paraffin and sectioned onto silanized glass slides.

Fresh Tissue Samples. Three paired tumor and normal tissue samples from primary HNSCC were snap frozen in liquid nitrogen. Tissue samples were frozen sectioned and stained with H&E to ensure that material contained normal or tumor tissue as appropriate. Samples were sectioned on ice and homogenized in 8 M urea lysis buffer as above.

CA IX Immunoblotting. Cell and tissue extracts were protein quantified using the Bio-Rad detergent-compatible protein assay (Bio-Rad, UK) to ensure even protein loading between lanes. Samples were diluted in phosphate buffered saline to give 50 µg of protein/well. RCC4 and RCC4/VHL extracts were used as positive and negative controls, respectively. Proteins were resolved in NuPage Bis Tris 4–12% gels (Novex, UK) and transferred with a wet blotter (Novex) to Immobilon-P membrane (Millipore, Bedford, MA) in 25 mM Tris base, 190 mM glycine, and 15% methanol. Membranes were developed using the Western Breeze chemiluminescent immunodetection system (Novex) with mouse MoAb M75, as described (27), at a dilution of 1:50 in assay diluent.

Archived Tumor Specimens. Previously untreated patients (79) with HNSCC presented to the Oxford Center for Head and Neck Oncology between 1995 and 1999 were studied (Table 1). All had surgery as their first line of management, with some receiving postoperative radiotherapy. Specimens of complete resections rather than biopsies were selected so that both normal and tumor tissue were present on each slide. Seven samples of lymph node metastases from patients in this series were also selected.

H&E-stained sections of all of the specimens were examined at low (×40) and medium (×100) power by two observers (N. B. and P. W.). Tumors were graded as well, moderate or poorly differentiated. The margin of tumor invasion into surrounding normal tissue was identified as either pushing or infiltrating. A pushing margin is recognized when there is a defined border between tumor and stroma; an infiltrating margin when there is no clearly defined border to the tumor and invasion occurs in thin filaments (28). The whole tumor area was examined, and the degree of necrosis was divided into three categories 0 < 5%, 5.1 < 25%, and >25.1%.

Immunostaining. Sections (4 µm) of formalin-fixed, paraffin-embedded tissue were cut onto silanized glass slides. They were cleared of paraffin in CitrocLEAR (HD Supplies, UK) and rehydrated through graded alcohol baths. After a rinse in tap water, they were placed in 3% hydrogen peroxide for 15 min.

CA IX. Slides were blocked in 10% normal human serum for 15 min, then incubated with 1:50 MoAb M75, as described (27), in TBS and 5% normal human serum for 30 min. They were rinsed twice in TBS and then developed using the Horse Radish Peroxidase Envision System (DAKO). Slides were counterstained with hematoxylin (Sigma Chemical Co. diagnostics, St. Louis, MO) and mounted with Aquamount (BDH, Poole, UK). Slides were examined at low (×40) and medium (×100) power by two observers (P. W. and N. B.). The percentage of tumor cells positive for CA IX in the whole tumor section was determined. Formalin-fixed, paraffin-embedded RCC4 and RCC4/VHL cell pellets were used as positive and negative controls, respectively.

CD34. Slides were pressure cooked for 3 min in Tris/EDTA lysis buffer (pH 9.0) and incubated with 1:100 MoAb Qbend 10 (DAKO) in TBS for 60 min. After two rinses in TBS, they were incubated with goat antimouse IgG

Table 1 Patient and tumour characteristics by category and CA IX expression

	n	CA IX expression ^a Median (range)
Age (yr) (median, 62) (range, 17–92)		
>62	39	20% (0–80%)
<62	40	20% (0–90%)
Sex		
Male	54	20% (0–90%)
Female	25	15% (0–90%)
Site		
Oral cavity	31	20% (0–90%)
Oropharynx	23	30% (0–75%)
Larynx	16	7.5% (0–80%)
Hypopharynx	9	25% (0–75%)
Stage		
T ₁	9	5% (0–20%)
T ₂	20	20% (0–75%)
T ₃	18	27.5% (0–90%)
T ₄	32	20% (0–90%)
Nodal stage		
N ₀	38	20% (0–90%)
N+	41	20% (0–80%)
Grade		
Well differentiated	12	25% (0–75%)
Moderately differentiated	57	20% (0–90%)
Poorly differentiated	10	10% (0–60%)
Margin		
Pushing	49	30% (0–90%)
Infiltrating	27	15% (0–80%)
Unable to assess	3	
Necrosis (median, 5%) (range, 0–75%)		
Low (<5%)	46	15% (0–75%)
Moderate (5–25%)	26	30% (0–90%)
High (>25%)	7	60% (5–90%)
MVD (median, 6%) (range, 0–7)		
Low (<5.7)	46	10% (0–90%)
High (>6)	30	35% (0–90%)

^a As a percentage of the tumour area involved.

(PO447, DAKO) for 30 min, washed in TBS, and then incubated with alkaline phosphatase anti-alkaline phosphatase for 30 min. The last two steps were repeated twice with 10-min incubations as described (29). New Fuchsin Red substrate was applied for 15 min, and slides were counterstained with hematoxylin and mounted with Aquamount. MVD was determined in tumor microvessel hotspots using a Chalkley point counting grid at high power (×250) by two observers (R. L. and N. B.). The average of the vessel counts in the three most vascular areas per section was taken (30).

Double Staining CA IX, CD34. Two representative slides demonstrating overexpression of CA IX and areas of necrosis were selected. CA IX immunostaining was carried out as above using the Horse Radish Peroxidase Envision System (DAKO) without counterstaining. Slides were then washed for 15 min in TBS, and immunostaining for CD34 was carried out as above. Slides were counterstained and mounted as above.

The distance from blood vessels marked with CD34 to the start of CA IX expression and necrosis was assessed using an eyepiece graticule calibrated against a graduated slide. Measurements were taken from both tumors in three different areas carefully selected to represent cross sections of a tumor cord, avoiding oval or longitudinal sections. Measurements were done in three different directions from a single vessel.

Statistics. Correlation between the level of CA IX expression in sections of primary tumor and nodal metastases was examined using Spearman's rank correlation. The difference in CA IX expression with age (two categories at the median age), MVD (two categories at the highest third), percentage of tumor necrosis (three categories: 0–5%, 5–25%, and >25%), sex, T stage (T_{1–4}), N stage (N₀ and N+), grade of tumor, and margin of invasion was compared using a Mann-Whitney U test or Kruskal Wallis test as appropriate. The difference in necrosis score with MVD (two categories at the highest third) was examined using the Mann-Whitney U test. For multivariate analysis, bivariate logistic regression was used and an odds ratio calculated. For this test, CA IX expression was divided at the median into two categories of high expression (>20%) and low expression (≤20%), necrosis into two categories present (>5%) or absent (≤5%), and T stage into early (T_{1,2}) and advanced (T_{3,4}). All statistics were done using SPSS software v9.0.

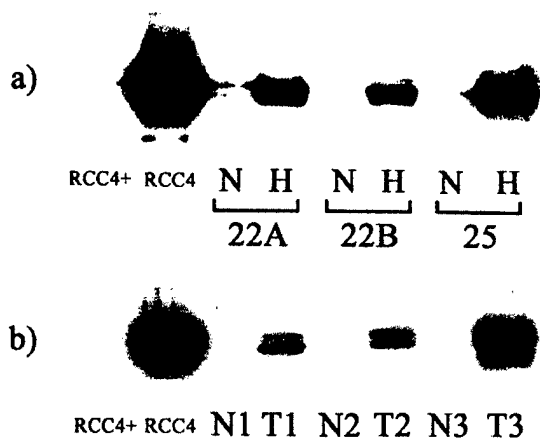


Fig. 1. *RCC4/VHL* (wt VHL), negative control; *RCC4* (empty vector), positive control. *a*, expression of CA IX in HNSCC cell lines (UM-SCC22A, UM-SCC22B, and SCC-25) on Western blotting in normoxia and hypoxia. *N*, normoxia; *H*, hypoxia (pO_2 0.1%). *b*, expression of CA IX in paired tumor and normal tissue from 3 patients with HNSCC. *T*, tumor tissue; *N*, paired normal tissue.

RESULTS

Expression of CA IX on Western Blotting in HNSCC Cell Lines and Tissue Samples. Because VHL mutation constitutively up-regulates HIF-1 α , controls for CA IX expression were extracts from the renal cell line RCC4 with VHL mutation. They showed marked up-regulation of CA IX in normoxia, in contrast to the control RCC4/VHL cell line transfected with wt VHL, where CA IX was minimal in

normoxia. It appeared as two bands related to glycosylation. CA IX was up-regulated in all three head and neck cell lines exposed to hypoxia (0.1% O_2 for 16 h) with little or no expression in normoxia (Fig. 1*a*). CA IX expression was clearly up-regulated in tumor samples compared with paired normal tissue taken at operation from patients with HNSCC (Fig. 1*b*).

Localization of CA IX Expression in HNSCC. CA IX was over-expressed in 71 of 79 HNSCC tumor sections examined; expression was confined to the perinecrotic region of these tumors (Fig. 2*a*). It was absent or very low in the normal epithelium overlying tumor tissue (Fig. 2*b*). Expression was confined to the cell membrane (Fig. 2*c*). In the eight tumor sections where no CA IX expression was seen, there was little or no tumor necrosis observed (0% necrosis in four cases, 5% necrosis in two cases, 20% necrosis in two cases). The level of expression was similar in both the primary and lymph node metastases from the same patient in all seven cases, although no significant correlation could be demonstrated because of the small numbers [primary median CA IX 50% (range, 5–60%), secondary median CA IX 35% (range, 20–80%), $n = 7$, $P = 0.093$, Spearman's correlation].

Distance between Blood Vessel and Necrosis and CA IX Expression. The median distance from a blood vessel to the start of necrosis was 130 μ m (range, 80–200 μ m; $n = 18$), and the median distance between a blood vessel and the start of CA IX expression was 80 μ m (range, 40–140 μ m; $n = 18$), as shown in Fig. 2*f*. Using a formula published by Tomlinson and Gray (31), which makes assumptions about oxygen diffusion and consumption on the basis of experiments done on squamous cell carcinoma of the lung, the partial pressure of oxygen at a given distance from the nearest vessel can be

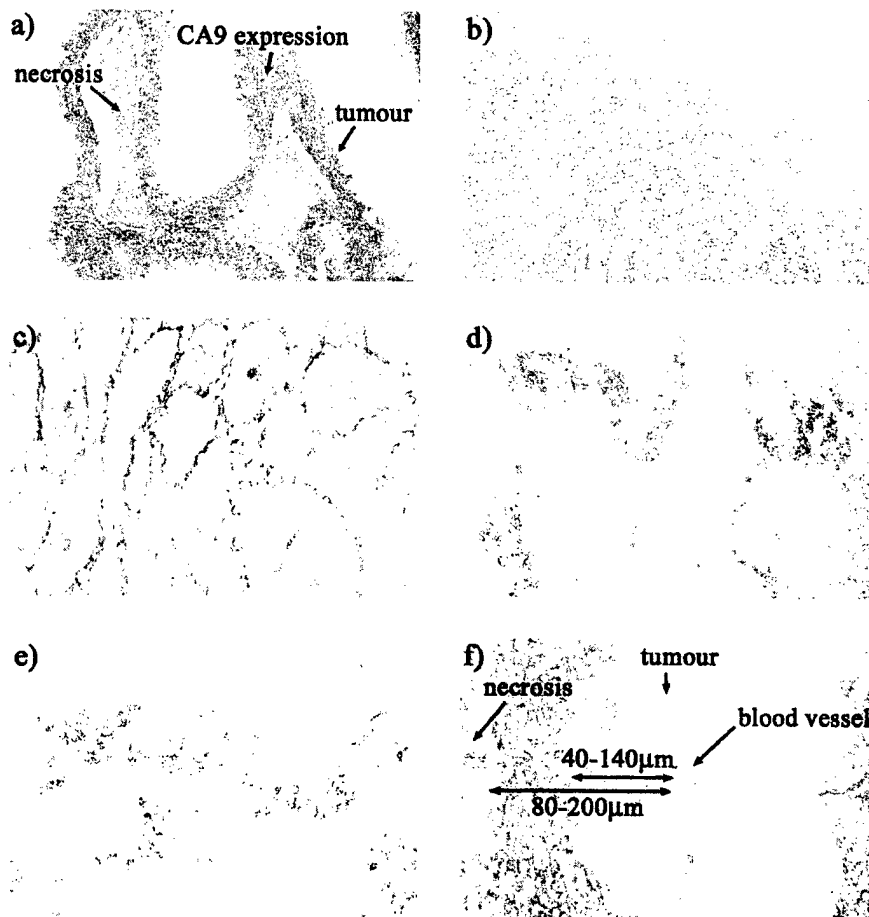


Fig. 2. Expression of CA IX on immunostaining in HNSCC. *a*, perinecrotic expression of CA IX ($\times 100$). *b*, overlying normal squamous epithelium ($\times 100$). *c*, membrane expression of CA IX ($\times 1000$). Expression of CA IX is shown in paired primary (*d*) and lymph node metastases (*e*; $\times 100$). *f*, range of distances between a blood vessel labeled with CD34 MoAb and the start of CA IX expression and necrosis ($\times 250$).

calculated (Fig. 3). In the HNSCC sections examined here, the median distance from a blood vessel to the start of CA IX expression of 80 μm (range, 40–140 μm) gives a tissue pO_2 of 1% (range, 0–2.8%). These results are only approximate because of the shrinkage of tissue on formalin fixation, the variation in sectioning of the tumor, and the assumptions made about oxygen diffusion and consumption.

Difference in CA IX Expression with MVD, Necrosis Score, and T Stage. CA IX expression was higher in tumors with a MVD in the top third of the range ($P = 0.02$, Mann-Whitney; Table 1), as shown in Fig. 4. CA IX expression was also higher as the percentage of tumor necrosis increased ($P = 0.001$, Kruskal Wallis; Table 1), as shown in Fig. 5. There was a significantly higher level of CA IX expression in more advanced tumors (T_{2-4}) compared with T_1 tumors ($P = 0.033$, Kruskal Wallis; Table 1). There was no significant difference in CA IX expression between categories of age, sex, N-stage, grade, or margin of invasion (Table 1). There was no significant difference in percentage of tumor necrosis with increasing T stage ($P = 0.37$, Kruskal Wallis, data not shown) or high and low MVD ($P = 0.47$, Mann-Whitney, data not shown).

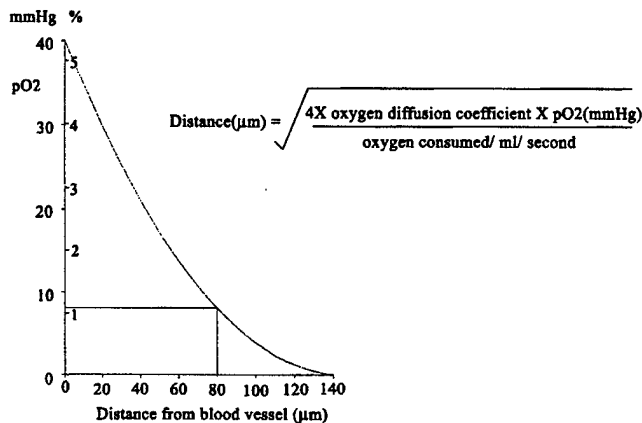


Fig. 3. Formula for the calculation of the oxygen tension at distances from a blood vessel (31). Shown is pO_2 (vertical axis) in mmHg and percentage of O_2 . The median distance from a blood vessel, 80 μm , and lower end of the range, 40 μm , are shown with their corresponding pO_2 .

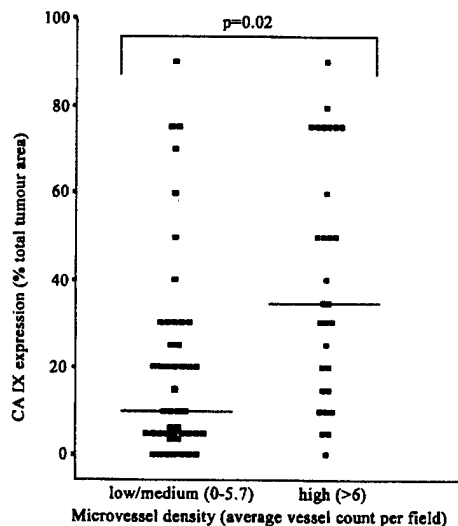


Fig. 4. Difference in CA IX expression with MVD measured by Chalkley vessel counting in HNSCC, $n = 76$. The percentage of total tumor area positive for CA IX is plotted against categories of MVD, low/medium (<5.7) and high (>6). There is a significant difference between the two categories, $P = 0.02$, Mann-Whitney U test.

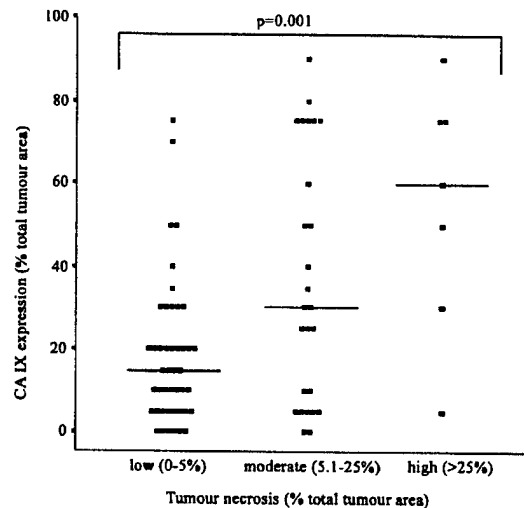


Fig. 5. Difference in CA IX expression with percentage area of tumor necrosis in HNSCC, $n = 79$. The percentage of total tumor area positive for CA IX is plotted against categories of necrosis, low ($<5\%$), moderate (5.1–25%), and high ($>25\%$). There is a significant difference between the three categories, $P = 0.001$, Kruskal Wallis test.

When the difference in CA IX expression between high and low groups of MVD, categories of necrosis, and T stage was examined using multivariate analysis, percentage of tumor necrosis ($P = 0.0003$; odds ratio, 10.0) and MVD ($P = 0.0019$; odds ratio, 7.3) remained significant factors associated with CA IX expression. The effect of T stage on CA IX expression was no longer seen.

DISCUSSION

Hypoxic regions are common within solid tumors because of disorderly vasculature, shunting of blood, and oxygen consumption out of balance with oxygen supply as rapid growth outstrips the blood supply (32–35). Tumor hypoxia has been shown to be important in resistance to radiotherapy and chemotherapy (25, 36–38) and has a significant effect on disease free and overall survival in HNSCC (22, 23, 37).

This study demonstrates that CA IX is overexpressed in HNSCC. It was clearly induced by hypoxia in cell lines *in vitro*, and on immunostaining expression, it was clearly localized to the perinecrotic regions of the tumor, which are known to be hypoxic. CA IX expression was seen at a median distance from blood vessels of 80 μm correlating with a calculated pO_2 in the range of 1% at the edge nearest the blood vessels. At the edge nearest the area of necrosis, the pO_2 would be $\sim 0.1\%$, which *in vitro* also gave strong induction of CA IX. There was a significant increase in CA IX expression as tumor necrosis increased. These observations suggest that CA IX is regulated by hypoxia *in vivo*. There was variability between tumors in distance from blood vessels to necrosis, which may reflect the susceptibility of the tumor cells to hypoxia-induced death, the heterogeneity of oxygen distribution within the tumor (39), or O_2 consumption by the tumor contributing to the final effect of necrosis. However, these variations also appear to affect CA IX expression concomitantly. CA IX expression was only seen in the cell membrane on immunostaining. It is a transmembrane glycoprotein that makes CA IX a potentially useful indicator of tissue hypoxia, as the protein cannot diffuse away from its point of origin. This is in contrast to vascular endothelial growth factor, which does not correlate with biomarkers of hypoxia, such as Pimonidazole (40). Although secreted proteins may be useful peripheral blood markers of hypoxia (41), CA IX is induced at the same oxygen tension at which HIF-1 α and its downstream

target genes are induced and provides a measure of the percentage of the tumor population that is hypoxic (42).

The correlation between CA IX and MVD is likely to be attributable to the overexpression of CA IX at the same oxygen tension as hypoxia-induced proangiogenic cytokines, such as vascular endothelial growth factor. The lack of correlation between MVD and necrosis may be because necrosis indicates both severe hypoxia, metabolic O_2 consumption by the tumor, and the ability of a cell to withstand hypoxia rather than being a simple measure of hypoxia, although one study in breast carcinoma did find a correlation between MVD and necrosis (43).

Tumor cells can undergo apoptosis in hypoxia, and therefore, there is strong selection for pathways to escape this fate, e.g., p53 mutation (44). Selection of these cells in the hypoxic microenvironment is an important mechanism for malignant progression (45). Hypoxic apoptosis is substantially mediated by an acidotic pHe, which occurs because of the switch from aerobic to anaerobic metabolism in hypoxia, *in vitro* studies (46). In that study, buffering the pH changes in hypoxia either by changing the medium or more concentrated buffers allowed cell survival under hypoxia. Thus, induction of genes able to regulate extracellular or pHi may help hypoxic cells survive. Several mechanisms exist at a cellular level to generate an acidotic pHe and maintain the pHi. It has been proposed that increased activity of the mitogen-sensitive Na^+/H^+ exchanger, increased function or expression of H^+ pumping ATPases, or an interaction between the tumor cell and its immediate environment may maintain the pHi at a normal level while lowering the pHe. Carbonic anhydrases have been suggested as one mechanism whereby the cell could maintain a difference in pH across its membrane (19, 47, 48).

Carbonic anhydrases catalyze the reversible conversion of H_2O and CO_2 to carbonic acid. During aerobic metabolism, CO_2 is generated. This moves out of the cell down a diffusion gradient as the extracellular CO_2 is maintained at a lower level by conversion to carbonic acid, which dissociates into H^+ and HCO_3^- . The bicarbonate ions are pumped back into the cell in exchange for chloride ions while the H^+ ions remain in the extracellular environment and lower the pHe. The induction by hypoxia of CA IX with its active extracellular enzyme site could theoretically help to lower the extracellular CO_2 and maintain the pHi at a normal level, preventing apoptosis and giving the cell a major survival advantage. A reduction in the pHe has advantages to tumor cells as it helps in the breakdown of the extracellular matrix, migration and invasion of tumor cells, induction of expression of growth factors, and reduction of the viability of nearby cells (49). This potential ability of hypoxia-induced CA IX to affect the pHi and pHe *in vitro* and *in vivo* is currently under investigation. The pH of a tumor is one of the most significant factors in mathematical models of tumor survival. (50). Chronic lowering of the pHi by inhibitors of the Na^+/H^+ exchanger or Na^+ -dependent HCO_3^-/Cl^- exchanger is directly cytotoxic to tumor cells and inhibits tumor growth (48).

The pH of a tumor may significantly alter the uptake of chemotherapy drugs, particularly if they are weak electrolytes (51). Chlorambucil and 5FU, both weak acids, have increased toxicity and are retained in tumors cells when there is a low pHe (52, 53). Doxorubicin and mitoxantrone, both weak bases, have reduced intracellular accumulation with low pHe (54, 55). Doxorubicin toxicity has been enhanced in an animal model by raising the pHe with bicarbonate in the drinking water (49).

Carbonic anhydrase inhibitors have been shown to inhibit tumor cell invasion *in vitro* (47), and in xenograft experiments, carbonic anhydrase inhibitors as part of a chemotherapy regimen enhanced the effect of chemotherapy drugs and helped delay tumor growth (56).

Thus, our demonstration of up-regulation of CA IX *in vivo* in a perinecrotic pattern suggests this may be an important pathway in

hypoxia, possibly regulating pHe to allow survival of a viable rim of cells under hypoxic conditions. This subpopulation of cells may be a suitable target for inhibitors of carbonic anhydrase. Use of CA IX as a target for radioimmunotherapy with MoAbs or use of CA IX to convert a pro-drug to an active drug may have potential problems because of its abundant expression normal human upper GI mucosa and GI-associated structures.

CA IX expression correlates with the oxygen diffusion distance and is expressed in a perinecrotic manner; this may be a marker for hypoxia in HNSCC. It is induced by hypoxia in HNSCC cells and is up-regulated in HNSCC. Up-regulation correlates with tumor necrosis and MVD. Overexpression may help to maintain the pHi, give tumor cells a survival advantage, and enhance resistance to radiotherapy and chemotherapy. CA IX provides a potential target for future therapy.

REFERENCES

- Opavsky, R., Pastorekova, S., Zelnik, V., Gibadulinova, A., Stanbridge, E. J., Zavada, J., Kettmann, R., and Pastorek, J. Human MN/CA9 gene, a novel member of the carbonic anhydrase family: structure and exon to protein domain relationships. *Genomics*, 33: 480-487, 1996.
- Pastorek, J., Pastorekova, S., Callebaut, L., Mornon, J. P., Zelnik, V., Opavsky, R., Zaf'oviova, M., Liao, S., Portetelle, D., Stanbridge, E. J., et al. Cloning and characterization of MN, a human tumor-associated protein with a domain homologous to carbonic anhydrase and a putative helix-loop-helix DNA binding segment. *Oncogene*, 9: 2877-2888, 1994.
- McKiernan, J. M., Buttyan, R., Bander, N. H., Stifelman, M. D., Katz, A. E., Chen, M. W., Olsson, C. A., and Sawczuk, I. S. Expression of the tumor-associated gene MN: a potential biomarker for human renal cell carcinoma. *Cancer Res.*, 57: 2362-2365, 1997.
- Nishimori, I., Fujikawa-Adachi, K., Onishi, S., and Hollingsworth, M. A. Carbonic anhydrase in human pancreas: hypotheses for the pathophysiological roles of CA isozymes. *Ann. N. Y. Acad. Sci.*, 880: 5-16, 1999.
- Pastorekova, S., Parkkila, S., Parkkila, A. K., Opavsky, R., Zelnik, V., Saarnio, J., and Pastorek, J. Carbonic anhydrase IX, MN/CA IX: analysis of stomach complementary DNA sequence and expression in human and rat alimentary tracts. *Gastroenterology*, 112: 398-408, 1997.
- Saarnio, J., Parkkila, S., Parkkila, A. K., Waheed, A., Casey, M. C., Zhou, X. Y., Pastorekova, S., Pastorek, J., Karttunen, T., Haukipuro, K., Kairaluoma, M. I., and Sly, W. S. Immunohistochemistry of carbonic anhydrase isozyme IX (MN/CA IX) in human gut reveals polarized expression in the epithelial cells with the highest proliferative capacity. *J. Histochem. Cytochem.*, 46: 497-504, 1998.
- Uemura, H., Nakagawa, Y., Yoshida, K., Saga, S., Yoshikawa, K., Hirao, Y., and Oosterwijk, E. MN/CA IX/G250 as a potential target for immunotherapy of renal cell carcinomas. *Br. J. Cancer*, 81: 741-746, 1999.
- Liao, S. Y., Aurelio, O. N., Jan, K., Zavada, J., and Stanbridge, E. J. Identification of the MN/CA9 protein as a reliable diagnostic biomarker of clear cell carcinoma of the kidney. *Cancer Res.*, 57: 2827-2831, 1997.
- McKiernan, J. M., Buttyan, R., Bander, N. H., de la Taille, A., Stifelman, M. D., Emanuel, E. R., Bagiella, E., Rubin, M. A., Katz, A. E., Olsson, C. A., and Sawczuk, I. S. The detection of renal carcinoma cells in the peripheral blood with an enhanced reverse transcriptase-polymerase chain reaction assay for MN/CA9. *Cancer (Phila.)*, 86: 492-497, 1999.
- Murakami, Y., Kanda, K., Tsuji, M., Kanayama, H., and Kagawa, S. MN/CA9 gene expression as a potential biomarker in renal cell carcinoma. *BJU Int.*, 83: 743-747, 1999.
- Brewer, C. A., Liao, S. Y., Wilczynski, S. P., Pastorekova, S., Pastorek, J., Zavada, J., Kurosaki, T., Manetta, A., Berman, M. L., DiSaia, P. J., and Stanbridge, E. J. A study of biomarkers in cervical carcinoma and clinical correlation of the novel biomarker MN. *Gynecol. Oncol.*, 63: 337-344, 1996.
- Liao, S. Y., and Stanbridge, E. J. Expression of the MN antigen in cervical papanicolaou smears is an early diagnostic biomarker of cervical dysplasia. *Cancer Epidemiol. Biomarkers Prev.*, 5: 549-557, 1996.
- Zavada, J., Zavadova, Z., Pastorekova, S., Ciampor, F., Pastorek, J., and Zelnik, V. Expression of MaTu-MN protein in human tumor cultures and in clinical specimens. *Int. J. Cancer*, 54: 268-274, 1993.
- Saarnio, J., Parkkila, S., Parkkila, A. K., Haukipuro, K., Pastorekova, S., Pastorek, J., Kairaluoma, M. I., and Karttunen, T. J. Immunohistochemical study of colorectal tumors for expression of a novel transmembrane carbonic anhydrase, MN/CA IX, with potential value as a marker of cell proliferation. *Am. J. Pathol.*, 153: 279-285, 1998.
- Turner, J. R., Odze, R. D., Crum, C. P., and Resnick, M. B. MN antigen expression in normal, preneoplastic, and neoplastic esophagus: a clinicopathological study of a new cancer-associated biomarker. *Hum. Pathol.*, 28: 740-744, 1997.
- Uemura, H., Kitagawa, H., Hirso, Y., Okajama, E., DeBruyne, C., Coaterwijk, E. Expression of tumour-associated antigen MN/G250 in urologic carcinoma: potential therapeutic target. *J. Urol.*, 157 (Suppl.): 377, 1997.
- Vermynen, P., Roufosse, C., Burny, A., Verhest, A., Bosschaerts, T., Pastorekova, S., Ninane, V., and Sculier, J. P. Carbonic anhydrase IX antigen differentiates between preneoplastic malignant lesions in non-small cell lung carcinoma. *Eur. Respir. J.*, 14: 806-811, 1999.

18. Iliopoulos, O., and Kaelin, W. The molecular basis of von Hippel-Lindau disease. *Mol. Med. Today*, 3: 289-293, 1997.
19. Ivanov, S. V., Kuzmin, I., Wei, M. H., Pack, S., Geil, L., Johnson, B. E., Stanbridge, E. J., and Lerman, M. I. Down-regulation of transmembrane carbonic anhydrases in renal cell carcinoma cell lines by wild-type von Hippel-Lindau transgenes. *Proc. Natl. Acad. Sci. USA*, 95: 12596-12601, 1998.
20. Maxwell, P., Weisner, M. S., Chang, G. W., Clifford, S. C., Vaux E. C., Cockman, M. E., Wykoff, C. C., Pugh, C. W., Maher, E. R., Ratcliffe, P. J. The tumour suppressor protein VHL targets hypoxia-inducible factors for oxygen-dependent proteolysis. *Nature (Lond.)*, 399: 271-275, 1999.
21. Wykoff, C., Beasley, N., Watson, P., Turner, L., Pastorek, J., Wilson, G., Turley, H., Maxwell, P., Pugh, C., Ratcliffe, P., and Harris, A. Hypoxia-inducible regulation of tumor-associated carbonic anhydrases. *Cancer Res.*, 60: 7075-7083, 2000.
22. Brizel, D. M., Dodge, R. K., Clough, R. W., and Dewhirst, M. W. Oxygenation of head and neck cancer: changes during radiotherapy and impact on treatment outcome. *Radiother. Oncol.*, 53: 113-117, 1999.
23. Stadler, P., Becker, A., Feldmann, H. J., Hansgen, G., Dunst, J., Wurschmidt, F., and Molls, M. Influence of the hypoxic subvolume on the survival of patients with head and neck cancer. *Int. J. Radiat. Oncol. Biol. Phys.*, 44: 749-754, 1999.
24. Sundfor, K., Lyng, H., and Rofstad, E. K. Tumour hypoxia and vascular density as predictors of metastasis in squamous cell carcinoma of the uterine cervix. *Br. J. Cancer*, 78: 822-827, 1998.
25. Vaupel, P., and Hoeckel, M. Predictive power of the tumor oxygenation status. *Adv. Exp. Med. Biol.*, 471: 533-539, 1999.
26. Carey, T. Head and neck tumor lines. In: R. Hay, A. Gazdar, and J-G. Park (eds.), *Atlas of Human Tumor Cell Lines*, pp. 79-120. Orlando, FL: Academic Press, Inc., 1994.
27. Pastorekova, S., Zavadvova, Z., Kostal, M., Babusikova, O., and Zavada, J. A novel quasi-viral agent, MaTu, is a two-component system. *Virology*, 187: 620-626, 1992.
28. Crissman, J. D., Liu, W. Y., Gluckman, J. L., and Cummings, G. Prognostic value of histopathologic parameters in squamous cell carcinoma of the oropharynx. *Cancer (Phila.)*, 54: 2995-3001, 1984.
29. Cordell, J. L., Falini, B., Erber, W. N., Ghosh, A. K., Abdulaziz, Z., MacDonald, S., Pulford, K. A., Stein, H., and Mason, D. Y. Immunoenzymatic labeling of monoclonal antibodies using immune complexes of alkaline phosphatase and monoclonal anti-alkaline phosphatase (APAAP complexes). *J. Histochem. Cytochem.*, 32: 219-229, 1984.
30. Fox, S. B. Tumour angiogenesis and prognosis. *Histopathology*, 30: 294-301, 1997.
31. Tomlinson, R., and Gray, L. The histological structure of some human lung cancers and the possible implications for radiotherapy. *Br. J. Cancer*, 9: 539-549, 1955.
32. Dewhirst, M. W., Secomb, T. W., Ong, E. T., Hsu, R., and Gross, J. F. Determination of local oxygen consumption rates in tumors. *Cancer Res.*, 54: 3333-3336, 1994.
33. Secomb, T. W., Hsu, R., Dewhirst, M. W., Klitzman, B., and Gross, J. F. Analysis of oxygen transport to tumor tissue by microvascular networks. *Int. J. Radiat. Oncol. Biol. Phys.*, 25: 481-489, 1993.
34. Secomb, T. W., Hsu, R., Ong, E. T., Gross, J. F., and Dewhirst, M. W. Analysis of the effects of oxygen supply and demand on hypoxic fraction in tumors. *Acta Oncol.*, 34: 313-316, 1995.
35. Kimura, H., Braun, R. D., Ong, E. T., Hsu, R., Secomb, T. W., Papahadjopoulos, D., Hong, K., and Dewhirst, M. W. Fluctuations in red cell flux in tumor microvessels can lead to transient hypoxia and reoxygenation in tumor parenchyma. *Cancer Res.*, 56: 5522-5528, 1996.
36. Moulder, J. E., and Rockwell, S. Tumor hypoxia: its impact on cancer therapy. *Cancer Metastasis Rev.*, 5: 313-341, 1987.
37. Gatenby, R. A., Kessler, H. B., Rosenblum, J. S., Coia, L. R., Moldofsky, P. J., Hartz, W. H., and Broder, G. J. Oxygen distribution in squamous cell carcinoma metastases and its relationship to outcome of radiation therapy. *Int. J. Radiat. Oncol. Biol. Phys.*, 14: 831-838, 1988.
38. Teicher, B. A. Hypoxia and drug resistance. *Cancer Metastasis Rev.*, 13: 139-168, 1994.
39. Helminger, G., Yuan, F., Dellian, M., and Jain, R. K. Interstitial pH and pO₂ gradients in solid tumors *in vivo*: high-resolution measurements reveal a lack of correlation. *Nat. Med.*, 3: 177-182, 1997.
40. Raleigh, J. A., Calkins-Adams, D. P., Rinker, L. H., Ballenger, C. A., Weissler, M. C., Fowler, W. C., Jr., Novotny, D. B., and Varia, M. A. Hypoxia and vascular endothelial growth factor expression in human squamous cell carcinomas using pimonidazole as a hypoxia marker. *Cancer Res.*, 58: 3765-3768, 1998.
41. Koong, A. C., Denko, N. C., Hudson, K. M., Schindler, C., Swiersz, L., Koch, C., Evans, S., Ibrahim, H., Le, Q. T., Terris, D. J., and Giaccia, A. J. Candidate genes for the hypoxic tumor phenotype. *Cancer Res.*, 60: 883-887, 2000.
42. Jiang, B. H., Semenza, G. L., Bauer, C., and Marti, H. H. Hypoxia-inducible factor 1 levels vary exponentially over a physiologically relevant range of O₂ tension. *Am. J. Physiol.*, 271: C1172-C1180, 1996.
43. Leek, R., Landers, R., Harris, A., and Lewis, C. Necrosis correlates with high vascular density and focal macrophage infiltration in invasive carcinoma of the breast. *Br. J. Cancer*, 79: 991-995, 1999.
44. Graeber, T. G., Osmanian, C., Jacks, T., Housman, D. E., Koch, C. J., Lowe, S. W., and Giaccia, A. J. Hypoxia-mediated selection of cells with diminished apoptotic potential in solid tumours. *Nature (Lond.)*, 379: 88-91, 1996.
45. Hockel, M., Schlenger, K., Aral, B., Mitze, M., Schaffer, U., and Vaupel, P. Association between tumor hypoxia and malignant progression in advanced cancer of the uterine cervix. *Cancer Res.*, 56: 4509-4515, 1996.
46. Schmaltz, C., Hardenbergh, P. H., Wells, A., and Fisher, D. E. Regulation of proliferation-survival decisions during tumor cell hypoxia. *Mol. Cell. Biol.*, 18: 2845-2854, 1998.
47. Parkkila, S., Rajaniemi, H., Parkkila, A. K., Kivela, J., Waheed, A., Pastorekova, S., Pastorek, J., and Sly, W. S. Carbonic anhydrase inhibitor suppresses invasion of renal cancer cells *in vitro*. *Proc. Natl. Acad. Sci. USA*, 97: 2220-2224, 2000.
48. Yamagata, M., and Tannock, I. F. The chronic administration of drugs that inhibit the regulation of intracellular pH: *in vitro* and anti-tumour effects. *Br. J. Cancer*, 73: 1328-1334, 1996.
49. Raghunand, N., He, X., van Sluis, R., Mahoney, B., Baggett, B., Taylor, C. W., Paine-Murrieta, G., Roe, D., Bhujwalla, Z. M., Gillies, R. J. Enhancement of chemotherapy by manipulation of tumour pH. *Br. J. Cancer*, 80: 1005-1011, 1999.
50. Gatenby, R. A. The potential role of transformation-induced metabolic changes in tumor-host interaction. *Cancer Res.*, 55: 4151-4156, 1995.
51. Gerweck, L. E. Tumor pH: implications for treatment and novel drug design. *Semin. Radiat. Oncol.*, 8: 176-182, 1998.
52. Kozin, S. V., and Gerweck, L. E. Cytotoxicity of weak electrolytes after the adaptation of cells to low pH: role of the transmembrane pH gradient. *Br. J. Cancer*, 77: 1580-1585, 1998.
53. Ojogo, A. S., McSheehy, P. M., Stubbs, M., Alder, G., Bashford, C. L., Maxwell, R. J., Leach, M. O., Judson, I. R., and Griffiths, J. R. Influence of pH on the uptake of 5-fluorouracil into isolated tumour cells. *Br. J. Cancer*, 77: 873-879, 1998.
54. Gerweck, L. E., Kozin, S. V., and Stocks, S. J. The pH partition theory predicts the accumulation and toxicity of doxorubicin in normal and low-pH-adapted cells. *Br. J. Cancer*, 79: 838-842, 1999.
55. Vukovic, V., and Tannock, I. F. Influence of low pH on cytotoxicity of paclitaxel, mitoxantrone, and topotecan. *Br. J. Cancer*, 75: 1167-1172, 1997.
56. Teicher, B. A., Liu, S. D., Liu, J. T., Holden, S. A., and Herman, T. S. A carbonic anhydrase inhibitor as a potential modulator of cancer therapies. *Anticancer Res.*, 13: 1549-1556, 1993.

Prognostic Significance of a Novel Hypoxia Regulated Marker – Carbonic Anhydrase IX in Invasive Breast Carcinoma

Stephen K. Chia¹, Charles C. Wykoff², Peter H. Watson³, Cheng Han², Russell D. Leek², Jaromir Pastorek⁴, Kevin C. Gatter⁵, Peter Ratcliffe⁶ and Adrian L. Harris²

¹ Division of Medical Oncology, British Columbia Cancer Agency, Vancouver, British Columbia, V5Z 4E6, Canada

² Imperial Cancer Research Fund Molecular Oncology Laboratory, University of Oxford, Institute of Molecular Medicine, John Radcliffe Hospital, Oxford, OX3 9DU, UK

³ Department of Pathology, University of Manitoba, Winnipeg, Manitoba, R3E 0W3, Canada

⁴ Institute of Virology, Slovak Academy of Sciences, Slovak Republic

⁵ University of Oxford, Nuffield Department of Clinical Laboratory Sciences, John Radcliffe Hospital, Oxford, OX5 9DU, UK

⁶ Wellcome Trust, University of Oxford, Churchill Hospital, Oxford, UK

Acknowledgments:

S.K.C supported by the Shane Fellowship and the Canadian Breast Cancer Foundation – British Columbia/Yukon Chapter.

P.H.W. is the recipient of a Medical Research Council of Canada Scientist Award, an Academic Award from the US Army Research and Material Command, and travel awards from Burroughs Wellcome Trust and the Royal College of Physicians and Surgeons of Canada.

Correspondence to: Adrian L. Harris, M.D., Imperial Cancer Research Fund Molecular Oncology Laboratory, University of Oxford, Institute of Molecular Medicine, John Radcliffe Hospital, Oxford, OX3 9DU, UK

ABSTRACT

Purpose: To assess the frequency of expression and the prognostic significance of a hypoxia regulated marker, carbonic anhydrase IX (CA IX), in a cohort of patients with invasive breast cancer.

Patients and Methods: CA IX expression was evaluated by immunohistochemistry with a murine monoclonal antibody, M75, in a series of 103 women treated surgically for early breast cancer. The majority of patients were treated with adjuvant hormonal or chemotherapy. The frequency of expression, its association with recognized prognostic factors and the relationship with outcome was evaluated by univariate and multivariate statistical analysis.

Results: CA IX expression was present within 51 of 103 cases (49.5 %). The level of CA IX expression was found to be significantly associated with tumor necrosis ($p < 0.001$), higher grade ($p = 0.02$) and negative estrogen receptor status ($p < 0.001$). Furthermore CA IX expression was associated with a higher relapse rate ($p = 0.004$) and a worse overall survival ($p = 0.001$). By multivariate analysis CA IX was also shown to be an independent predictive factor for overall survival (hazard ratio 2.61; 95% C.I. 1.01-6.75, $p = 0.05$).

Conclusion: CA IX expression was associated with a worse relapse free and overall survival in an unselected cohort of invasive breast carcinoma patients. A potential role as a marker of hypoxia within breast carcinomas was also confirmed by a significant association with necrosis. Further work assessing its prognostic significance in breast cancer is warranted, particularly interactions with radiotherapy and chemotherapy resistance.

INTRODUCTION

The benefits of adjuvant chemotherapy and hormonal therapy for the treatment of invasive breast cancer are now well proven [1-2]. However many women still undergo treatment without necessarily achieving benefit. Much work has been done on determining prognostic factors that will improve our capability to predict the risk of breast cancer relapse and death in women following the diagnosis of primary breast cancer. The value of factors such as axillary lymph node status, tumor size, tumor grade, and hormonal receptor status are well-established [3- 6]. However earlier diagnosis and changes in clinical practice have made it more difficult to apply all these factors as the majority of women now present with small, node negative tumors. Further work is required to refine relapse risk so as to determine the group of women most in need of adjuvant treatment as well as sparing those whose prognosis is favorable without further therapy. Also factors that may modify the effectiveness of therapy are important to establish, since they may provide new targets for modification of resistance.

Hypoxia has been implicated as an important component in tumor progression and spread. The degree

of tumor hypoxia has been shown to be inversely correlated with response to treatment and overall survival [7]. This is partly related to radiation resistance but is also independently a risk factor for poor outcome [8-9]. Hypoxia is also a vital factor in the etiology of tumor necrosis and the latter parameter has also been demonstrated, though perhaps not widely appreciated, to be a prognostic factor for a worse relapse-free and overall mortality rate in both node negative and node positive breast cancer [10]. A correlation has been established between the degree of tumor necrosis and angiogenesis [11-12]. Lastly the degree of angiogenesis, as quantified by microvessel density and analysis of angiogenic factors such as vascular endothelial growth factor (VEGF) in tumor tissue samples, has been found to be prognostic for relapse-free and overall survival in cohorts of women with node positive and node negative breast carcinoma [13-18]. Taken together it appears that hypoxia, tumor necrosis, and angiogenesis are intimately associated biologically and prognostically in breast carcinoma.

We have recently found that carbonic anhydrase 9 (CA IX) gene is directly regulated by hypoxia in several epithelial cell lines via a hypoxia response element in the 5' UTR of the gene. Furthermore the upregulation of this enzyme was dependent on hypoxia inducible factor-1 (HIF-1) [manuscript submitted]. CA IX belongs to the family of zinc metalloenzymes responsible for the reversible inter-conversion of carbon dioxide and water to carbonic acid. The carbonic anhydrase family has an essential role in physiologic functions in the human body, in particular maintaining pH, water and ion equilibrium [19-20]. CA IX was first identified in HeLa cells (a human cervical carcinoma cell line) and then found to be a novel tumor marker in human ovarian, endometrium and cervical cancer specimens but not their corresponding normal tissues, and was termed MN [21]. Subsequently the MN gene has been cloned and the transmembrane protein product showed structural and functional homology with the carbonic anhydrase enzymes and as such renamed CA IX [22]. CA IX is found in normal tissue in the gastrointestinal tract [23-24]. Further work has shown that CA IX is expressed in renal cell carcinoma [25-26], esophageal carcinoma [27], non-small cell lung carcinoma [28] and colorectal tumors [29]. These studies have also revealed that the expression of this biomarker is restricted to transformed, dysplastic and malignant epithelial cells and is rarely expressed in benign tumors or normal tissue.

To date there have been no published reports investigating the presence of CA IX in human breast cancer or on the potential prognostic significance of CA IX in any human cancer series. Therefore, in light of our recent findings that CA IX may be a marker for hypoxia

in vivo, and the fact that alterations in tissue pH may affect drug uptake and hence drug resistance, the aims of this study were to assess the expression of CA IX in invasive breast carcinoma in relation to tumor necrosis and to determine whether this novel biomarker is an independent prognostic factor for subsequent breast cancer relapse and death.

MATERIALS AND METHODS

Patients and tissues

A series of 103 surgically resected invasive breast carcinomas treated at the John Radcliffe Hospital and the Churchill Hospital, Oxford, with a median follow-up of 6.2 years, was assessed. The majority of the cohort underwent either modified radical mastectomy or lumpectomy with breast irradiation. Axillary lymph node status was confirmed histologically. If lymph node involvement was found then adjuvant radiotherapy to the axilla was delivered. Adjuvant systemic treatment consisted of Tamoxifen at 20 mg daily for 5 years for post-menopausal women regardless of hormonal receptor status and six cycles of intravenous cyclophosphamide, methotrexate and 5-fluorouracil delivered every 3 weeks for pre-menopausal women. All patients were assessed in follow-up every 3 months for the first 18 months and every 6 months thereafter. Treatment for confirmed recurrent disease was by endocrine manipulation for soft tissue or skeletal metastasis or by chemotherapy for visceral disease and failed endocrine therapy. The clinicopathologic characteristics of the entire cohort are summarized in Table 1.

Immunohistochemistry (IHC)

Immunohistochemical staining for CA IX was performed on 5 µm serial sections on coated slides from paraffin embedded blocks. All slides were first deparaffinized with standard techniques and then placed in 0.5% hydrogen peroxide for 15 minutes to saturate endogenous peroxidases. Incubation with 10% normal human serum in Tris buffered saline (TBS) for 15 minutes was then performed to block non-specific uptake of the antibody. The murine monoclonal antibody M75 at a dilution of 1:50 in TBS with 5% normal human serum for 30 minutes was utilized to assess for expression of CA IX. This antibody has previously been characterized with Western blot analysis to confirm its specificity [24]. Next a 30 minute incubation with a peroxidase conjugated to goat anti-mouse immunoglobulins (Dako EnVision + System, Peroxidase, Mouse; Dako, Carpinteria, CA, USA) was performed. Slides were then stained with 3,3'-diaminobenzidine chromogen solution for 8 minutes and then counterstained with haematoxylin and mounted

with aquamount. All staining was performed on an automated immunohistochemical stainer (MiniPrep 75, Tecan; Reading, UK) at room temperature. Following successive incubations (except the normal human serum block) the slides were washed twice with TBS for 5 minutes.

Assessment of CA IX expression

Immunostaining was quantified for CA IX by light microscopy and semi-quantitative scoring by one author (P.H.W) blinded to the cohort's clinical data and outcome. In brief, a score of 0 - 3 for the intensity of staining in the majority of the entire section with invasive carcinoma was given (0: no staining; 1: weak staining; 2: moderate staining; and 3: strong staining). All slides were evaluated by light microscopy and the percentage of tumor cells throughout the section that were stained positive was estimated and the product of the intensity staining and the percentage of tumor then produced a final immunostaining score (IHC-score) of 0 - 300.

Tumor hormone receptor status

Estrogen receptor (ER) analysis was performed using an enzyme linked immunosorbent assay technique (Abbott Laboratories, USA). Tumors with cytoplasmic estrogen levels greater than 10 fmol per milligram of protein were considered positive. Epidermal growth factor receptor (EGFR) was determined using ligand binding of [¹²⁵I]EGF to tumor membranes as previously described [30]. Tumors with an EGFR level of greater than or equal to 20 fmol per milligram of membrane protein were considered positive.

Assessment of tumor necrosis

Tumor necrosis was scored on haematoxylin and eosin stained sections adjacent to those sections subjected to immunohistochemistry. The entire section was assessed and the percentage of necrosis within the invasive tumor component was scored by one author (P.W.H) independently from the IHC analysis and blinded to the cohort's clinical data and outcome. Necrosis within in-situ carcinoma components was not scored. For statistical analysis the percentage of necrosis was either categorized into four categories of levels (negative, low, medium, or high) or divided into negative or positive (where the presence of any necrosis was considered positive) as previously described [11].

Statistical analysis

For statistical analysis CA IX expression was evaluated as both a continuous and a discontinuous variable. In the latter case, the median IHC score for the series was used as a cut-point (i.e. an IHC score ≥ 1 , corresponding to

the presence of any staining, was considered as positive for CA IX expression). CA IX was evaluated in relation to a range of established prognostic variables using the Mann Whitney test and Kruskal-Wallis tests where appropriate. The association with relapse free and overall survival was assessed by univariate (Log-rank test and Kaplan-Meier method) and multivariate (Cox regression model) analysis. All tests were performed using the Stata 5.0 statistical analysis software (Stata Corporation, College Station, Texas, USA).

RESULTS

In this unselected cohort of 103 women with invasive breast cancer the clinicopathologic features are representative of that of a general population of breast cancer patients (Table 1). Amongst these patients, the median age was 59 years, the median tumor size was 2.4 cm, 58% were axillary node-positive disease and 68% were estrogen receptor positive. Necrosis was present in 50 cases, and amongst this subset marked necrosis ($\geq 25\%$ of tumor) was present in 14 cases. The mean percentage necrosis was 17% (+/- SD of 16%). The majority of cases (90) were invasive ductal carcinomas, with 11 patients having an invasive lobular pathology and 2 with tubular carcinomas. The median duration of follow-up for the entire cohort is 6.2 years and to date 41 (40%) of the cohort have relapsed and 32 (31%) have died.

CA IX expression in relation to clinicopathological variables

The specificity of the M75 antibody for detection of CA IX expression in breast tissue sections was initially confirmed by comparison of IHC scores with the detection of the 58kD and 54kD bands corresponding to the CA IX protein in western blots performed on the same tumor specimens [Wykoff et al, DCIS paper, manuscript submitted].

CA IX expression was detectable in 49.5 % of cases as strong membranous staining within epithelial tumor cells. The pattern of expression however was predominantly very focal within the tumor and typically limited only to tumor cells immediately adjacent to areas of necrosis. Expression was also occasionally seen adjacent to areas of dense collagenous stromal scar within the central regions of some tumors. The focal nature of expression was also reflected in the distribution of IHC scores (range 0-225, median 0, mean 23) with only 14% of tumors having an IHC score of greater than 50. Representative examples of tumors showing low, moderate and high CA IX expression are illustrated in Figure 1.

CA IX expression was compared with several established clinicopathological prognostic variables (Table 2). As anticipated from the pattern of staining, significant associations were seen between both the presence and level of CA IX expression and the presence of necrosis ($p < 0.001$), higher tumor grade ($p = 0.02$) and negative estrogen receptor status ($p < 0.001$) within the entire cohort. Otherwise there was no apparent relationship with other prognostic variables such as age, nodal status, tumor size, tumor type and EGFR status. In parallel, necrosis was also assessed in relation to ER status and grade and was significantly associated with ER negative status ($p = 0.002$) and high grade ($p < 0.0001$).

Relationship of CA IX to relapse free survival (RFS) and overall survival (OS)

Univariate analysis of established prognostic factors and their relationship to survival confirmed that nodal status, grade, and ER status were all significantly related to both RFS (p values = < 0.001 , 0.04 , 0.03 respectively) and OS (p values = < 0.001 , 0.04 , 0.02 respectively) in this cohort. Tumor size was also predictive of RFS ($p = 0.04$), while patient age was found predictive of OS ($p = 0.05$). The presence of CA IX expression was then considered and showed a significant association with a shorter RFS ($p = 0.004$) and a poorer OS ($p = 0.001$) (Figure 2). Similarly, the level of CA IX expression was also significant in terms of RFS ($p = 0.04$) and OS ($p < 0.001$). For the latter, every 10 unit increase in CA IX IHC score was associated with a hazard ratio of 1.12 (95% CI 1.06-1.2). Interestingly the presence of necrosis was also significantly associated with OS ($p = 0.03$). In multivariate Cox proportional hazard analysis, where nodal status, age, tumor size, grade and necrosis were considered together with the CA IX status, only positive lymph node status and CA IX presence emerged as significant independent predictors of OS ($p = 0.004$ and $p = 0.05$ respectively) in this cohort (Table 3).

DISCUSSION

We have recently shown that a marked upregulation of the CA IX mRNA and protein occurs in human cancer cell lines exposed to hypoxic conditions, with barely detectable basal expression in normoxia (manuscript submitted). In this current study we have extended this observation and shown that CA IX is expressed in invasive breast carcinoma *in vivo*, with the expression restricted to regions of necrosis. We have also demonstrated that CA IX is associated with several poor prognostic factors including high tumor grade, ER negative status and the presence of necrosis. Finally, CA IX expression is predictive for reduced relapse free and

overall survival in univariate analysis and is an independent factor for overall survival in multivariate analysis.

CA IX was first identified in a human cervical carcinoma (HeLa) cell line [31] and was subsequently found to be present only in the extracts from human carcinoma cell lines and clinical tumor specimens but not from corresponding normal tissue [21]. Further evidence for a role in tumorigenesis came from the demonstration that transfection of a cell line (NIH3T3) with the MN gene resulted in the transfected cells acquiring features of a transformed phenotype (altered morphology, enhanced DNA synthesis with shorter doubling times, and capacity for anchorage-independent growth) [22]. The MN gene was subsequently cloned and four distinct regions of the protein product were identified. These include an N-terminal region with structural features to suggest involvement in intercellular communication and proliferation, an extracellular domain with close homology to other known members of the carbonic anhydrase gene family, a transmembrane region, and an intracytoplasmic C-terminal tail [22,32-33]. The structural features suggest a function in control of extracellular pH, and are compatible with our recent observation that CA IX is upregulated in epithelial tumor cells under hypoxic conditions.

In the current study CA IX expression was closely correlated with the presence of necrosis, believed to be an indicator of local hypoxia, within invasive breast tumors. In a recent study, conducted on a similar size cohort of invasive breast cancers, we found that the presence of necrosis correlated with high vascular density, high tumor grade and ER negative status [11]. However necrosis was not related to RFS or OS. In the present cohort, we have also confirmed that necrosis is associated with ER negative and high grade tumors, but necrosis also showed a significant relationship with poor overall survival, but not with relapse free survival, in uni-variate analysis. The explanation for this difference is not clear, however the current cohort has a longer duration followup (74 months vs 63 months).

Previous work has been done on CA IX expression in other solid tumors and has shown a similar pattern of membranous expression in malignant cells, with no expression in normal or benign tissue (with the exception of gastrointestinal tract) [25-29]. In a recent series of 65 non-small cell lung carcinoma (NSCLC) specimens the frequency of positive immunostaining was 80%, with no correlation with histologic subtype or tumor differentiation [28]. In series of 147 renal cell carcinomas, immunohistochemistry demonstrated strong expression of MN/CA IX in 87% of the tumors.

Interestingly there was a significant inverse relationship between MN/CA IX staining and tumor grade and stage, with a greater proportion of malignant cells staining positive in the lower grade and stage tumors [34]. This inverse correlation of level of expression of CA IX and histological grade and other poor prognostic factors (e.g. depth of invasion, lymph node metastasis) has also been shown in studies with cervical carcinoma [35], colorectal carcinoma [29] and esophageal cancer [27]. This is different from the results of our study, where there is a positive correlation between level of expression of this biomarker and the grade of tumor, as indicated by both histologic grade and ER status. The reason for this difference is unknown, however one possibility is that while hypoxia associated with visible necrosis appears to be a dominant factor in the regulation of CA IX in breast tissues, there may be other factors involved in the regulation of the CA IX gene in other tissues and related tumor types. Certainly an association with areas of necrosis, and thus hypoxia, has not previously been noted in these other studies.

An explanation for the association seen in breast tumors between CA IX expression and poor prognosis may lie in the nature of its functional involvement in pH regulation in breast tissue. Carbonic anhydrase proteins exert their effect by catalyzing the reversible interconversion of carbonic acid to carbon dioxide. Evidence exists that the extracellular pH of solid tumors is significantly more acidic than in normal tissue [36-37], whereas the intracellular pH in tumors is neutral or slightly more alkaline compared to normal cells [37-39]. This reversal in pH gradient has hypothetical implications for resistance to weakly basic chemotherapeutic agents. In fact, a recent study has demonstrated enhanced efficacy for doxorubicin in

human breast cancer cells *in vitro* and *in vivo* when the pH is raised from 6.8 to 7.4 [40]. CA IX may allow for adaptation intracellularly to a hypoxic acidic environment while simultaneously contributing to chemotherapeutic and radiation resistance through modification of the extracellular micro-environment.

Lastly the utility of this novel biomarker may have diagnostic and therapeutic implications. Besides its specificity by immunohistochemistry for malignant cells, a recent study has shown that RT-PCR detection of CA IX can be highly specific for detecting circulating renal carcinoma cells [41]. Likewise, work has already been done on a radiolabelled antibody to CA IX (mAbG250) for scintigraphic diagnosis of renal cell carcinoma [42], and this same antibody has also been shown to exert anti-tumor effects on a renal cell carcinoma xenograft model [43]. However a direct biological effect for CA IX on the growth of breast cancer remains to be established.

In conclusion, we have shown that CA IX expression is closely associated with necrosis in breast carcinoma and this is consistent with previous evidence indicating that CA IX is regulated by hypoxia. We have shown that this novel biomarker also has prognostic significance for a shorter relapse free and a worse overall survival in an unselected series of invasive breast carcinomas. It remains to be seen whether expression of CA IX is just an indicator of response to necrosis caused by local hypoxia or whether it actively contributes to the process of cell survival by influencing extracellular pH. This could affect anthracycline resistance and also be a marker for radiation resistance, but this will require analysis in randomised prospective studies.

REFERENCES

1. Early Breast Cancer Trialists' Collaborative Group: Polychemotherapy for early breast cancer. *Lancet* 352:930-942, 1998
2. Early Breast Cancer Trialists' Collaborative Group: Tamoxifen for early breast cancer: An overview of the randomized trials. *Lancet* 351:1451-1467, 1998
3. Fisher B, Bauer M, Wickerham DL et al. Relation of number of positive axillary nodes to the prognosis of patients with primary breast cancer: an NSABP update. *Cancer* 52:1551, 1983
4. Davies BW, Gelber D, Goldhirsch A et al. Prognostic significance of tumor grade in clinical trials of adjuvant therapy for breast cancer with axillary lymph node metastasis. *Cancer* 58:2662, 1986
5. Koscielny S, Tubiana M, Le MG et al. Breast cancer: relationship between the size of the primary tumor and the probability of metastatic dissemination. *Br J Cancer* 49:709, 1984
6. Clark GM and McGuire WL. Steroid receptors and other prognostic factors in primary breast cancer. *Semin Oncol* 15:20, 1988
7. Dachs GU and Stratford IJ. The molecular response of mammalian-cells to hypoxia and the potential for exploitation in cancer therapy. *Br J Cancer* 74:S126-S132, 1996

8. Hockel M, Schlenger K, Aral B, et al. Association between tumor hypoxia and malignant progression in advanced cancer of the uterine cervix. *Cancer Res* 56:19;4509-4515, 1996
9. Walenta S, Wetterling M, Lehrke M, et al. High lactate levels predict likelihood of metastases, tumor recurrence and restricted patient survival in human cervical cancer. *Cancer Res* 60:916-921, 2000
10. Fisher ER, Anderson S, Redmond C et al. Pathologic findings from the National Surgical Adjuvant Breast Project protocol B-06. 10 year pathologic and clinical prognostic discriminants. *Cancer* 71:2507-2514, 1993
11. Leek RD, Landers RJ, Harris AL et al. Necrosis correlates with high vascular density and focal macrophage infiltration in invasive carcinoma of the breast. *Br J Cancer* 79:991-995, 1999
12. Kato T, Kimura T, Miyakawa R et al. Clinicopathologic study of angiogenesis in Japanese patients with breast cancer. *World J Surg* 21:49-56, 1997
13. Weidner N, Semple JP, Welch WR, et al. Tumor angiogenesis and metastasis-correlation in invasive breast carcinoma. *N Engl J Med* 324:1-8, 1991
14. Horak ER, Leek R, Klenk N, et al. Angiogenesis, assessed by platelet/endothelial cell adhesion molecule antibodies, as indicator of node metastasis and survival in breast cancer. *Lancet* 340:1120-1124, 1992
15. Fox SB, Leek RD, Smith K, et al. Tumor angiogenesis in node-negative breast carcinomas: Relationship with epidermal growth factor receptor and survival. *Breast Cancer Res Treat* 29:109-116, 1994
16. Gasparini G, Weidner N, Bevilacqua P, et al. Tumor microvessel density, p53 expression, tumor size and peritumoral lymphatic vessel invasion are relevant prognostic markers in node-negative breast carcinoma. *J Clin Oncol* 12:454-466, 1994
17. Gasparini G, Toi M, Gion M et al. Prognostic significance of vascular endothelial growth factor protein in node-negative breast carcinoma. *J Natl Cancer Inst* 89:139-147, 1997
18. Linderholm B, Grankvist K, Wilking N, et al. Correlation of vascular endothelial growth factor content with recurrences, survival, and first relapse site in primary node-positive breast carcinoma after adjuvant treatment. *J Clin Oncol* 18:1423-1431, 2000
19. Maren TH. Carbonic anhydrase: chemistry, physiology and inhibition. *Physiol Rev* 47:595-743, 1967
20. Tashian RE. The carbonic anhydrases: Widening perspectives on their evolution. expression and function. *Bioessays* 10:186-192, 1989
21. Zavada J, Zavadova Z, Pastorekova S et al. Expression of MaTu-MN protein in human tumor cultures and in clinical specimens. *Int J Cancer* 54:268-274, 1993
22. Pastorek J, Pastorekova S, Callebaut I et al. Cloning and characterization of MN, a human tumor-associated protein with a domain homologous to carbonic anhydrase and a putative helix-loop-helix DNA binding segment. *Oncogene* 9:2877-2888, 1994
23. Pastorekova S, Parkkila S, Parkkila AK et al. Carbonic anhydrase IX, MN/CA IX: analysis of stomach complementary DNA sequence and expression in human and rat alimentary tracts. *Gastroenterology* 112:398-408, 1997
24. Saarnio J, Parkkila S, Parkkila AK et al. Immunohistochemistry of carbonic anhydrase isozyme IX (MN/CA IX) in human gut reveals polarized expression in the epithelial cells with the highest proliferative capacity. *J Histochem Cytochem* 46:497-504, 1998
25. Liao SY, Aurelio ON, Jan K et al. Identification of the MN/CA 9 protein as a reliable diagnostic biomarker of clear cell carcinoma of the kidney. *Cancer Res* 57:2827-2831, 1997
26. McKiernan JM, Buttyan R, Bander NH et al. Expression of the tumor-associated gene MN: a potential biomarker for human renal cell carcinoma. *Cancer Res* 57:2362-2365, 1997
27. Turner JR, Odze RD, Crum CP et al. MN antigen expression in normal, preneoplastic, and neoplastic esophagus: a clinicopathological study of a new cancer associated biomarker. *Hum Pathol* 28:740-744, 1997
28. Vermylen P, Roufosse C, Burny A et al. Carbonic anhydrase IX antigen differentiates between

- preneoplastic malignant lesions in non-small cell lung carcinoma. *Eur Respir J* 14:806-811, 1999
29. Saarnio J, Parkkila S, Parkkila AK et al. Immunohistochemical study of colorectal tumors for expression of a novel transmembrane carbonic anhydrase, MN/CA IX, with potential value as a marker of cell proliferation. *Am J Pathol* 153:279-285, 1998
 30. Fox FB, Smith K, Hollyer J, et al. The epidermal growth factor receptor as a prognostic marker: results of 370 patients and review of 3009 patients. *Breast Can Res Treat* 29:41-49, 1994
 31. Stanbridge EJ, Flandermeyer RR, Daniels DW et al. Specific chromosome loss associated with the expression of tumorigenicity in human cell hybrids. *Somat Cell Genet* 7:699-712, 1981
 32. Opavsky R, Pastorekova S, Zelnik V et al. Human MN/CA9 gene, a novel member of the carbonic anhydrase family: structure and exon to protein domain relationships. *Genomics* 33:480-487, 1996
 33. Peles E, Nativ M, Campbell P et al. The carbonic anhydrase domain of receptor tyrosine phosphatase β is a functional ligand for the axonal cell recognition molecule contactin. *Cell* 82:251-260, 1995
 34. Uemura H, Nakagawa Y, Yoshida K et al. MN/CA IX/G250 as a potential target for immunotherapy of renal cell carcinomas. *Br J Cancer* 81:741-746, 1999
 35. Brewer C, Liao SY, Wilczynski SP et al. A study of biomarkers in cervical carcinoma and clinical correlation of the novel biomarker MN. *Gynecol Oncol* 63:337-344, 1996
 36. Wike-Hooley JL, Haveman J and Reinhold HS. The relevance of tumour pH to the treatment of malignant disease. *Radiother Oncol* 2:343-366, 1984
 37. Gerweck LE and Seetharaman K. Cellular pH gradient in tumor versus normal tissue: potential exploitation for the treatment of cancer. *Cancer Res* 56:1194-1198, 1996
 38. Griffiths JR. Are cancer cells acidic? *Br J Cancer* 64:425-427, 1991
 39. Negendank W. Studies of human tumours by MRS: a review. *NMR Biomed* 5:303-324, 1992
 40. Raghunand N, He X, van Sluis R et al. Enhancement of chemotherapy by manipulation of tumour pH. *Br J Cancer* 80:1005-1011, 1999
 41. McKiernan JM, Buttyan R, Bander NH et al. The detection of renal carcinoma cells in the peripheral blood with an enhanced reverse transcriptase-polymerase chain reaction assay for MN/CA 9. *Cancer* 86:492-497, 1999
 42. Steffens MG, Boerman OC, Oosterwijk-Wakka JC et al. Targeting of renal cell carcinoma with iodine -131-labeled chimeric monoclonal antibody G250. *J Clin Oncol* 15:1529-1537, 1997
 43. Van Dijk J, Uemura H, Beniers AMJC et al. Therapeutic effects of monoclonal antibody G250, interferons and tumor necrosis factor, in mice with renal cell carcinoma xenografts. *Int J Cancer* 56:262-268, 1994

Table 1. Patient Demographics

Patient Characteristics	Number
Total patients	103
Age (median, range) years	59 (28-82) years
< 50	27
≥ 50	76
Surgical treatment	
Lumpectomy	5
Lumpectomy + RT	63
Mastectomy	35
Tumor size (median, range) cm	2.4 cm (0.8-8.0 cm)
< 2 cm	43
≥ 2 cm	58
Node status	
Positive (range of positive nodes)	58 (1-16)
Negative	45
Grade	
1	15
2	48
3	40
ER status	
Positive	70
Negative	33
EGFR status	
Positive	56
Negative	46
Adjuvant therapy	
Chemotherapy	27
Hormonal therapy (Tamoxifen)	80
Median duration follow-up (median, range) years	6.2 years (0.4-10.1)
Relapses	41
Deaths	32

Figure 1

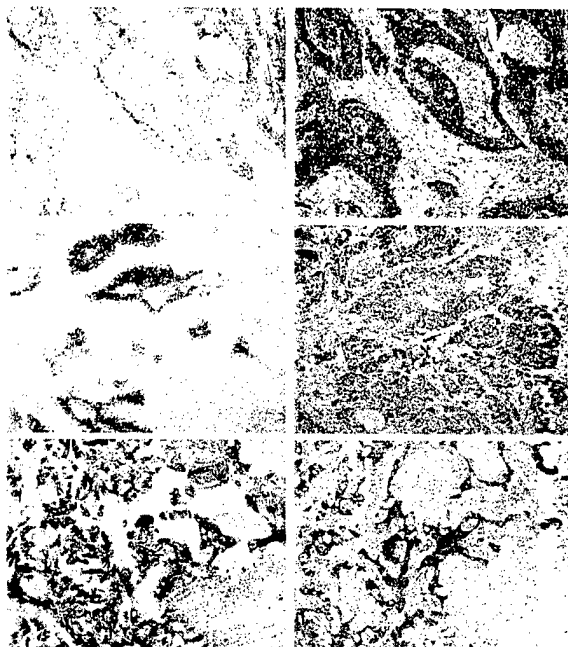


Figure 2

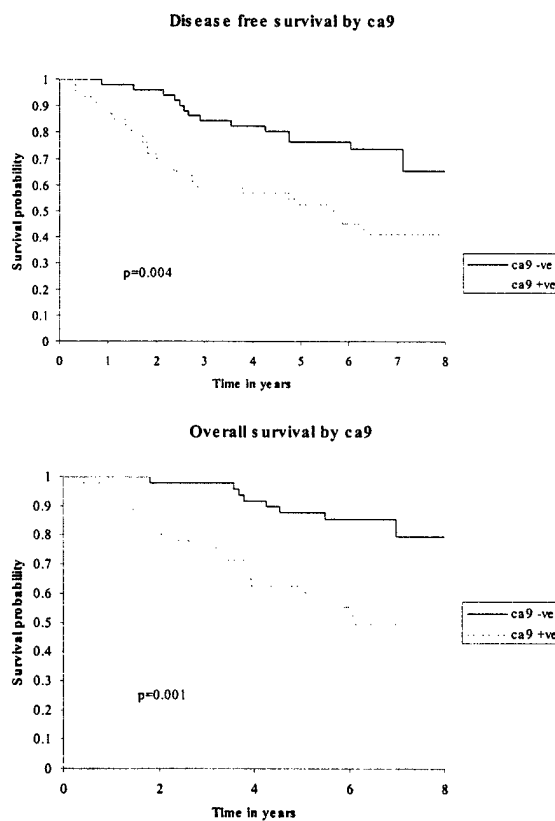


Table 1

Patient Characteristics	Number
Total patients	103
Age (median, range) years	59 (28-82) years
< 50	27
≥ 50	76
Surgical treatment	
Lumpectomy	5
Lumpectomy + RT	63
Mastectomy	35
Tumor size (median, range) cm	2.4 cm (0.8-8.0 cm)
< 2 cm	43
≥ 2 cm	58
Node status	
Positive (range of positive nodes)	58 (1-16)
Negative	45
Grade	
1	15
2	48
3	40
ER status	
Positive	70
Negative	33
EGFR status	
Positive	56
Negative	46
Adjuvant therapy	
Chemotherapy	27
Hormonal therapy (Tamoxifen)	80
Median duration follow-up (median, range) years	6.2 years (0.4-10.1)
Relapses	41
Deaths	32

Table 2

Association between CAIX expression and prognostic parameters

		CA IX IHC score		p-value
		mean	SD	
Grade	I	8	14	0.02
	II	19	43	
	III	33	47	
ER	-ve	50	59	<0.001
	+ve	10	24	
Necrosis	-ve	9	25	<0.001
	+ve	38	52	

Table 3

Cox's multivariate survival analysis

variable	Odds ratio	95% CI	significance
Nodal status	5.52	2.02-15.08	0.001
Ca9	1.16	1.06-1.27	0.002
Grade	1.39	0.64-3.01	ns
Size	1.32	0.57-3.03	ns
ER	0.78	0.32-1.91	ns
Necrosis	0.9	0.32-2.43	ns

HIF-1-dependent regulation of hypoxic induction of the cell death factors BNIP3 and NIX in human tumours¹

Heidi M. Sowter, Peter J. Ratcliffe, Peter H. Watson, Arnold H. Greenberg and Adrian L. Harris². Institute of Molecular Medicine, John Radcliffe Hospital, Oxford, OX3 9DS, UK (H.M.S. and A.L.H.); Wellcome Trust Centre for Human Genetics, Oxford, OX3 7BN, UK (P.J.R.)

Running title: Expression of BNIP3 and NIX in human tumours

Key words: BNIP3, NIX, tumour, hypoxia, HIF-1

Abbreviations:

The abbreviations used are: HIF-1, hypoxia-inducible factor-1; VHL, von Hippel-Lindau. ¹ This work was supported by the Imperial Cancer Research Fund. ² To whom requests for reprints should be addressed: Adrian L. Harris, Institute of Molecular Medicine, John Radcliffe Hospital, Oxford, OX3 9DS, UK.

Abstract

Solid tumours contain regions of hypoxia, a physiological stress that can activate cell death pathways and so result in the selection of cells resistant to death signals and anti-cancer therapy. BNIP3 is a cell death factor that is a member of the Bcl-2 proapoptotic family, recently shown to induce necrosis rather than apoptosis. Using cDNA arrays and SAGE, we found that hypoxia induces upregulation of BNIP3 and its homologue, NIX. Analysis of human carcinoma cell lines showed that they are regulated in many tumour types, as well as in endothelial cells and macrophages. Regulation was hypoxia inducible factor-1 (HIF-1) dependent, and HIF-1 expression was suppressed by von Hippel-Lindau protein (pVHL) in normoxic cells. Northern blotting and *in situ* hybridisation analysis has revealed that these factors are highly expressed in human tumours compared to normal tissue, and that BNIP3 is upregulated in peri-necrotic regions of the tumour. This study shows that hypoxia regulates a specific necrosis pathway and may be a key drive to tumour evolution.

Introduction

Solid tumours are poorly oxygenated compared to normal tissues, and contain regions of hypoxia. Induction of apoptosis by hypoxia is one mechanism by which stress-damaged cells can be destroyed, and most tumour cells retain the ability to undergo apoptosis in response to hypoxic stress (1). However, hypoxia increases the mutation rate of cells (2), resulting in the selection of mutations that make cells more resistant to apoptosis and less responsive to cancer therapy (3; 4). Hypoxia-inducible factor-1 (HIF-1) is a heterodimeric transcription factor consisting of an oxygen-regulated alpha subunit (Hif-1 α) and a stable nuclear factor, Hif-1 β /ARNT, and has been well-characterised as a mediator of hypoxic response (for review see 5). Under normoxic conditions, Hif-1 α is rapidly degraded by the proteasome after being targeted for ubiquitination, a process that is dependant on the product of the von Hippel-Lindau gene (pVHL; 6). Under hypoxic conditions, degradation of Hif-1 α is suppressed, and transcription of mRNAs encoding hypoxically-responsive genes can occur. HIF-1 has been shown to be a factor mediating hypoxia-induced apoptosis; hypoxia increases apoptosis in Hif-1 α ++ embryonic stem cells and chinese hamster ovary (CHO) cells, but this process is strikingly reduced in the same cells in which the gene has been disrupted (7). We screened for genes induced by hypoxia in a breast carcinoma cell line (T47D) using gene expression arrays, and detected an upregulation of BNIP3. Also, using the SAGE map website (<http://www.ncbi.nlm.nih.gov/SAGE>), virtual subtraction of genes expressed by a glioblastoma cell line (H247) under normoxic and hypoxic conditions revealed

upregulation of NIX in hypoxia (8). BNIP3 (Nineteen kD interacting protein-3) is a pro-apoptotic mitochondrial protein that was isolated through its interaction with E1B 19K and Bcl-2 (9). Overexpression of BNIP3 and its homologue NIX (10-12) in Rat-1 fibroblasts and MCF-7 breast carcinoma cells induces cell death within 12 h. BNIP3 and NIX are expressed ubiquitously in most human tissues as assessed by Northern blotting (12), although it is not known which cell types express BNIP3 and NIX, or if their pattern of expression differs in malignant tissue. A recent study has shown that BNIP3 mRNA levels increase in response to hypoxia in a CHO cell line, and that this effect is mediated via Hif-1 α (13). We have characterised the response of BNIP3 and NIX to hypoxia in human cell lines, and shown that BNIP3 and NIX are overexpressed in human tumours compared to normal tissue.

Materials and Methods

Cell Culture. Human cell lines were obtained from the ICRF cell service, and grown in DMEM, RPMI or Hams F-12 supplemented with 10 % fetal calf serum (Gibco), L-glutamine (2 μ M), penicillin (50 IU/ml) and streptomycin sulphate (50 μ g/ml). The human cell lines investigated were: SKBr, T47D, MDA468, MCF7, MDA231 (breast cancer); SKOV3 (ovarian cancer); HT1080 (fibrosarcoma), MKN45 (stomach cancer); C32, LS174T (colon cancer); EJ (bladder cancer); DU145 (prostate cancer); U937, THP-1 (macrophage); RZM (EBV-transformed normal human lymphocytes); HUVEC (endothelial). RCC4 (renal cancer) cell lines expressing pVHL or empty vector have been described previously (6). The Chinese hamster ovary (CHO) cell lines used were KA13 (mutated to be defective for Hif-1 α) and C4.5 (the parent cell line), and have been described previously (14). Parallel incubations were performed on flasks of cells approaching confluence in normoxia (humidified air with 5 % CO₂) or hypoxia (hypoxic conditions were generated in a Napco 7001 incubator (Precision Scientific) with 0.1 % O₂, 5 % CO₂ and balance N₂).

Western Blotting. Cells were homogenised in a lysis buffer containing 8M urea, 10% SDS, 1M DTT and protease inhibitors. Proteins were electrophoresed on a 10% SDS-PAGE gel and transferred onto a PVDF membrane (Millipore). BNIP3 protein was detected using a mouse anti-human BNIP3 monoclonal antibody (10) followed by goat anti-mouse HRP (Dako) and ECL developing reagents (Amersham). Blots were exposed to film for between 30 s and 2 min.

Immunohistochemistry. Formalin-fixed paraffin-embedded tissue (John Radcliffe Hospital pathology archives) or cell pellets (created by washing and centrifuging cell lines which had been scraped from tissue culture flasks) were sectioned onto 3-aminopropyltriethoxysilane (Sigma) coated slides. Sections were dewaxed and rehydrated before blocked in 10 % horse serum. A rabbit polyclonal antibody to BNIP3, which has been described previously (15) or a mouse

monoclonal antibody to human CD68 (Dako) was applied to the sections at 1/500 and 1/10. Biotinylated horse anti-mouse IgG or goat anti-mouse IgG (1/200) and ABC complex AP conjugate were applied consecutively for 30 min each at room temperature, and visualised using AP substrate (Vectastain).

Probe Production. Regions of BNIP3 and NIX selected to avoid areas of homology were amplified by RT-PCR from cDNA synthesised from MCF-7 cells subjected to hypoxia. BNIP3 cDNA was amplified between base pairs 277 and 431, using 5'-ACCAACAGGGCTTCTGAAAC-3' as the upstream primer and 5'-GAGGGTGGCCGTGCGC-3' as the downstream reverse complement primer. NIX cDNA was amplified between base pairs 716 and 798 using 5'-AGTAGCTTATTTGAACCTGAGACCATTG-3' as the upstream primer and 5'-TGAGGGTTACTGGAATTGGATATGTA-3' as the downstream reverse complement primer. The purified PCR products were labelled for Northern blotting with ³²P[CTP] (T7 Quickprime kit; Pharmacia) and unincorporated label was separated from the probe by running the mixture through a NICK column (Pharmacia) followed by precipitation in 5M ammonium acetate and ethanol, using yeast tRNA as a carrier. For in situ hybridisation the purified PCR products were cloned into pCR-script SK (Stratagene, Cambridge, UK), and sequenced to confirm their identity and orientation. Riboprobes were transcribed (MAXIScript in vitro transcription kit, Ambion AMS Ltd, Witney, Oxon, UK) from linearised plasmids with ³³P-UTP (Amersham), before phenol extraction and ethanol precipitation.

RNA preparation and Northern blotting. Total RNA was prepared according to Chomczynski and Sacchi and assessed by absorbance at 260/280nm. 20 µg aliquots were electrophoresed in 1% agarose gels containing formaldehyde, and transferred to Hybond N membranes by capillary blotting in 10x SSC (1x SSC consists of 150 mM sodium chloride, 15 mM tri-sodium citrate, pH 7.0). After fixation, blots were incubated overnight at 68°C with 32P-labelled cDNA probes and washed in several changes of 1x SSC/0.1% SDS before exposing to X-ray film for up to 7 days. The consistency of RNA loading and transfer was assessed by staining of the 28S rRNA with ethidium bromide.

In Situ Hybridisation. The in situ hybridisation protocol used in this study has been described previously (16). Briefly, the riboprobes were diluted to 30,000 cpm/µl in hybridisation buffer, and incubated on the sections for 18 h at 55°C. The slides were then washed and treated with RNase A before being coated with autoradiographic emulsion and exposed to film for 21 days at 4°C.

Results

Expression of BNIP3 protein in human cell lines. The 18 human cell lines described above, representing epithelial tumours, sarcomas, endothelium, lymphocytes and macrophages, were subjected to 0.1% hypoxia or normoxia for 16 h, before making protein extractions. Western blot analysis for BNIP3 revealed that an increase of both the 30 KDa and 60 KDa forms of BNIP3 protein occurred after hypoxia in 15 of the 18 cell lines (results from 6 cell lines are shown in Fig. 1a). The induction was concordant for both protein forms. Of these cell lines, 12 were derived from carcinomas (SKBR, T47D, MDA468, MDA231, MCF7, SKOV3, EJ, MKN45, C32, LS174T, RCC4 and DU145), 2 from macrophages (U937 and THP-1) and 1 from endothelial cells (HUVEC). The RZM (lymphocyte) and HT1080 (fibrosarcoma) cell lines expressed very low levels of BNIP3 protein under normoxic conditions, but protein levels did not increase in response to hypoxia (Fig. 1A). Further analysis of the MCF7 cell line revealed that BNIP3 protein production was upregulated within 8 h of exposure to

hypoxia, and persisted for at least 24 h in the continued presence of hypoxia (data not shown).

Hif-1 dependent induction of BNIP3 protein. The RCC4 cell line, which is derived from renal carcinoma cells defective for VHL, showed constitutive upregulation of BNIP3 under normoxic conditions (Fig. 1B). When VHL was re-introduced into this cell line, levels of BNIP3 in normoxia were suppressed and became inducible by hypoxia (Fig. 1B). To further check the role of Hif-1 in BNIP3 induction, CHO KA13 and C4.5 cells were subjected to normoxia or hypoxia for 16 h, before being analysed immunohistochemically for BNIP3 protein. Neither cell line expressed BNIP3 protein under normoxic conditions, although after treatment with hypoxia, BNIP3 expression was markedly increased in the C4.5 cells. The KA13 cells, which are defective for Hif-1, showed little, if any, increase in BNIP3 protein after hypoxia (Fig. 2).

Expression of NIX and BNIP3 mRNA in human cell lines. The HT1080 cell line and 4 of the cell lines showing increased protein levels under hypoxia (EJ, T47D, MDA231, MDA468) were subjected to normoxia or hypoxia for 16 h, before extracting total RNA. Northern blot analysis identified transcripts of 4.5 kb and 1.4kb (NIX) and 5kb and 1.7kb (BNIP3), which, in concordance with the BNIP3 protein expression, increased under hypoxia in all of the cell lines except HT1080 (Fig. 3). The increase in expression was concordant for both transcripts of NIX and BNIP3.

Expression of NIX and BNIP3 mRNA in human normal breast and breast tumour tissue. RNA was extracted from tumour and distant normal breast obtained from mastectomy samples, and analysed for NIX and BNIP3 expression using Northern blotting. Levels of NIX and BNIP3 mRNA were higher in the tumour samples compared to normal tissue in 5/5 and 3/5 cases respectively (Fig. 3). The expression of BNIP3 mRNA in the remaining 2 cases was unchanged. Both transcripts of NIX mRNA were present in human tissue, but the 5 kb transcript of BNIP3 was only detected in the tumour sample of one of the cases.

Localisation of BNIP3 mRNA in human tumours. In order to localise BNIP3-expressing cells in human tissue, formalin-fixed blocks of normal breast and tumour from two of the patients described above, as well as blocks from various other types of human epithelial tumours, were subjected to in situ hybridisation analysis. BNIP3 mRNA was detectable in 5/9 tumours, consisting of 1/2 SSC head and neck carcinomas, 1/2 ovarian carcinomas, 1 pancreas carcinoma and 2 breast carcinomas. BNIP3 expression was not detected in 1 lung carcinoma, 1 lymphoma and 2 case of normal breast tissue. BNIP3 mRNA was expressed on epithelial carcinoma cells in perinecrotic areas of the tumour (Fig. 4) in all samples except one breast carcinoma, where hybridisation was seen in epithelial cells from a well-vascularised area of the tumour (data not shown). No specific hybridisation was detected when the sections were hybridised with the sense control probe for BNIP3 (Fig. 4).

Discussion

In this study we have demonstrated that the cell death factors BNIP3 and NIX are hypoxically inducible in a wide range of human epithelial, endothelial and macrophage cell lines, but not in lymphocyte or fibrosarcoma cell lines. This result has been confirmed at the protein level for BNIP3 and at the mRNA level for both BNIP3 and NIX. Time course studies in a breast carcinoma cell line indicated that BNIP3 protein markedly increased after 8 h of hypoxia; this result demonstrates that induction is relatively rapid in tumour cells and contrasts with a recent study, where BNIP3 protein was only detectable in a CHO-K1 cell line after 4 days of hypoxic culture (13).

It is probable that the hypoxic induction of BNIP3 in human cells is mediated via Hif-1, since RCC4 cells lacking wildtype pVHL have high levels of BNIP3 protein under both normoxic and hypoxic conditions. Re-introduction of pVHL to this cell line restores degradation of Hif-1 under normoxic conditions (6), and reduces BNIP3 expression. As well as this, BNIP3 protein is not markedly induced under hypoxic conditions in CHO cells defective for Hif-1. These results confirm recent data that suggested a HIF-1-dependent response based on mutational analysis of the BNIP3 promoter (13).

Importantly, our study has also demonstrated that mRNAs encoding NIX, and in most cases BNIP3, are expressed at higher levels in clinical material from human breast tumours, when compared to normal breast tissue. This result is consistent with upregulation of the HIF-1 pathway in human tumours, but somewhat surprising in light of other studies that have shown downregulation of BNIP3 in keloid cells compared to normal tissue (17) and human T-cell leukemia virus type I injected cells (18). These differences may relate to different patterns of microenvironmental hypoxia. In our material, in situ hybridisation analysis of RNA expression in human tumours revealed that it is expressed by peri-necrotic areas of tumour, which result from hypoxic stress.

Areas of necrosis are commonly found in solid tumours, and correlate with poor prognosis. Also, cell death by necrosis is seen more commonly than apoptosis in hypoxic tumours. BNIP3 activates caspase-independent necrosis-like cell death as a consequence of opening the mitochondrial permeability transition pore (19), and may be the pathway mediating hypoxia-induced necrotic cell death in cancer. HIF-1 activation regulates many pathways advantageous to tumour growth, such as angiogenesis, glycolysis and glucose uptake (5), although our results suggest that activation of HIF-1 during the evolution of cancer also co-selects pathways such as BNIP3/NIX that have the potential for anti-tumour effects.

Most tumour cells retain the ability to undergo apoptosis in response to hypoxic stress (1), although paradoxically, this loss of apoptotic-sensitive cells leads to the selection of viable cells which are more resistant to treatment and contribute to tumour relapse (3). Hockel et al. have determined that a subset of hypoxic cervical carcinomas have a low apoptotic index, and that these tumours are highly aggressive (20). The mechanism by which hypoxia selects for cells resistant to apoptosis is unclear. Striking upregulation of the BNIP3/NIX gene products by hypoxia and enhanced expression in clinical tumours suggests that further analysis of this pathway in normal and tumour tissue may be helpful in understanding this important process.

References

1. Shimizu, S., Eguchi, Y., Kamiike, W., Itoh, Y., Hasegawa, J., Yamabe, K., Otsuki, Y., Matsuda, H. and Tsujimoto, Y. Induction of apoptosis as well as necrosis by hypoxia and predominant prevention of apoptosis by Bcl-2 and Bcl-XL. *Cancer Res.*, 56: 2161-2166, 1996.
2. Reynolds, T.Y., Rockwell, S. and Glazer, P.M. Genetic instability induced by the tumour microenvironment. *Cancer Res.*, 56: 5754-5757, 1996.
3. Schmaltz, C., Hardenbergh, P.H., Wells, A. and Fisher, D.E. Regulation of proliferation-survival decisions during tumor cell hypoxia. *Molecular & Cellular Biology*, 18: 2845-54, 1998.
4. Graeber, T.G., Osmanian, C., Jacks, T., Housman, D.E., Koch, C.J., Lowe, S.W. and Giaccia, A.J. Hypoxia-mediated selection of cells with diminished apoptotic potential in solid tumours. *Nature*, 379: 88-91, 1996.
5. Semenza, G.L. Regulation of mammalian O₂ homeostasis by hypoxia-inducible factor 1. *Annu. Rev. Cell Dev. Biol.*, 15: 511-578, 1999.
6. Maxwell, P.H., Wiesner, M., Chang, G.-W., Clifford, S., Vaux, E., Cockman, M., Wycoff, C., Pugh, C., Maher, E. and Ratcliffe, P. The tumour suppressor protein VHL targets hypoxia-inducible factors for oxygen-dependent proteolysis. *Nature*, 399: 271-275, 1999.
7. Carmeliet, P., Dor, Y., Herbert, J.-M., Fukumura, D., Brusselmans, K., Dewerchin, M., Neeman, M., Bono, F., Abramovitch, R., Maxwell, P., Koch, C.J., Ratcliffe, P., Moons, L., Jain, R.K., Collen, D. and Keshet, E. Role of HIF-1 α in hypoxia-mediated apoptosis, cell proliferation and tumour angiogenesis. *Nature*, 394: 485-490, 1998.
8. Lal, A., Lash, A.E., Altschul, S.F., Velculescu, V., Zhang, L., McLendon, R.E., Marra, M.A., Prange, C., Morin, P.J., Polyak, K., Papadopoulos, N., Vogelstein, B., Kinzler, K.W., Strausberg, R.L. and Riggins, G.J. A public database for gene expression in human cancers. *Cancer Res.*, 59: 5403-5407, 1999.
9. Boyd, J.M., Malstrom, S., Subramanian, T., Venkatesh, L.K., Scheper, U., Elangovan, B., D'Sa-Eipper, C. and Chinnadurai, G. Adenovirus E1B 19 kDa and Bcl-2 proteins interact with a common set of cellular proteins. *Cell*, 79: 341-351, 1994.
10. Matsushima, M., Fujiwara, T., Takahashi, E.-I., Minaguchi, T., Eguchi, Y., Tsujimoto, Y., Suzumori, K. and Nakamura, Y. Isolation, mapping and functional analysis of a novel human cDNA (BNIP3L) encoding a protein homologous to human BNIP3. *Genes, Chrom. Cancer*, 21: 230-235, 1998.
11. Chen, G., Cizeau, J., Vande Velde, C., Hoon Park, J., Bozek, G., Bolton, J., Shi, L., Dubik, D. and Greenberg, A.H. NIX and BNIP3 form a subfamily of pro-apoptotic mitochondrial proteins. *J. Biol. Chem.*, 274: 7-10, 1999.
12. Yasuda, M., Han, J.-W., Dionne, C.A., Boyd, J. and Chinnadurai, G. BNIP3a: a human homologue of mitochondrial proapoptotic protein BNIP3. *Cancer Res.*, 59: 533-537, 1999.
13. Bruik, R.K. Expression of the gene encoding the proapoptotic BNIP3 protein is induced by hypoxia. *Proc. Natl. Acad. Sci. USA*, 97: 9082-9087, 2000.
14. Wood, S. M., Wiesener, M.S., Yeates, K.M., Okada, N., Pugh, C.W., Maxwell, P.H. and Ratcliffe, P.J. Selection and analysis of a mutant cell line defective in the hypoxia-inducible factor-1 α -subunit (HIF-1 α). *J. Biol. Chem.*, 273: 8360-8368, 1998.
15. Ray, R., Chen, G., Vande Velde, C., Cizeau, J., Hoon Park, J., Reed, J.C., Gietz, R.D. and Greenberg, A.H. BNIP3 heterodimerises with Bcl-2/Bcl-XL and induces cell death independent of a Bcl-2 homology 3 (BH3) domain at both mitochondrial and nonmitochondrial sites. *J. Biol. Chem.*, 275: 1439-1448, 2000.

16. Clark, D.E., Smith, S.K., Sharkey, A.M., Sowter, H.M. and Charnock-Jones, D.S. Hepatocyte growth factor/scatter factor and its receptor c-Met: Localisation and expression in the human placenta throughout pregnancy. *J. Endocrinol.*, 151: 459-467, 1996.

17. Sayah, D.N., Soo, C., Shaw, W.W., Watson, J., Messadi, D., Longaker, M.T., Zhang, X. and Ting, K. Downregulation of apoptosis-related genes in keloid tissues. *J. Surg. Res.*, 87: 209-216, 1999.

18. Harhaj, E.W., Good, L., Xiao, G. and Sun, S.-C. Gene expression profiles in HTLV-I-immortalized T cells: deregulated expression of genes involved in apoptosis regulation. *Oncogene*, 18: 1341-1349, 1999.

19. Vande Velde, C., Cizeau, J., Dubak, D., Alimonti, J., Brown, T., Israels, S., Hakem, R. and Greenberg, A.H. BNIP3 and genetic control of necrosis-like cell death through the mitochondrial permeability transition pore. *Mol. Cell. Biol.*, 20: 5454-5468, 2000.

20. Hockel, M., Schlenger, K., Hockel, S. and Vaupel, P. Hypoxic cervical cancers with low apoptotic index are highly aggressive. *Cancer Res.*, 59: 4525-4528, 1999.

Blots were probed with an antibody to BNIP3 (Top panel) or α -tubulin (bottom panel). (A) Cell lines shown are: HT1080 (1); EJ (2); MKN45 (3); HUVEC (4); LS174T (5); DU145 (6). (B) Cell lines shown are RCC4 (7) and RCC4-VHL (8).

Figure 2. Immunohistochemical analysis of BNIP3 expression by C4.5 cells (A and B) and KA13 cells (C and D) after treatment with normoxia (A and C) and hypoxia (B and D).

Figure 3. Northern blot analysis of RNA extracted from HT1080 (1), EJ (2), T47D (3), MDA231 (4) and MDA468 (5) cell lines after 16 h treatment with normoxia (N) or hypoxia (H), and RNA extracted from normal (N) and tumorous (T) breast tissue from 5 patients (6-10). Blots were probed for NIX (A) and BNIP3 (B). The positions of ethidium bromide labelled 28 S and 18 S rRNA were used to estimate the size of the transcripts; the 28 S ribosomal band is shown in panel C as a loading control.

Figure 4. In situ hybridisation analysis of BNIP3 mRNA in human tissue. Hybridisation, visualised as silver granules under dark field conditions, was detected in perinecrotic areas of tumour. Necrotic areas of tissue are denoted N, and vascularised areas of the tissue are denoted V. (A and B): A section of an ovarian carcinoma hybridised with BNIP3 antisense probe, shown under dark-field (A) and bright-field conditions. (C and D): A section of a SSC head and neck carcinoma hybridised with BNIP3 antisense probe, shown under dark-field (C) and light-field (D) conditions. (E): A section of normal breast tissue hybridised with BNIP3 antisense probe and shown under dark field conditions. (F): A section of an ovarian carcinoma hybridised with BNIP3 sense probe, shown under dark-field conditions.

Figure Legends

Figure 1. Western blot analysis of protein extracted from various cell lines after treatment with normoxia (N) or hypoxia (H) for 16 h.

Figure 1

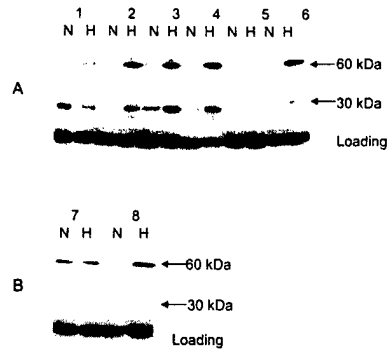


Figure 2

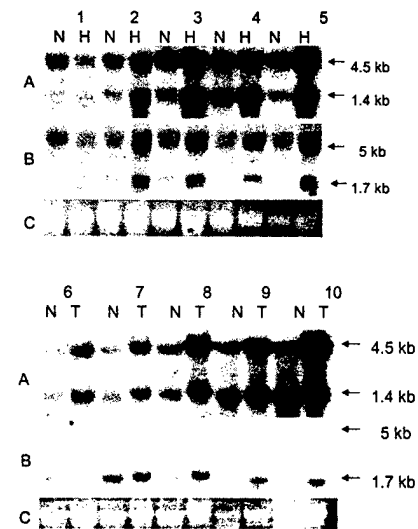


Figure 3

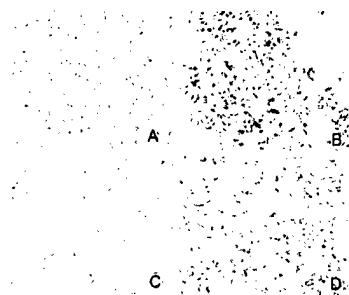
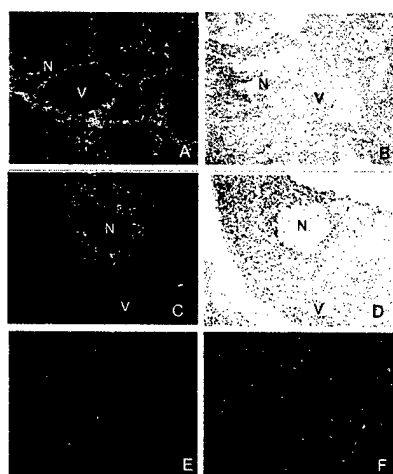


Figure 4



Title: Genetic model of multi-step breast carcinogenesis involving the epithelium and stroma: clues to tumour-microenvironment interactions**Authors:** Keisuke Kurose^{1,2}, Stacy Hoshaw-Woodard³, Adewale Adeyinka⁴, Stan Lemeshow³, Peter Watson⁴ and Charis Eng^{1,2,5,*}**Affiliations:** ¹Clinical Cancer Genetics and Human Cancer Genetics Programs, Comprehensive Cancer Centre, and Division of Human Genetics, Department of Internal Medicine; ²Division of Human Cancer Genetics, Department of Molecular Virology, Immunology and Medical Genetics; and ³Center for Biostatistics, Comprehensive Cancer Centre, The Ohio State University, Columbus, OH 43210, USA; ⁴Department of Pathology, University of Manitoba Health Sciences Centre, Winnipeg, Manitoba R3E 0W3, Canada; ⁵CRC Human Cancer Genetics Research Group, University of Cambridge Cambridge CB2 2QQ, UK***To whom correspondence should be addressed at:** Charis Eng, MD, PhD, Human Cancer Genetics Program, The Ohio State University Comprehensive Cancer Centre, 420 West 12th Avenue, Room 690C TMRF, Columbus, OH 43210, USA.
Tel: +1 614 292-2347; Fax: +1 614 688 3582 or 4245; E-mail: eng-1@medctr.osu.edu**ABSTRACT**

Although numerous studies have reported that high frequencies of loss of heterozygosity (LOH) at various chromosomal arms have been identified in breast cancer, differential LOH in the neoplastic epithelial and surrounding stromal compartments has not been well examined. Using laser capture microdissection, which enables separation of neoplastic epithelium from surrounding stroma, we microdissected each compartment of 41 sporadic invasive adenocarcinomas of the breast. Frequent LOH was identified in both neoplastic epithelial and/or stromal compartments, ranging from 25% to 69% in the neoplastic epithelial cells, and from 17% to 61% in the surrounding stromal cells, respectively. The great majority of markers showed a higher frequency of LOH in the neoplastic epithelial compartment than that in the stroma, suggesting that LOH in neoplastic epithelial cells might precede LOH in surrounding stromal cells. Furthermore, we sought to examine pair-wise associations of particular genetic alterations in either epithelial or stromal compartments. Seventeen pairs of markers showed statistically significant associations. We also propose a genetic model of multi-step carcinogenesis for the breast involving the epithelial and stromal compartments and note that genetic alterations occur in the epithelial compartments as the earlier steps followed by LOH in the stromal compartments. Our study strongly suggests that interactions between breast epithelial and stromal compartments might play a critical role in breast carcinogenesis and several genetic alterations in both epithelial and stromal compartments are required for breast tumour growth and progression.

INTRODUCTION

Breast cancer is the most common and second most lethal cancer in women in Western countries. Numerous studies have focused on the role of chromosome abnormalities and gene mutations in sporadic breast cancer, but to date no clear model of the critical events or delineation of primary abnormalities has emerged. Various chromosome arms have been observed to be affected by a high frequency of structural or numerical abnormalities (1-5). Although several of these chromosome arms appear to be the sites of putative tumour suppressor genes (TSGs), the number and identity of TSGs relevant for mammary carcinogenesis is unknown. At the molecular level, several somatic mutations in genes residing in these regions have been described (1, 6-9). Despite this abundance of data, the relevance, role, and timing of most of the described

genetic abnormalities in sporadic breast cancer are still unclear. It is also not known whether specific mutations play relevant roles as causative factors or are the consequence of the general genomic instability and progression in breast tumours.

A few studies have previously demonstrated that loss of heterozygosity (LOH) identified at various chromosomal loci at high frequency in invasive cancer is already present in *in situ* carcinoma, atypical ductal hyperplasia, non-atypical hyperplasia of the breast, and perhaps adjacent normal epithelial cells, although these studies predated laser capture microdissection (LCM), hence, contamination from clearly malignant tissue cannot be excluded (10-15). These observations are also found in colonic adenomas (16), Barrette oesophageal metaplasia (17, 18), and lung hyperplasias (19). These reports indicate that the majority of premalignant or precursor lesions share their LOH phenotypes with invasive disease in the same organs, providing novel biologic evidence that they are genetically and perhaps evolutionarily related. Nonetheless, until recently, any cancer such as breast cancer was treated as a single amorphous entity. Most such genetic studies were uniformly performed on the entire tumour without regard to its components despite the fact that a few groups were quite aware of both epithelial and stromal components of tumours, and the cell biology of the tumour "microenvironment" has been described for the last 20 years. Thus, until now, when a genetic alteration, be it intragenic mutation, regional amplification, or deletion manifested by LOH is attributed to a breast cancer, it is unclear if the alteration is actually occurring in the epithelial compartment, the surrounding stromal compartment or both.

The effects of the metabolism of the tumour stroma, locally as well as systemically, are largely unknown. Although the stroma has generally been considered a silent bystander during epithelial carcinogenesis, the concept that the microenvironment is central to maintenance of cellular function and tissue integrity provides the rationale for the idea that its disruption can contribute to neoplasia (20). Several studies performed *in vivo* and *in vitro* indicated that the growth and invasive potentials of carcinoma cells are influenced through interactions with host stromal cells (21-23). Despite these progressive cell biological studies, the precise genetic mechanisms leading to tumour progression remain unclear. Even less clear is the role of differential genetic alterations in the epithelial neoplastic component and its surrounding stroma.

Recently, Moinfar *et al.* reported the high frequency of LOH in the mammary stroma with breast cancer (5). They examined 11 patients with ductal carcinoma *in situ*, including five cases with invasive ductal carcinoma, and found LOH in the stromal cells. Although these investigators identified frequent genetic alterations in the mammary stroma, each component of the breast carcinoma was manually microdissected; thus cross-contamination cannot be excluded. Further, they examined a limited number of samples and a limited number of microsatellite markers on only 5 chromosome arms. In this present study, we sought to systematically examine for genetic alterations in the epithelial and stromal components of invasive adenocarcinomas of the breast with the DNA extracted from cells from each compartment obtained by LCM. We found frequent LOH in both epithelial and/or stromal components of breast cancer and identified associations among LOH at various chromosomal regions, suggesting that genetic alterations in the epithelial and surrounding stromal cells are involved in the breast tumorigenesis through concurrent and independent pathways.

RESULTS

LCM of each specimen was performed to selectively obtain normal epithelial or stromal cells, carcinomatous epithelial cells, and stromal cells surrounding the epithelial carcinoma (eg, Fig. 1A). LOH at each of the 13 chromosomal regions were detected in epithelial and/or stromal compartments among the 41 invasive adenocarcinomas of the breast (eg, Fig. 1B). Table 1 summarises the frequencies of LOH observed at 13 loci in neoplastic epithelial and surrounding stromal cells. Among the 13 microsatellite markers examined, the LOH frequency ranged from 25% (9/36) at D3S1581 (3p14-q21) to 69% (22/32) at D17S796 (17p13) in the neoplastic epithelial compartment; and from 17% (6/36) also at D3S1581 to 61% (20/33) at D2S156 (2q34) in the surrounding stromal component (Table 1). D2S156 (2q34) and perhaps D6S437 (6q25) were the only two markers demonstrating a higher frequency of LOH in the surrounding stromal compartment compared to the neoplastic epithelial cells. In contrast, the great majority of markers showed a higher frequency of LOH in the neoplastic epithelial compartment compared to the surrounding stromal cells (Table 1).

On further inspection of the differential LOH data, it can be noted that for certain markers, LOH predominates in the neoplastic epithelial compartment; for others, LOH predominates in the stromal compartment, and for yet other markers, it predominates in both compartments (Table 1). For instance, LOH at 16q24.3 (D16S413) was identified more frequently only in the neoplastic epithelial cells (11 tumours) than in only the stromal cells (3 tumours, $P=0.0325$, McNemar's test). The number of tumours that showed LOH at 17p13 (D17S796) only in stromal cells (2 tumours) was significantly fewer than that having LOH at 17p13 in both epithelial and stromal cells or only in the neoplastic epithelial cells (12 tumours or 10 tumours, $P=0.0209$, McNemar's test).

We then looked for pair-wise associations of dependency or independency of particular genetic alterations with one another in either epithelial or stromal compartments (Fig. 2). We found that there were statistically significant associations in 17 pairs (17/325; 5.3%) of markers (Fig. 2). Fifteen pairs (15/17; 88%) showed positive associations, and 2 pairs (2/17; 12%) negative associations (Fig. 2). LOH at 4

markers, D10S1765, D11S912 and D17S579 in the surrounding stromal compartment and D2S156 in the neoplastic epithelial compartment, were associated with ≥ 3 sites of LOH (Fig. 2). Of note, LOH at D10S1765 in the stromal compartment was associated with LOH at D17S579 and D22S277 in the stromal compartments and also with LOH at D2S156 in the neoplastic epithelial compartments. LOH at D17S579 in the stromal compartment, in turn, was found to be associated with LOH at D2S156 and D13S155 in the neoplastic epithelial compartment and at D10S1765 in the surrounding stromal compartment. In contrast, LOH at D8S264 (8p23.2) in the neoplastic epithelial cells is negatively correlated with LOH at D1S228 (1p36) in the surrounding stromal cells. Interestingly, LOH at D8S264 in the surrounding stromal compartment is negatively correlated with LOH at D1S228 in the neoplastic epithelial compartment.

DISCUSSION

In this present study, we have found frequent LOH in both neoplastic epithelial and surrounding stromal cells of invasive adenocarcinomas of the breast. In our series of 41 breast cancer samples, we identified LOH in the neoplastic epithelial compartment, ranging from 25% (9/36) to 69% (22/32), and in the stromal compartment, ranging from 17% (6/36) to 61% (20/33), respectively. Of note, the great majority of markers demonstrated a higher frequency of LOH in the neoplastic epithelial compartment compared to the surrounding stromal cells (Table 1). Further inspection of the differential LOH data indicated that the frequency of LOH only in the stromal compartment occurred among fewer tumours than that in both neoplastic epithelial and surrounding stromal compartments, or that in only the neoplastic epithelial cells (Table 1). In the field of human cancer genetics, it has been shown that markers with the highest frequency of LOH represent those with the earliest genetic alterations, the so-called first "hits" and the one with the lowest frequency of LOH, the latest "hit" in carcinogenesis (16). Thus, under this assumption, from our data, we can propose a genetic model of multistage, stepwise carcinogenesis in the breast, according to the relative frequencies of LOH in the epithelial and stromal compartments (Fig. 3). Our proposed model encompasses data that shows a higher frequency of LOH in breast epithelial cells occurs earlier than that in the stromal compartment (Fig. 3). Although Moinfar *et al.* (5) worked without the advantage of LCM and used markers representing only 5 chromosomal regions and a sample size of 11, their observations of relative frequencies of LOH in the neoplastic epithelium (occurring in 1/4 to 3/3 tumours) compared to presumably surrounding stroma (occurring in 1/4 to 4/5) might be interpreted as concurrent with ours. These data together with our observations suggest that genetic alterations in the epithelial compartment, at least in some chromosomal regions, precede the genetic changes in the surrounding stromal cells. If in fact we may extrapolate that each region of LOH represents at least one putative TSG, then it is possible that the same putative gene involved in epithelial carcinogenesis plays some role in the stroma at a later stage, with the possible exception of D2S156. In our study, the earliest genetic alterations occurred at D8S264, D16S413 and D17S796 in the epithelium as well as D2S156 in the stroma (Fig. 3). It is almost certain that the D17S796 marker represents *TP53*, and indeed, *TP53* alterations have been noted amongst the most frequent and

earliest somatic alterations in prior studies involving "whole" breast carcinomas (24, 25). The regions of D8S264 and D16S413 have yet to yield convincing tumour suppressor genes involved in breast carcinogenesis. Our data would strongly support the existence of one or more tumour suppressor genes residing in these two regions which when mutated participate in the initiation of cancer within the breast epithelium. Of interest, LOH at D2S156 in the stromal cells is also scored as an early event (Fig. 3). This has not been a region noted to have LOH in whole breast cancers. Nonetheless, our data suggest that there will be at least one important gene residing in that interval which plays a prominent role in the initiation of breast carcinogenesis, possibly from a microenvironmental or "landscaper" point of view (26). The genetic model proposed (Fig. 3) assumes for simplicity that frequency of occurrence reflects temporal sequence. This in turn assumes an equivalent effect on tumorigenesis and early progression between all alterations. However, it is recognised that an alternative possibility is that some alterations may be dominant while others may require the cooperation of parallel or multiple complex alterations at other sites to facilitate progression, and that this would influence the prevalence of the alteration in advanced tumours. In the case of these different assumptions, a lower frequency of stromal alterations could reflect the fact that stromal alterations are not dominant and only exert an indirect effect on the adjacent epithelium or only exert an effect in collaboration with others, to influence the overall process of tumorigenesis.

The apparent asynchronous LOH at each marker between epithelium and stroma might suggest that while the neoplastic epithelium is clonal as is the stroma, these observations may support one viewpoint that epithelium and stroma derive from different cellular origins. However, there are advocates of a common cellular origin of both epithelium and stroma (27). If this latter is true, then in the context of our observations, the LOH in epithelium and stroma occurred after the divergence of epithelial and stromal cell from the presumed common cell.

Despite a relatively small sample size, we were able to examine pair-wise associations between regions and compartments where LOH occurred (Fig. 2). For example, LOH at D17S579 in the neoplastic epithelial cells was associated with LOH at D17S796 and D10S1765 in the neoplastic epithelial compartments. These chromosomal loci contain several putative TSGs. The polymorphic markers, D17S579 (17q21), D17S796 (17p13) and D10S1765 (10q23.3), are in proximity to the *BRCA1* gene, *TP53* gene, and *PTEN* gene, respectively. Previous reports have identified that there are significant associations between LOH of *BRCA1* and *TP53* (28, 29) or *PTEN* gene (28) in sporadic heterogeneous breast cancer samples. Crook *et al.* found a high proportion of "whole" breast and ovarian tumours from *BRCA1* mutation carriers had *TP53* mutations (30). Our proposed genetic model does suggest that LOH at D17S796 in the neoplastic epithelial cells is the earliest hit, LOH at D17S579 in the neoplastic epithelial cells is the second one, then LOH at D10S1765 in the neoplastic epithelial cells is the third hit in these consequences (Table 1 and Fig. 3). The association between LOH of *BRCA1* and *PTEN* is, therefore, one of the genetic alterations that might be expected to occur as a consequence of the loss of *BRCA1* and *TP53*. LOH at

D2S156 in the neoplastic epithelial compartment was associated with LOH at 3 markers, D10S1765, D11S912 and D17S579 in the surrounding stromal compartments. The reciprocal interaction between epithelial and stromal cells plays a key role in the morphogenesis, proliferation, and differentiation of epithelial cells (31-33). Most of the intercellular substances, extracellular matrix (ECM) molecules that are required for tumour growth and progression are produced by the stromal cells (34). It is well demonstrated that altered gene expression occurs between normal and neoplastic breast stroma (35) and that stromal cells play a critical role in the production and possible dissolution of the ECM (36, 37). Thus, genetic alterations in the stromal cells may change the interaction between epithelial cells and ECM molecules and influence the tumour invasion and dissemination (22, 23). Our results suggest that LOH at 2q34 (D2S156) might precede LOH of 3 chromosomal loci in the stromal compartments (Figs. 2 and 3). Therefore, we hypothesised that loss of a putative TSG on 2q34 might play an important role in genetic alterations of stromal compartments, which in turn might influence tumour invasion and dissemination through ECM remodelling. If this hypothesis is correct, then we can further hypothesise that genetic alterations in the stroma might predict for poorer prognosis due to increased tumour invasiveness.

In summary, we have found frequent LOH in both neoplastic epithelial and surrounding stromal compartments in invasive adenocarcinomas of the breast and statistically significant associations among the LOH at various chromosomal regions. We also propose a multi-step genetic model of breast carcinogenesis involving epithelium and stroma, which can help build further hypotheses and guide future studies of reciprocal interactions between breast neoplastic epithelial and stromal cells in tumour initiation, progression, invasion and metastases. Such studies might eventually lead to novel therapeutic strategies, which selectively target epithelium or stroma.

MATERIALS AND METHODS

Breast cancer samples

Forty-one archival (formalin-fixed and paraffin-embedded) tissues that were distinct cases of clinically sporadic primary invasive adenocarcinomas of the breast were used. Twenty-six samples were obtained from the National Cancer Institute of Canada Manitoba Breast Tumour Bank and 15 were from the Department of Pathology of The Ohio State University.

Microdissection of tissue and DNA extraction

Microdissection of carcinomatous epithelial cells, surrounding stromal cells, and normal epithelial or stromal cells from fixed, paraffin-embedded sections of breast was done by use of an Arcturus PixCell II Laser Capture microdissecting microscope (Arcturus Engineering, Inc., Mountain View, CA). This system utilises a transparent thermoplastic film applied to the surface of the tissue section on standard histopathology slides. The breast cancer epithelial, surrounding stromal, and normal epithelial or stromal cells to be microdissected were identified and targeted through a microscope, and a narrow (~15 µm) carbon dioxide laser-beam pulse specificity activated the film above these cells. The resulting strong focal adhesion allowed selective procurement of only the targeted cells (38) (Fig. 1A). The cells removed in Fig. 1A are the neoplastic epithelial component. The surrounding stromal fibroblasts are

immediately adjacent to the removed cells (Fig. 1A, arrow). It is acknowledged that while LCM minimises cross-contamination of cell types, it does not guarantee against it. However, the very "clean" LOH (virtually all or none) which we have obtained does suggest that any cross-contamination is not significant.

DNA from microdissected tissue was extracted in 50 μ l of solution containing 0.04% proteinase K, 1% Tween-20, 10 mM Tris-HCl (pH 8.0), and 1 mM EDTA at 37°C overnight followed by heat inactivation at 95°C for 10 minutes.

LOH analysis

For purposes of this study, genomic DNA, extracted from paraffin embedded tissues, served as template for polymerase chain reactions (PCR) amplification of 13 microsatellite markers selected from a comprehensive genetic map of the human genome (39). Fluorescent-labelled polymorphic markers, including D1S228 (1p36), D2S156 (2q34), D3S1581 (3p14.2-21.2), D3S1286 (3p24.3-25.1), D6S437 (6q25.3), D8S264 (8p23.2), D10S1765 (10q23.3), D11S912 (11q23), D13S155 (13q14), D16S413 (16q24.3), D17S796 (17p13), D17S579 (17q21), and D22S277 (22q12.2-13.1), were used for this analysis. All subsequent PCRs were carried out using 0.5 μ M each of forward and reverse primer in 1X PCR buffer (Qiagen, Valencia, CA), 1.5 mM MgCl₂ (Qiagen), 1X Q-buffer (Qiagen), 1.25 units of HotStar Taq polymerase (Qiagen), and 200 μ M of each dNTP (Gibco, Gaithersburg, MD) in a final volume of 25 μ l. After a denaturation at 95°C for 14 minutes, reactions were subjected to 40 cycles of 94°C for 1 minute, 55°C to 60°C for 1 minute, and 72°C for 1 minute followed by 10 minutes at 72°C. PCR reactions and genotyping were repeated at least a second time to confirm the data. Amplified PCR products were separated by electrophoresis through 6% denaturing polyacrylamide gels, and the signal was detected with an Applied Biosystems model 377xl semi-automated DNA sequencer (Applied Biosystems, Perkin-Elmer Corp., Norwalk, CT). The results were analysed by automated fluorescence detection using the GeneScan collection and analysis software (GeneScan, Applied Biosystems). Scoring of LOH was initially performed by inspection of the GeneScan analysis output. A conservative ratio of peak heights of alleles between germline DNA and somatic DNA greater than or equal to 1.9:1 will be used to define LOH in this study (40).

Statistical analysis

Comparisons for statistical significance were performed by using either the standard Fisher's exact test (2-tailed) or the McNemar's test for matched pairs at the $p=0.05$ level of significance. McNemar's test was used when interest focused on differences in proportions of patients with LOH in either stromal or epithelial cells, but not both. This test determines whether, in these cases of discordance, there is a disproportionate number of patients with LOH in one of the two sites. McNemar's test is used in recognition of the fact that the stromal and epithelial cells are taken from the same breast tissue and, hence, are matched. However, the Fisher's exact test was also employed because it is unclear from a biological point of view whether each data point (ie LOH at any one marker) is dependent on the next (ie LOH at other markers).

ACKNOWLEDGMENTS

We thank Fred Wright and Sandya Liyanarchchi for providing statistical assistance. Part of this work was performed in the Laser Capture Microdissection core facility in the Tissue Procurement Shared Resources Service of the Comprehensive Cancer Centre. This work was supported in part by the Jimmy V Golf Classic Award for Basic and Clinical Cancer Research from the V Foundation (to CE) and a grant from the National Cancer Institute, Bethesda, MD (P30CA16058 to The Ohio State University Comprehensive Cancer Centre).

REFERENCES

1. Devilee, P. and Cornelisse, C.J. (1994) Somatic genetic changes in human breast cancer. *Biochim Biophys Acta*, **1198**, 113-130.
2. Bieche, I. and Lidereau, R. (1995) Genetic alterations in breast cancer. *Genes Chromosomes Cancer*, **14**, 227-251.
3. Kerangueven, F., Noguchi, T., Coulier, F., Allione, F., Wargniez, V., Simony-Lafontaine, J., Longy, M., Jacquemier, J., Sobol, H., Eisinger, F. *et al.* (1997) Genome-wide search for loss of heterozygosity shows extensive genetic diversity of human breast carcinomas. *Cancer Res*, **57**, 5469-5474.
4. O'Connell, P., Pekkeli, V., Fuqua, S.A., Osborne, C.K., Clark, G.M. and Allred, D.C. (1998) Analysis of loss of heterozygosity in 399 premalignant breast lesions at 15 genetic loci. *J Natl Cancer Inst*, **90**, 697-703.
5. Moynfar, F., Man, Y.G., Arnould, L., Brathauer, G.L., Ratschek, M. and Tavassoli, F.A. (2000) Concurrent and independent genetic alterations in the stromal and epithelial cells of mammary carcinoma: implications for tumorigenesis. *Cancer Res*, **60**, 2562-2566.
6. Li, J., Yen, C., Liaw, D., Podsypanina, K., Bose, S., Wang, S.I., Puc, J., Miliareis, C., Rodgers, L., McCombie, R. *et al.* (1997) PTEN, a putative protein tyrosine phosphatase gene mutated in human brain, breast, and prostate cancer. *Science*, **275**, 1943-1947.
7. Done, S.J., Arneson, N.C., Ozcelik, H., Redston, M. and Andrulis, I.L. (1998) p53 mutations in mammary ductal carcinoma in situ but not in epithelial hyperplasias. *Cancer Res*, **58**, 785-789.
8. Feilolter, H.E., Coulon, V., McVeigh, J.L., Boag, A.H., Dorion-Bonnet, F., Duboue, B., Latham, W.C., Eng, C., Mulligan, L.M. and Longy, M. (1999) Analysis of the 10q23 chromosomal region and the PTEN gene in human sporadic breast carcinoma. *Br J Cancer*, **79**, 718-723.
9. Negrini, M., Monaco, C., Vorechovsky, I., Ohta, M., Druck, T., Baffa, R., Huebner, K. and Croce, C.M. (1996) The FHIT gene at 3p14.2 is abnormal in breast carcinomas. *Cancer Res*, **56**, 3173-3179.
10. Rosenberg, C.L., de las Morenas, A., Huang, K., Cupples, L.A., Faller, D.V. and Larson, P.S. (1996) Detection of monoclonal microsatellite alterations in atypical breast hyperplasia. *J Clin Invest*, **98**, 1095-1100.
11. Lakhani, S.R., Collins, N., Stratton, M.R. and Sloane, J.P. (1995) Atypical ductal hyperplasia of the breast: clonal proliferation with loss of heterozygosity on chromosomes 16q and 17p. *J Clin Pathol*, **48**, 611-615.

12. Lakhani, S.R., Slack, D.N., Hamoudi, R.A., Collins, N., Stratton, M.R. and Sloane, J.P. (1996) Detection of allelic imbalance indicates that a proportion of mammary hyperplasia of usual type are clonal, neoplastic proliferations. *Lab Invest*, **74**, 129-135.
13. Jensen, R.A., Page, D.L. and Holt, J.T. (1994) Identification of genes expressed in premalignant breast disease by microscopy-directed cloning. *Proc Natl Acad Sci USA*, **91**, 9257-9261.
14. Noguchi S., Motomura, K., Inaji, H., Imaoka, S. and Koyama H. (1994) Clonal analysis of predominantly intraductal carcinoma and precancerous lesions of the breast by means of polymerase chain reaction. *Cancer Res*, **54**, 1849-1853.
15. Deng, C., Lu, Y., Zlotnikov, G., Thor, A.D. and Smith, H.S. (1996) Loss of heterozygosity in normal tissue adjacent to breast carcinomas. *Science*, **274**, 2057-2059.
16. Fearon, E.R. and Vogelstein, B. (1990) A genetic model for colorectal tumorigenesis. *Cell*, **61**, 759-767.
17. Blount, P.L., Galipeau, P.C., Sanchez, C.A., Neshat, K., Levine, D.S., Yin, J., Suzuki, H., Abraham, J.M., Meltzer, S.J. and Reid, B.J. (1994) 17p allelic losses in diploid cells of patients with Barrett's esophagus who develop neoplasia. *Cancer Res*, **54**, 2292-2295.
18. Zhuang, Z., Vortmeyer, A.O., Mark, E.J., Odze, R., Emmert-Buck, M.R., Merino, M.J., Moon, H., Liotta, L.A. and Duray, P.H. (1996) Barrett's esophagus: metaplastic cells with loss of heterozygosity at the APC gene locus are clonal precursors to invasive adenocarcinoma. *Cancer Res*, **56**, 1961-1964.
19. Hung, H., Kishimoto, Y., Sugio, K., Virmani, A., McIntire, D.D., Minna, J.D. and Gazdar, A.F. (1995) Allele-specific chromosome 3p deletions occur at an early stage in the pathogenesis of lung carcinoma. *JAMA*, **273**, 554-563.
20. Bissell, M.J. and Barcellos-Hoff, M.H. (1987) The influence of extracellular matrix on gene expression: is structure the message? *J Cell Sci Suppl*, **8**, .
21. Picard, D., Rolland, Y. and Poupon, M.F. (1986) Fibroblast-dependent tumorigenicity of cells in nude mice: implication for implantation of metastases. *Cancer Res*, **46**, 3290-3294.
22. Grey, A.M., Schor, A.M., Rushton, G., Ellis, I. and Schor, S.L. (1989) Purification of the migration stimulating factor produced by fetal and breast cancer patient fibroblasts. *Proc Natl Acad Sci USA*, **86**, 2438-2442.
23. Camps, M.L., Chang, S.M., Hsu, T.C., Freeman, M.R., Hong, J., Zhou, H.E., von Eschenbach, A.C. and Chung, L.W. (1990) Fibroblast-mediated acceleration of human epithelial tumor growth in vivo. *Proc Natl Acad Sci USA*, **87**, 75-79.
24. Coles, C., Condie, A., Chetty, U., Steel, C.M., Evans, H.J. and Prosser, J. (1992) p53 mutations in breast cancer. *Cancer Res*, **52**, 5291-5298.
25. Buchhorn, T.A., Weil, M.M., Story, M.D., Strom, E.A., Brock, W.A. and McNeese, M.D. (1999) Tumor suppressor genes and breast cancer. *Radiat Oncol Invest*, **7**, 55-65.
26. Kinzler, K.W. and Vogelstein, B. (1998) Landscaping the cancer terrain. *Science*, **280**, 1036-1037.
27. Pierce, G.B. and Speers, W.C. (1988) Tumors as caricatures of the process of tissue renewal: prospects for therapy by directing differentiation. *Cancer Res*, **48**, 1996-2004.
28. Hanby, A.M., Kelsell, D.P., Potts, H.W., Gillett, C.E., Bishop, D.T., Spurr, N.K. and Barnes, D.M. (2000) Association between loss of heterozygosity of BRCA1 and BRCA2 and morphological attributes of sporadic breast cancer. *Int J Cancer*, **88**, 204-208.
29. Tong, D., Kucera, E., Schuster, E., Schmutzler, R.K., Swoboda, H., Reinthaller, A., Leodolter, S. and Zeillinger, R. (2000) Loss of heterozygosity (LOH) at p53 is correlated with LOH at BRCA1 and BRCA2 in various human malignant tumors. *Int J Cancer*, **88**, 319-322.
30. Crook, T., Crossland, S., Crompton, M.R., Osin, P. and Gusterson, B.A. (1997) p53 mutations in BRCA1-associated familial breast cancer. *Lancet*, **350**, 638-639.
31. Cunha, G.R., Bigsby, R.M., Cooke, P.S. and Sugimura, Y. (1985) Stromal-epithelial interactions in adult organs. *Cell Differ*, **17**, 137-148.
32. Donjacour, A.A. and Cunha, G.R. (1991) Stromal regulation of epithelial function. *Cancer Treat Res*, **53**, 335-364.
33. Hom, Y.K., Young, P., Wiesen, J.F., Miettinen, P.J., Derynck, R., Werb, Z. and Cunha, G.R. (1998) Uterine and vaginal organ growth requires epidermal growth factor receptor signaling from stroma. *Endocrinology*, **139**, 913-921.
34. Hanahan, D. and Folkman, J. (1996) Patterns and emerging mechanisms of the angiogenic switch during tumorigenesis. *Cell*, **86**, 353-364.
35. Leygue, E., Snell, L., Dotzlaw, H., Hole, K., Hiller-Hitchcock, T., Roughley, P.J., Watson, P.H. and Murphy, L.C. (1998) Expression of lumican in human breast carcinoma. *Cancer Res*, **58**, 1348-1352.
36. Wolf, C., Rouyer, N., Lutz, Y., Adida, C., Lorient, M., Bellocq, J.P., Chambon, P. and Basset, P. (1993) Stromelysin 3 belongs to a subgroup of proteinases expressed in breast carcinoma fibroblastic cells and possibly implicated in tumor progression. *Proc Natl Acad Sci USA*, **90**, 1843-1847.
37. Noel, A., Hajitou, A., L'Hoir, C., Maquoi, E., Baramova, E., Lewalle, J.M., Remacle, A., Kebers, F., Brown, P., Calberg-Bacq, C.M. *et al.* (1998) Inhibition of stromal matrix metalloproteinases: effects on breast-tumor promotion by fibroblasts. *Int J Cancer*, **76**, 267-273.
38. Emmert-Buck, M.R., Bonner, R.F., Smith, P.D., Chuaqui, R.F., Zhuang, Z., Goldstein, S.R., Weiss, R.A. and Liotta, L.A. (1996) Laser capture microdissection. *Science*, **274**, 998-1001.
39. Dib, C., Faure, S., Fizames, C., Samson, D., Drouot, N., Vignal, A., Millasseau, P., Marc, S., Hazan, J., Seboun, E. *et al.* (1996) A comprehensive genetic map of the human genome based on 5,264 microsatellites. *Nature*, **380**, 152-154.
40. Marsh, D.J., Zheng, Z., Zedenius, J., Kremer, H., Padberg, G.W., Larsson, C., Longy, M. and Eng, C. (1997) Differential loss of heterozygosity in the region of the Cowden locus within 10q22-23 in follicular thyroid adenomas and carcinomas. *Cancer Res*, **57**, 500-503.

Table 1. LOH frequencies and distribution in the epithelial and stromal cells

Chromosomal Region	Marker	Cases with LOH in Ep ^a / informative cases	Cases with LOH in St ^b / informative cases	Cases with LOH in either Ep or St / informative cases	Cases with LOH only in Ep	Cases with LOH only in St	McNemar's Test <i>p</i> -value (exact <i>p</i> -value)
1p36	D1S228	16/34 (47%)	10/34 (29%)	21/34 (62%)	11	5	0.1336 (0.2101)
2q34	D2S156	16/33 (48%)	20/33 (61%)	26/33 (79%)	6	10	0.3173 (0.4545)
3p14.2-21.2	D3S1581	9/36 (25%)	6/36 (17%)	11/36 (31%)	5	2	0.2568 (0.4531)
3p24.3-25.1	D3S1286	17/37 (46%)	14/37 (38%)	23/37 (62%)	9	6	0.4386 (0.6072)
6q25.3	D6S437	14/29 (48%)	15/29 (52%)	20/29 (69%)	5	6	0.7630 (1.000)
8p23.2	D8S264	21/32 (66%)	18/32 (56%)	25/32 (78%)	7	4	0.3657 (0.5488)
10q23.3	D10S1765	15/36 (42%)	10/32 (31%)	16/32 (50%)	6	5	0.7630 (1.000)
11q23	D11S912	19/37 (51%)	16/37 (43%)	25/37 (68%)	9	6	0.4386 (0.6072)
13q14	D13S155	18/33 (55%)	16/33 (48%)	23/33 (70%)	7	5	0.5637 (0.7744)
16q24.3	D16S413	20/31 (65%)	13/32 (41%)	23/31 (74%)	11	3	0.0325 (0.0574)
17p13	D17S796	22/32 (69%)	14/32 (44%)	24/32 (75%)	10	2	0.0209 (0.0386)
17q21	D17S579	17/32 (53%)	11/32 (34%)	21/32 (66%)	10	4	0.1088 (0.1796)
22q12.2-13.1	D22S277	15/37 (41%)	15/37 (41%)	21/37 (57%)	6	6	1.000 (1.000)

^aEp, epithelium; ^bSt, stroma.**ABBREVIATIONS**

LOH: loss of heterozygosity

ROH: retention of heterozygosity

LCM: laser capture microdissection

TSG: tumour suppresser gene

ECM: extracellular matrix

PCR: polymerase chain reactions

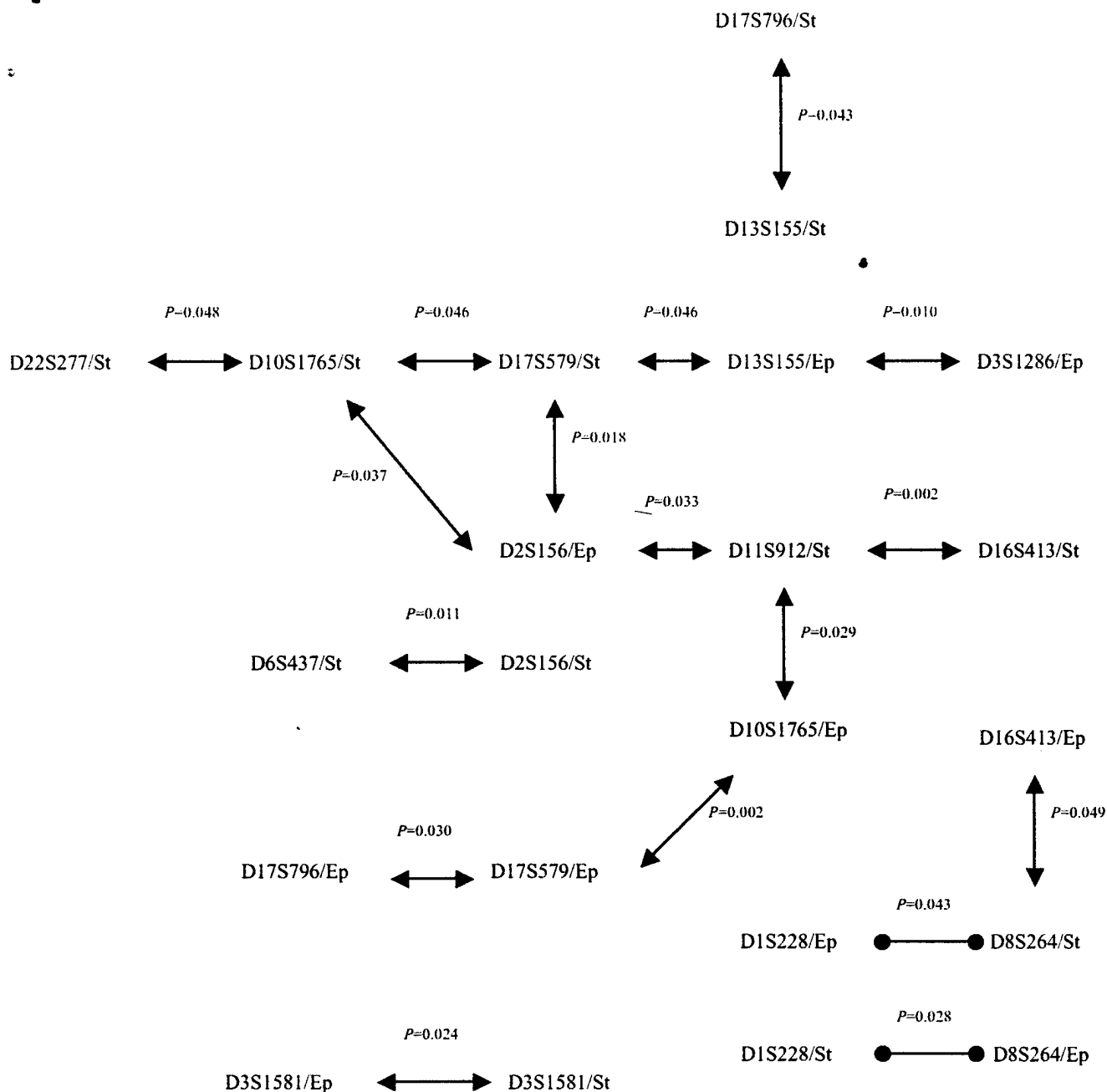


Figure 2. Positive and negative associations between markers in epithelial and stromal compartments of adenocarcinomas of the breast. Double-headed arrows denote positive correlations while double-knobbed lines negative correlations. Numbers above the arrows or lines are *P* values (Fisher's exact test). Ep, epithelial cells; St, stromal cells.

A

Before



After

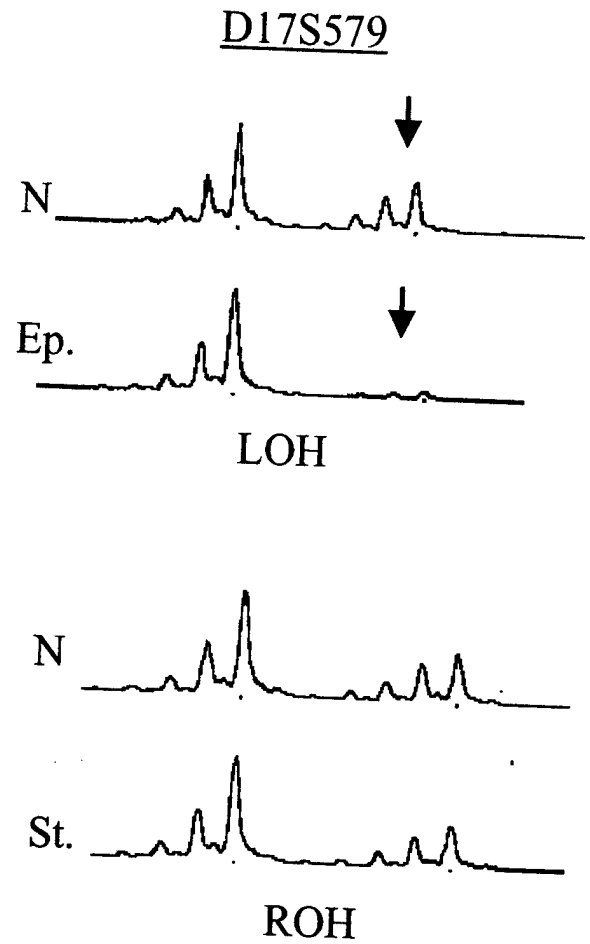
Captured
cells**B**

Figure 1. A: Laser capture microdissection (LCM) from breast cancer specimen. Captured cells are the neoplastic epithelial component. The surrounding stromal fibroblasts are immediately adjacent to the removed cells (arrow). **B:** Illustrative examples of LOH (arrows) and retention of heterozygosity (ROH) at D17S579. N, normal cells; Ep, epithelial cells; St, stromal cells.

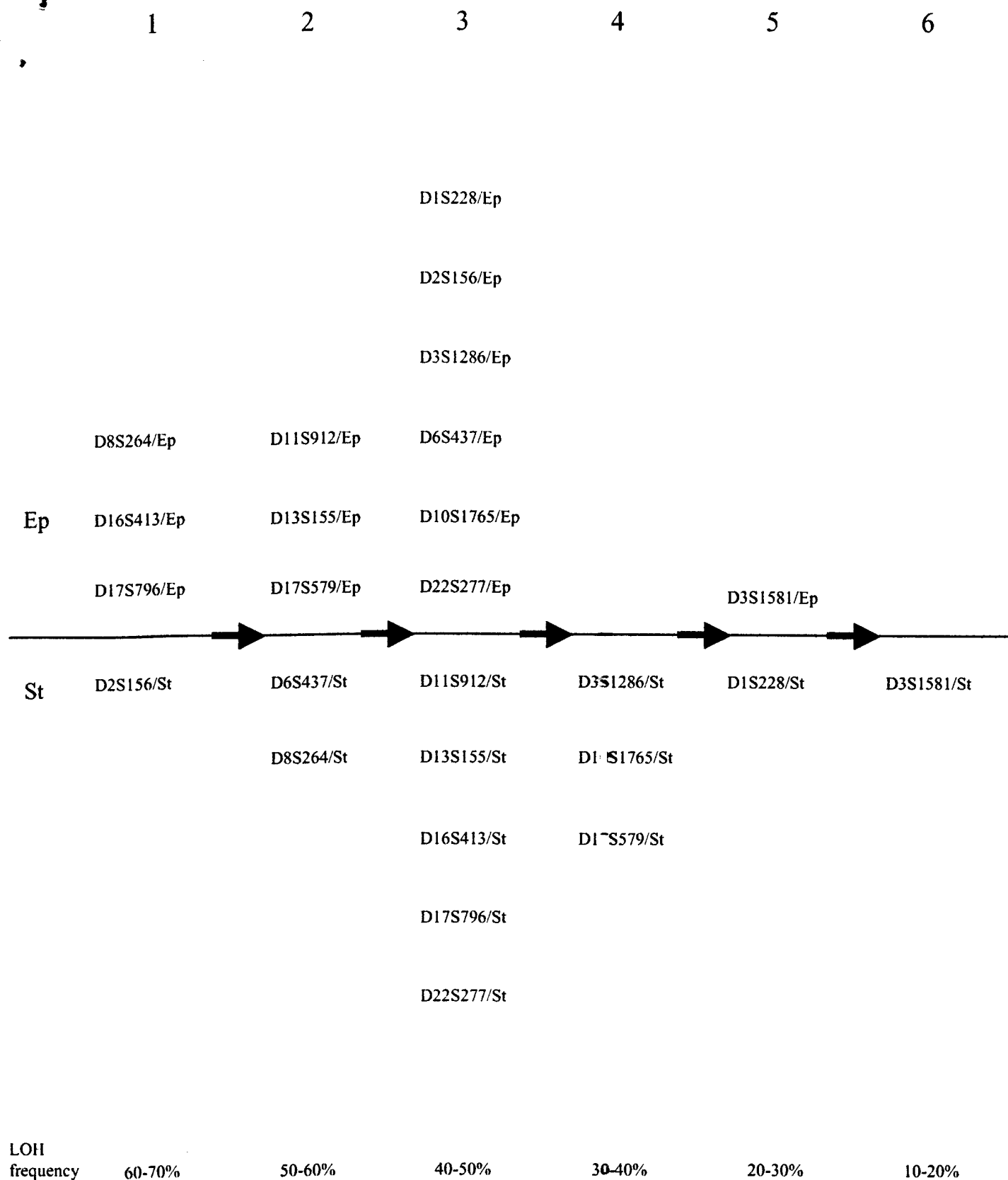


Figure 3. Proposed genetic model of multistage, stepwise carcinogenesis in the breast involving the epithelial and stromal compartments. Ep, epithelial cells; St, stromal cells.